शैक्षणिक प्रतिवेदन

Academic Report
2017-18

होमी भाभा राष्ट्रीय संस्थान
Homi Bhabha National Institute

(परमाणु ऊर्जा विभाग की एक सहायक संस्था और यूजीसी अधिनियम 1956 की धारा 3 के तहत विश्वविद्यालय माना जाता है
An aided institution of the Department of Atomic Energy and a Deemed to be University Under section 3 of the UGC Act.1956)

Location of HBNI Central Office, Constituent Institutions & Off Campus Centre

Homi Bhabha National Institute

Academic Report 2017-18

Training School Complex, Anushaktinagar,
Mumbai 400094

Contents

From the Vice-Chancellor

I take great pleasure in presenting the academic report of HBNI for the year 2017-18. During the year, HBNI continued its progress by way of introducing innovative programs and fine tuning the academic processes. We crossed the prestigious milestone of producing 1000 PhDs, during the year. The total number of PhDs awarded by HBNI till 31st March 2018 stands at 1132.

In the MHRD's National Institutional Ranking Framework (NIRF) exercise for the academic year 2016-17, results of which were announced in April 2018, HBNI received 26th Rank in University category among a total of 296 participants. An analysis of the data with respect to the ranking parameters gives us the confidence that HBNI will improve its ranking substantially in the coming years. HBNI has also been included in the list of institutions to be given a higher degree of autonomy by UGC.

The quality of the PhD programs undertaken by HBNI students is obvious through a perusal of the highlights of the thesis included in the volume of the academic report that accompanies this annual report. The mission of DAE and the research ambience, infrastructure and knowledge base in the institutions under HBNI provide the necessary ingredients for the choice of challenging problems at the frontiers of science and technology for the research programs of the students. In addition, HBNI has also been offering programs that contribute to skill development. The courses in Oncology, clinical research and nursing are making impactful contributions to the country's human resource base in these vital areas.

During the year, HBNI introduced several innovative schemes to provide additional academic exposure to its PhD students. One such scheme is the study tour of research scholars to another Constituent Institution (CI) of HBNI. CIs are also encouraged to organize meetings of the research scholars to share the results of their work, as well as their research experience and also to provide an avenue for identifying areas where they could collaborate or use the infrastructure available in other CIs. Several quality improvement measures have been undertaken including a review of the ordinances and introduction of faculty assessment program. HBNI also started a colloquium program during the year, to enable the HBNI functionaries to obtain the perspectives and advice from eminent academicians in the country. A technical lecture series has also been started to archive, in video format, lectures on a variety of topics of high relevance to the Department, particularly in the area of nuclear and radiation safety, delivered by acclaimed experts. Collaboration with other academic institutions in the country through MoUs is continuing to expand; for instance, steps were taken during the year to collaborate with INSTN, France in design and delivery of educational material in the areas of mutual interest in the domain of nuclear science and technology. Such programs of international collaboration in the field of education and research get added impetus through the increased autonomy now provided by UGC.

HBNI has established itself as one of the best research universities in the country, encouraging research in various facets of nuclear science and technology including mathematics, and providing valuable human resources to the country in a variety of domains, including superspecialities in medicine. There are, of course, domains where further improvement can be realized, and with the efforts of a dedicated team at the Central office and the faculty distributed across the CIs, we can hope to see further progress in a variety of aspects. I would like to place on record our gratitude to Dr. Sekhar Basu, Chairman, Council of Management, HBNI and Secretary, DAE and other members of the CoM, for providing all necessary guidance and support to HBNI in furthering its objectives. Thanks are particularly due to Prof. R.B.Grover, Emeritus Professor, HBNI who has been a source of inspiration to the HBNI team. Thanks are also due to members of the Academic Council and the Planning and Monitoring Board for their critical advice and valuable contributions towards introducing innovative schemes.

(P R Vasudeva Rao)

Introduction

The HBNI has the following as its Constituent Institutions (CIs)/ Off Campus Centre (OCC)

1. Bhabha Atomic Research Centre (BARC), Mumbai
2. Indira Gandhi Centre for Atomic Research (IGCAR), Kalpakkam
3. Raja Ramanna Centre for Advanced Technology (RRCAT), Indore
4. Variable Energy Cyclotron Centre (VECC), Kolkata
5. Saha Institute of Nuclear Physics (SINP), Kolkata
6. Institute for Plasma Research (IPR), Gandhinagar
7. Institute of Physics (IOP), Bhubaneswar
8. Harish-Chandra Research Institute (HRI), Allahabad
9. Institute of Mathematical Sciences (IMSc), Chennai, and
10. Tata Memorial Centre (TMC), Mumbai.
11. National Institute of Science Education and Research (NISER), Bhubaneswar (from February 5, 2016)

The role of HBNI is to nurture in-depth capabilities in nuclear science and engineering and to serve as a catalyst to accelerate the pace of basic research and facilitate its translation into technology development and applications through academic programs, viz., Master's and Ph.D. degrees in Engineering, Physical, Chemical, Mathematical, Life and Health Sciences while encouraging inter-disciplinary research. Additionally, a Strategic Studies program has also been identified to ensure availability of adequate qualified human resources to address issues pertaining to nuclear law, economics of nuclear power, nuclear security, nuclear proliferation, intellectual property rights etc.

Academic Programs of the Institute

The HBNI offers a range of academic programs in chemical sciences, engineering sciences, health sciences, life sciences, mathematical sciences and physical sciences. All institutions, except NISER, conduct programs at post-graduate level. Various programs offered are the following.

Ph.D. in varied disciplines is offered at all CIs/OCC. HRI, IMSc and NISER also offer an integrated Ph.D. program where students study for M.Sc. as well as Ph.D.

M.Tech. in engineering sciences and **M.Phil.** in physical sciences, chemical sciences and life sciences. These programs consist of one year of course work and one year of project/dissertation work. The course work is offered at all campuses of BARC Training School and IPR Training School. Project/Dissertation work is offered at BARC, IGCAR, RRCAT, VECC, IPR and some other units of DAE. Those who are not interested in project/dissertation work get a post graduate diploma in lieu of M.Tech. or M.Phil degree.

M.Sc. (Engg) in which research content is more than that in a M.Tech. program. The duration of the project work under this program is one and half year, while the duration of the course work is up to one year. This program is offered at BARC, IGCAR, VECC, RRCAT and IPR.

Integrated M.Sc.of five-year duration at NISER

Super Specialty Health Science Courses at TMC

- **D.M.** (Medical Oncology)
- **D.M.** (Pediatric Oncology)
- **D.M.** (Gastroenterology)
- **D.M.** (Critical Care Medicine)
- **D.M.** (Interventional Radiology)
- **M.Ch.** (Surgical Oncology)
- **M.Ch.** (Gynecological Oncology)
- **M.Ch.** (Plastic Surgery)
- **M.Ch.** (Head & Neck Oncology)

Post Graduate Health Science Courses at TMC

- **M.D.** (Pathology) #
- **M.D.** (Anesthesia) #
- **M.D.** (Radio-diagnosis)#
- **M.D**. (Radiotherapy)##
- **M.D**. (Microbiology) #
- **M.D**. (Nuclear Medicine)
- **M.D.** (Palliative Medicine) #
- **M.D.**(Immuno-Hematology &Blood Transfusion)

M.Sc. (Nursing) at TMC

M.Sc. (Clinical Research) at TMC

Dip.R.P. Diploma in Radiological Physics at BARC

DMRIT Diploma in Medical Radio Isotope Techniques at BARC

PGDFIT PGDiploma in Fusion Imaging Technology at TMC

In addition, the TMC also offers a two-year Certified Fellowship Program in 23 different areas related to Oncology. Most of the Ph.D. programs are multi-disciplinary in nature having guides and co-guides from different branches of science and engineering. 785 students are admitted in different programs during 2017-18, out of which 336 students are for PhD program. HBNI has awarded 225 Ph.D., 94 M.Tech., 22 M.Sc. (Engg), 89 M.Sc., 108 post graduate medical degrees, 5 M.Sc.(Nursing) and 38 PG diplomas in radiation protection (DipRP),medical radioisotope technology (DMRIT), radiation medicine (DRM) and fusion imaging technology (DFIT) during this period.

All the Constituent Institutions have excellent library facilities having a large collection of books and subscribe to a large number of research journals. All journals are available to researchers on their desktops.

Composition of the Bodies of the Institute

Management of the Institute

The Council of Management is the principal organ for management of the Institute.

COUNCIL OF MANAGEMENT [CoM]

Dr. Sekhar Basu Chairman, AEC	Chairman
Prof. B. K. Dutta/ Prof. P.R. Vasudeva Rao Vice-Chancellor	Member
Shri K.N. Vyas Director, BARC	Member
Prof. P.A. Naik Director, RRCAT	Member
Prof. R.A. Badwe Director, TMC	Member
Prof. A.K. Mohanty Director, SINP	Member
Member for Finance, AEC	Member
Secretary Higher Education, MHRD	Member
Prof. Surendra Prasad Former Director, IIT Delhi and Chairperson, NBA	Member
Prof. Arun Nigavekar Trustee & Senior Advisor, Science & Technology Park, University of Pune	Member
Prof. Sudhir K. Sopory Former Vice-Chancellor, JNU, New Delhi	Member
Prof. B. K. Dutta Dean	Member
Prof. B. K. Dutta/Prof.D.K. Maity Registrar	Non-Member Secretary

All academic issues are handled by the Academic Council which functions on advice of the Board of Studies.

ACADEMIC COUNCIL

Prof. B. K. Dutta/ Prof. P R Vasudeva Rao	Vice Chanceller (Chairman)
Shri K.N. Vyas	Director, BARC
Prof. A.K. Bhaduri	Director, IGCAR
Prof. P.A.Naik	Director, RRCAT
Prof. S. Chaturvedi	Director, IPR
Prof. A. Roy	Director, VECC
Prof. R. A. Badwe	Director, TMC
Prof. A.K. Mohanty	Director, SINP &Convener, BoS (Physical Sciences)
Prof. V. Arvind	Director, IMSc
Prof.P. Mazumdar	Director, HRI
Prof. Sudhakar Panda	Director, IoP
Prof. Dipan Ghosh	IIT-Bombay
Prof. K. Muralidhar	IIT-Kanpur
Prof. E. D. Jemmis	IISc, Banglore
Prof. Srinivasan Ramakrishnan	TIFR, Mumbai
Prof. Jaikumar Radhakrishnan	TIFR, Mumbai
Prof. B.K. Dutta	Dean, HBNI
Prof. R.B. Grover	Convener, BoS (Applied Systems Analysis)
Prof. S. Chattopadhyay/Prof. S. Chiplunkar	Convener,BoS(Life Sciences)
Prof. B. Ramakrishnan	Convener, BoS (Mathematical Sciences)
Prof. G.K. Dey/Prof. A.P. Tiwari	Convener, BoS (Engineering Sciences)
Prof. B.S. Tomar/Prof. P.D. Naik	Convener, BoS (Chemical Sciences)
Prof. K. S. Sharma	Convener, BoS(Health Science)
Prof. B. K. Dutta/ Prof.D.K. Maity	Registrar (Non-Member-Secretary)

Advisory Committee			
Secretary, DAE and Chairman, AEC	Chairman	Director, TMC	Member
Vice Chancellor, HBNI	Member	Director, IMSc	Member
Director, BARC	Member	Director, TIFR	Member
Director, IGCAR	Member	Director, NISER	Member
Director, RRCAT	Member	Director, HRI	Member
Director, VECC	Member	Director, IOP	Member
Director, IPR	Member	Dean, HBNI	Member -Secretary
Director, SINP	Member		

Officers of the Institute			
Academic		**Administrative and Accounts**	
Prof. P. R. Vasudeva Rao	Vice Chancellor (From Oct. 4th, 2017)	Shri Himanshu Shankar	Finance Officer
Prof. B. K. Dutta	Vice Chancellor (Till Oct. 3rd, 2017)	Prof. D.K.Maity	Registrar (Officiating, w.e.f. 01/01/2017)
Prof. B. K. Dutta	Dean	Shri M.S.Gandle	Deputy Registrar
Prof. D. K. Maity	Associate Dean	Shri Swaminathan K	Administrative Officer
Prof. A. K. Dureja	Associate Dean	Ms. Bharati Suverna	Asst. Registrar

Board of Studies

- Applied Systems Analysis (A)
- Chemical Sciences (C)
- Engineering Sciences (E)
- Medical and Health Sciences (H)
- Life Sciences (L)
- Mathematical Sciences (M)
- Physical Sciences (P)
- Integrated Masters Programme (I)

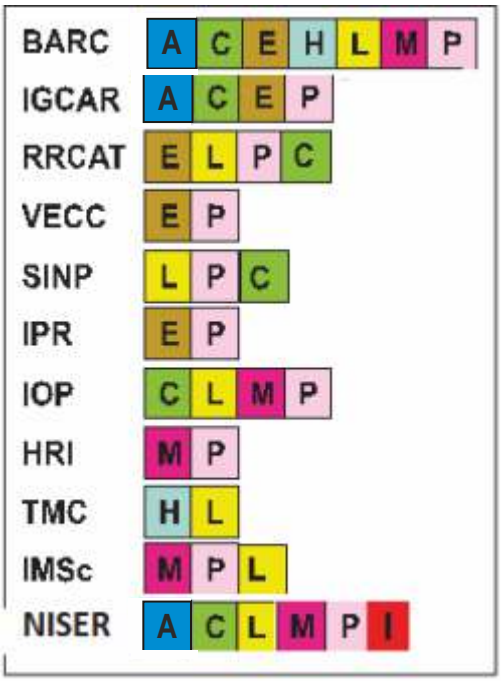

To manage affairs of the Institute at the level of Constituent Institutions (CIs)/Off Campus Centre (OCC), each CI/OCC has one or more Deans-Academic and a university cell. CIs/OCC have also established a robust framework for admission, evaluation of performance and monitoring the progress of research by the students.

Board of Studies of HBNI (As on 31st of March 2018)

BoS (Chemical Sciences)

1. Prof. B. S. Tomar, BARC - Convener
2. Prof. P. D. Naik, BARC – Co-Convener
3. Prof. D. K. Maity, HBNI
4. Prof. P. K. Pujari, BARC
5. Prof. H. Pal, BARC
6. Prof. A. K. Tyagi, BARC
7. Prof. S. Kannan, BARC
8. Prof. A. Srinivasan, NISER
9. Prof. Sharmila Banerjee, RMC
10. Prof. N. Sivaraman, IGCAR

Balancing Members

1. Prof. A. K. Mohanty, SINP
2. Prof. S. Chiplunkar, TMC

BoS (Engineering Sciences)

1. Prof. A. P. Tiwari, BARC-Convener
2. Prof. K. Velusamy, IGCAR-Co- Convener
3. Prof. Archana Sharma, BARC
4. Prof. P. V. Varde, BARC
5. Prof. A. K. Nayak, BARC
6. Prof. J. Chattopadhyay, BARC
7. Prof. C. P. Paul, RRCAT
8. Prof. Paramita Mukherjee, VECC
9. Prof. S. K. Pathak, IPR
10. Prof. V. Kain, BARC

Balancing Members:

1. Prof. A. K. Bhattacharjee, BARC
2. Prof. A. K. Dureja, HBNI

BoS (Health Sciences)

1. Prof. K. S. Sharma, TMC - Convener
2. Prof. Sandeep Basu, RMC-Co-Convener
3. Prof. N. Roy, BARC
4. Prof. Nalini Shah, K.E.M.Hospital, Mumbai
5. Prof. Suleman Merchant, L.T.M.G. Hospital, Mumbai
6. Dr. S. K. Srivastava, TMC
7. Dr. S. V. Kane, TMC
8. Dr. S. B. Banavali, TMC
9. Prof. P. S. Yadav, TMC
10. Prof. D. D. Deshpande, TMC

Balancing Members:

1. Prof. S. V.Chiplunkar, ACTREC,TMC
2. Prof. A. K. Dureja, HBNI

BoS (Life Sciences)

1. Prof. (Mrs.) S. Chiplunkar, ACTREC-Convener
2. Prof. V. P. Venugopalan, BARC-Co-Convener
3. Prof. AbhijitChakraborty, SINP
4. Prof. B. J. Rao, TIFR
5. Prof. Rajiv Sarin, ACTREC
6. Prof. S. Santoshkumar, BARC
7. Prof. P. Suprasanna, BARC
8. Prof. S. Gautam, BARC
9. Prof. H. S. Mishra, BARC
10. Prof. HarapriyaMohaptra, NISER

Balancing Members:

1. Prof. K. S. Sharma, TMC
2. Prof. D. K. Maity, HBNI
3. Prof. Rahul Siddharthan, IMSc

BoS (Mathematical Sciences)

1. Prof. B. Ramakrishnan, HRI-Convener
2. Prof. Meena Mahajan, IMSc-Co-Convener
3. Prof. R. R. Puri, IIT Gandhinagar
4. Prof. MahuyaDatta, ISI-Kolkata
5. Prof. Jugal K. Verma, IIT Bombay

6. Prof. B. Sury, ISI-Bangalore
7. Prof. K. N. Raghavan, IMSc
8. Prof. K. V. Subrahmanyam, CMI-Chennai
9. Prof. V. Muruganandam, NISER
10. Prof. D. S. Ramana, HRI

Balancing Member

1. Prof. A. K. Dureja, HBNI

BoS (Physical Sciences)

1. Prof. A. K. Mohanty, SINP-Convener
2. Prof. Pinaki Majumdar, HRI-Co-Convener
3. Prof. G. Amarendra, IGCAR
4. Prof. Sudip Sengupta, IPR
5. Prof. N. K. Sahoo, BARC
6. Prof. S. C. Gadkari, BARC
7. Prof. D. Indumathi, IMSc
8. Prof. Shikha Varma, IoP
9. Prof. K. S. Bindra, RRCAT
10. Prof. B. Mohanty, NISER

Balancing Members:

1. Prof. D. K. Maity, HBNI
2. Prof. Jane Alam, VECC

BoS (Applied Systems Analysis)

1. Prof. R. B. Grover, HBNI-Convener
2. Prof. KamachiMudali, IGCAR Co-Convener
3. Dr. K. Raghuraman, Ex-DAE, Navi Mumbai
4. Prof. G. Ravikumar, BARC
5. Prof. Pranay Swain, NISER
6. Prof. SurinderJaswal, TISS
7. Prof. S. Kannan-BARC

BoS (Undergraduate Studies)

1. Director, NISER-Convener (Ex-Officio)
2. Dean/Faculty-In-Charge (Academics), NISER Co-Convener (Ex-Officio)
3. Dean/Faculty-In-Charge (Student Affairs), NISER (Ex-Officio)
4. Chair School of Life Sciences, NISER (Ex-Officio)
5. Chair School of Chemical Sciences, NISER (Ex-Officio)
6. Chair School of Mathematics, NISER (Ex-Officio)
7. Chair School of Physical Sciences, NISER (Ex-Officio)
8. Chair, Undergraduate Studies Committee of Institute, NISER (Ex-Officio)

Balancing Members:

1. Prof. Pinaki Majumdar, HRI
2. Prof. D. K. Maity, HBNI
3. Prof. Meena Mahajan, IMSc
4. Prof. S. Chiplunkar, TMC

Deans Academics at Constituent Institutions(CIs)/Off-Campus Centre (OCC)

(As on January 1st, 2018)

Sr. No.	Name of the CI/Off-campus Centre	Discipline	Name Of the Dean Academic
1	Bhabha Atomic Research Centre	Life Sciences	Prof. (Ms.) Hema Rajaram
		Chemical Sciences	Prof. A.K. Tyagi
		Physical & Mathematical Sciences	Prof. B.K. Nayak
		Engineering Sciences (Stream-I)	Prof. Vivekanand Kain
		Engineering Sciences (Stream-II)	Prof. Anup K. Bhattacharjee
		Health Sciences	Dr. Sandip Basu
2	Indira Gandhi Centre for Atomic Research	Chemical Sciences	Prof. N. Sivaraman
		Physical Sciences	Prof. N.V. Chandra Sekhar
		Engineering Sciences	Prof. (Ms.) G. Sasikala
3	Raja Ramanna Centre for Advanced Technology	All Disciplines	Prof. Arup Banerjee
4	Variable Energy Cyclotron Centre	Physical Sciences	Prof. Jane Alam
		Engineering Sciences	Prof. (Ms.) Paramita Mukherjee
5	Saha Institute of Nuclear Physics	Chemical & Life Sciences	Prof. Abhijit Chakrabarti
		Physical Sciences	Prof. Debades Bandhopadhyay
6	Institute for Plasma Research	All Disciplines	Prof. Subroto Mukherjee
7	Institute of Physics	Physical Sciences	Prof. Pankaj Agrawal
8	Institute of Mathematical Sciences	Mathematical Sciences	Prof. Vijay Kodiyalam
		Physical Sciences	Prof. Rahul Sinha
		Life Sciences	Prof. Gautam Menon
9	Harish -Chandra Research Institute	All Disciplines	Prof. Dileep Jatkar
10	Tata Memorial Centre	All Disciplines	Prof. K.S. Sharma
11	National Institute of Science Education and Research	All Disciplines	Prof. (Ms.) Harapriya Mohapatra

Faculty List (as on January 1st, 2018)

HBNI

1. Banerjee S.
2. Vasudeva Rao P R
3. Dutta B K
4. Grover Ravi Bhushan
5. Joshi J B
6. Tomar B S
7. Basu Saibal
8. Maity Dilip Kumar
9. Dureja Adarsh Kumar

BARC

❖ **CHEMICAL SCIENCES**

10. A. L. Rufus
11. Achary S. N.
12. Acharya Raghunath
13. Adhikari Soumyakanti
14. Agarwal Renu
15. Amit Kunwar
16. Ankita Rao
17. Anupkumar B
18. Arunasis Bhattacharyya
19. Arya Ashok Kumar
20. Awadhesh Kumar
21. Balaji P Mandal
22. Bandyopadhyay Tusar
23. Banerjee Aparna
24. Banerjee Dayamoy
25. Banerjee Sharmila
26. Bhardwaj Y. K.
27. Bhasikuttan A C
28. Bindal R. C.
29. Chandrakumar K R S
30. Chatterjee Suchandra
31. Choudhury Niharendu
32. Das Tapas
33. Dash Ashutosh
34. Deo Mukul Narayan
35. Dey Ghasiram
36. Dey Sandip
37. Dibakar Goswami
38. Drishty Satpati
39. Dubey Abhinav Kumar
40. Dutt G. B.
41. Dutta Choudhury Sharmistha
42. Dutta Dimple
43. Ganguly R
44. Ghanty Tapan Kumar
45. Ghosh Asim Kumar
46. Ghosh Hirendra Nath
47. Ghosh Subir Kumar
48. Ghosh Sunil Kumar
49. Goswami Madhumita
50. Gupta Vinita Grover
51. Hassan P A
52. J. Selvakumar
53. Jha S K
54. K Indira Priyadarsini
55. K. Bhattacharyya
56. K. C. Barick
57. K. K. Swain
58. Kadam Ramakant Mahadeo
59. Kapoor Sudhir
60. Kaushik Chetan Prakash
61. Kedarnath G.
62. Korde Aruna

63. Kshirsagar R J
64. Kumar Pradeep
65. Kumar Sangita D.
66. Kumar Sanjiv
67. Kumar Sanjukta A.
68. Kumar Sunil Jai
69. Kumar Virendra
70. Kumbhakar Manoj
71. Majumder Chiranjib
72. Manmohan Kumar
73. Mishra Adya Prasad
74. Mishra R
75. Misra N L
76. Mohanty J.
77. Mohapatra Prasanta Kumar
78. Mondal Jahur A
79. Mukerjee S K
80. Murali M. S.
81. Musharaf Ali S. K.
82. Naik Devidas B
83. Naik Prakash Dattatray
84. Nandita Maiti
85. Nath Sukhendu
86. Nayak A. K.
87. Nayak Sandip Kumar
88. Neetika Rawat
89. Ningthougam Raghumani Singh
90. Pabby Anil Kumar
91. Pai Mrinal R.
92. Pal Haridas
93. Pandey Ashok Kumar
94. Pandey Usha
95. Pandit Gauri Girish
96. Parida Suresh Chandra
97. Patra Chandra Nath
98. Prabhat K Singh
99. Prasad Phadnis
100. Pujari Pradeep Kumar
101. R. J. Kshirsagar
102. R. Sasikala
103. Rahul Tripathi
104. Raje Naina
105. Ramkumar Jayshree
106. Rangarajan S
107. Rath M.C.
108. Ravi P. M.
109. Ray Alok Kumar
110. Roy Mainak
111. S. Kannan
112. Sali S. K.
113. Salil Varma
114. Samanta Alok Kumar
115. Sandeep Nigam
116. Sarkar Arnab
117. Satpati Ashis Kumar
118. Sawant Shilpa N.
119. Sharma Manoj Kumar
120. Sharma Pramod
121. Singh Ajay K
122. Singh Kumar Dhurva
123. Singhal Anshu
124. Singhal Rakesh Kumar
125. Smruti Dash
126. Sodaye Hemant Shivram
127. Sodaye Suparna
128. Soumyaditya Mula
129. Sreenivas T
130. Srinivasan M. P
131. Srivastava Ritu M.
132. Suchismita Mishra

133. Sudarsan V.
134. Sudarshan Kathi
135. Sunny Febby
136. Tripathi A. K.
137. Tripathi R M
138. Tyagi A K
139. Upadhyaya Hari Prasad
140. Varshney Lalit
141. Vatsa R K
142. Velmurugan S

❖ **Engineering Sciences**

143. Awasthi Alok
144. Badodkar D N
145. Bajpai R. K.
146. Balasubramaniam R
147. Betty C A
148. Bhargava Kapilesh
149. Bhattacharjee Anup Kumar
150. Biswas Aniruddha
151. Chakraborty Sankar Prasad
152. Chakraborty Sudipta
153. Chakravarty Anindya
154. Chandraker Dinesh Kumar
155. Chattopadhyay Jayanta
156. Das Ramkrishna
157. Dikshit Biswaranjan
158. Dwarakanath T A
159. Gopalakrishnan Sugilal
160. Gopika Vinod
161. Kain Vivekanand
162. Kapoor Rajeev
163. Kar D C
164. Kar Soumitra
165. Khan Imran Ali
166. Kinshuk Dasgupta
167. Laik Arijit
168. Mahata Tarasankar
169. Maheshwari N K
170. Maiti Namita
171. Majumdar Sanjib
172. Mandal D.
173. Mukhopadhyay Siddhartha
174. Mukhopadhyaya Sulekha
175. Nayak Arun Kumar
176. Pal Sangita
177. Patankar V H
178. Prakash Deep
179. Reddy G R
180. Roy Debanik
181. Roy S B
182. Samal M K
183. Sengupta Pranesh
184. Sharma Archana
185. Singh Gurusharan
186. Singh Jung Bahadur
187. Singh K. K.
188. Singh R K
189. Singh Ram Niwas
190. Sinha Amit
191. Tewari P K
192. Tewari Raghvendra
193. Tiwari A P
194. Topkar Anita Vinay
195. Vaidya Abhijeet Mohan
196. Varde Prabhakar V
197. Verma Rishi
198. Vijayan P K
199. Vincent Tessy
200. Vinod Kumar A

❖ **Health Sciences**

201. Basu Sandip
202. Gadgil Anita
203. Jadhav D. S.
204. Jadhav R. V.
205. Kalbhande
206. Khandekar A. J.
207. Kulkarni A. R.
208. Malhotra Gaurav
209. Malpani B. L.
210. Mishra Satish
211. More N. N.
212. Pendse R. R.
213. Saha Swapnil
214. Sharma Sunil Dutt
215. Shejul Yogesh K
216. Tamboli Ninad

❖ **Life Sciences**

217. Acharya Celin
218. Amit Kumar
219. Apte Shree Kumar
220. B K Das
221. Badigannavar Anand M.
222. Ballal Anand D.
223. Banerjee Manisha
224. Bhakti Basu
225. Bhat Nagesh
226. Bhilwade Hari Narayan
227. Chada Sonia
228. Chawla S. P.
229. Chittela Rajanikant
230. Das Birajalaxmi
231. Fulzele Devanand Pralhadrao
232. Gagan Deep Gupta
233. Ganapathi T R
234. Ghosh Anu
235. Gopalakrishnan Roja
236. Jambulkar Sanjay J
237. Jamdar S. N.
238. Kota Swathi
239. Kulkarni Savita
240. Kulkarni Vishvas M
241. M G R Rajan
242. Makde Ravindra D.
243. Manish Goswami
244. Manjaya Joy G.
245. Maurya Dharmendra Kumar
246. Melo J S
247. Mishra Himanshi N
248. Misra Hari S
249. Mukherjee Archana
250. Mukherjee Prasun Kumar
251. Mukhopadhyaya Rita
252. Nancharaiah Y. V.
253. Pandey B. N.
254. Patro Birija Sankar
255. R Shashidhar
256. Rachna Agarwal
257. Rajaram Hema
258. Ramesh Hire
259. Rath Devashish
260. Reddy kandali S.
261. S. T. Mehetre
262. Saha Joshi Archana
263. Saini Ajay
264. Sainis Krishna Balaji
265. Santosh Kumar S.

266. Satyendra Gautam
267. Shankar Bhavani S.
268. Sharma Deepak
269. Souframanien J.
270. Subramanian Mahesh
271. Sukhendu Bikash Ghosh
272. Suprasanna P
273. Suvendu Mondal
274. Toleti Subba Rao
275. Uppal Sheetal
276. Variyar Prasad S
277. Venugopalan V P

❖ **Physical Sciences**

278. Ahmed Zafar
279. Amit P. Srivastava
280. Aswal Dinesh Kumar
281. Aswal V K
282. B.N. Raja Sekhar
283. Bakshi Ashok Kumar
284. Bandyopadhyay Tapas
285. Bera Santanu
286. Bhattacharya Debarati
287. Bhattacharyya Dibyendu
288. Bhattacharyya Soumen
289. Bhushan Dhabekar
290. Biswas Debabrata
291. Biswas Dhruba Jyoti
292. Biswas Dipak Chandra
293. Chakraborty Keka R
294. Chandratre Vinay Bhaskar
295. Chaplot Samrath Lal
296. Chauhan Anil Kumar
297. Das Amitabh
298. Das Swapan
299. Dasgupta Kamlesh
300. Datta Debabrata
301. Debnath A K
302. Dev Vas
303. Dighe Priyamvada M
304. Dutta Dipanwita
305. Gadkari Sanjay C
306. Gaitonde D M
307. Garg Alka B
308. Garg Nandini
309. Ghorui Srikumar
310. Goswami Binoy Krishna
311. Gupta Anurag
312. Gupta N K
313. Gupta Shiv Kumar
314. Jain Sudhir Ranjan
315. Jayasekharan T.
316. Jha Shambhu Nath
317. John Bency V
318. Joshi Keshaw Datt
319. K. K. Yadav
320. Kannan Umasankari
321. Karmakar Debjani
322. Kaur Manmeet
323. Kaushik Trilok Chand
324. Koul Dileep Kumar
325. Krishnani P D
326. Kulkarni Mukund Shrinivas
327. Kumar Aniruddha
328. Kumar Mukesh
329. Kumar Munish
330. Kumar Vinay
331. Mahata Kripamay
332. Mazumder Subhashish
333. Mishra D. R.

334. Mishra Rosaline
335. Mitra Abhas Kumar
336. Mitra Subhankur
337. Mittal Ranjan
338. Mukherjee Goutam Dev
339. Mukhopadhyay Ramaprasad
340. Murli Chitra
341. Nakhate S G
342. Nayak Basanta Kumar
343. Nilaya J. Padma
344. Pant Lalit Mohan
345. Paritosh Modak
346. Pradhan Swarupananda
347. Rajarajan A. K.
348. Ramaniah Lavanya
349. Rannot R C
350. Rao Divakar K.
351. Rao Mala N
352. Rao Pushpa M
353. Rao Rekha
354. Rao Turumella V Chandrasekhar
355. Ravikumar G.
356. Ray Aditi
357. Renju George Thomas
358. Roy Bidyut Jyoti
359. S. Anand
360. Sahoo N K
361. Sahu Sanjay Kumar
362. Salunkhe Hemanth Govind
363. Sangeeta
364. Santra Satyaranjan
365. Sapra B K
366. Sastry U P
367. Saxena Alok
368. Saxena Vibha
369. Selvam T. Palani
370. Sen Debasis
371. Shastri Aparna
372. Shivanand Chaurasia
373. Shrivastava Aradhana
374. Shukla Prashant
375. Singh Ajay
376. Singh Pitamber
377. Singh Surendra
378. Sinha Amar
379. Srinivasan Krishnagopal
380. Subir Bhattacharyya
381. Sucharita Sinha
382. Sukanta Karmakar
383. Suryanarayana M. V.
384. Thakare Sanjay V.
385. Tickoo A K
386. Tripathy S P
387. Udupa Dinesh Venkatesh
388. Wagh Pratap Baburao
389. Warrier Manoj Kumar
390. Yeram Shashwati Sen
391. Yusuf S M

IGCAR

❖ **Chemical Sciences**

392. A. Suresh
393. Bandi Prabhakara Reddy
394. Das Arindam
395. Durairaj Ponraju
396. Ganesan Rajesh
397. Jain Ashish
398. Jena Hrudananda
399. K. I. Gnanasekar
400. K. Sundararajan

401. Kannan Sankaran
402. Krishnamurthy Ananthasivan
403. M G Pujar
404. M. Joseph
405. N Sivaraman
406. Nagarajan K
407. Ningshen Sublime
408. Panigrahi Bhabani Shankar
409. R V Subba Rao
410. R. Venkata Krishnan
411. S. Ramya
412. Satpathy Kamala Kanta
413. Savari Anthonysamy
414. T. S. Lakshminarasimhan
415. V. Jayaraman

❖ **Engineering Sciences**

416. Aniruddha Moitra
417. Anish Kumar
418. Arun Kumar Bhaduri
419. B Purna Chandra Rao
420. Binod Kumar Choudhary
421. C. K. Mukhopadhyay
422. G Sasikala
423. M. Vasudevan
424. Mythili R
425. Nagesha A
426. P Parameswaran
427. P. Mangarjuna Rao
428. S Murugan
429. Saroja Saibaba
430. Shaju K Albert
431. Shankar Vani
432. Sharma Anil Kumar
433. Sudha C
434. V.S. Srinivasan
435. Velusamy K.

❖ **Physical Sciences**

436. Arup Dasgupta
437. Awadhesh Mani
438. B Sundaravel
439. B Venkataraman
440. C Venkata Srinivas
441. Chinnappan Ravi
442. Dhara Sandip Kumar
443. Divakar Ramachandran
444. G Amarendra
445. G Mangamma
446. G Raghavan
447. John Philip
448. K Devan
449. M Kamruddin
450. M T Jose
451. Mathi Jaya S
452. N Subramanian
453. N V Chandra Shekar
454. Niranjan Kumar
455. Panigrahi B K
456. Prabhakar K
457. Prasad Arun K
458. R Baskaran
459. R Govindraj
460. R Rajaraman
461. R Ramaseshan
462. R Venkatesan
463. R. Krishnan
464. Ravindran Nithya
465. Ravindran T R
466. S Amrithapandian

467. S Ganesamoorthy
468. S Sivakumar
469. S Tripura Sundari
470. S. Abhaya
471. Sharat Chandra
472. T N Sairam
473. Tom Mathews
474. V Sivasubramanian
475. V Sridharan

RRCAT

❖ **Chemical Scien**

476. Das Kaustuv
477. Nanda Dipankar

❖ **Engineering Sciences**

478. Gupta Prabhat Kumar
479. Paul Christ Prakash
480. Shukla Rahul

❖ **Life Sciences**

481. Dube Alok
482. Sharma Mrinalini S.

❖ **Physical Sciences**

483. Banerjee Arup
484. Bhaumik Indranil
485. Bindra Kushvinder Singh
486. Chakera J. A.
487. Chakrabarti Aparna
488. Chari Rama
489. Chattopadhyay Maulindu Kumar
490. Dasgupta Raktim
491. Dixit Kumar Vijay
492. Dixit Sudhir Kumar
493. Ganguli Tapas
494. Ghosh Haranath
495. Gupta Pooja
496. Gupta Surya Mohan
497. Ingale Alka A.
498. Jayabalan J.
499. Joshi Mukesh
500. Karnal A.K
501. Kumar Vinit
502. Kunwar Singh Bartwal
503. Majumder Shovan K
504. Mishra Satya Ram
505. Misra Pankaj
506. Modi Mohammed Hussein
507. Moorti Anand
508. Mukherjee Chandrachur
509. Mukhopadhyay P. K.
510. Naik Prasad Anant
511. Nayak Maheswar
512. Om Prakash
513. Pal Suparna
514. Roy Sindhunil Barman
515. S. Satapathy
516. Sagdeo Archana
517. Senecha Vinod Kumar
518. Shailendra Kumar
519. Sharma Avnish K.
520. Sharma Tarun Kumar
521. Singh Chandra Pal
522. Singh Manoranjan P.
523. Sinha A.K.
524. Srivastava Arvind Kumar
525. Tiwari Manoj Kumar
526. Tiwari Vibhuti Bhushan
527. Tiwari Vidya Sagar

528. Verma Sunil

VECC

❖ **Chemical Science**

529. Sen Pintu

❖ **Engineering Sciences**

530. Mukherjee Paramita
531. Nabhiraj P. Y.
532. Pal Sandip
533. Pal Sarbajit
534. Roy Tapatee Kundu

❖ **Physical Sciences**

535. Bandyopadhyay Arup
536. Banerjee Gayathri N
537. Banerjee Kaushik
538. Basu Devasish Narayan
539. Bhattacharaya Chandana
540. Bhattacharjee Tumpa
541. Bhattacharyya Sarmishtha
542. Bhowmick Debasis
543. Chakrabarti Alok
544. Chattopadhyay Subhasis
545. Chaudhuri Gargi
546. Das Nisith Kumar
547. Das Parnika
548. Dubey Anand Kumar
549. Ghosh Premomoy
550. Ghosh Tilak Kumar
551. Jane Alam
552. Karmakar Prasanta
553. Md. Haroon Rashid
554. Mukherjee Gopal
555. Mukhopadhyay Supriya
556. Naik Vaishali
557. Nayak Tapan Kumar
558. Ray Ayan
559. Sadhukhan Jhilam
560. Sailajananda Bhattacharya
561. Sanyal Dirtha
562. Sarkar Sourav
563. Srivastava Dinesh Kumar
564. Zubayer Ahammed

SINP

❖ **Chemical Science**

565. Basu Samita
566. Hazra Montu K.
567. Lahiri Susanta
568. Mishra Padmaja Prasad
569. Senapati Dulal

❖ **Life Sciences**

570. Bagh Sangram
571. Banerjee Subrata
572. Bhattacharyya Dhananjay
573. Biswas Sampa
574. Chakrabarti Abhijit
575. Chakrabarti Oishee
576. Das Chandrima
577. Garai Gautam
578. Manna Soumen Kanti
579. Mukhopadhyay Debashis
580. Raghuraman H
581. Saha Partha
582. Sarkar Munna
583. Sen Udayaditya
584. Sengupta Kaushik

❖ **Physical Sciences**

585. Agrawal Bijay Kr.
586. Bandyopadhyay Bilwadal
587. Bandyopadhyay Debades

588. Banerjee Rahul
589. Banerjee Sangam
590. Basu Abhik
591. Basu Chinmay
592. Bhattacharya Satyaki
593. Bhattacharyya Gautam
594. Bhattacharyya S. R.
595. Bhunia Satyaban
596. Chakraborti Nikhil
597. Chakraborty Supratic
598. Chattopadhyay Sukalyan
599. Chini Tapas Kr.
600. Das Debasish
601. Das Indranil
602. Das Mala
603. Datta Ushasi
604. De Asit K.
605. De Sankar
606. Dey Chandi Charan
607. Dutta Koushik
608. Dutta Suchandra
609. Garg Arti
610. Ghosal Ambar
611. Ghosh Amit
612. Goswami Asimananda
613. Gupta Kumar Sankar
614. Hazra Satyajit
615. Karmakar Biswajit
616. Kundu Arnab
617. Majumdar Debasish
618. Majumdar Nayana
619. Majumdar Pratik
620. Mallick Bireswar Basu
621. Mandal Prabhat Kr.
622. Mathews Prakash
623. Mazumdar Chandan
624. Menon Krishnakumar S.R.
625. Mohanty Ajit K
626. Mohanty Pradeep Kr.
627. Mukherjee Anjali
628. Mukherjee Manabendra
629. Mukhopadhyay Mrinmay Kumar
630. Mukhopadhyay Supratik
631. Mustafa Munshi Golam
632. Mylavarapu Sita Janaki
633. Nandy Maitreyee
634. P. M. G. Nambissan
635. Pal Barnana
636. Pradhan Kalpataru
637. Roy Pradip Kr.
638. Roy Shibaji
639. Roy Subinit
640. Saha Satyajit
641. Sarkar Maitreyee Saha
642. Sarkar Sandip
643. Sarkar Subir
644. Satpati Biswarup
645. Sharan Manoj K.
646. Singh Harvendra
647. Sinha Tinku
648. Yarlagadda Sudhakar

IPR

❖ **Chemical Sciences**

649. Sudhir Kumar Nema

❖ **Engineering Sciences**

650. Chaturvedi Shashank
651. Paritosh Chaudhuri
652. Pathak Surya Kumar
653. Tanna Vipulkumar L

654. Gupta Suryakant B
655. Kumar Rajesh

❖ **Physical Sciences**

656. Anitha V P
657. Bandopadhyay Mainak
658. Bipul K Saikia
659. Bisai Nirmal Kumar
660. Bora Dhiraj
661. Chandra Debasis
662. Chattopadhyay Asim Kumar
663. Chattopadhyay Prabal Kumar
664. D Chenna Reddy
665. Das Amita
666. Deshpande Shishir P
667. G. Ravi
668. Ganesh Rajaraman
669. Ghosh Joydeep
670. Gourab Bansal
671. Hiteshkumar B. Pandya
672. Jana Mukti Ranjan
673. Joshi Hem Chandra
674. Khirwadkar Samir S.
675. Kulkarni Sanjay V.
676. Kumar Ajai
677. Lalit Mohan Awasthi
678. Mrityunjay Kundu
679. Mukherjee Subroto
680. P V Subhash
681. Pintu Bandyopadhyay
682. Pradhan Subrata
683. Pramod Kumar Sharma
684. Raju Daniel
685. Ramasubramanian N
686. Ranjan Mukesh
687. Sen Abhijit
688. Sengupta Sudip
689. Shantanu Kumar Karkari
690. Sharma Devendra
691. Smruti R. Mohanty
692. Srinivasan R
693. Vinay Kumar

IOP

❖ **Physical Sciences**

694. Agrawal Pankaj
695. Bhattacharjee Somendra Mohan
696. Das Debottam
697. Debakanta Samal
698. Debasish Chaudhuri
699. Ghosh Kirtiman
700. Jayannavvar A. M.
701. Mandal Saptarshi
702. Mitra Manimala
703. Mukherji Sudipta
704. Nayak Aruna Kumar
705. Ota S B
706. Panda Sudhakar
707. Patra Suresh Kumar
708. Saha Arijit
709. Sahoo Satyaprakash
710. Sahu Pradip Kumar
711. Sanjib Kumar Agarwalla
712. Satyam Parlapalli Venkata
713. Sekhar Biju Raja
714. Shamik Banerjee
715. Som Tapobrata
716. Srivastava Ajit Mohan
717. Topwal Dinesh
718. Tripathy Goutam
719. Varma Shikha

720. Virmani Amitabh

HRI

❖ **Mathematical SciencesI**

721. Batra Punita
722. Chakraborty Kalyan
723. Dalawat Chandan Singh
724. Kumar Manoj
725. Prakash Gyan
726. Raghavendra Nyshadham
727. Ramakrishnan B.
728. Ramana D. Surya
729. Ratnakumar P.K.
730. Shah Hemangi Madhusudan
731. Thangadurai Ravindranathan

❖ **Physical Scienc**

732. Basu Anirban
733. Choubey Sandhya
734. Das Tapas Kumar
735. Datta Asesh krishna
736. De Aditi Sen
737. Gandhi Raj
738. Gopakumar Rajesh
739. Jatkar Dileep Prabhakar
740. Maharana Anshuman
741. Majumdar Pinaki
742. Mukhopadhyaya Biswarup
743. Naik Satchidanand
744. Pai G. Venketeswara
745. Pareek T. P.
746. Pati Arun Kumar
747. Rai Santosh Kumar
748. Rao Sumathi
749. Sen Ashoke
750. Sen Prasenjit
751. Sen Ujjwal

TMC

❖ **Health Sciences**

752. Agarwal Jai Prakash Hanuman Prasad
753. Agarwal Vandana
754. Agrawal Archi Ramesh
755. Alahari Aruna
756. Ambulkar Reshma
757. Amin Nayana Shekar
758. Ashok Kumar M.S.
759. Badwe Rajendra Achyut
760. Bagal Bhausaheb Pandurang
761. Bajpai Jyoti
762. Bakshi Ganesh Kailas
763. Bakshi Sumitra Ganesh
764. Bal Munita Meenu
765. Balasubramaniam Ganesh
766. Banavali Shripad Dinanath
767. Bhat Vivek Gajanan
768. Bhosale Shilpushp Jagannath
769. Biswas Sanjay
770. Budrukkar Ashwini Narsingrao
771. Chakraborty Santam
772. Chatterjee Aparna Sanjay
773. Chaturvedi Pankaj
774. Chaukar Devendra Arvind
775. Chinnaswamy Girish
776. D Cruz Anil Keith
777. Daddi Anuprita Dilip
778. Deodhar Jayita Kedar
779. Deodhar Kedar Kamalakar
780. Desai Madhavi Dattatraya
781. Desai Priti Dhansukhbhai
782. Desai Sangeeta Bhikaji

783. Deshmukh Anuja Dhananjay
784. Deshpande Deepak Dattatray
785. Desouza Ashwin Luis
786. Dholam Kanchan Parashuram
787. Digumarti Raghunadharao
788. Dikshit Rajesh Prabhakar
789. Divatia Jigeeshu Vasishtha
790. Doctor Jeson Rajan
791. Engineer Reena Zarir
792. Epari Sridhar
793. Ganesan Subramanian Papagudi
794. Ghosh Jaya
795. Ghosh Laskar Sarbani
796. Goda Jayant Sastri
797. Goel Mahesh
798. Gujral Sumeet
799. Gulia Ashish
800. Gulia Seema
801. Gupta Sudeep
802. Gupta Tejpal
803. Gurav Sandeep Vivek
804. Jain Hasmukh Kantilal
805. Jain Parmanand
806. Jaiswal Dushyant
807. Jalali Rakesh
808. Janu Amit Kumar
809. Jiwnani Sabita Shambhulal
810. Joshi Amit Prakashchandra
811. Joshi Malini Premkumar
812. Joshi Shalaka Prakash
813. Kane Shubhada Vijay
814. Karimundackal George
815. Kelkar Rohini Subhash
816. Kembhavi Seema Ashish
817. Kerkar Rajendra Achyut
818. Khanna Nehal Rishi
819. Khattry Navin
820. Kinhikar Rajesh Ashok
821. Kothekar Amol Trymbakrao
822. Krishnatry Rahul Naresh Chand
823. Kulkarni Atul Prabhakar
824. Kulkarni Suyash Sureshchandra
825. Kumar Rajiv
826. Laskar Siddhartha Sankar
827. Mahajan Abhishek
828. Mahantshetty Umesh Murgendra
829. Maheshwari Amita
830. Mehta Shaesta Abdulaziz
831. Menon Santosh
832. Mishra Gauravi Ashish
833. Mittal Neha
834. Moiyadi Aliasgar V.
835. Murthy Vedang
836. Myatra Sheila Nainan
837. Nair Deepa Ravindranathan
838. Nair Nita Sukumar
839. Narula Gaurav
840. Noronha Vanita Maria
841. Ojha Shashank
842. Ostwal Vikas Sureshchand
843. Pai Prathamesh Srinivas
844. Pantvaidya Gouri Himalaya
845. Parab Swapnil Yeshwant
846. Parmar Vani
847. Patil Asawari Jingonda
848. Patil Prachi Sunil
849. Patil Vijay Maruti
850. Patil Vijaya Prakash
851. Patkar Nikhil Vijay
852. Pimple Sharmila Anil

853. Popat Palak Bhavesh
854. Prabhash Kumar
855. Prakash Gagan
856. Prasad Maya
857. Purandare Nilendu Chandrakant
858. Puri Ajay
859. Qureshi Sajid Shafique
860. Rajadhyaksha Sunil Bhagwant
861. Ramadwar Mukta Ravindra
862. Ranganathan Priya
863. Rangarajan Venkatesh
864. Rekhi Bharat
865. Rugmini Sudhir Vasudevan Nair
866. Sable Nilesh Pandurang
867. Saklani Avanish Parmesh
868. Salins Naveen Sulakshan
869. Sarin Rajiv
870. Sastri Supriya Jayant
871. Sawant Sheela Prashant
872. Sengar Manju
873. Shah Sneha Ashok
874. Shankhdhar Vinay Kant
875. Shanmugham Pramesh Conjeevaram
876. Sharma Kailash Sampatlal
877. Sharma Sudivya Prashast
878. Shet Tanuja Manjanath
879. Shetmahajan Madhavi Gopalkrishna
880. Shetty Nitin Sudhakar
881. Shetty Prakash Mahabal
882. Shrikhande Shailesh Vinayak
883. Solanki Sohan Lal
884. Surappa Shylasree Thumkur
885. Tembhare Prashant Ramesh
886. Thakur Meenakshi Haresh
887. Thiagarajan Shiva Kumar
888. Thota Raghu Sudarshan
889. Trivedi Bhakti Dushyant
890. Vora Tushar Shailesh
891. Wadasadawala Tabassum Abdul Wahid
892. Yadav Prabha Subhash

❖ **Life Sciences**

893. Bhattacharyya Dibyendu
894. Bose Kakoli
895. Chilkapati Murali Krishna
896. Chiplunkar Shubhada Vivek
897. Dalal Sorab Nariman
898. De Abhijit
899. Dutt Amit
900. Dutt Shilpee
901. Gota Vikram Suryaprakash
902. Govekar Rukmini Balkrishna
903. Gupta Sanjay
904. Hasan Syed Khizer
905. Kode Jyoti A.
906. Mahimkar Manoj Balkrishna
907. Ray Pritha
908. Shirsat Neelam Vishwanath
909. Teni Tanuja Rajendra
910. Varma Ashok
911. Venkatraman Prasanna
912. Waghmare Sanjeev

IMSc

❖ **Life Sciences**

913. Menon Gautam I.
914. Samal Areejith
915. Siddharthan Rahul
916. Sinha Sitabhra
917. Vemparala Satyavani

❖ **Mathematical Sciences**

918. C.R. Subramanian
919. Chakraborty Partha Sarathi
920. Chatterjee Pralay
921. Gun Sanoli
922. Iyer Jaya N.
923. Kodiyalam Vijay
924. Lodaya Kamal
925. Mahajan Meena Bhaskar
926. Mohari Anilesh
927. Mukhopadhyay Anirban
928. Nagaraj D.S.
929. Prasad Amritanshu
930. R. Ramanujam
931. Raghavan K.N.
932. Roy Indrava
933. S Viswanath
934. Sankaran Parameswaran
935. Saurabh Saket
936. Sharma Vikram
937. Srinivas Kotyada
938. V. Arvind
939. Venkatesh Raman
940. Venugopalan Sushmita

❖ **Physical Sciences**

941. Adhikari Ronojoy
942. Ashok Sujay K.
943. Bagchi Manjari
944. Balachandran Sathiapalan
945. Chandrashekar C.M.
946. Chaudhuri Pinaki
947. D. Indumathi
948. Date Ghanshyam D.
949. Digpal Sanatan
950. Ganesh Ramachandran
951. Ghosh Sibasish
952. Gopalakrishnan Shrihari
953. Laad Mukul S.
954. Mukhopadhyay Partha
955. Nemani Venkata Suryanarayana
956. R. Shankar
957. Ravindran Rajesh
958. Ray Purusattam
959. S. Kalyana Rama
960. Sinha Nita
961. Sinha Rahul
962. Syed Raghib Hassan
963. V. Ravindran

NISER

❖ **Applied Systems Analysis**

964. Das Amarendra
965. Khuntia Rooplekha
966. Pattanaik Debashis
967. Swain Pranaya Kumar
968. Yeldho Joe Varghese

❖ **Chemical Sciences**

969. Barman Sudip
970. Behera Jogendra Nath
971. Bhargava B.L.
972. Biswal Himansu Sekhar
973. Chakrabarty Suman
974. Chandrashekar T.K.
975. Chidambaram Gunanathan
976. Ghosh Arindam
977. Ghosh Subhadip
978. Kar Sanjib
979. Mal Prasenjit
980. Moloy Sarkar

981. Nembenna Sharanappa
982. Purohit Chandra Shekhar
983. Ravikumar P. C.
984. Saravanan Peruncheralathan
985. Sharma Nagendra Kumar
986. Srinivasan Alagar
987. Upakarasamy Lourderaj
988. Venkatasubbaiah Krishnan

❖ **Life Sciences**

989. Acharya Rudresh
990. Aich Palok
991. Alone Debasmita Pankaj
992. Alone Pankaj Vidyadhar
993. Bhattacharyya Asima
994. Chattopadhyay Subhasis
995. Chowdary Tirumala Kumar
996. Dixit Manjusha
997. Goswami Chandan
998. Konkimalla Venkat Sai Badireenath
999. Mathew Renjith
1000. Mohapatra Harapriya
1001. Panigrahi Kishore Chandra Sekhar
1002. Singru Praful S.
1003. Srinivasan Ramanujam

❖ **Mathematical Sciences**

1004. Anisur Rahaman Molla
1005. Dalai Deepak Kumar
1006. De Shyamal Krishna
1007. Jana Nabin Kumar
1008. K. Senthil Kumar
1009. Karn Anil Kumar
1010. Keshari Dinesh Kumar
1011. Meher Jaban
1012. Mukherjee Ritwik
1013. Muruganandam Varadharajan
1014. Panchugopal Bikram
1015. Parui Sanjay
1016. Patra Kamal Lochan
1017. Roy Sutanu
1018. Sahoo Binod Kumar
1019. Sahoo Manas Ranjan
1020. Sahu Brundaban
1021. Tripathi Amit

❖ **Physical Sciences**

1022. A.V. Anil Kumar
1023. Ajaya Kumar Nayak
1024. Basak Subhasish
1025. Bedanta Subhankar
1026. Benjamin Colin
1027. Bhattacharjee Joydeep
1028. Das Ritwick
1029. Gowdigere Chethan N
1030. Khandai Nishikanta
1031. Mal Prolay Kumar
1032. Mohanty Bedangadas
1033. Mohapatra Ashok Kumar
1034. Mukherjee Anamitra
1035. Rahaman Abdur
1036. Rengaswamy Ramesh
1037. Roy Victor
1038. Sahoo Pratap Kumar
1039. Samal Prasanjit
1040. Senapati Kartikeswar
1041. Srivastava Yogesh Kumar
1042. Sumedha
1043. Swain Sanjay Kumar
1044. V. Ravi Chandra

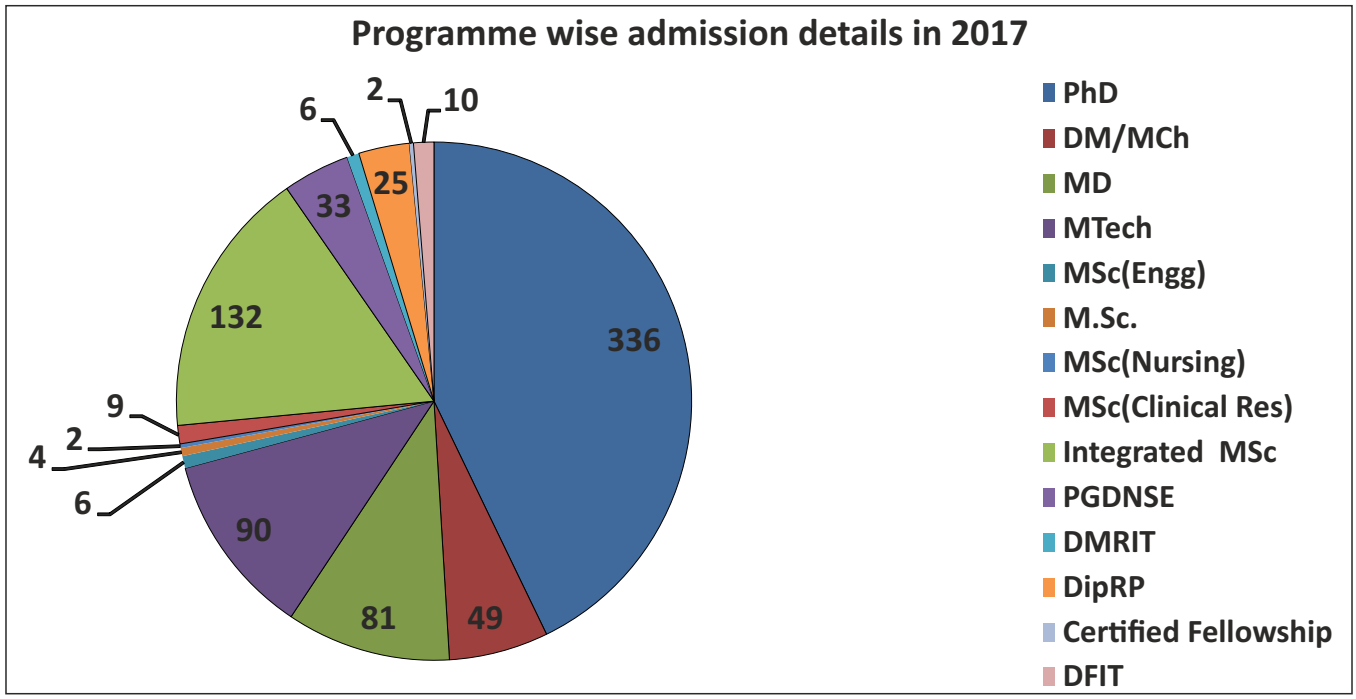

Total=785

Constituent Institution (CI) wise and programme-wise number of students admitted in 2017

	BARC	IGCAR	RRCAT	VECC	SINP	IPR	TMC	IoP	IMSc	HRI	NISER	Total
Ph.D./Int. Ph.D.	75	44	17	7	31	16	17	9	22	9	89	336
MTech/ PG Diploma	94	29										123
MSc(Engg)	2	4										6
MD	2						79					81
DM/MCh							49					49
MSc/ Int. MSc										4	132	136
MSc Nursing							2					2
MSc Clinical Research							9					9
Certified fellowship							2					2
Dip. RP	25											25
DFIT							10					10
DMRIT	6											6
Total	204	77	17	7	31	16	168	9	22	13	221	**785**

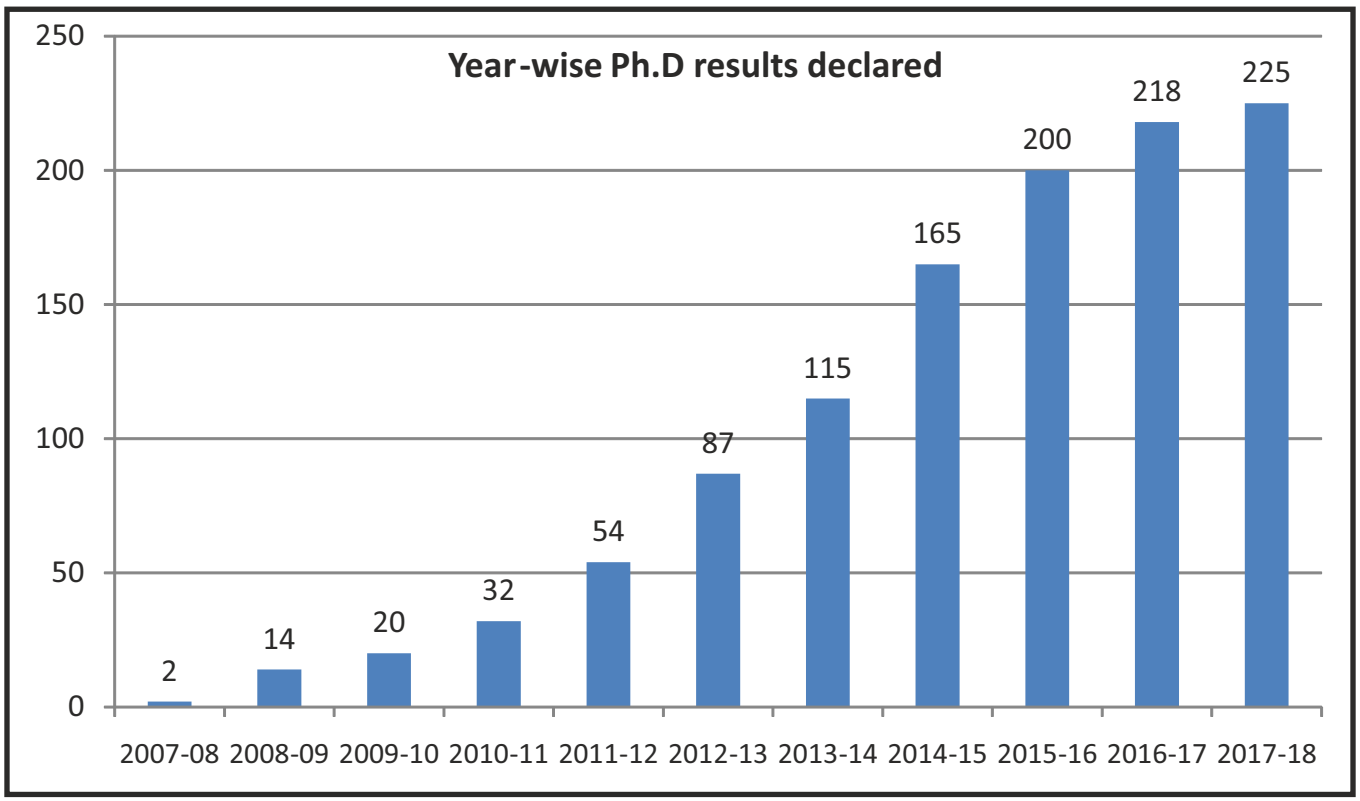
Year-wise Ph.D results declared
250
200
150
100
50
0
2
14
20
32
54
87
115
165
200
218
225
2007-08
2008-09
2009-10
2010-11
2011-12
2012-13
2013-14
2014-15
2015-16
2016-17
2017-18

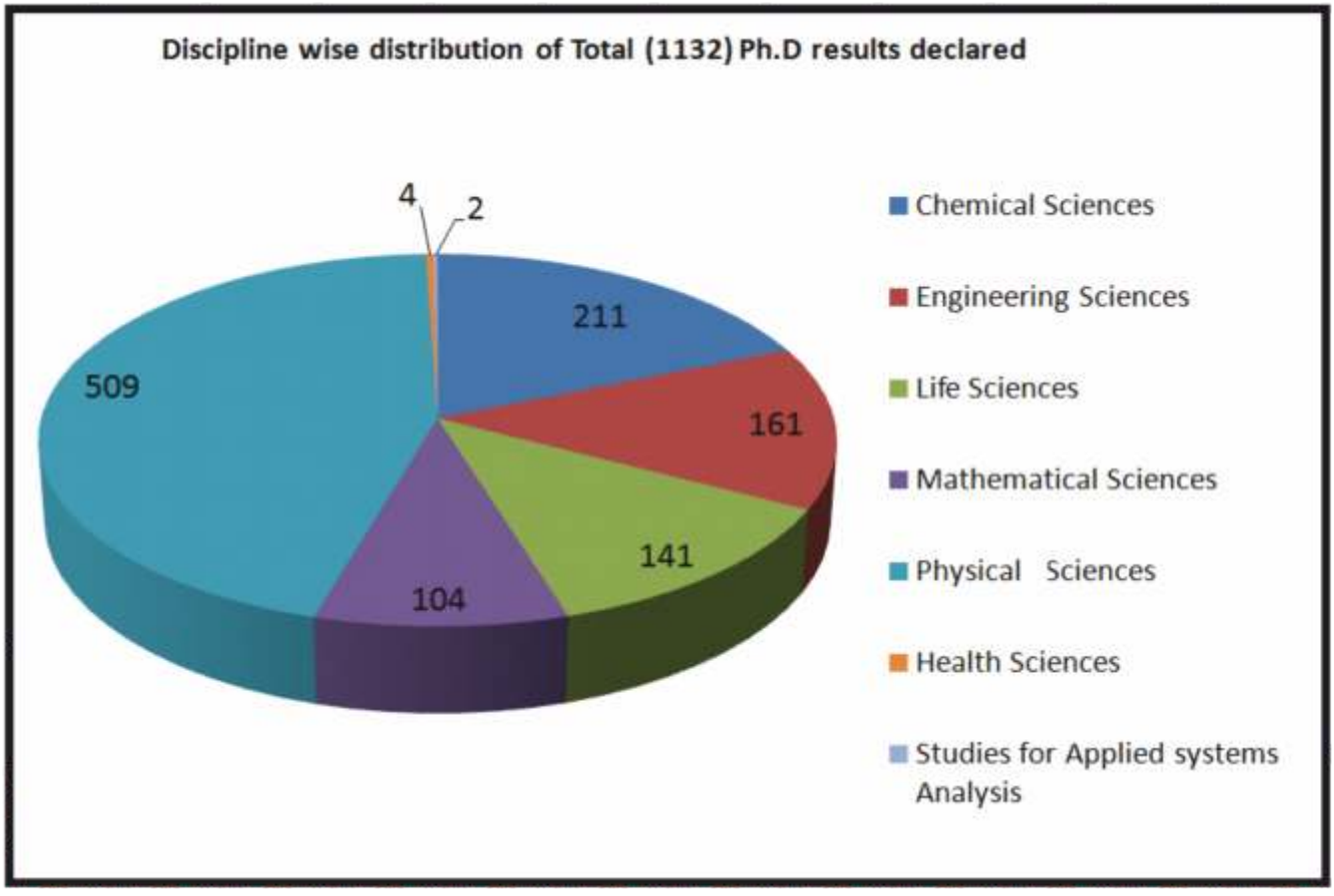
Discipline wise distribution of Total (1132) Ph.D results declared
4
2
211
161
141
104
509
Chemical Sciences
Engineering Sciences
Life Sciences
Mathematical Sciences
Physical Sciences
Health Sciences
Studies for Applied systems Analysis

CIs/OCC wise declared PhD results

Year	BARC	IGCAR	RRCAT	VECC	SINP	NISER	IPR	IOP#	HRI	TMC	IMSc	TOTAL
2007-08								2				2
2008-09					1			4	2		7	14
2009-10					1			2	7		10	20
2010-11	5				2			6	9		10	32
2011-12	15	2	2		1		5	3	9		17	54
2012-13	45	7	4	8	2		3	4	5	4	5	87
2013-14	34	23	2	7	6		8	9	4	6	16	115
2014-15	62	33	15	6	8		1	8	5	14	13	165
2015-16	86	29	13	7	13		5	10	11	18	8	200
2016-17	71	33	5	10	11	16	7	5	14	23	23	218
2017-18	71	27	10	11	18	16	13	8	16	15	20	225
TOTAL	389	154	51	49	63	32	42	61	82	80	129	1132

#Includes NISER Results till 2015-16

CIs/OCC & Discipline wise PhD results declared during 2017-18

	BARC	IGCAR	RRCAT	VECC	SINP	NISER	IPR	IOP	HRI	TMC	IMSc	Total
Chem	25	10				10		1				46
Engg	24	11	1	2								38
Health										2		2
Life	4					5				13		22
Math									4		9	13
Physical	18	6	9	9	18	1	13	7	12		11	104
Total	71	27	10	11	18	16	13	8	16	15	20	225

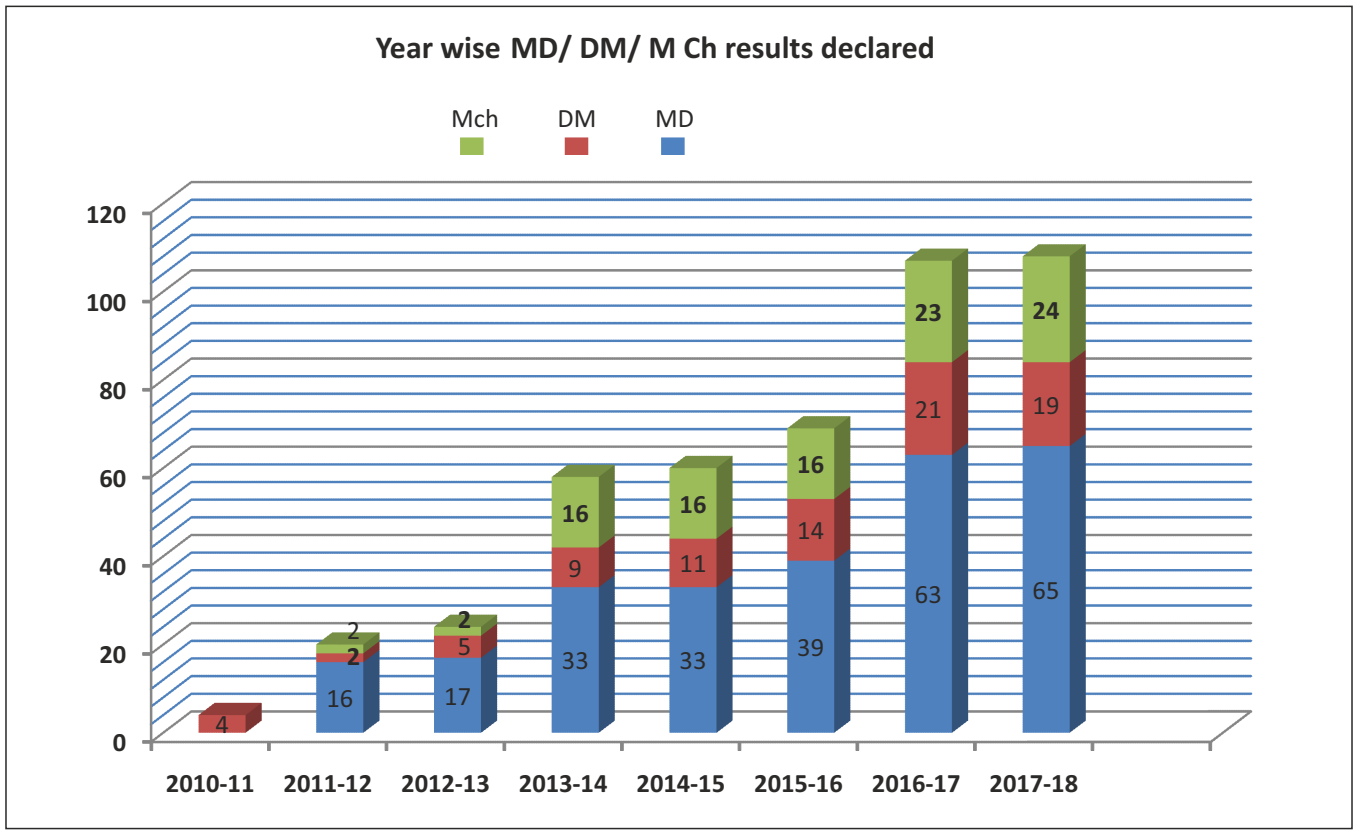
Year wise MD/ DM/ M Ch results declared
Mch
DM
MD
120
100
80
60
40
20
0
4
2
2
16
2
5
17
16
9
33
16
11
33
16
14
39
23
21
63
24
19
65
2010-11
2011-12
2012-13
2013-14
2014-15
2015-16
2016-17
2017-18

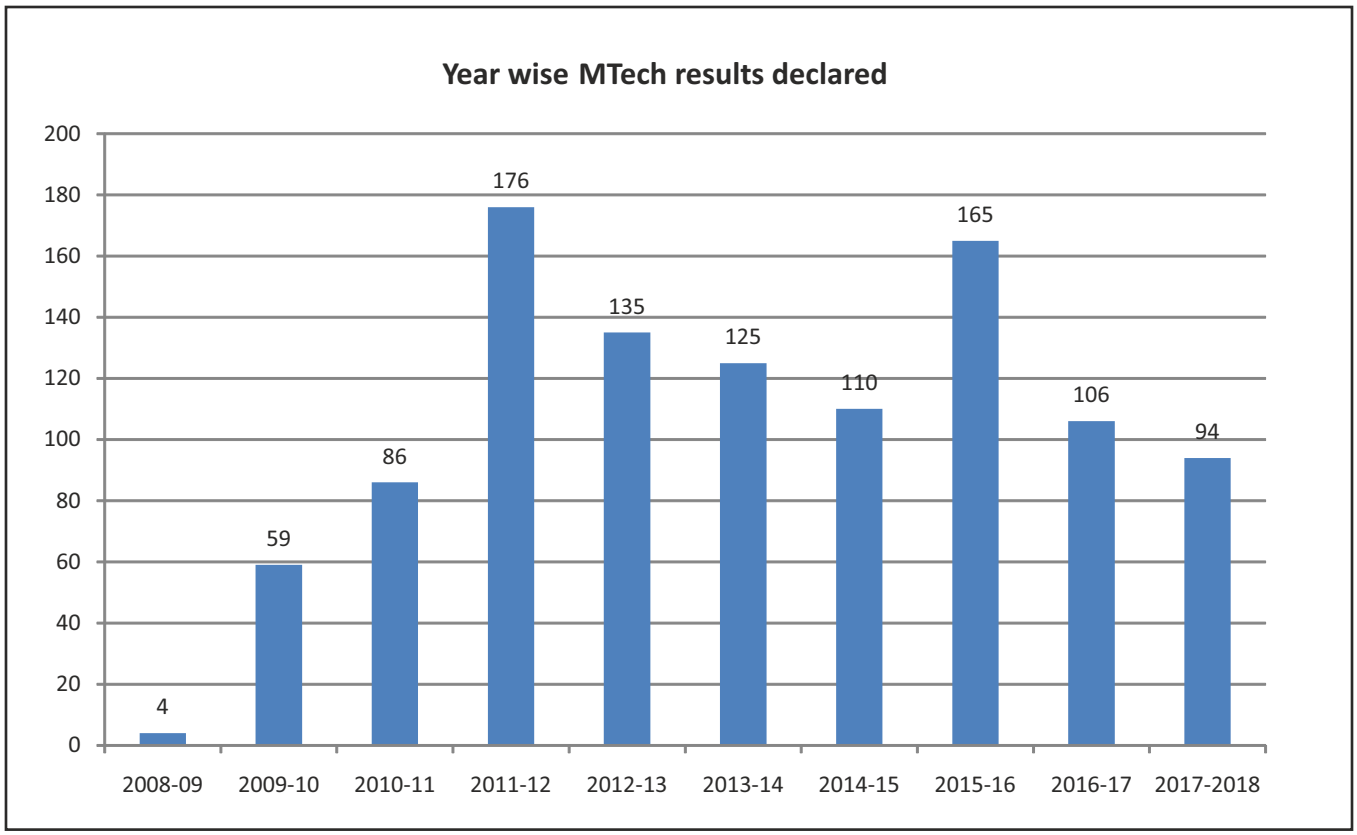
Year wise MTech results declared
200
180
160
140
120
100
80
60
40
20
0
4
59
86
176
135
125
110
165
106
94
2008-09
2009-10
2010-11
2011-12
2012-13
2013-14
2014-15
2015-16
2016-17
2017-2018

Section-II

Scientific and Technical Achievements During Present Period Through Completed Ph.D. Work

1. Chemical Sciences

During the period, HBNI has awarded Ph.D. degree to 46 students in Chemical Sciences on successful completion of academic programmes. Research topics are from a variety of areas including environment chemistry, actinide separation & speciation, nano & polymeric material and molecular modelling towards selective metal ion extraction. Highlights of a few doctoral theses are outlined below.

1.1. Bhabha Atomic Research Centre

Finding efficient sorbents for remediation of contaminated water is a tricky affair which needs both chemical intuition and experimental validation. One doctoral thesis reports that the biomaterial chitosan is cross-linked with sodium tripolyphosphate and the modified sorbent (CTPP) is found to have better sorption properties for the sorption of heavy metal ions U(VI) and Cr(III) than unmodified chitosan. Stability in aqueous solution and the sorption capacity are higher for the new sorbent and chemical characterisation showed that the newly added phosphate groups are the principal binding sites for the metal ions. Further, immobilisation of humic acid (HA) is achieved on CTPP to get a novel stable solid HA based sorbent (HA-CTPP), which is found to be effective for the removal of metal ions such as U(VI) and Pb(II) from aqueous solutions. HA immobilisation by this route is observed not to affect the sorption capacity of HA for Pb(II) but is found to be deteriorated in case of U(VI). In another attempt, complex behaviour of bio-nano systems in environmental remediation is demonstrated by a comparative study of sorption of U(VI) on to synthesised bare and humic acid coated magnetite (HA-magnetite) nanoparticles. Red-ox processes are involved in the sorption of U(VI) onto bare magnetite but not in case of HA-magnetite. The latter is also having higher sorption capacity and better kinetics for the sorption of U(VI) and is found to be more stable in solution systems against undesirable characteristics such as aggregation.

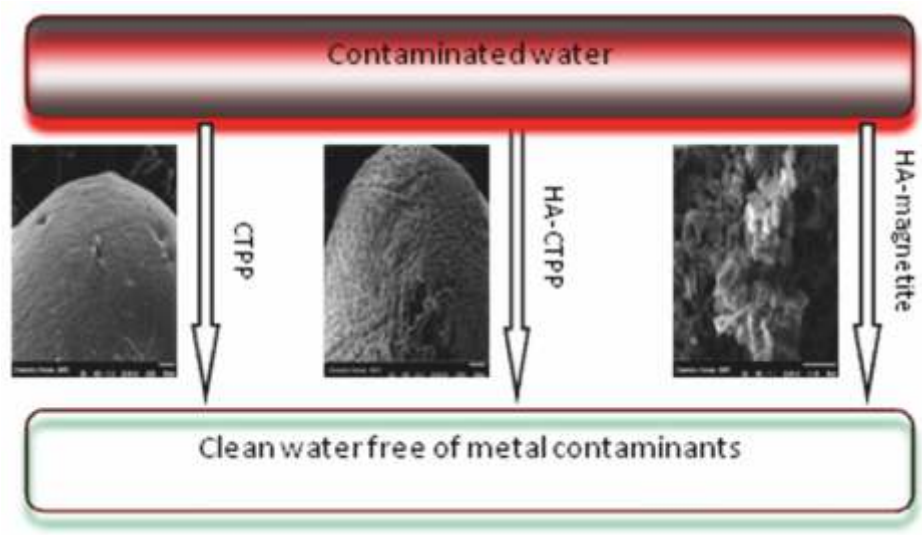

Figure 1.1.1. Modified biomaterials such as CTPP and HA-CTPP and bio-nano composites such as HA-magnetite are superior adsorbents for remediation of water contaminated with heavy metals and radionuclides.

Further, the subtle differences of the humic acid fractions for field application for arresting migration of metal ion contaminant is bought out by carefully designed experiments using HA fractions, BHA and GHA with U(VI). BHA is seen to bind and hold the contaminant for more time than GHA and the differences are attributed to their characteristic functional group distributions and supramolecular behaviour.

Trace metals are having great importance in the marine ecosystem. So determination of trace metals in different compartments (seawater, sediment and biota) of marine ecosystem is necessary. Thane Creek receives large concentrations of trace metals due to effluents

discharged from different industries and urban effluents. Very limited information is available on trace metals pollution in the estuaries of India.

A student has reported results based on studies at Thane Creek, Mumbai, India in another doctoral thesis. Estimation of trace metals in seawater is a difficult task because of the very low concentrations of trace metals and high salt content. Instruments capable of trace metal analysis in ppb range needs matrix separation prior to analysis. Accordingly, the separation and pre-concentration of trace metals is usually involved in the analytical procedures used for the determination of trace metals in seawater. Solvent extraction procedure is optimized for accurate determination of trace metals in seawater samples. Sediments are considered as sink of trace metals in marine environment. So trace metal concentrations are determined in the collected sediment samples. Different geochemical indices are calculated to understand the pollution load in the Thane Creek area due to trace metals burden. Trace metal concentrations in sediment samples also depend on different physico-chemical parameters.

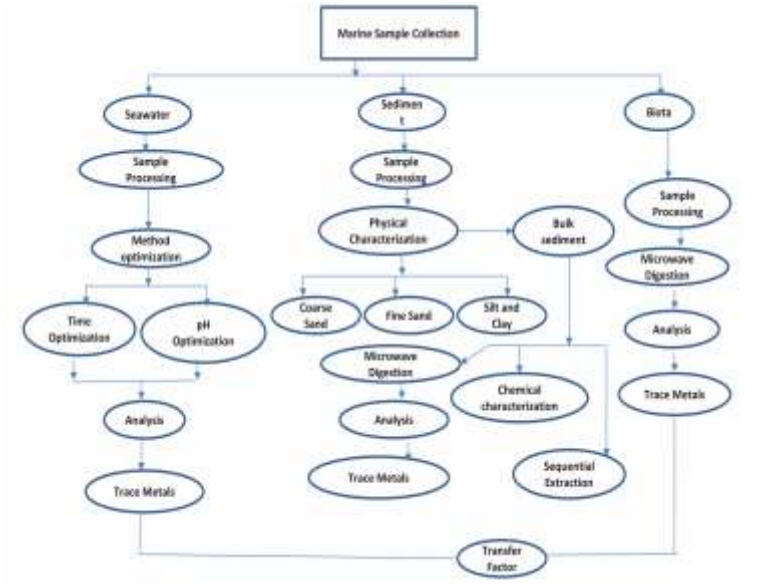

Figure 1.1.2. Study Framework

Different physico-chemical parameters are studied in sediment samples. Correlation studies are carried out to understand the major contributing parameter for trace metal concentrations in sediment samples. Total trace metal concentrations do not give exact idea of toxicity in sediment samples. Therefore binding behaviour of trace metals in sediment samples are studied using sequential extraction procedure. Trace metals though occur at extremely low concentrations in seawater, are accumulated by marine organisms and concentrations in their body Figure 1.1.2. Study Frameworktissue can be hundreds of times greater than seawater. As human being consume different marine organisms like biota, can lead potential health problem. Trace metal concentrations are determined in whole body biota and as well as edible part of biota. Transfer factors for trace metals are determined from seawater to biota. Health hazard in human beings due to trace metals through consumption of biota across Thane Creek area, Mumbai, India are also investigated. In summary, the hazard quotient (HQ) values shows that steady consumption of biota found in this study is not hazardous. The sum of all HQ values representing the hazard index (HI) also found to be less than unity. So the consumption of fish or biota as a whole as such is not hazardous from the given location for the reported trace metals.

Human beings get exposed to natural radiation externally from cosmic rays and terrestrial radiation and also receive internal exposure primarily due to inhalation and ingestion of radionuclides of terrestrial origin. People residing in high background radiation area (HBRA) of thorium rich monazite deposit along the coastal belt of Kanyakumari district, Tamilnadu are likely to get exposed to ^{232}Th ingestion intake compared to inhabitants of normal background radiation areas. Hence, it is important to evaluate the annual ingestion committed effective dose due to intake of ^{232}Th by consumption of diet/food and drinking water. A student has carried out this work due to non-existent of literature data on dietary ingestion intake

of thorium by the Inhabitants of the above study area. In the thesis, low level ^{232}Th concentrations in food items (from local market) and duplicate diet (DD, from four villages) and drinking water (from three villages) are quantified using instrumental neutron activation analysis (INAA) and inductively coupled plasma mass spectrometry (ICP MS), respectively. The concentration (µg kg-1fresh) range in the food items from market basket study (MBS) is 0.3 (tomato)-136 (anchovy curated fish), which corresponds to average annual effective ingestion dose of 3.4 µSv y-1. The ^{232}Th concentration in DD varied between 4.1 and 31.3 µg kg-1 fresh. The average annual effective ingestion dose to the adult using DPS is 7.7 µSv y-1 which is higher than that is evaluated using MBS (3.4 µSvy-1), indicating DPS is a preferred method for realistic biokinetic studies. ^{232}Th in water samples measured using ICP-MS ranged from 2.4 to 18.3 ngL-1 and the equivalent calculated annual dose is 13.6 nSv y-1, which very less compared diet samples. Both INAA and ICP-MS methods were advantageously utilized for low concentration level of Th in a large number of samples. The results presented in the thesis are important as it gives new data on dietary ingestion intake of ^{232}Th, which in turn gives idea about ingestion dose to the inhabitants in the study area. Figure 1.1.3. Annual effective dose from ^{232}Th from ingestion intake to inhabitants of High background radiation area, Tamilnadu, India.The evaluated ^{232}Th intake will serve as important input parameter for biokinetic or epidemiological studies to be carried in this region.

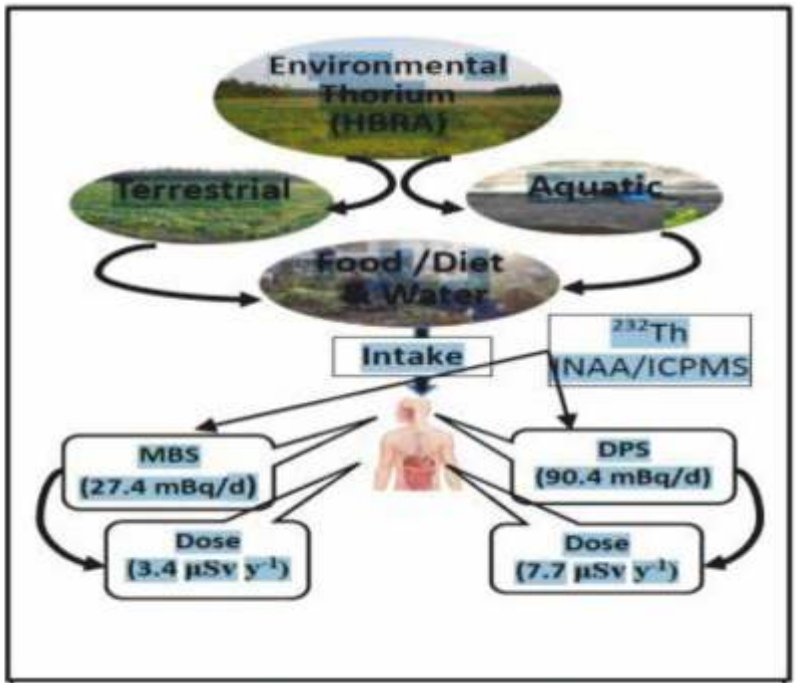

Figure 1.1.3. Annual effective dose from 232Th from ingestion intake to inhabitants of High background radiation area, Tamilnadu, India.

Safe management of high level radioactive liquid waste (HLW) produced during the reprocessing of irradiated nuclear fuel is a demanding task. Vitrification of HLW in borosilicate glass is considered to be one of the most suitable immobilization methods available today. Ni-Cr-Fe based superalloy 690 is used as the process pot, susceptor in multi-zone induction heated metallic melter pot furnace and the electrodes in Joule heated ceramic melter pot used for HLW immobilization process. To increase the service life of vitrification furnace materials, efforts are being made to develop suitable coatings on superalloy substrates. However, detailed interaction of aluminide coatings with simulated waste solution and borosilicate melt has not been studied so far. Interaction of pack aluminized (high Al-containing pack; 10 wt.% Al) and thermally oxidized Alloy 690 substrates with simulated nuclear waste solution at 373 K for 216 hours and with sodium borosilicate melt at 1248 K for 192 hours were carried out. In one thesis, exposed samples were characterized using Raman spectroscopy, X-ray photoelectron spectroscopy (XPS) and Electron probe micro-analysis (EPMA). Analyses of sodium borosilicate glass that interacted with coated specimen having high aluminium content, using Fourier-Tranform infrared spectroscopy (FT-IR) and XPS indicated a modified glass structure due to incorporation of Al^{+3} in the glass network.

In order to decrease the Al activity and avoid the inclusion of Al^{+3} in glass network, aluminium content in the pack aluminization mixture are reduced to 2 wt. %. Aluminized (low aluminium containing pack (2 wt.%)) and thermally oxidized Alloy 690 specimen were subjected to interaction with simulated nuclear waste and sodium borosilicate melt at similar experimental conditions. The analysis results clearly depicts that low Al containing pack aluminization composition (2 wt.% Al, 2 wt.% NH_4Cl and 96 wt.% Al_2O_3) is acceptable for synthesis of aluminized coatings on Alloy 690 specimens, that is used in metallic and ceramic melter pots for the vitrification of high level nuclear waste.

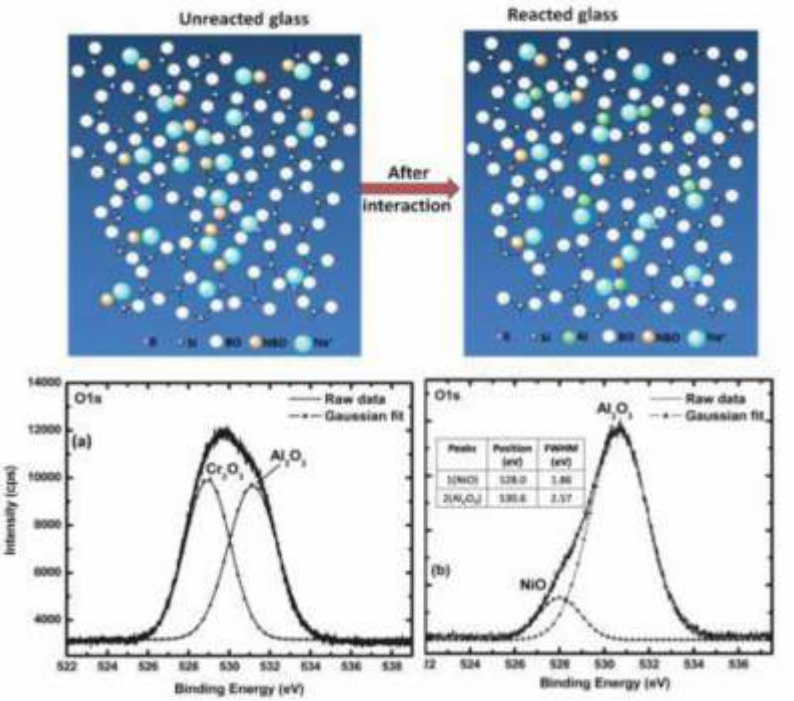

Figure .1.4. Pictorial representation of modified sodium borosilicate glass structure due to incorporation of Al3+ from high Al containing coating. O1s XPS spectra of coated samples exposed to (a) simulated nuclear waste and (b) sodium borosilicate glass are also shown

The study reported in this thesis reveals new polymeric sorbents prepared for the removal of cobalt and antimony during dilute chemical decontaminations of nuclear power plants. Selective removal of these radioactive ions, in presence of large excess of other non-active competitor ions such as iron, will lead to a large reduction in the volume of radioactive waste generated during decontamination, and will make the process more economical and environment friendly. The second most abundant biopolymer chitosan was studied in detail to understand its metal ion removal properties from complex matrices. Plausible mechanisms that operate during the metal sorption under different solution conditions were found out. It was shown that chitosan selectivity for a particular metal ion could be varied according to the pH and nature of the speciation profile in the solution. A Co(II)-ion imprinted chitosan was synthesized and a reversal in biosorbent selectivity through metal ion imprinting technique was achieved. This was the first ever report on such selectivity reversal of a biosorbent through metal ion imprinting. Co(II) imprinted chitosan's ability to remove low level Co(II) in presence of large excess of Fe(II), from

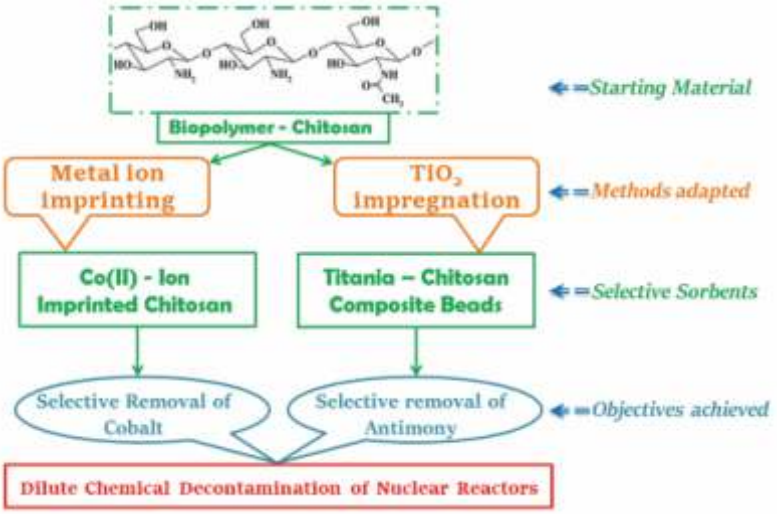

Figure 1.1.5 Materials/methods used during the study with objectives

typical decontamination formulations containing strong complexing agents was demonstrated.

Comparative analysis of six different sorbents, for antimony removal efficacy, reveal the importance of solution pH and antimony speciation in the solution on antimony uptake by the sorbents. Among the six sorbents studied, titania based materials are found to be more suitable for antimony removal, but not in a format suitable for large scale applications. Hence, the possibility of preparing a nano-titania based sorbent in a format suitable for large scale column applications by combining with chitosan was explored. A procedure for the synthesis of nano TiO_2-chitosan composite sorbent in bead format was standardized, and the antimony removal efficacy of the synthesized composite beads has been demonstrated under simulated dilute chemical decontamination conditions. The results showed that it is possible to have good control over the properties of the beads prepared through rational choice of composition of the constituents in the pre-polymerisation mixture during preparation of the beads, and by employing suitable solution conditions during sorption. As a spin-off; successful removal of arsenic, a ground water contaminant of concern, by the nano TiO_2-chitosan beads prepared is also demonstrated.

In nuclear reactors, ^{137}Cs and ^{90}Sr are produced as fission products. ^{137}Cs is highly gamma radioactive with a half life of 30 years. It emits high gamma energy of 662 keV. ^{90}Sr is a fission product having a half-life of 28 years which is generated in the nuclear fuel cycle and has to be separated from nuclear waste. Uranium is a radioactive metallic element and its compounds are more chemically toxic than its radio toxicity. Similarly, tannery industries often generate hexavalent chromium, whereas copper and hexavalent chromium are among the list of metals by-products from metal plating industry. Higher concentration level of heavy metals, more than the safe permissible limit, is lethal and detrimental for living beings. Thus the treatment of heavy metals is of special concern due to their recalcitrance and persistence in the environment.

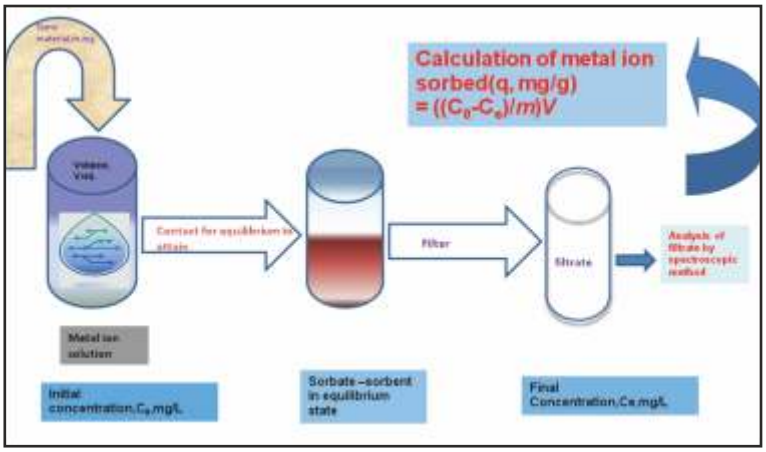

Figure 1.1.6 Schematic diagram of a general sorption reaction.

Nanomaterials are nowadays gaining much attention for their more chemically active nature than macroscopic materials for sorption studies due to their relatively greater surface area to volume ratio and tailor made structural properties. In this context, manganese dioxide, nano molybdate and tungstate of strontium and yttrium, bare magnetite, oleic acid coated magnetite, silica coated magnetite nano materials have been synthesized, characterized by a series of experimental techniques and uptake studies has been carried out. The main focus of this work was to study the potential use of these nano sorbents for removal of radionuclide, viz. uranium(VI), cesium(I) and strontium(II) as well as heavy metal ion particularly hexavalent chromium and divalent copper. The potential of $SrWO_4$, $SrMoO_4$, Y_2WO_6 and $Y_2Mo_3O_{12}$ nanomaterials as sorbents for removal of toxic species was also explored. The effects of various experimental conditions on the sorption efficiency, kinetics, mechanism of the sorption process give satisfactory results for successful design and development of sorption system for practical purpose of radioactive waste management.

The main aspire of this thesis is the investigation of exciton, bi-exciton and charge transfer processes in Quantum Dots (QDs) and metal semiconductor nanohybid materials followed by their photocatalytic and photovoltaic applications. To accomplish the project, metal nanoparticles (MNP), different QDs and metal semiconductor nanohybid material (NHM) are synthesised. The synthesized materials have been characterised by X-Ray Powder diffraction and high resolution transmission electron microscopy techniques.

To boost the power conversion efficiency (PCE) of quantum dot solar cell (QDSC) by long lived charge separated state, CdSe{Au} nanohybrid material (NHM) which acts as a better light harvester than CdSe quantum dot (QD) alone is introduced. Steady state absorption studies show broadening of the absorption band of CdSe{Au} NHM up to 800 nm. The steady state and time resolved luminescence studies reveal ultrafast electron transfer from CdSe QD to Au nanoparticles (NP), forming a charge separated state. The measured PCE of the CdSe{Au} NHM is 4.39% which is significantly higher than pure CdSe QDs (3.37%). The ultrafast TA studies suggest sub-picosecond electron transfer from CdSe QDs to Au NP and slower charge recombination in NHM. Interestingly three times higher recombination resistance at the interface of TiO_2-CdSe{Au} as compared to TiO_2-CdSe is shown by EIS measurements which has also explained the enhancement of PCE by the NHM. To understand the inner mechanism of higher charge separation processes within the hybrid materials CdSe@CdS{Au} nano hetero-structures with different size Au nanoparticles (NP) are synthesized and ultrafast charge transfer dynamics have been monitored with the help of Femto-second transient spectroscopy. Steady state and time-resolved luminescence spectroscopy suggest electron transfer from photo-excited CdSe@CdS core-shell to Au NP within the hetero-structure. Transient absorption studies revealed both hot and thermalized electron transfer take place from core-shell QDs to metal NPs with time constants of 150 fs and 300 fs, respectively. Hot electron transfer from QDs to Au NP found to take place predominantly in the hetero-structures depending on the sizes of the metal nanoparticles. Photo-degradation of rhodamin B (Rh-B) in presence of CdSe@CdS{Au} HS under visible radiation suggests that hot electron in the hetero-structure play a major role in photo-catalytic degradation. This thesis has significant contribution in fundamental charge transfer processes of nanohybrid material and solar energy application as well.

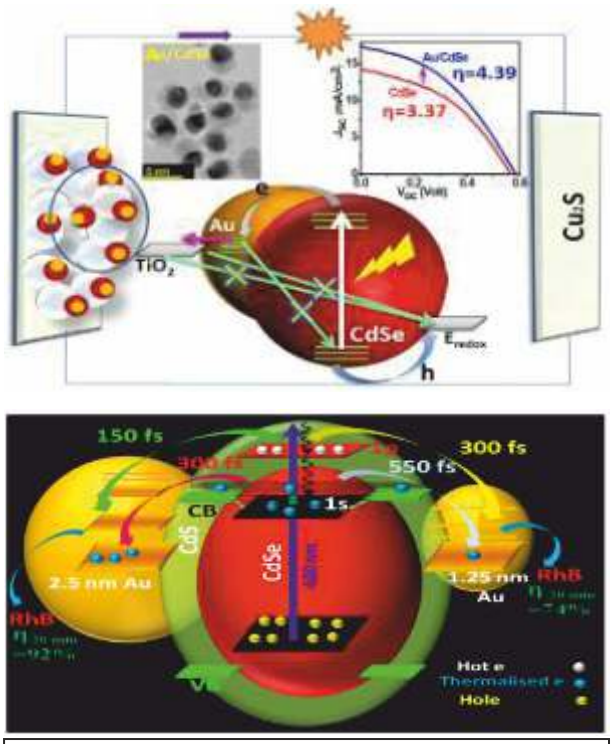

Figure 1.1.7 Upper Panel Schematic diagrame of the role of Au NP in CdSe{Au} NHM solar cell. Lower Panel Hot and Thermalsed electron transfer dynamics in metal-semiconductor NHM.

The present work involves the evaluation of room temperature ionic liquids (RTILs) for the solvent extraction and electrochemical studies of lanthanides and actinides. Even though a large number of methods and materials are available for the separation of actinides from dissolver solution and HLLW, processes based on room temperature ionic liquids (RTILs) are being proposed as possible substitute to the

traditional methods. RTILs are organic salts molten at temperature below 100°C. They have several superior properties suitable for industrial exploitation and nuclear fuel cycle application. They are, extraordinary extraction of metal ions from aqueous solutions when RTILs used in conjunction with traditional extractants, possibility of tailoring ionic liquids for task specific applications, feasibility of separating target metals from aqueous wastes and recover by electro-deposition directly from ionic liquid phase etc. Therefore, it is envisaged that employment of ionic liquids in the area of nuclear fuel cycle applications would lead to the development of environment benign process that generates minimum waste.

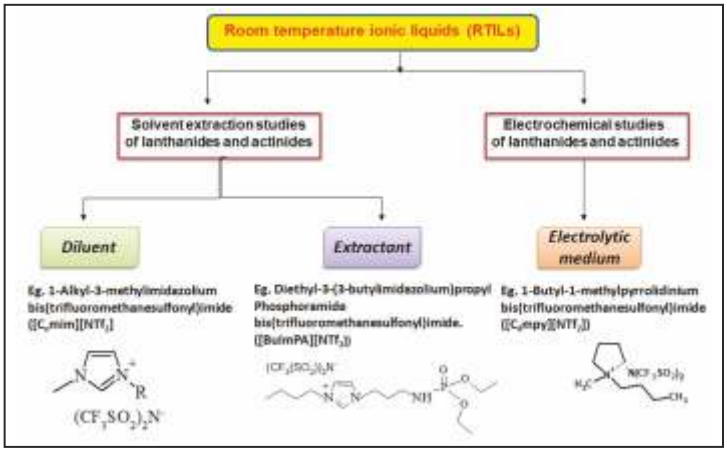

Figure 1.1.8 Different roles of RTILs for solvent extraction and electrochemical studies

In the present work, RTILs are explored for three different roles; i). as diluent, ii). as extractant and iii). as electrolytic medium. In solvent extraction studies, RTIL is explored as diluent as well as extractant. Separation of actinides, U(VI), Pu(IV) and Am(III) from nitric acid medium using a solvent phase composed of molecular extractants dissolved in imidazolium / pyrrolidiniumbis(trifluoromethanesulfonyl)imide ionic liquid diluent and the loading behaviour of Eu(III) in imidazolium ionic liquid diluent at higher Eu(III) loading conditions is investigated. Moreover, a new phosphoramide functionalized ionic liquid and a tetraalkyl ammonium phosphate ionic liquid are explored as extractant for the separation of actinides, U(IV) and Pu(IV), from nitric acid medium.In electrochemical studies, RTIL is explored as electrolytic medium and the electrochemical behavior of U(VI) and Eu(III) in the presence of molecular extractants dissolved imidazolium and pyrrolidiniumbis(trifluoromethanesulfonyl)imide ionic liquids is studied.

Recovery of radio-cesium from PUREX-HLLW is one of the most challenging tasks at the back end processes of nuclear fuel cycle and has been the sole objective of the present thesis work. This has been attempted in present thesis using solvent extraction and membrane based techniques using calix-crown-6 ligands in phenyltrifluoromethylsulphone diluents. Extensive solvent extraction studies involving Cs(I) have shown the order of extractability and separation efficiency CBC > CNC > CMC > CC under identical experimental conditions. Further studies using CBC and CMC have shown that these ligands can be used for selective recovery of Cs from uranium depleted HLLW. Solvent extraction parameters are optimized initially for quantitative extraction and stripping of Cs from pure nitric acid medium.

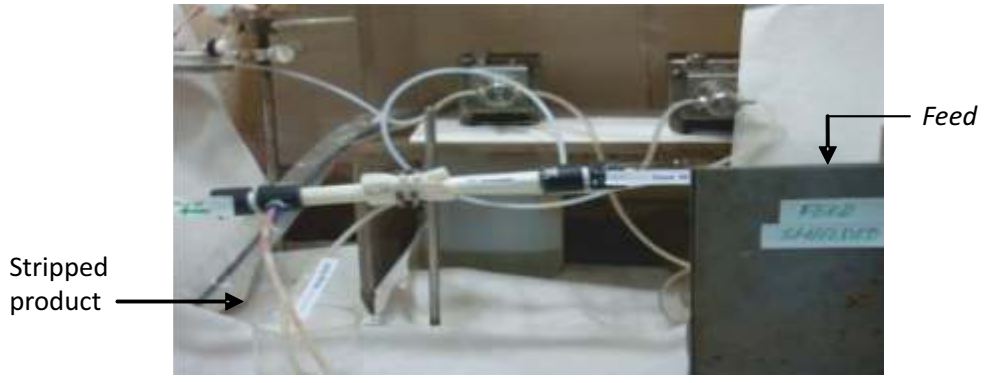

Figure 1.1.9 Separation from HLLW using hollow fiber contactor

Study is extended to simulated HLLW which is finally deployed to recover radio cesium from actual HLLW solutions at laboratory scale. About 10 mCi of radio-cesium is recovered from actual HLLW using the solvent extraction method. Radiation stability of these ligands has also been established. Encouraged by solvent extraction results, further studies are carried out using supported liquid membrane based separation. Efficient transport of Cs from real waste solutions has been demonstrated using CMC (0.01M in 40% iso-decanol + 60% n-dodecane). Both solvent extraction and transport data are used to optimise the transport conditions of Cs in hollow fibre supported liquid membrane configuration. Recovery >90% are shown in ~20h which was reproduced even after long period of 50 days. These results will find application for large scale recovery of Cs from acidic waste solution.

This thesis work mainly demonstrates the possible application of polymer inclusion membrane (PIM) based separation of U(VI), Pu(IV), Th(IV) and Am(III) from dilute nitric acid feed solutions using several diglycolamide (DGA) ligands viz. *N,N,N',N'*-tetra-*n*-octyl diglycolamide (TODGA), *N,N,N',N'*-tetra (2-ethyl hexyl) diglycolamide (T2EHDGA), *N,N,N',N'*-tetra-*n*-pentyl diglycolamide (TPDGA), *N,N,N',N'*-tetra-*n*-hexyl diglycolamide (THDGA) and *N,N N',N'*-tetra-*n*-decyl diglycolamide (TDDGA) and multiple DGA-functionalized ligands viz., tripodal diglycolamide (T-DGA) and DGA functionalized calix[4]arene(C4DGA) as the carrier extractants. The PIMs were prepared following standard methods and their physical characterization was carried out using techniques, e.g., TGA, XRD, SEM, AFM, FTIR and TIMM. The effect of the concentrations of the carriers, the plasticizer and the polymer on the uptake of the actinide ions by the PIMs was investigated in detail to get the optimum composition of the PIMs. The uptake and transport profiles of actinide ions were evaluated at varying feed compositions by the PIMs. The uptake and transport studies suggested that the uranyl ion was least effectively extracted by the DGA based PIMs indicating possible steric constraints in accommodating the ligand molecules along the equatorial plane of the metal ion that hindered the extraction. The transport studies of the actinides ions using the above mentioned PIMs indicated that significant amounts of the actinide ions were held up within the PIM and longer time was required for >90% transport. The T-DGA-containing PIMs were found to be more efficient than the TODGA-based PIMs in the batch uptake studies of actinides. A comparatively slower uptake and transport of actinide ions was observed with the C4DGA containing PIM. Different transport parameters e.g., permeability coefficients, diffusion coefficient for the actinides with the PIMs were determined experimentally and compared with the available data obtained with analogous SLMs. The reusability and stability studies of the DGA-based PIMs indicate the limited lifetime of the PIMs. The mechanism of extraction of trivalent actinide ions (Eu^{3+} was taken as a surrogate of Am^{3+}) was studied in detail with T2EHDGA and T-DGA based PIMs by fitting the uptake data with various kinetic and isotherm equations. Finally, a polymeric membrane electrode containing TODGA as the ionophore was prepared and studied for possible potentiometric determination of Eu (III) ions.

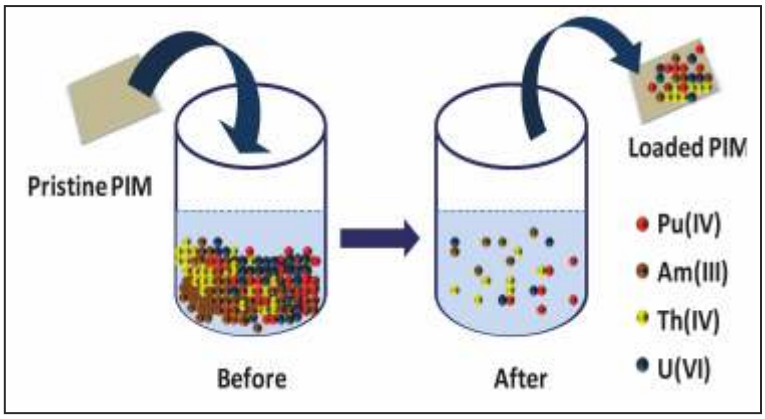

This thesis aimed at the important problems related to reprocessing of the nuclear waste and zinc isotope separation using computational and experimental studies. The work is mainly focused on the micro-

hydration of metal ions, partition coefficient of extractants, interaction between host-guest. The microhydration of Rb^+ and Sr^{2+} ions using electronic structure calculations provide the valuable insights in the bulk hydration. The partition coefficients of variety of crown ethers in selected water-organic bi-phasic system including ionic liquids were calculated using COSMO-RS theory and compared with the available experimental results. The study of Li^+ ion with model crown ethers demonstrates the effect of different donor, cavity and electron donating/withdrawing groups on the complexation. In another study suitable crown ether architectures were established for encapsulation of Cs^+ and Sr^{2+} ions using DFT.

The work on selectivity of metal ions with different lignads using computational and experiments include ; i) the enhanced selectivity of Cs^+ ion over Na^+ ion with hybrid calix[4]-bis-crown macrocyclic ligand compared to 18-crown-6 ether and further enhancement in the Cs^+ selectivity by tuning hybrid calix-crown ether using DFT, ii) the preferential selectivity of bivalent Sr^{+2} ion over tetravalent Th^{+4} ion with dicyclo-hexano-18-crown-6 (DCH18C6) using DFT, iii) combined experimental and theoretical study to investigate the complexation behaviour of Pu^{4+} and UO_2^{2+} with DHOA in different diluents, iv) the enhanced selectivity of Am^{3+} over Eu^{3+} with CyMe4-BTPhen compared to CyMe4-BTBP using DFT. In all these studies the computational results are compared with the available experimental results and found to be in good agreement. The suitable conformer of DCH18C6 is explored for the zinc isotope fractionation using DFT validated by experimental results. The present studies will definitely provide the fundamental insights for the selective separation of metal ions. Thus, these studies will be useful for the future design of extractants.

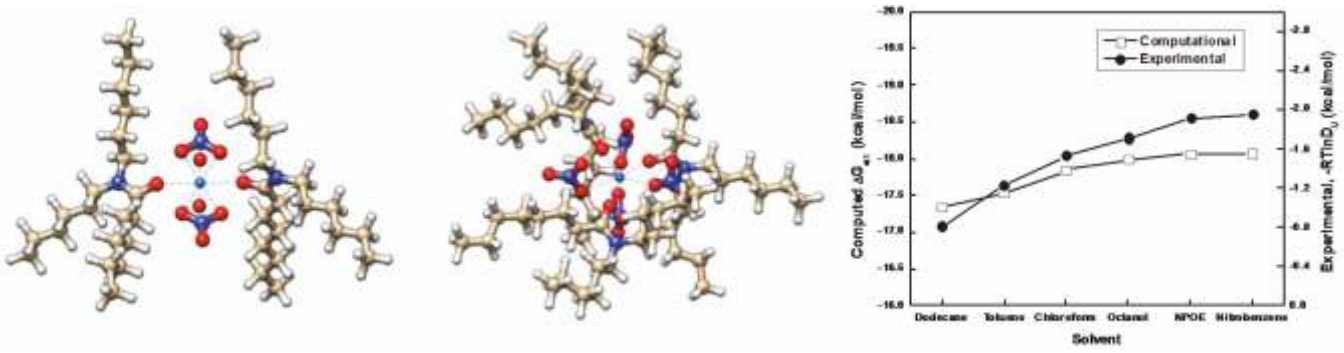

Figure 1.1.10 Optimized structures of $UO_2(DHOA)_2(NO3)_2$ and $Pu(DHOA)_3(NO3)_4$ using DFT. The experimentally observed 'D' and theoretically predicted 'Gext' values for UO_2^{2+} with DHOA.

Acidic solutions are ubiquitous in nature and hence microscopic description of hydrated acids would help in understanding a broad spectrum of topics ranging from proton transport in biological systems to the problem of acid rain. The aim of this doctoral thesis is to understand hydration of acids at the molecular level and to obtain a correlation between molecular and bulk level acid strength. It is reported that on successive addition of water molecules to isolated carboxylic acid molecule, O–H bond of –COOH group becomes longer and weaker and finally acid dissociation occurs with the formation of contact ion-pair as an intermediate. During the process, the distance between H atom of the acid molecule and O atom of the immediate neighboring water molecule decreases. The number of water molecules (n) needed to dissociate the acid molecule depends on the strength of the A-H bond. The weakening of the O-H bond of the acid molecule, with the addition of water molecules, and subsequent formation of contact ion pair are reflected in the bond dipole moment, H bond energy, IR spectra and bond dissociation energy profiles of

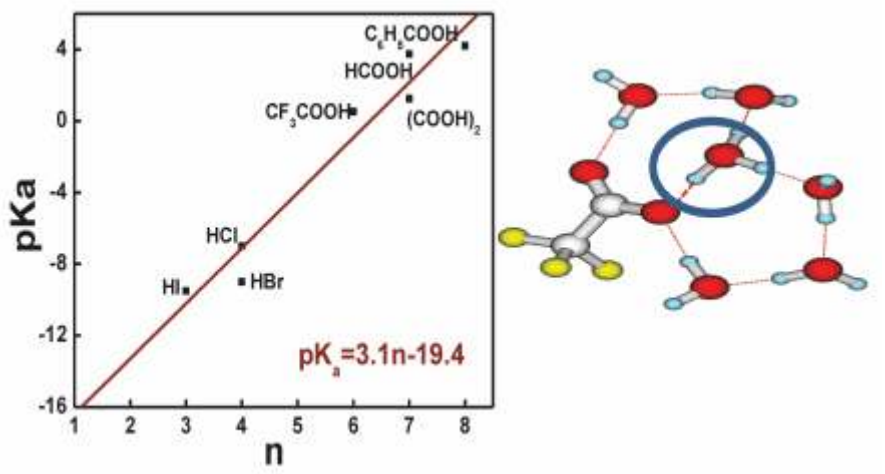

Figure 1.1.11 Plot of pKa versus the number of water molecules (n) needed to dissociate an acid molecule. The minimum energy equilibrium conformfer of $CF_3COOH.6H_2O$, showing contact ion pair formation, is also given.

the O-H bond of the acid molecule in the hydrated acid clusters. On successive addition of solvent water molecules, the barrier for proton transfer from the acid molecule to the neighboring solvent water molecule reduces. After a critical number of solvent water molecules, proton transfer process becomes barrier less and spontaneous. Micro hydration of photo acid is also considered by taking 2-naphthol as a case study. It is also reported that fewer number of water molecules are required to dissociate 2-naphthol in the first excited singlet state compared to its ground and first excited triplet state. A linear relation is observed between the number of water molecules needed to dissociate an acid molecule and its pKa. The thesis for the first time presents a non-thermodynamic route to calculate pKa of an acid. This also provides a route to calculate local pH in a biological systems and this has far reaching consequences study behavior of proteins under different environment.

2-[^{18}F]Fluro-2-deoxy-glucose ([^{18}F]FDG) is a PET-imaging radiopharmaceutical, that is widely used in oncology as it has very significantly improved diagnosis and management of cancers, by virtue of their increased uptake of glucose. However, [^{18}F]FDG has some limitations as it is not a selective tracer for cancers. [^{18}F]FDG is also taken up significantly in the normal brain, in sites of infection and inflammationand wherever there is increased muscle activity. In neurology, specifically brain tumours, which requires early and unequivocal diagnosis, [^{18}F]FDG is of very limited use as it gives low contrast images. In this context, [^{18}F]-labelled amino acids are found to be more specific, as their uptake by normal brain tissue is low and tumours are seen with much higher contrast.

The thesis work is focused on the production of [^{18}F]fluoro-ethyl tyrosine ([^{18}F]FET), which has been reported to be a useful brain tumour imaging agent. [^{18}F]FET was prepared by more than one method, with attention paid to optimizing the reaction yields, using non-HPLC purification steps post-synthesis, so that this important PET-imaging agent can be produced in existing FDG production facilities thatare available in all medical cyclotron centres. [^{18}F]FET was synthesized from the O-(2'-tosyloxethyl)-N-trityl-L-tyrosine-tert-butyl ester (TET) precursor, after carefully standardizing the reaction conditions, purification methods and quality control procedures so that the final product will meet approval for human clinical studies. The studies showed that high quality of [18F]FET can be produced economically with 2 mg of precursor and solid-phase extraction (SPE) purification with an neutral alumina cartridge column.[^{18}F]FET is now

routinely produced by this method under GMP and being used for human studies after approval from DAE-Radio pharmaceuticals Committee.

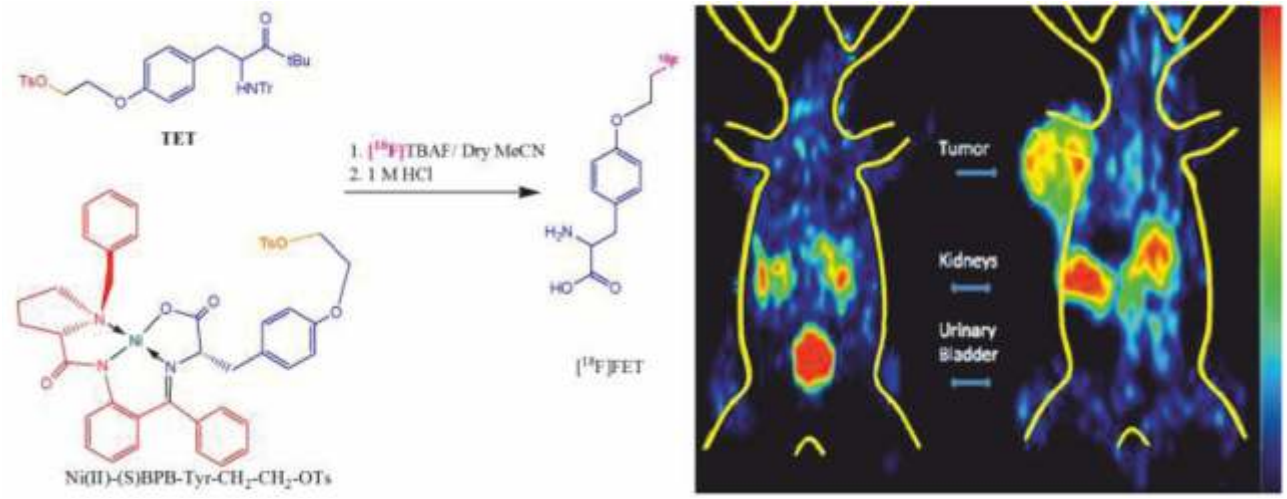

Figure 1.1.12. Radio synthesis of [^{18}F]FET Micro PET imaging studies in B16F10 Melanoma bearing C57BL/6

A fully automated radio-synthesis of [^{18}F]FET using SPE procedure was also developed using the novel Ni(II)-(S)BPB-Tyr complex based precursor with 94% L-enantiomeric purity. The method has been standardized and evaluated to produce the radiopharmaceutical of a quality that is required for human studies. A simplified route for precursor synthesis was developed, reducing the number of steps and time significantly. A simplified, fast, efficient and economic purification procedure termed as Serial Column Flash Chromatography (SCFC) method, was also applied for purification of various Ni(II)-SBPB complex based precursors for 18F-labelled fluoro-amino acids. Radiosynthesis of 1-[^{18}F]Fluoro-propyl tyrosine ([^{18}F]FPT) using Ni(II)-SBPB complex based precursors, and purification using SPE were also shown. The quality of the product was evaluated by standard methods and the uptake was evaluated by micro-PET imaging studies and found to be satisfactory.In conclusion (i) GMP compliant [^{18}F]FET can be produced by SPE purification using TET precursor. (ii) [^{18}F]FET can be synthesized efficiently and economically using Ni(II)-(S)BPB complex based precursor. (iii) Ni(II)-(S)BPB-amono acid Schiff's base precursor can be an efficient method for synthesis of [^{18}F]fluoro-amino acid for PET, due to its ease of production and high chemical stability.

One doctoral thesis has been accepted in the area of biophysical chemistry. Free radicals and molecular oxidants, collectively known as reactive oxygen species (ROS) are important entities generated during various biochemical reactions in the cells. However, excess generation of ROS causes oxidative stress which has been implicated in onset of several diseases. To protect from oxidative stress, cells utilize different enzymes like glutathione peroxidase (GPx) and low molecular weight molecules like vitamins, thiols, etc., collectively called as 'antioxidants'. Low molecular weight organo-selenium compounds represent a special class of antioxidants which can exhibit both GPx like catalytic activity or free radical scavenging activity, through the intermediacy of selenoxides. Even though the enzymatic activity of organo-selenium compounds have been studied extensively, there are not many reports on free radical reactions and electron transfer reactions of these compounds which are necessary for understanding their role in GPx and antioxidant activity.Here, the electron transfer reactions of structurally related organo-selenium

compound sand their gold nano composites have been explored using techniques like, nanosecond pulse radiolysis stopped flow techniques and quantum chemical calculations, followed by identification and estimation of the transient intermediates and reaction products. The study showed that chemical kinetic parameters along with molecular descriptors like highest occupied molecular orbital (HOMO), non-bonding interaction, enthalpy change, etc can be used for designing organo-selenium based antioxidants with enhanced activity against both free radicals and molecular oxidants. Also, conjugation of these compounds with nanoparticles of noble metals like gold (GNP) and provide an alternative route for modulation of redox properties of these compounds through formation of selenium-GNP nano composites.

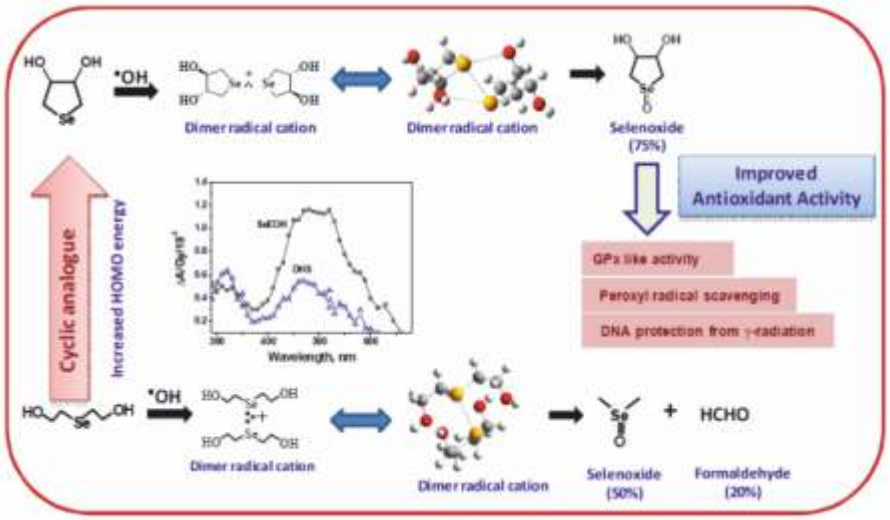

Figure 1.1.13. Comparative antioxidant activity of linear (SeEOH) and cyclic (DHS) organoselenium systems.

1.2. Indira Gandhi Centre for Atomic Research

Luminescence determination of lanthanides and actinides is a major challenge in aqueous medium due to their poor molar absorptivities and low quantum yield. In order to overcome these problems, ligand sensitized luminescence has been widely used for lanthanide determination. Ligand sensitized luminescence, which is a popular way to enhance the luminescence of lanthanides, however, is not useful in the case of uranium as most of the ligands do not sensitize the luminescence intensity of uranium. Though, there are plenty of ligands which enhance the luminescence of lanthanides, only a few such as 2,6-pyridine di-carboxylic acid and trimesic acid were reported to enhance the luminescence of uranyl ion (Uo_2^{2+}).

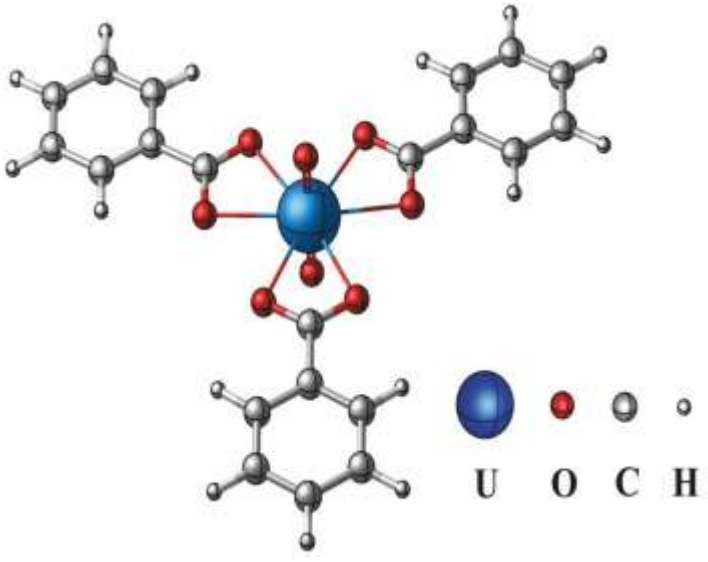

Figure 1.2.1 Uranyl tris complex $[UO_2(C_6H_5COO)_3]^-$ in acetonitrile with D_3h symmetry.

This thesis deals with the luminescence studies of Eu^{3+} and UO_2^{2+} complexed with aromatic carboxylic acid ligands in acetonitrile medium. In this thesis work, six ligands have been employed to examine the Eu^{3+} and UO_2^{2+} luminescence and complexation. Ligands used in this study are benzoic acid, ortho toluic acid, meta toluic acid, para toluic acid, pyridine-2-carboxylic acid or picolinic acid, pyridine-2,6- dicarboxylic acid or dipicolinic acid. The coordination and luminescence behavior of Eu^{3+} and UO_2^{2+} complexes is found to be different in acetonitrile compared to that of aqueous medium. In contrary to aqueous medium where Eu3+ and UO_2^{2+} benzoates form 1 1 and 1 2 species, present study reveals formation of highly luminescent 1 3 complexes in acetonitrile medium. Luminescence lifetime studies are also carried out in order to understand the complexation behavior of these complexes. Among all the ligands studied in this work, dipicolinic acid shows the highest enhancement for both of the metal ions, Eu^{3+} and UO_2^{2+} leading to the detection limits of $4x10^{-11}$ M for Eu^{3+} and $1x10^{-9}$ M for UO_2^{2+} in acetonitrile. These detection limits of europium and uranium achieved in acetonitrile medium is far better than that obtained in aqueous medium.

The present thesis involves the synthesis of various diglycolamic acid based extractants and their evaluation for the mutual separation of lanthanides and actinides. Diglycolamic acid is an acid derivative of diglycolamide. Diglycolamides are the popular reagents for the separation of trivalent lanthanides and actinides from concentrated nitric acid medium (3-4 M nitric acid). A pictorial representation of various extraction methods adopted for the mutual separation of Ln(III)-An(III) using diglycolamic acid ligand in the present study is shown in figure 1.1.9. Two extractants bis(2-ethylhexyl) diglycolamic acid (HDEHDGA) and its sulfur derivative, bis(2-ethylhexyl) thiodiglycolamic acid (HDEHSDGA) were developed for the mutual separation of lanthanides and actinides by liquid-liquid extraction method. Feasibility of separation was demonstrated using a 20 stage mixer-settler. Several solid phase adsorbents with diglycolamic acid as ligand were also developed suitable for the separation of micro-quantities of radionuclides present in a large volume of feed solution. In connection with this, a number of diglycolamic acid impregnated resins and a chemically modified anchored resin in which polyamine resin matrix was modified with diglycoamic acid was also developed. Similarly, a couple of adsorbents with inorganic matrices such as silica and iron oxide were also developed. The extraction studies with these adsorbents confirmed the feasibility of separating Am(III) from Eu(III) with high separation factors.

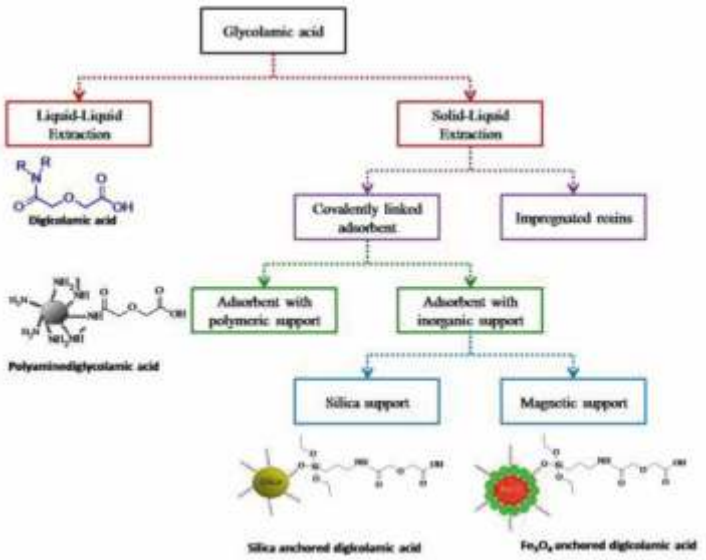

Figure 1.2.2 Different types of extractants with glycolamic acid

The thesis deals with the synthesis, characterization and application studies of zero-dimensional, two-dimensional carbon materials and its composites. Zero dimensional graphitic carbon nitride quantum dots (g-CNQDs) were synthesized from formamide and it has application in fluorescence sensing. Carbon quantum dots synthesized from formic acid has application in electrochemical sensing. Two-dimensional

(2D) carbon nitride and graphene were fabricated by bottom up fabrication method from g-CNQDs and CQDs respectively and 2D carbon nitride was used as toxic Hg^{2+} ion sensor by electro chemical method and graphene was used as H_2O_2 sensor by electro chemical method. The composite materials of carbon nitride such as Iron oxide nanoparticles embedded on carbon nitride matrix (Fe_3O_4-CNx), Platinum nanoparticles on graphitic carbon nitride (Pt/CNx) and Zinc doped porous carbon nitride microsphere (Zn-CNx) have application in photo catalysis, electro oxidation and heavy metal ion removal studies from waste water.

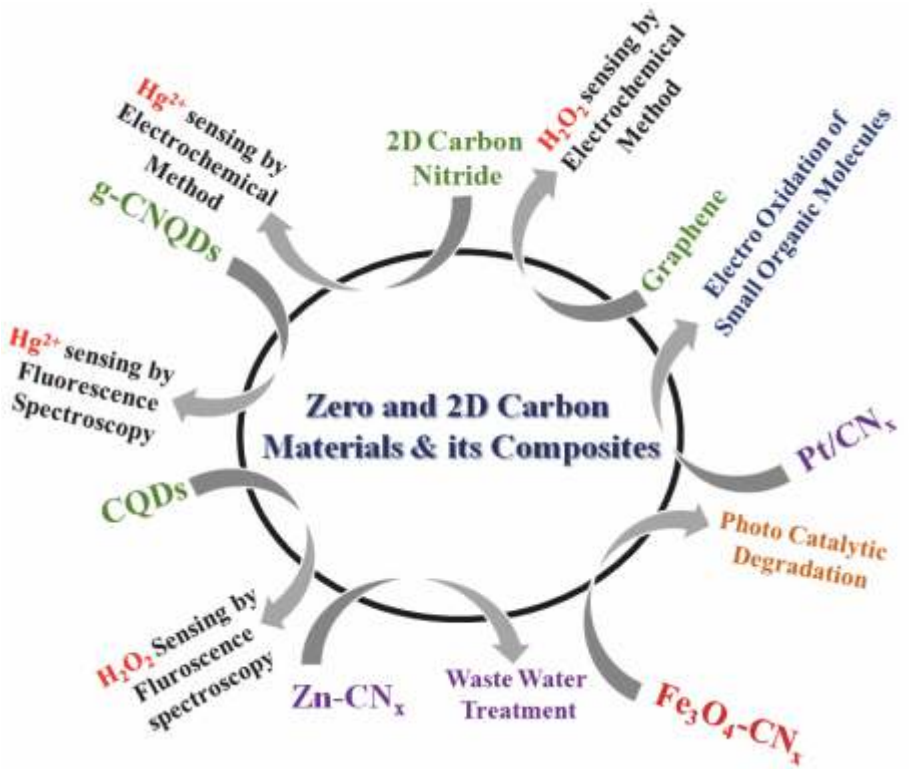

High-level liquid waste (HLLW) is generated during reprocessing of spent nuclear fuels. Partitioning and transmutation (P&T) strategy is a viable option for the safe management of HLLW. The current practice of trivalent actinide partitioning is a two cycle approach. It involves the separation of trivalent actinides and lanthanides together from the HLLW in the first cycle by using neutral extractants followed by lanthanide (Ln)-actinide (An) separation using acidic extractant in the second-cycle. This process may be simplified by combining both neutral and acidic extractant in a single-cycle approach. In single-cycle approach, both trivalent actinides and lanthanides can be extracted from HLLW followed by selective separation of actinides from lanthanides. The present work involves testing of various combinations of neutral and acidic extractant in order to use them in a single-cycle approach and their evaluation for the mutual separation of lanthanides and actinides. Studies reported in the thesis aimed at the development of single-cycle approach for the mutual separation of trivalent actinides from trivalent lanthanides. Several combinations such as unsymmetrical diglycolamide (UDGA)- HDEHDGA, TODGA-HDEHP, TEHDGA - HDEHP etc. are studied to examine the feasibility of mutual separation of trivalent lanthanides and actinides. Based on the several combinations of extractants, a flow sheet for minor actinide partitioning in single-cycle process was proposed which is shown in Figure 1.2.3. In this process, both U(VI) and Pu(IV) can be separated from the spent fuel using PUREX process. HLLW contains all trivalent lanthanides and actinides along with other fission products. The trivalent actinides and lanthanides are extracted using 0.1 M TEHDGA-0.25 M HDEHP

in n-dodecane from HLLW. The extraction of trouble some fission products can be minimized using 0.05 M CyDTA in HLLW solution. CyDTA selectively forms complex with Zr(IV), Pd(II) and reduces the extraction of these metal ions. Other metal which was not extracted by the solvent phase was remained in aqueous phase known as high active raffinate. Selective stripping of actinides from the loaded organic phase could be achieved using 0.05 M DTPA+0.5 M citric acid at pH 3. Most of the lanthanides will be present in the solvent phase after the selective stripping of actinides.In order to reuse same solvent in the successive steps, these lanthanides should be separated from organic phase. These lanthanides can be separated using aqueous soluble tetraethyldiglycolamide (TEDGA).

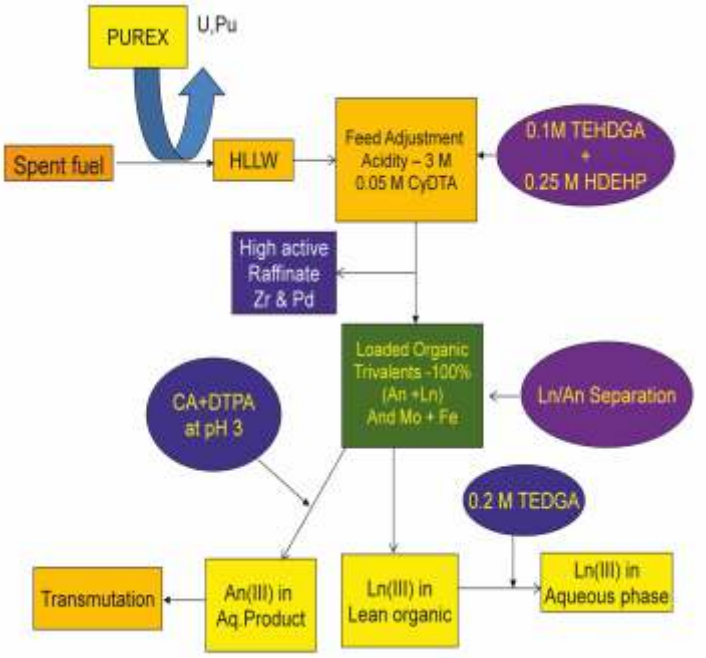

Figure 1.2.3 Proposed Flow sheet for minor actinide partitioning in single-cycle process.

In this doctoral thesis work, several symmetrical trialkyl phosphates (TalP) have been investigated towards identification of an alternate extractant to TBP for fast reactor fuel reprocessing and these studies have indicated tri-iso-amyl phosphate (TiAP) as a suitable extractant. Prior to the deployment of a novel solvent, TiAP /n-dodecane (n-DD) in an actual reprocessing plant, it is essential to understand the various aspects of this solvent system. In this context, the present study mainly focused on the issues arising from reprocessing of fast reactor fuels. The extraction behavior of actinides (U, Pu and Am), troublesome fission products (e.g. Zr, Ru, Tc) and some of the lanthanides (La, Pr, Nd, Sm, Eu) as fission product representatives with TiAP were investigated and compared with the TBP/n-DD system under identical experimental conditions. Continuous counter-current solvent extraction runs with TiAP based solvent using a mixer-settler have been carried out under various experimental conditions. Preliminary studies have been also carried out to develop an alternate method for the processing of metallic alloy fuels by aqueous route using PUREX process with TiAP based system. Thermal and radiolytic stability of TiAP system have been investigated and the results of TiAP solvent are compared with TBP. Studies carried out in the present work

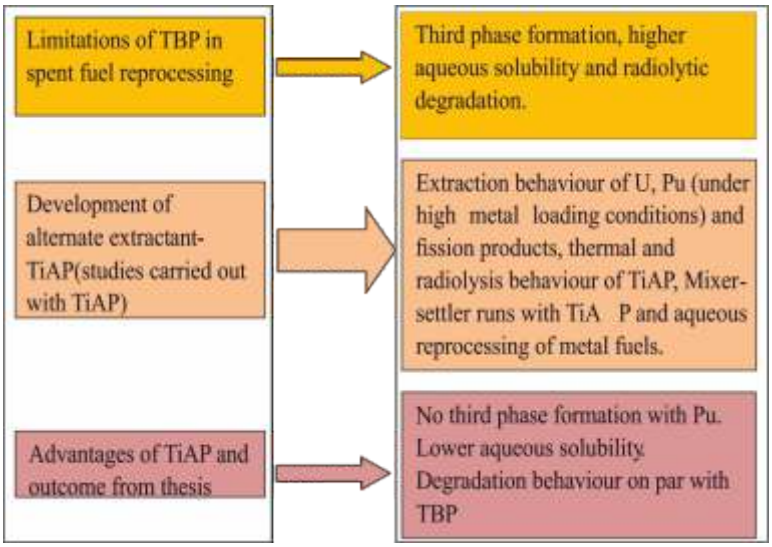

Figure 1.2.4 Graphical abstract of development of alternate extractnat, TiAP for spent fuel reprocessing

on various physicochemical and extraction properties as well as third phase formation phenomena have established that tri-iso-amyl phosphate is a suitable extractant for fast reactor fuel reprocessing.

Lead-bismuth eutectic alloy (LBE) is considered as coolant and spallation target in Accelerator Driven Systems (ADS) and as a candidate coolant in nuclear reactors. However, the high solubility of the alloying elements of steel in LBE leads to corrosion of structural steel. This can be reduced by forming a passive oxide layer over the steel surface by maintaining controlled oxygen levels in the coolant. To understand the thermochemical characteristics of this oxide film, details on phase diagrams of Pb-M-O and Bi-M-O (M =Fe, Cr) systems as well as the thermo chemical data of the ternary compounds in these systems are needed. Iron and chromium being the major components of structural steel, phase diagram and thermo chemical studies on Bi-Fe-O and Bi-Cr-O systems were carried out in the present work.

Though pseudo-binary phase diagrams of Bi_2O_3-Fe_2O_3 and Bi_2O_3-CrO_3 systems are reported in literature, the ternary phase diagrams of Bi-Fe-O and Bi-Cr-O systems have not been reported. In this work, phase fields of these systems were established by equilibrating compacted mixtures of bismuth and iron or chromium powders along with their oxides in sealed containers for prolonged periods at temperatures between 773 and 1023 K and characterizing the resulting phases by XRD. The phases coexisting with liquid bismuth were also identified by equilibrating samples in liquid Bi and characterizing the resulting phases by XRD. The ambiguity in the temperature range of stability of $BiFeO_3$was eliminated by carrying out long term equilibrations with $BiFeO_3$ under air and vacuum and confirmed that $BiFeO_3$ is metastable at low temperatures and becomes thermodynamically stable only around 940 K.

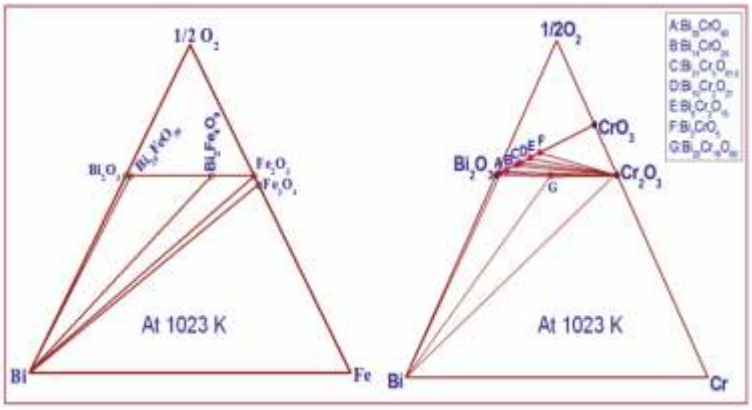

Equilibrations in Bi-Cr-O system revealed the existence of a new compound of composition '$Bi_{22}Cr_{18}O_{60}$'which was characterized by XRD, SEM-EDS and TEM. Pseudo-isopiestic equilibrations carried out under different oxygen partial pressures revealed that '$Bi_{22}Cr_{18}O_{60}$' appear as a stable phase in liquid Bi at a temperature between 891 and 956 K. From these results, ternary phase diagrams of BiFe-O and Bi-Cr-O systems have been constructed at 773 and 1023 K.

Equilibrium oxygen potentials in the relevant phase fields of Bi-Fe-O and Bi-CrO systems have been measured using solid oxide electrolyte based emf cells and from this data Gibbs energies of formation of some of the ternary compounds in these systems have been deduced. Oxygen potential measurements carried out in the Bi-Cr_2O_3-'$Bi_{22}Cr_{18}O_{60}$' phase field delineated the temperature of formation of the new compound i.e., '$Bi_{22}Cr_{18}O_{60}$' to be 907 K. Standard molar enthalpies of formation of the ternary compounds, $Bi_2Fe_4O_9$ and $Bi_{25}FeO_{39}$ were determined by acid solution calorimetry. Heat capacities of these compounds were also measured by differential scanning calorimetry. Internal consistency of the measured thermochemical data also checked. Based on the results of this work on Bi-Fe-O and Bi-Cr-O systems and the data on solubility of oxygen in liquid bismuth from literature, the nature of passive oxide layer formed over the structural steel has been assessed.

Strontium chloroapatite ($Sr_{10}(PO_4)_6Cl_2$, abbreviated as SrApCl) and various borosilicate glass (BSG) bonded composites are loaded with simulated pyrochemical chloride waste. These composites are an alternate candidate matrix for the immobilization of pyrochemical chloride waste discharged from the non-aqueous reprocessing of metallic fuel. The synthesis of SrApCl+20 BSG, SrApCl+10wt.% waste, SrApCl+(10wt.% to 16wt.%)waste+20BSG composites were done by solid state reaction route. The waste loading to the matrices were optimized based on PCT requirements. These composites were characterized by XRD, TG-DTA and SEM-EDAX. Thermal expansion of these composites was measured by dilatometry and HTXRD. The heat capacity (*Cp*) of these compositions was measured by drop calorimetry and DSC. The glass transition temperature (*Tg*) of the glass phase was measured by DSC, TMA (dilatometry) and electrical conductivity at elevated temperatures. The leaching resistance of the composites / compositions was investigated by soxhlet and other techniques.

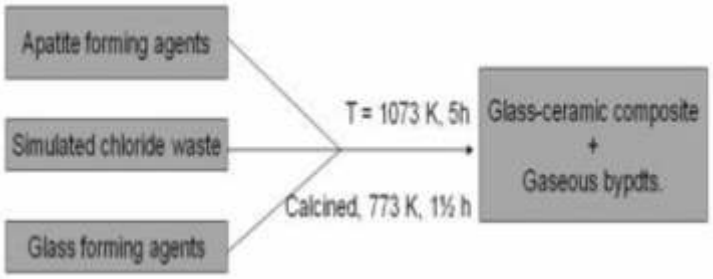

Figure 1.2.6 The flow sheet of glass-bond ceramic composites

The SrApCl and 10 wt. % waste loaded compositions were bonded with three different glasses apart from BSG such as alumino borosilicate glass (AlBSG), Ba-borosilicate glass (BaBSG) and lead–BSG (PbBSG). These composites were investigated to explore the improvement of required properties by changing the glass composition for the radwaste fixation. SrApCl+10w+20 AlBSG composition was synthesized by solid state reaction route and characterized by all the techniques used for SrApCl+10w+20 BSG composites as mentioned in the first paragraph. Similarly, SrApCl+10w+ 20BaBSG and SrApCl+10w+20PbBSG compositions were synthesized and their properties were measured to compare their performance with each other.The leaching studies on these composites were carried outby soxhlet and static methods. The normalized leach rate obtained in these experiments are ~ 10^{-5} to 10^{-6} g cm^{-2} d^{-1} which is within the range of values reported in the literature for various other matrices. From the above studies it was observed that 10-13 wt. % simulated pyrochemical waste loading is possible into these SrApCl-glass bonded composites against ~ 8 wt. % into the glass bonded sodalite matrix reported in the literature.

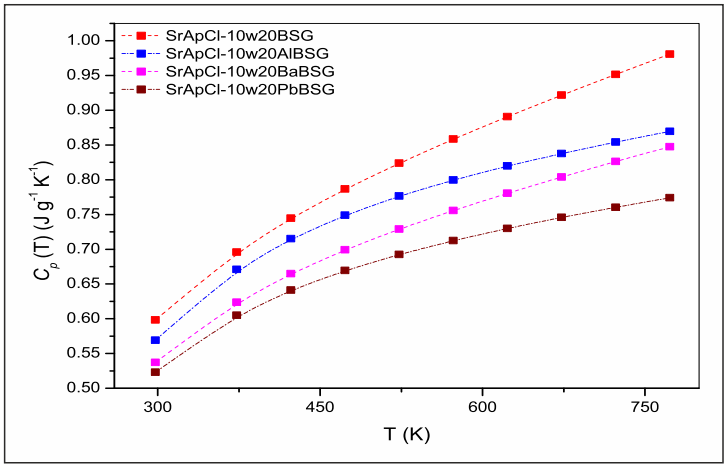

Figure 1.2.7 Cp vs. T for the glass-bond ceramic composites

1.3 National Institute of Science Education and Research

In recent years, pincer and half sandwich ruthenium complexes have gained enormous importance as efficient catalysts by offering benign routes in organic transformations and emerged as powerful and potent tools for atom economical synthetic protocols. In presence of well-defined ligand environment the catalytic properties of ruthenium complexes can be tuned further to attain diverse reactivity. The discovery

of Metal-Ligand Cooperation (MLC) in tridentate pincer complexes opened a new class of bond activation mode and consequently, an assortment of small molecules have been activated and utilized efficiently to provide benevolent routes in organic transformations. The current thesis is an attempt to extend these scopes further.The part A of the thesis mainly emphases the catalysis based on ruthenium pincer complexes in selective deuteration of alcohols, and terminal alkynes by employing D_2O as deuterium source. Also an efficient protocol of C1 feedstock generation from DMF to synthesize urea derivatives is developed.

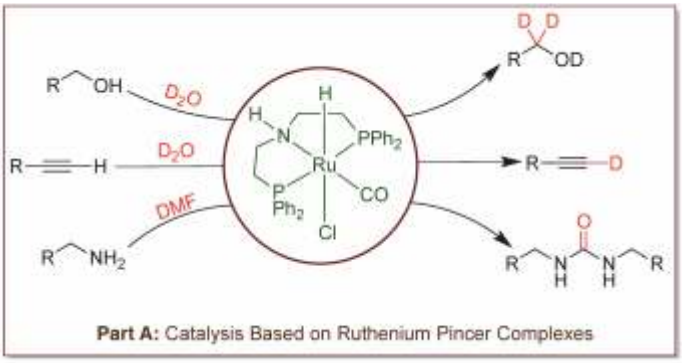

Figure 1.3.1 Part A describes catalysis based on ruthenium pincer complex.

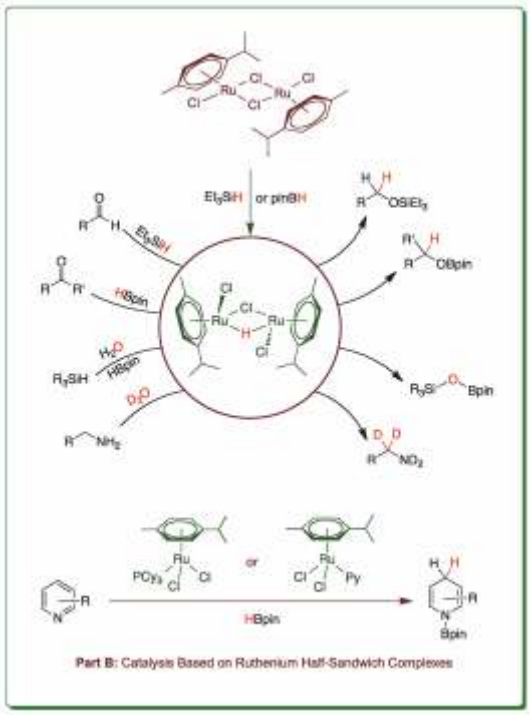

Figure 1.3.2 Part B describes catalysis based on half sandwich ruthenium complexes.

The part B of the thesis encompasses the reactivity of half-sandwich ruthenium complexes in various convenient catalytic transformations. Several ruthenium half sandwich complexes were synthesized, characterized and employed as catalyst in selective deuteration of amines, amino acids as well as in hydroelementation reactions, such as hydroboration, hydrosilylation and in atom-economical synthesis of borylsilyl ether. Important reactive intermediates were also isolated in most of the cases and characterized by spectroscopy and x-ray analysis. The information gathered from stoichiometric and catalytic investigations were utilized to rationalize the proposed mechanism for these processes.

In summary the thesis describes efficient and atom-economical approach towards important and useful catalytic transformations.

The present thesis presents a detail discussion on the speciation of actinides or their lighter homologues (lanthanides) under different aquatic environments and in presence of few important anthropogenic ligands that are co-disposed in the actinide waste and have significant presence in the waste confinements and near disposal facilities. The thermodynamic parameters reported in the present studies showed that these ligands form very strong and multiple complexes (MLi, i = 1-4) with the actinides and hence can be potential agents for migration of actinides from their source of origin.

Further, the actinide colloid formation is a key factor in deciding the solubility limits and the limiting solid phases. The accountancy of colloids helps in re-estimation the solubility products for accurate measurement of actinide concentration in aquatic conditions. The thesis also presents detailed study on colloid characterization in thorium samples kept for prolonged equilibration (~1080 days) at various pH and ionic strengths. The quantitative determination of colloid contribution helps not only in predicting

accurate solubility products but also to fractionate the dissolved thorium content to ionic, polymeric and colloid fractions. The present studies revealed the formation of colloids of range 14-37 nm at concentrations 0.06 to 6.38 ppb. The solubility products were found to be lower than the reported values upon taking into consideration the formation of colloids.

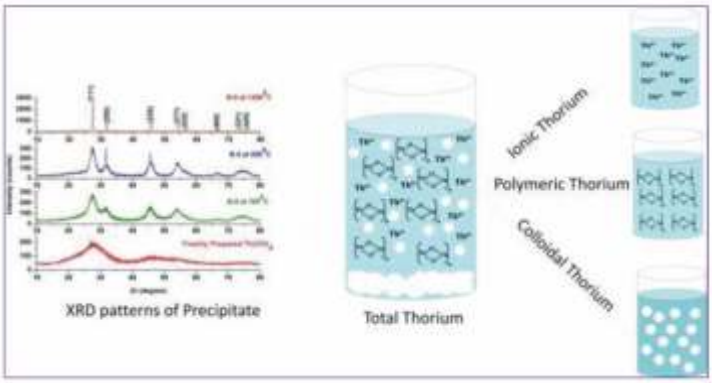

Figure 1.3.3 Fractionation of Aged Thorium Perchlorate solutions kept for an equilibration period of 1080 days into ionic, polymeric, colloidal and precipitated thorium parts.

The thesis involves the study of atomic-level mechanisms of photoinduced excited state intramolecular double proton transfer (ESIDPT) in diformyl dipyrromethanes, quantum chemical and ab initio chemical dynamics simulation of thermal denitrogenation of 1-pyrazolines, and denitrogenation of cis and trans-3,5-dimethyl-1-pyrazolines in the presence of external force.

The mechanism of photoinduced ESIDPT in diformyl dipyrromethanes is investigated using DFT methods. It was found that enolization by proton transfer processes resulted in a red shifted absorption spectra specific to diaryl substitution at the meso carbon atom of diformyl dipyrromethane and the enolization was observed to follow a step-wise mechanism i.e. diketo monoenol dienol (Figure 1.3.4). Quantum chemical calculations and ab initio classical trajectory simulations were performed to study the thermal denitrogenation of 1-pyrazoline using CASSCF methods. From the simulation results, it was seen that both the synchronous and asynchronous paths were equally probable (Figure 1.3.5). The effect of external force on the denitrogenation of cis and trans-3,5-dimethyl-1-pyrazoline was also investigated using CASSCF methods by varying the force from 0 nN to 11 nN along the vector connecting C3 and C5 atoms. It was observed that for trans-3,5-dimethyl-1-pyrazoline, the barriers for denitrogenation paths decreased with the increase in external force where as for cis-3,5-dimethyl-1-pyrazoline the barriers increased with the increase in external force up to 6 nN and then they decreased.

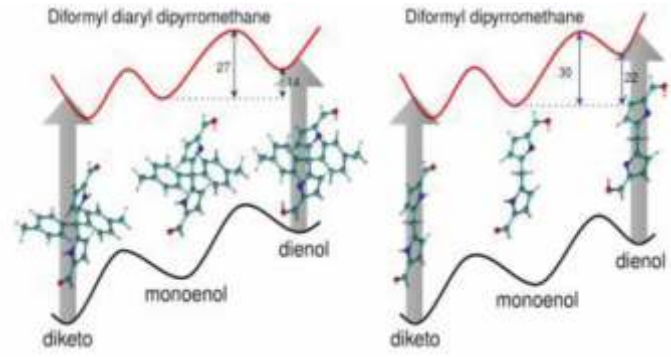

Figure 1.3.4 Potential energy profile for ESIDPT in diformyl dipyrro methanes

This thesis deals with hypervalent iodine(III) mediated C-N bond formation reactions. Transition metal-free, environmentally benign iodine(III) reagent $PhI(OAc)_2$ (PIDA) has been used for the synthesis of structurally important several heterocyclic molecules like benzimidazole, carbazole as well as non-heterocyclic nitrogenous compounds as portrayed in Figure 1.3.6. Mainly, two types of C-N bond formation reactions have been developed, first one type is dehydrogenative $C(sp^2)$-N and second type is non-dehydrogenative $C(sp^3)$-N.

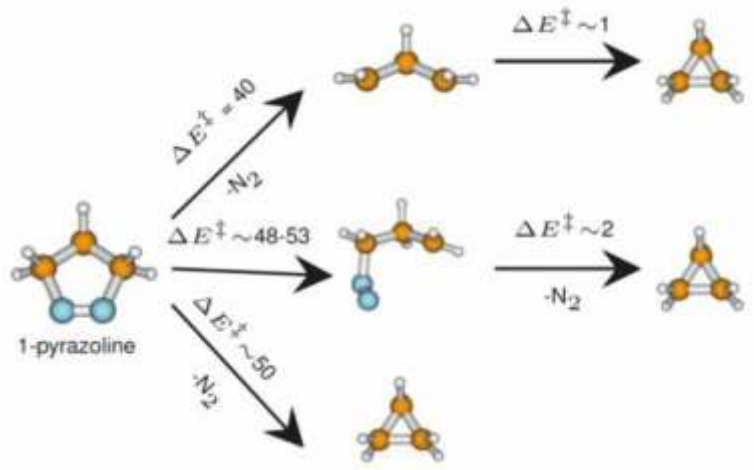

Figure 1.3.5 denitrogenation of 1-pyrazoline

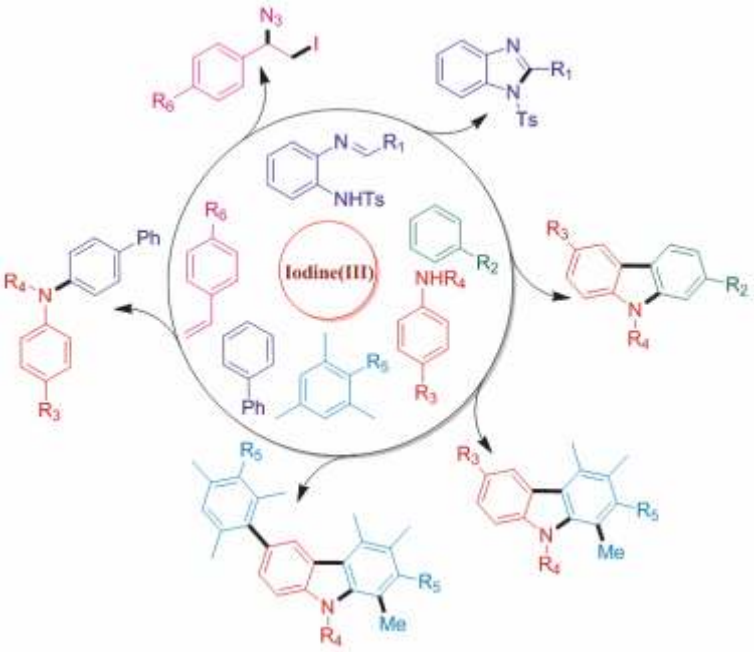

Figure 1.3.6 Schematic representation of C-N bond formation reactions

This thesis reports successfully designed and synthesized new unnatural d-amino acid, Troponylaminoethylglycine (*Traeg*) containing troponyl moiety as substituent on aminoethylglycine backbone. The formation of eight-membered ring hydrogen bonding between the troponyl carbonyl and amide NH is established (Figure 1.3.7 A).

An unusual cleavage of the classical acyclic amide bond derived from *Traeg*-aa under mild acidic conditions is established. The *Traeg* derived amide was cleaved into ester in alcoholic solvents and in acetonitrile, cationic troponyl lactone was obtained. In fact, the formation of cationic troponyl lactone from Traeg amide and other *N*-alkyl troponylglycinate amides is also an unusual and interesting transformation. Further, cationic troponyl lactone facilitated reversible amidation is established. So far, there no reports as

reversible amidation. Most interestingly, direct conversion of *N*-alkyl troponylglycinate esters into amides via cationic troponyl lactone without peptide coupling reagents is established at room temperature. The advantage with troponylglycinate esters is, they can be easily attached to free amine via amide bond and easily cleavable. Hence, N-alkyl troponylglycinates could be used as protecting groups for amine functionality (Figure 1.3.7 B&C).

Moreover, the reaction mechanism of *Traeg* derived amide and ester cleavage was elucidated. The role of troponyl ring and glycinate methylene group is established by performing control experiments and also deuterium labeling by entrapping deuterium at glycinate methylene group (Figure 1.1.25 B&C) Syntheses of cyclic amino troponimines and their fluorescent properties (solvent and pH dependent) are also demonstrated. Boron amino troponimines were successfully synthesized as novel fluorescent molecules containing tropolonoid aromatic system as analogues of BODIPY. The photophysical properties of boron-aminotroponimines are examined (Figure 1.3.7 D). Syntheses of sequence symmetric hexa-peptides by connecting proline tri-peptides at N-terminus through C-N bond by using alkyl linkers is established. Circular Dicroism studies revealed that these peptides are most probably aggregating at high concentration. Overall, this method could be useful for the syntheses of peptides for applications in nano material fabrication (Figure 1.3.7 E). Palladium compounds containing at least one metal-carbon bond intra molecularly stabilized by at least one donor atom termed cyclopalladated compounds or palladacycles are one of the most popular classes of organopalladium derivatives.

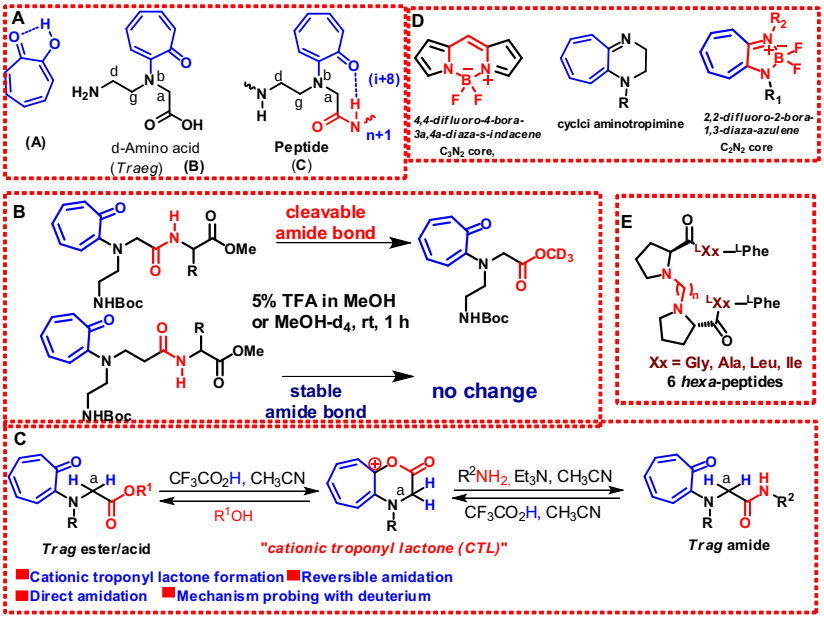

Figure 1.3.7 A) Chemical structure of synthesized unnatural amino acid; B) Unusual cleavage of Traeg amide bond; C) Direct/reversible amidation of Trag esters/amides; C) Chemical structure of boron-aminotroponimiines; C) Chemical structures of sequence symmetric hexa-peptides.

In 1995 Herrmann and co-workers successfully synthesized tri(o-tolyl)phosphine based palladacycle and utilized as precatalyst in Heck, Suzuki, and Buchwald-Hartwig reactions. Since then numerous palladacycles were synthesized and studied for a variety of organic transformations. Although ample reports exist for the synthesis of pyrazole-based palladacycles, their applications towards catalysis are scarcely studied. In my doctoral work, synthesis and characterization of a variety of pyrazole-based cyclometalated palladium compounds via C–H bond activation and exploration of their potential applications as pre-catalysts in C–C and C–N bond formation reactions are studied. We have synthesized and examined C–H bond activation of 3,5-diphenyl-1-(R-phenyl)- 1H-pyrazoles (R = H, Me, F and CF_3) from commercially available simple starting materials as ligands with $Pd(OAc)_2$ via nitrogen directed cyclopalladation of the aromatic ring. To our delight, we have demonstrated, for the first time, an efficient and economically attractive palladacyles catalyzed alkylation / methylation of ketones and amines using

alcohols as a greener and more sustainable alkylating / methylating agent, following the catalytic borrowing hydrogen strategy. Key to the success is the use of CF_3 group incorporation on palladacycle catalyst.

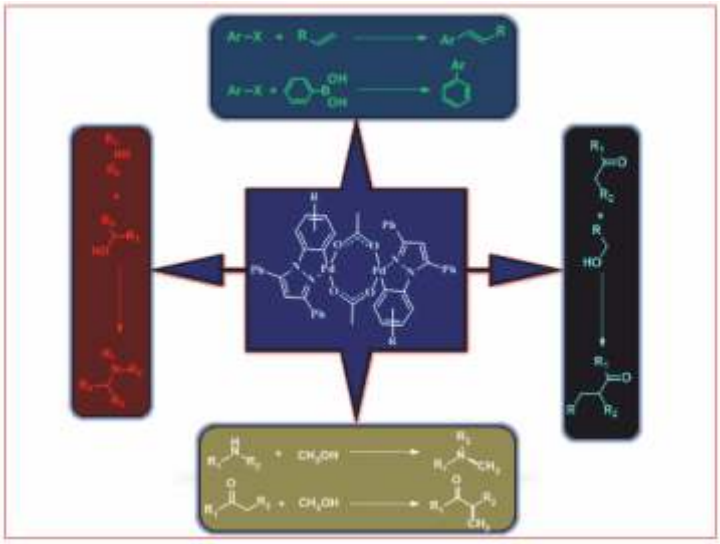

Figure 1.3.8 1,3,5-Triphenyl pyrazole-based palladacycles and their applications in C-C andC-N bond formation reactions

In this thesis work, student has successfully synthesized the tetrarylimidazole boron compounds by varying the substituents on N-phenyl & para-position of 2-phenol of tetraaryl imidazole. All these compounds are studied for their photophysical, electro- chemical, electro-luminescence and thermal properties. Pyrazole based N,C- chelate boron compounds have been designed and synthesized by varying substituents at the 4-position of N-phenyl. The photophysical properties reveal that these compounds exhibit fine tuning in emission maxima. Pyrazole and Phenanthrene imidazole based N,C- chelate dinuclear boron compounds with different pi-conjugation lengths are synthesized by varying the pi-conjugation spacer. All these dinuclear boron compounds exhibited high thermal stability and fluorescence emission both in solution and solid state. Tetraaryl pyrazole supported polymers and cyclophosphazenes were synthesized, characterized and studied their photophysial properties in the aggregated and the non-aggregated form reveals that they exhibit the aggregation induced emission enhancement (AIEE) phenomenon. Furthermore, we show that these polymers and cyclophosphazenes function as fluorescent chemosensors for the detection of explosives like picric acid.

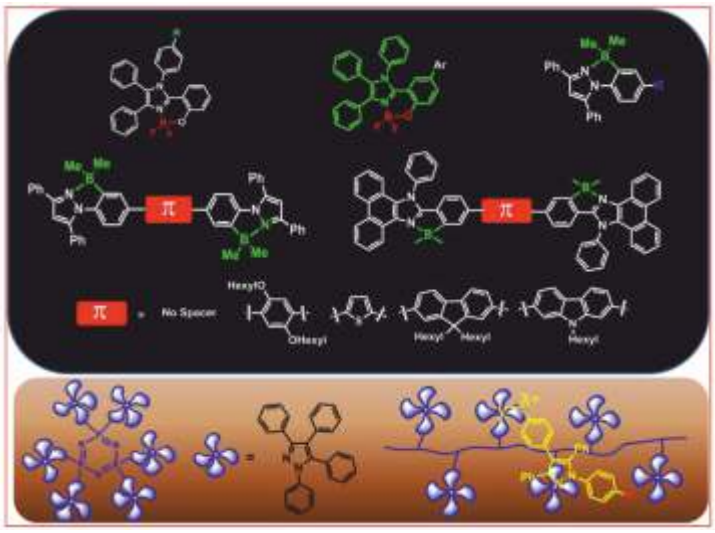

Figure 1.3.9 N, O-, N, C- chelate tetra-coordinate fluorescent boron compounds & tetraaryl pyrazole supported polymers and cyclophosphazene

2. Engineering Sciences

During this period, HBNI has awarded Ph.D. degrees to 38 students in Engineering Sciences on successful completion of academic programmes. Research topics are from a variety of areas including thermal hydraulic studies, mechanical property correlations, fluid flow & heat transfer, computer science, non-destructive evaluation, nuclear reactor engineering, computational fluid dynamics, biomedical signal processing, fracture mechanics, cavitation damage, instrumentation & control, classification algorithms, low noise electronics and embedded systems. Highlights of a few doctoral theses are outlined below.

2.1. Bhabha Atomic Research Centre (BARC)

Pool type research reactor often gets preference for production of radioisotopes as well as carrying out various irradiation experiments, due to its simpler design with easy accessibility from the core top. As reactor core top is open, radioactive coolant has a tendency to reach towards the pool top due to inertia and buoyancy leading to increase in radiation level at the pool top. Since, pool top activity level should be limited during normal operation; these reactors often use an open chimney structure at the reactor core outlet. Objective of the study is to identify major parameters which affect the mixing phenomena inside the chimney structure and to establish the design so that radioactive coolant from reactor core will be suppressed well within the chimney region.

Scaling philosophy was arrived by non-dimensionalising conservation equations. Numerical simulations were carried out for prototype and scaled chimney models with different core flow, bypass flow, chimney height and nozzle inclination using CFD code PHOENICS. Experiments were carried out in a chimney model (2 9) and flow visualisation & temperature measurements were done to establish the effect of buoyancy on the mixing behaviour. Correlations were developed for temperature profile, stagnation height, vortex spread height and pool temperature front height. Experiments were also carried out in a scaled (1 18) model using Particle Image Velocimetry (PIV) technique and dimensionless velocity distribution is compared with the computational results of prototype and chimney model to validate the scaling philosophy as well as the CFD code predictions.

Figure 2.1.1 Experimental set up for PIV

Figure 2.1.2 Experimental test facility

It was established by analyses and experiments that the core bypass flow sent to the pool is drawn in the downward direction inside the chimney which is able to suppress the upward flow. C hanges in inclination angles vary the height up to which effect of upward flow is felt. The higher is the angle, the lower is the stagnation height of the upward jet. Change in height of the chimney does not have significant effect on the stagnation height. The minimum bypass flow required to be sent to the pool is about 10% of the core flow. The minimum height of the chimney is 6 times the hydraulic diameter of the chimney.

Reliable predictions of annular flow dryout and post dryout heat transfer are one of the long standing issues of interest to nuclear reactor thermal-hydraulics. Annular flow dryout represents a thermal-hydraulic operating limit for BWRs. Beyond dryout, there is a severe deterioration of the heat transfer coefficient which would lead to a sudden rise in clad surface temperature. The magnitude of the rise (which is the point of concern in fuel safety) depends on local heat flux and flow conditions which may exist at dryout. The ability to predict the temperature rise depends on the adequacy of post dryout models.

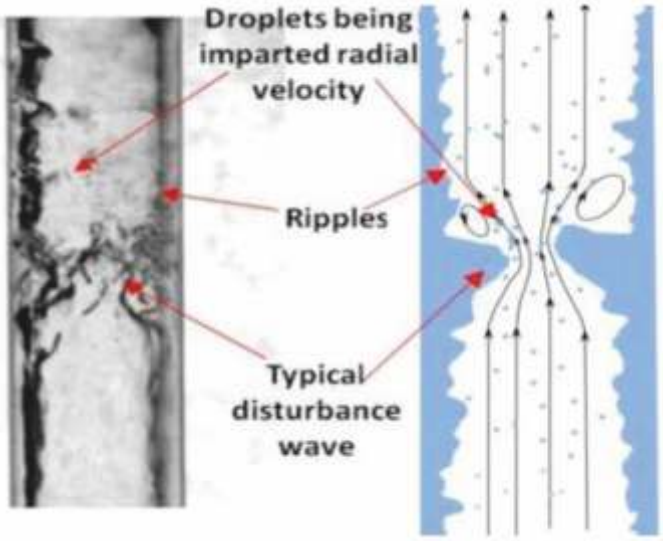

Figure 2.1.3 Visualization of annular two-phase flow and representation of main features

In the present work new models have been developed for prediction of annular flow dryout. Specifically, a new closure model has been developed for the estimation of fraction of liquid entrained as droplets at the point of transition to annular flow. This has led to noticeable improvement in dryout predictions for both tubes and rod bundles. The model development has been aided by conducting experiments to determine the film flow rate and thickness. These measurements were made by possible by in-house development of advanced sensors. Apart from this, visualization experiments and image processing have led to a novel technique for distinguishing churn flows from annular flows. These studies also led to a re-interpretation of the physical mechanism for onset of entrainment in annular two-phase flows.

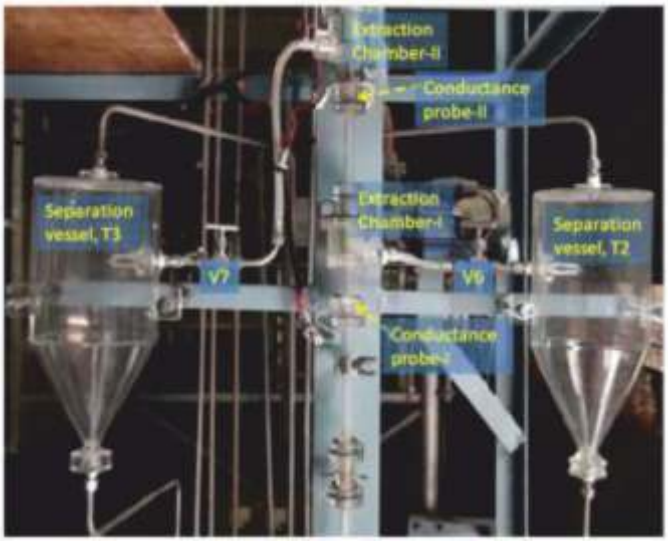

Figure 2.1.4 Air-water experimental facility with advanced instrumentation for film flow and thickness measurements.

In the post-dryout phase, the flow essentially consists of droplets in a stream of superheated vapour. These droplets play a very important role in precursory cooling of heated surface after dryout. In the present work, an analytical model has been developed to predict the heat transfer from heated wall to the droplets. The predictions of this model have been compared against experimental data available in literature and a good concurrence was observed.

All models generally rely on certain assumptions. Research over the years, has led to gradual reduction of the ad-hoc nature of some of these assumptions and development of new closures. The work reported in this thesis has been able to provide similar improvements to the general dryout and post-dryout models. Though certainly, there is still much scope for improvements.

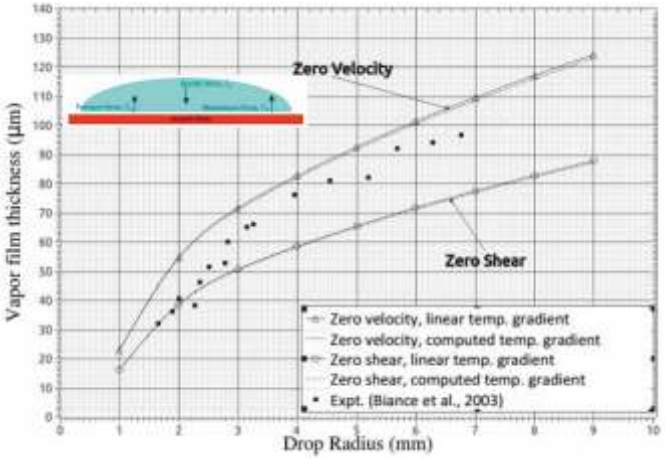

Figure 2.1.5 Prediction of wall-to-drop heat transfer with the developed model

One of the students worked on Use of Wavelets and Filter Banks in 2D Gel Electrophoresis Images in Spot Picker Robot for Precise Protein Identification. The main aim of this thesis was to bring in novel advanced techniques for the analysis of two-dimensional gel electrophoresis (2DGE) images, to provide more accurate protein spot detection in the field of proteomics. 2DGE is an important and the most widely used technique for analyzing protein expression in this field. By this technique, a very large number of proteins can easily and simultaneously be separated, identified and characterized. Due to very tedious and laborious work involved in the separation of thousands of proteins, a completely automated integrated system for the analysis of 2DGE images and spot excision is increasingly in demand. The nature of 2DGE images poses some great challenges, such as very noisy and inhomogeneous background with several irregular protein spots. These irregular protein spots are of varying size, shape and intensity. In this Thesis, problems of noise removal and methods of image segmentation are addressed to solve various challenges, such as faint or weak spots, overlapped spots and streaks, to a great extent. These challenges lead us to develop three novel segmentation methods; each method provides different insights into the problem and exhibits significant improvements over the available commercial software and methods for 2DGE images.

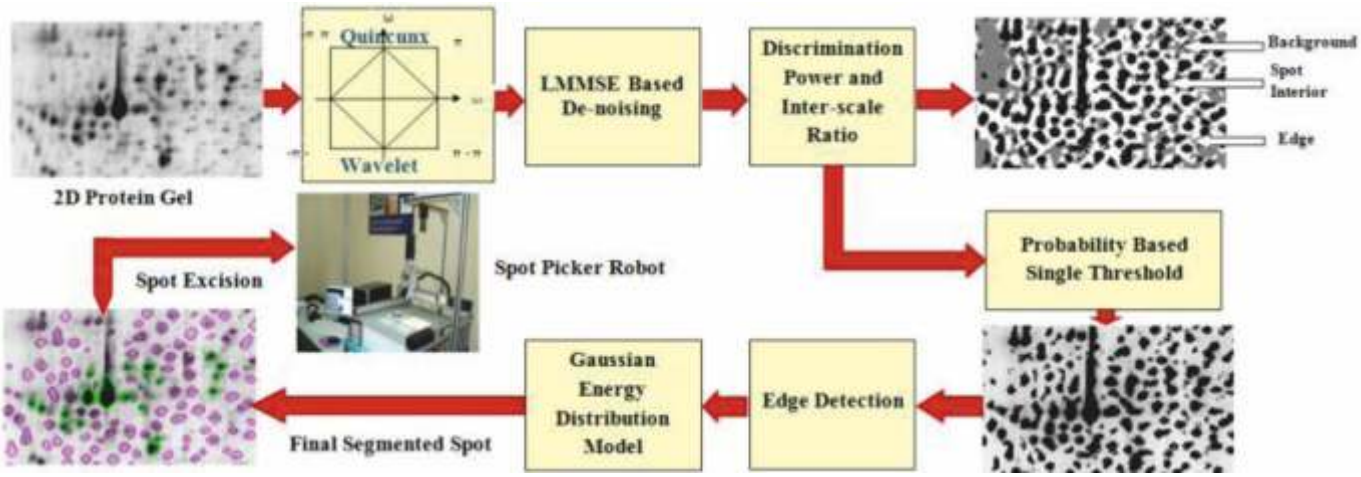

Figure 2.1.6 Analysis of 2D-Gel Images for Detection of Protein Spots Using Non-Separable Wavelet

The main contribution of the proposed algorithms is the use of nonseparable wavelets to study the nature of protein spots in the scale-space paradigm and to formulate efficient strategies for recognition. The first method analyzes the difference between streaks and spots, which are characterized in a nonseparable wavelet domain and combined with the watershed method for complete segmentation. In the second method, we have devised a technique to find out the faint spots by using inter-scale ratios of the wavelet coefficients. This technique is based on a single threshold and is independent of the gray value of the image. It copes with the inhomogeneities in the 2DGE images up to a large extent, which is helpful for finding the protein spots accurately. The third method emphasizes the minimization of artifacts and actual blob region identification in the noisy inhomogeneous background, by using kernel density estimation technique in the nonseparable wavelet domain.

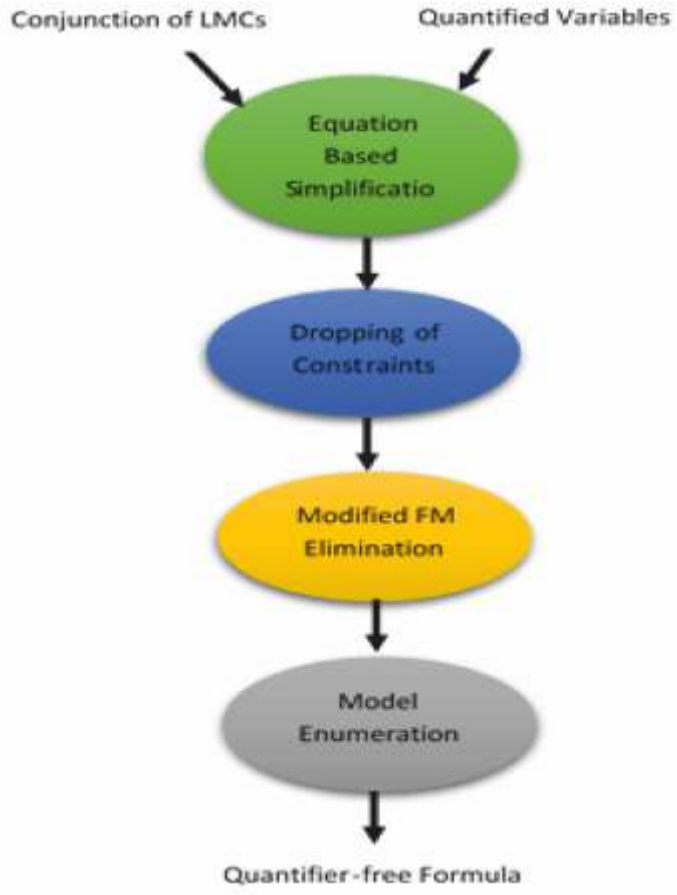

Figure 2.1.7 Quantifier Elimination Algorithm for Conjunctions of LMCs

Quantifier elimination is the process of converting a logic formula containing quantifiers into a semantically equivalent quantifier-free formula. This has a number of important applications in formal verification and analysis of hardware and software systems. Many key operations performed by formal verification and analysis tools essentially reduce to quantifier elimination from logic formulas. In this thesis entitled "Scalable Quantifier Elimination Techniques for Formal Verification", practically efficient and scalable techniques for quantifier elimination from logic formulas are presented that can improve the performance of such formal verification and analysis tools.

Boolean combinations of linear equalities, disequalities and inequalities on fixed-width bit-vectors, collectively called linear modular constraints (LMCs), is an important fragment of the theory of fixed-width bit-vector logic. A practically efficient and bit-precise algorithm for quantifier elimination from conjunctions of linear modular constraints is presented (see Figure 1). Techniques to extend this algorithm to work with arbitrary Boolean combinations of LMCs are then presented. Experiments indicate that these techniques significantly outperform alternative quantifier elimination techniques, and demonstrate the utility of these techniques in formal verification of word-level RTL designs. Next, Skolem function-based techniques for quantifier elimination from formulas in propositional logic are presented. Techniques for generating Skolem functions are of significant interest not only in quantifier elimination, but also in certification of solvers, synthesis of programs and circuits from specifications, and disjunctive decomposition of sequential circuits. In many such applications, the input formula is given as a conjunction of simpler sub-formulas, called factors, each of which depends on a small subset of variables. Here a SAT solving based algorithm for generating Skolem functions for

propositional formulas is presented that exploits factored representation of input formulas. In contrast to existing algorithms, this algorithm neither requires a proof of satisfiability nor uses composition of monolithic conjunctions of factors. Experiments indicate that on several large problem instances, this algorithm generates smaller Skolem functions and runs faster when compared to existing Skolem function generation algorithms.

One of the students investigated two sound focusing techniques using an integrated approach involving linear array and synthetic aperture focusing technique (SAFT) viz. Synthetic Focusing using Linear Array (SFLA) and Phased Array-SAFT (PA-SAFT). The approach is based on acquiring the raw data by a divergent sound beam using a linear array and carry out post-processing of the acquired data by time-based SAFT algorithm. Since the beam divergence is a key parameter in achieving fine focusing, an empirical relationship for its evaluation for miniature piezoelectric elements has been established. Contrary to what is widely reported in the literate, this study has shown that while dealing with miniature piezoelectric element, the lateral resolution achieved by SAFT depends on the wavelength,and is affected by array as well as SAFT processing parameters. An empirical relationship between the focal spot size, and the ratio of the size of the piezoelectric element to the wavelength, has been derived.

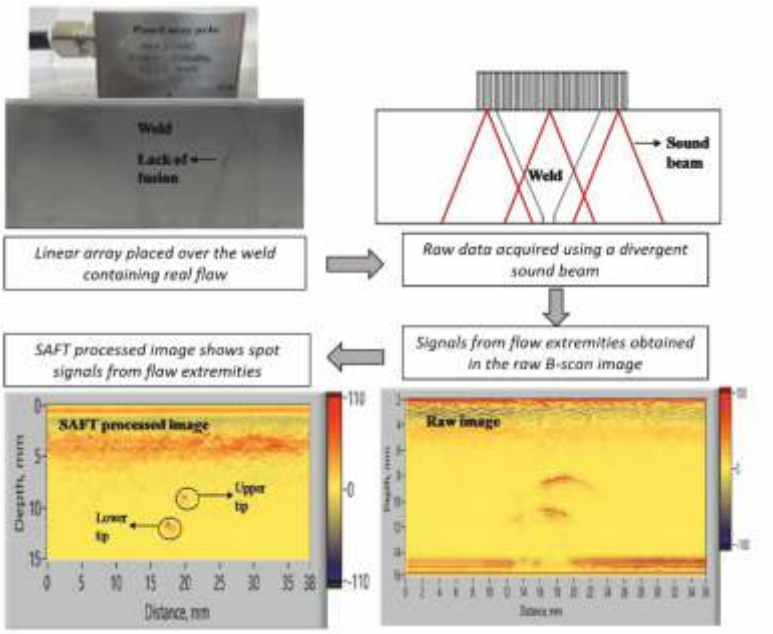

Figure 2.1.8 Characterization of flaws using an integrated approach involving the use of linear array and SAFT

The capabilities of SFLA and PA-SAFT techniques for characterization of planar and volumetric flaws has been studied on simulated and real weld flaws. The study has shown that both the techniques can accurately characterize flaws, with PA-SAFT technique showing better results on thick sections. The present investigation has shown that SFLA and PA-SAFT techniques require significantly lesser resources in terms of instrumentation hardware and data processing capabilities as compared to the existing array based techniques for sound beam focusing. The results on the characterization of real weld flaws by these techniques have shown that SFLA and PA-SAFT techniques hold a very good potential for field applications involving ultrasonic non-destructive evaluation.

A new process developed for the fabrication of nuclear fuels namely, coated agglomerate pelletization (CAP) process, was extensively investigated in the study to explore its feasibility as an alternative to present conventional process of powder processing and pelletization (POP) for addressing issues related to fabrication of thorium based fuels having high specific radioactivity and also due to multiple advantages like reduced man-rem problems, increased production rate, reduced radioactive liquid waste generation and improved safety it offered.

The research work investigated the effect on characteristics and thermal properties of the CAP pellets and

POP pellets due to substantial difference in fissile material distribution (homogeneity) in the pellets using simulation studies with surrogate materials and validated using real PuO2 thereby enabling comparison of simulant material and real fuel behaviors. The CAP and POP samples were prepared and synthesized under identical conditions and investigated for their characteristics and properties. The shrinkage studies brought out the mechanisms and factors responsible for different behavior between the CAP and POP pellets and resultant differences in their characteristics.

The characterization studies were carried out for density, microstructure, chemical purity and homogeneity which have pronounced effect on in-reactor fuel performance and on the thermal properties of the fuel. Due to high radioactive nature of the samples and the availability of characterization techniques being limited, alternate techniques were developed and employed for investigations. The studies showed characteristics possessed by CAP pellets compared to POP pellets to be favourable for better fuel behavior during irradiation. Theoretical understanding of thermal behavior of Th based MOX fuels of relevant compositions using Molecular Dynamics (MD) simulations for pellets with actual imperfections has been developed and performed and subsequently verified with experimental results. Thermal properties were extrapolated to higher temperatures for different compositions through molecular dynamic simulation by developed methodology.

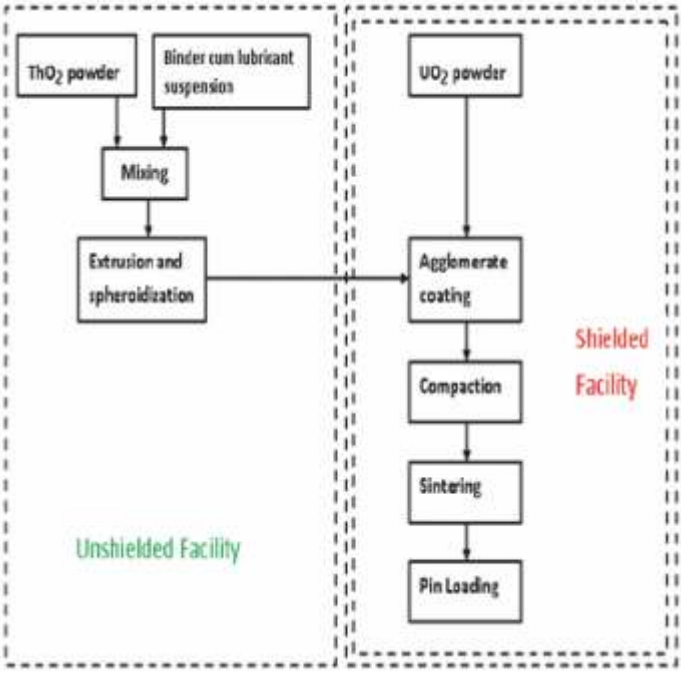

Figure 2.1.9 Flowsheet of Coated Agglomerate Pelletization (CAP) process.

From the studies conducted on surrogate systems and actual (Th,Pu)O2 system, it could be concluded that heterogeneous distribution of plutonium observed in the CAP pellets does not significantly impact the thermal conductivity of the fuel and therefore should be able to meet the desired linear heat rating of the fuel. In fact, some features of these pellets should result in improved in reactor behavior of the fuel due to reduced fission gas release and reduced pellet clad mechanical interaction.

The design and operation of nuclear reactors ensure that the likely hood of malfunction, leads to unsafe condition is small, such failures are still postulated and safety systems are provided to minimise the impact of such failures. The Shut Down System is one of the safety system which brings the reactor to safe shutdown state that is subcritical state from any operational state including design basis accidents and can hold the reactor in subcritical state. In Advanced Heavy Water Reactor (AHWR) two active, independent, functionally diverse, fast acting shut down systems are provided. Shut Down System-1 (SDS-1) consists of mechanical shut off rods and Shut Down System-2 (SDS-2) is based on liquid poison injection into the moderator. Gadolinium nitrate solution acts as neutronic poison, which is injected in heavy water moderator through a set of nozzles located inside calandria vessel. In this research, liquid poison injecting by shut down system-2 has been taken for the investigation of various associated thermal hydraulic and fluid dynamics phenomena.

In AHWR calandria, 513 calandria tubes and total 640 injection nozzles of diameter 6 mm as shown in Figure 2.1.10. To model such complex problem, a computer code has been developed which provides time varying input conditions for all the nozzles for distributing the poison into the calandria. Inlet condition of poison was modelled as the source term in the conservation equations used in the CFD code. Effect of heat generation in the moderator on the flow pattern and mixing characteristic of the poison in to the moderator is also investigated. Experiments show that progression of jet injected in axial direction of bundle is more compared to that injected in cross bundle. However, lateral spread of jet is more in cross bundle compared to axial bundle. CFD simulation of experiment with poison moderator interface shows that though the poison injection is delayed due to moderator inventory present between poison moderator interface and calandria, poison front penetrates at a faster rate due to partially developed nature of the jet before the poison injection and apparently catches the velocity front with time. CFD simulation of full calandria with 640 numbers of injection nozzles revealed that poison reaches the significant volume of calandria in given time to shut down the reactor. Results show that poison, having concentration more than 1% of initial concentration covers 65% volume of active core in 2 seconds. Based on the above studies it is found that shut down system-2 of AHWR works effectively for the configuration considered in the study.

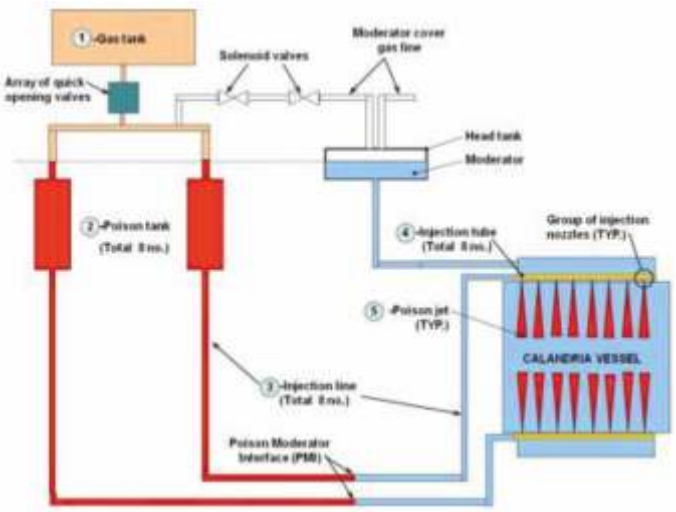

Figure 2.1.10 Schematic of Shut Down System -2 (SDS-2)

The Gen-IV International Forum's proposal of considering Supercritical Water Reactor (SCWR) in next generation nuclear reactors gave motivation to study flow and heat transfer characteristics of supercritical systems. Research on supercritical systems started with experimental work on supercritical flow in pipes followed by CFD simulations. The steep change in fluid properties around the pseudo-critical point makes supercritical heat transfer characteristics much different from subcritical ones. The behavior of a SPNCL will be much different than subcritical NCL because of different thermo-physical properties of the working fluid under these two conditions.

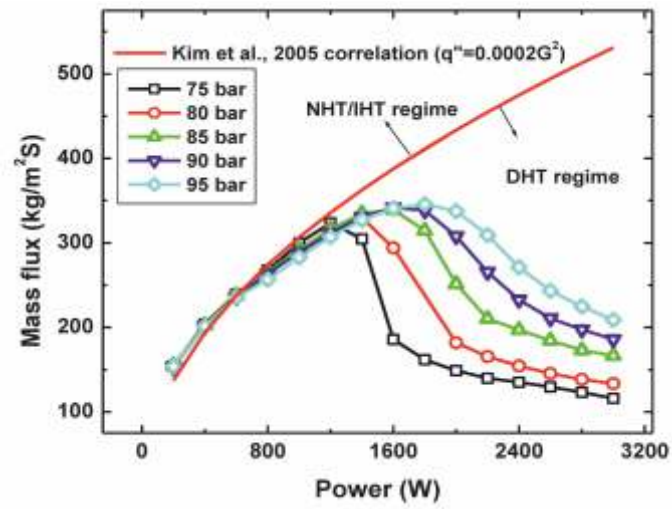

Figure 2.1.11 Prediction of onset of heat transfer deterioration

Computational investigation is performed to study the steady state and transient characteristics of SPNCL. For this purpose a 1D and a 2D (axi-symmetric) CFD codes are developed. Both these codes are validated with available experimental data, simulation results and correlations. Detailed flow and heat transfer analyses of vertical heater vertical

cooler (VHVC) configuration of SPNCL have been carried out at different operating pressures. Heat transfer analysis is done to identify regime of heat transfer namely normal, enhanced and deteriorated heat transfer. The onset of heat transfer deterioration is tested with Kim et al. correlation as shown in Figure 2.1.11. A new correlation is also derived for predicting the steady state characteristics. Proposed correlation is validated with experimental data and simulation results from present investigations as well as published literature as shown in Figure 2.1.12.

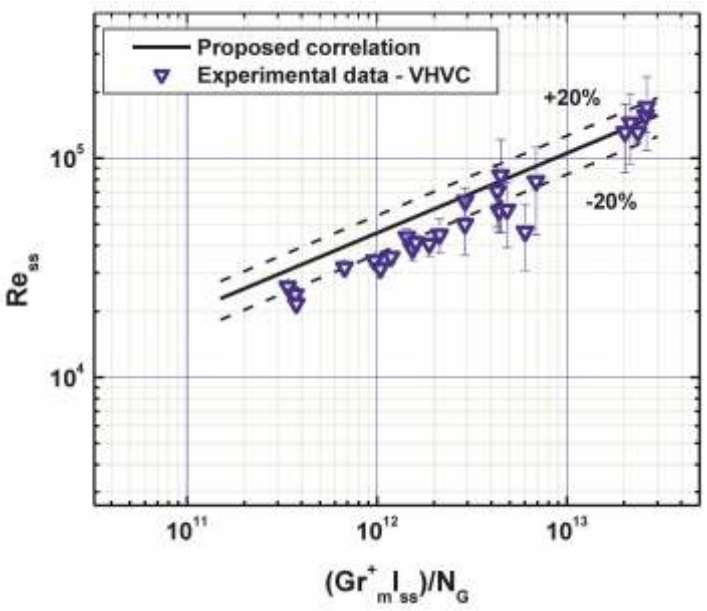

Figure 2.1.12 Validation of proposed correlation with experimental data with VHVC orientation

Comprehensive transient analyses of VHVC configuration of SPNCL are carried out. Various transients include flow initiation, power step up and power step back transients are studied. Effect of geometrical parameters such as pipe diameter, elevation difference between cooler and heater, heater length, cooler length and effect of operating parameters such as operating pressure, power, secondary side coolant flow rate etc. on flow initiation transient are studied.

One of the students worked on evaluation of mechanical properties of structural materials using miniature tensile and small punch test techniques. Miniature specimen test techniques are only options for evaluation of mechanical properties where limited material is available. There are certain issues which need to be addressed for tapping the vast potential of miniature specimen test techniques. In this thesis, issues related to miniature tensile and small punch test techniques have been highlighted; and attempts have been made to address them. Experimental, analytical and metallurgical studies were carried out to determine the minimum thickness and other geometries of miniature tensile specimen which could give tensile properties comparable to those from standard tensile test specimens.

Further, small punch test (SPT) technique has been used for estimating the ultimate tensile strength (UTS) using the load-displacement plot, obtained from a small disk of 3mm diameter and 0.25mm thickness. It is shown that UTS correlation should be based on the load which is corresponding to necking region of the SPT specimen; and not on Pmax value (used by others) of the load-displacement plot. A new UTS correlation, based on the necking region of the SPT disk specimens of 3mm diameter and 0.25mm thickness, has been proposed as UTS=130*$\frac{P_{0.48}}{t_0^2}$ +6.

Aging management of irreplaceable or not easily replaceable equipment is one among the many application areas of miniature test techniques. In this thesis, the methodology has been demonstrated by scooping of small volume of material using a boat sampling device, Figure 2.1.13(a); fabrication of various types of miniature test specimens using electro-discharge machining; Figure 2.1.13(b); and conducting the experiments. Figure 2.1.13(c) and (d) show UTM equipped with Video extensometer and special grips, respectively, for conducting miniature tensile tests.

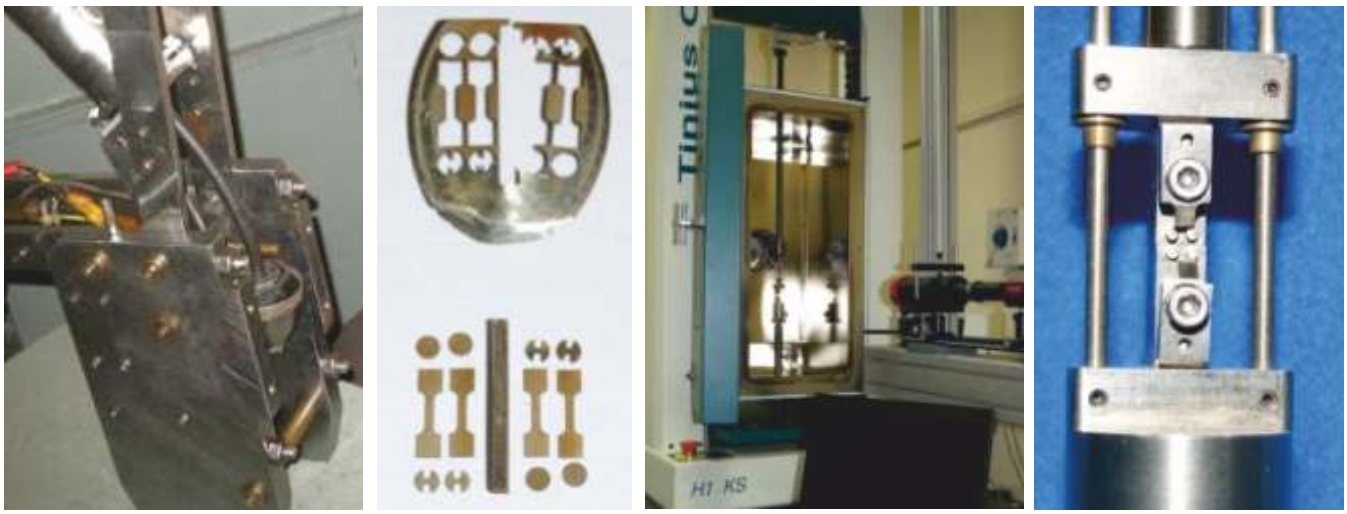

Figure 2.1.13 Boat Sampling Device, (b) Fabrication of Miniature Specimens from Boat Sample of size 25mm width x 40mm length x 3mm thickness, (c) UTM with Video Extensometer for Testng Miniature Tensile Specimens, and (d) Fixture for Miniature Tensile Specimens

Another student worked on investigations towards enhancing power output of a pressure tube type BWR using annular fuel rod cluster. Inside and outside cooled annular fuel pins have significant advantages like reduced peak fuel temperature and actual heat flux. Hence several studies have been reported using annular fuel pin cluster for up rating the power in PWRs. Increasing the power rating also increases the power density and hence reduces the reactor pressure vessel size for the same rating. Exploratory studies have also been carried out for FBRs and GCRs using annular fuel pin clusters. No study is yet reported on their use in BWRs for power up rating. Hence, a study is made using annular fuel rod cluster to enhance the power rating of a vertical Pressure Tube type Boiling Water Reactor (PTBWR). The existing design of the reference PTBWR selected for the study use solid fuel cluster with its maximum power limited to 920 MW. The up rated reactor with annular fuel cluster shall satisfy the Minimum Critical Heat Flux Ratio (MCHFR) criterion besides achieving negative void reactivity and high burnup. As a design objective at least 20 % power uprating was considered acceptable with annular fuel cluster for the reference PTBWR.

The existing thermal hydraulic codes required modification to account for the heat flux and flow split between the inner and outer passages of the annular fuel cluster while the physics codes could be used as it is. Seven annular fuel cluster designs were chosen and examined from physics and thermal hydraulics requirements and finally a 19 pin annular fuel rod cluster shown in Figure 2.1.14 was acceptable. With the selected 19-rod annular fuel rod cluster, a whole core calculation was performed. A coupled neutronic thermal hydraulic

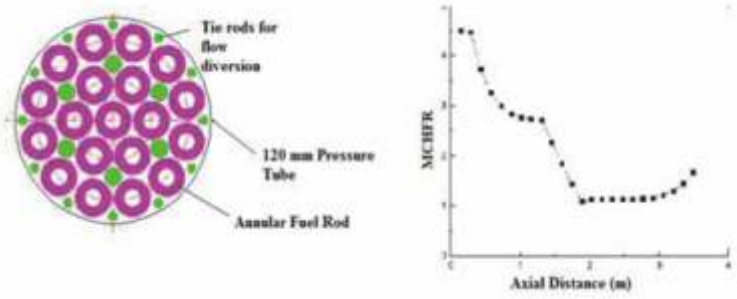

Figure 2.1.14 19 Pin annular fuel rod cluster with MCHFR curve with 23% power uprating

analytical technique was used for the whole core calculations. Reactor physics calculations were carried out by FEMINA and thermal hydraulic calculations were carried out by coupling codes ARTHA and ANUFAN. Power up rating of approximately 23% without any major design modifications in the original design of the reactor could be achieved by the 19-rod cluster. This up rating increases reactor thermal power up to 1132 MW and the burn up to 60,000 MWd/ton. The designed bundle has negative coolant void reactivity and adequate thermal margin.

One of the students worked on determination and validation of fracture properties using small punch test specimens for nuclear reactor materials. This thesis deals with the development of new correlations and methodologies to predict fracture toughness using SPT experimental data. The procedure to calculate fracture toughness using conventional SPT specimen has two steps. The first step is to calculate biaxial-strain at the minimum cross section of the SPT specimen using central deflection measured during punching. The second step is to calculate fracture toughness using biaxial-strain at fracture. In both the steps, the calculations are done using empirical correlations. In the present work, some improved empirical correlations have been developed to calculate biaxial-strain using central deflection and also fracture toughness using biaxial-fracture-strain. The SPT experiments are conducted using number of nuclear structural materials. The proposed correlations are tested using these experimental data.

In addition to proposed empirical correlations, a methodology has been also proposed to generate complete J-R curve of a material using SPT experimental data. The predictive capabilities of the proposed correlations and new methodology are validated against material toughness parameters quoted in the literature determined using ASTM E1820 standard specimens. Present work also addresses determination of crack initiation toughness using pre-cracked SPT, popularly known as p-SPT. A new methodology is suggested to determine crack initiation point during p-SPT experiment by using principles of damage mechanics.

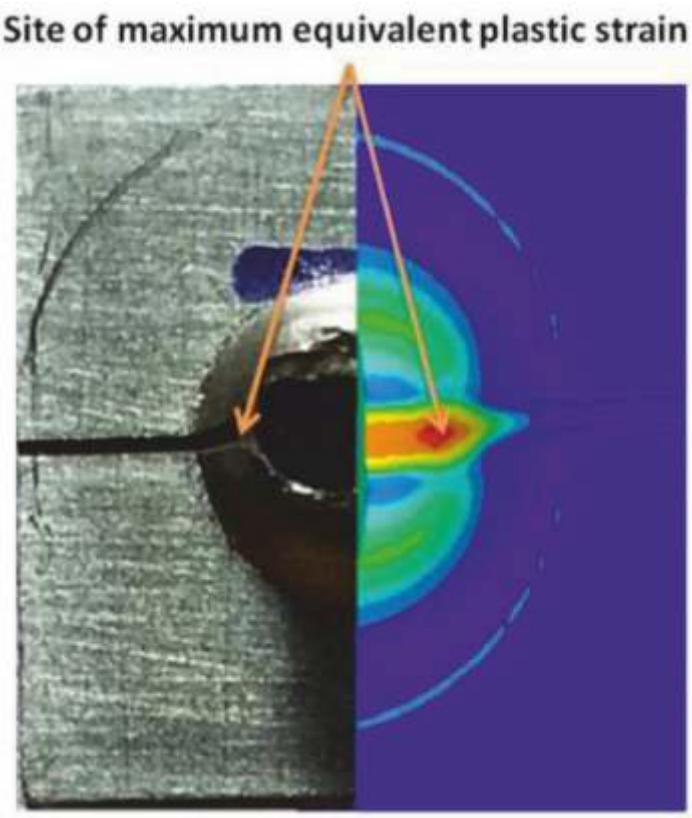

Figure 2.1.15 Location of crack initiation and through thickness fracture of p-SPT specimen at maximum equivalent plastic strain

2.2. Indira Gandhi Centre for Atomic Research (IGCAR)

Cavitation is a phenomenon which occurs in liquid systems when the static pressure at any point in the system falls below the vapor pressure causing vaporization of the liquid. This thesis work entitled “Studies on Cavitation Erosion Resistance of Reactor Materials” is devoted to the study of cavitation erosion produced in reactor materials in liquid sodium environment with specific reference to austenitic stainless

steel SS 316L and its hard faced variants, viz. hard faced with Stellite6 and Colmonoy5. The work done consisted of (a) design and commissioning of a vibratory cavitation system for the study of cavitation damage in liquid sodium (b) modeling of single bubble collapse to estimate the collapse pressure (c) weight loss measurement, SEM examination and surface roughness measurements to evaluate the cavitation damage resistance of the materials tested.

Austenitic stainless steel SS316L and its hard-faced variants (i.e. hard-faced with Stellite6 and Colmonoy5) were tested in sodium at 200°C, 250°C, 300°C and 400°C.

Following are the major conclusions

1. Cavitation erosion resistance of hardfaced coatings is significantly better than that of the austenitic stainless steel 316LN. Hard carbides and borides resists deformation of the surfaces during bubble collapse and this gives the cavitation erosion resistance to hardfaced coatings. In contrast, austenitic stainless steel surface deforms easily under cavitation resulting in damage. Stellite 6 hardfaced coating is more resistant to cavitation erosion than Colmonoy 5 coatings though hardness is higher for the latter. This is attributed to higher fracture toughness and lower stacking fault energy of the former. Transformation of FCC matrix phase of Stellite 6 coating to HCP under stress is another reason for the improved wear resistance of the alloy. All the three alloy systems show an initial increase in cavitation erosion with temperature followed by a decrease in cavitation erosion with further increase in temperature.
2. The evaluation of cavitation damage resistance on the basis of roughness measurement results in a similar ranking of various materials as that from weight loss due to cavitation damage.
3. Modelling of collapse pressure using Gilmore's equation shows that collapse pressure increases marginally between 200°C and 300°C and decreases on further increase in temperature. This trend is similar to that observed in the variation of weight loss rate with temperature.

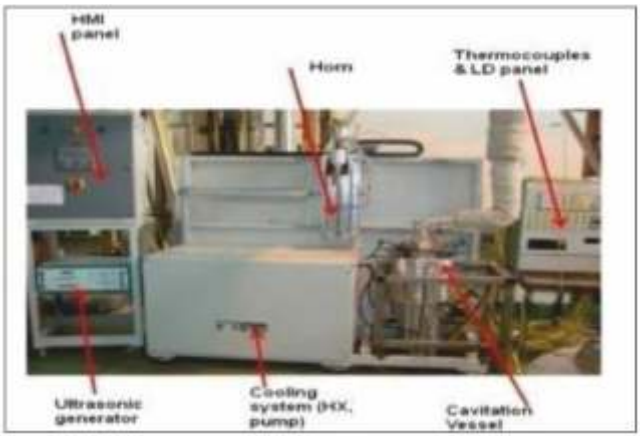

Figure 2.2.1 Ultrasonic vibratory cavitation device

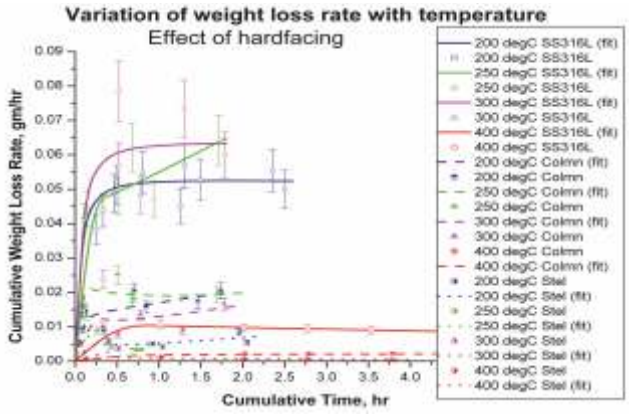

Figure 2.2.2 Comparison of weight loss from cavitation damage

The identification of slow occurring events in a nuclear power plant can be achieved using supervised classification algorithms. These algorithms are basically machine learning algorithms which uses historical data sets which is huge in number and processing such amount of data is computationally complex. In order to reduce the complexity of the classifier, reduction in the data size is achieved by discarding the

irrelevant features and samples termed as dimensionality reduction. Principal component analysis (PCA) is one such technique which is elucidated in the thesis. In PCA, the features are transformed into another dimension and arranged in the decreasing order of their eigen values of the covariance. The screen plot is used to select the boundary beyond which the features are discarded as they have very less eigen values which means they hardly contributed towards the covariance. It is experimentally demonstrated that classification of some of the malfunctions occurring in the steam water system of a sodium cooled fast reactor, is more accurate by undergoing dimensionality reduction up to 40% using PCA. In another approach, reduction in the sample size is experimented using training dataset reduction where the samples are discarded whose euclidean distance is beyond a hypothetical boundary. This approach produced better accuracy by reducing sample size up to 60% of the original size.

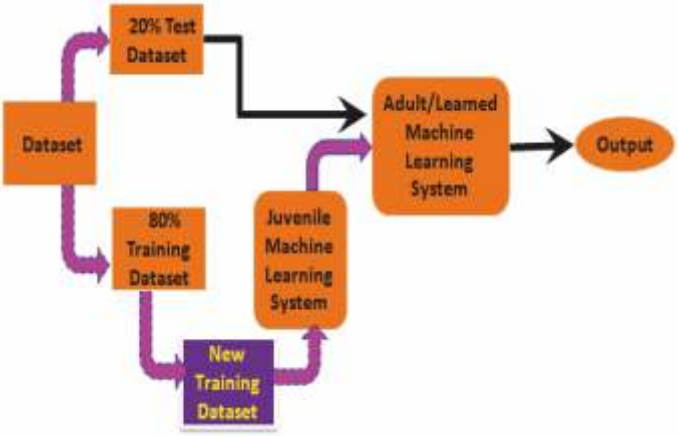

Figure 2.2.3 Block diagram of preprocessing of dataset for supervised classification problems

Another common issue associated with any classification dataset is the problem of imbalanced dataset. Traditionally, the classification accuracy is biased towards majority class thereby neglecting the minority class. One of the solutions to such problem is oversampling of the minority class samples known as synthetic minority oversampling technique (SMOTE), wherein, each minority sample generates equal number of synthetic data in order to make the dataset balanced. In the thesis, a modification to SMOTE which solves the imbalanced dataset problem, termed as weighted SMOTE is studied. In this algorithm, instead of oversampling each minority sample with same amount of synthetic data, different weights are assigned to each minority sample. Based on the weights assigned, the generation of the amount of synthetic data varies for each minority sample. Finally, the performance of the weighted SMOTE on various real world imbalanced datasets along with nuclear power plant events produced better result compared to the traditional SMOTE.

Spallation target cooling in cyclotrons involves high heat fluxes of the order of 15 MW/m^2. From a comprehensive literature review it is found that for high heat flux applications jet impingement method can be used. Helium jet impingement cooling has been selected for heat removal up to about 1 kW. Even though the amount of heat removal is less, helium cooling system is a simple system due to its non-radioactive nature. First an experimental facility has been established to carryout various jet cooling experiments with air as the cooling medium. The air flow rate was varied from 0 to 15 m^3/hr. Thin specimen of the order of 20 mm x 20 mm x 0.5 mm have been heated by joule heating. Using the experimental facility various

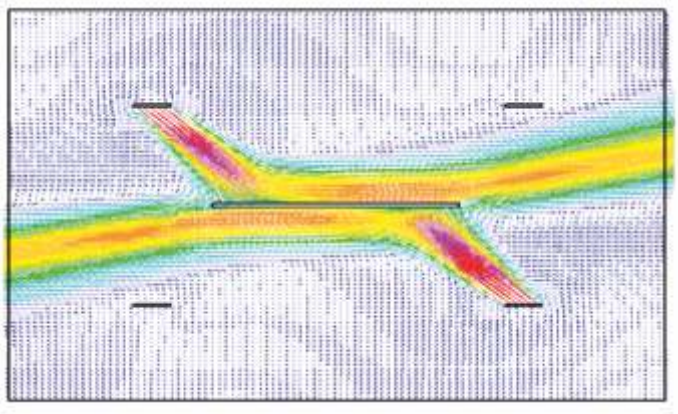

Figure 2.2.4 Velocity distribution for two jets at 450 one on each side

single and multi jet air cooling experiments have been carried out. Slot jet and single array of circular jet nozzles have been used. Temperature measurements have been carried out using thermocouples and infrared thermal imaging technique. The jet cooling phenomena are also simulated numerically using two-dimensional computational fluid dynamic analyses. Commercially available CFD code is used for this purpose. An investigation of the performance of various turbulence models shows that prediction of heat transfer behaviour by eddy viscosity models, viz., k-e and k-e RNG are close to those predicted by Reynolds Stress models and large eddy simulation. Parametric study by varying the distance between jet and target plate has also been performed to ascertain the influence. Studies on multiple inclined jets impinging on a target plate show that the interaction between jets makes the thermal hydraulic behaviour unsteady. Flow from one jet is found to mask that from the other jet. Hence, the heat transfer is not that effective compared to that in the case of vertical jet impingement. As the inclination of the jet approaches towards vertical, the heat transfer coefficient increases. However, even with two impinging jets, 60^{o} inclined to horizontal, the predicted heat transfer coefficient is less than that of single vertical jet. From the correlations available in literature, Martin correlation is selected and is compared with the experimental as well as numerical results. Further, the CFD studies indicate that cooling by two jets one on either side is more effective in heat removal compared to four jets on all the sides due to the effect of spent flow. This configuration also gives low temperature difference across the sample. Multi air jet experiments also confirm that two jet cooling gives higher heat transfer coefficient compared to four jet cooling and also more uniform temperature distribution across the specimen. Hence this configuration is recommended for spallation target cooling in cyclotrons.

The rotary angular position and speed of a motor shaft are important to sense and control various motor drive systems. Positional sensors and their associated converters are used to extract these parameters. Traditionally, synchros have been used in harsh environments involving noise, high temperature and vibration. Further, Fast Breeder Test Reactor (FBTR) experience for the past 30 years with successful synchro operation as positional sensor is the prime motivation towards this work. At present Synchro-to-Digital Converter (SDC) is increasingly used for precise measurement of rotary position, such as control rod, guide tube, gripper assembly etc. in fast reactor programme.

Firstly, this work highlights the functional simulation of synchro and SDC.It is useful in non-ideal characteristics study of synchro & their impact on angular measurement of SDC. A novel approach (shown in Figure 1) based on Pulse Width Modulation (PWM) is implemented to compute angular position and speed of synchro shaft. The basic idea of the scheme is the linear evaluation of peak amplitudes of synchro signals using Time Duration Windows (TDW) and division of TDWs followed by the inverse tangent operation to get rotor shaft angle.TDW is the time gap between rising edge of triangular signal and falling edge of PWM signal in every cycle of V_S (or) V_C.This method utilizes simple components and the computation of speed of rotor shaft doesn't require any separate

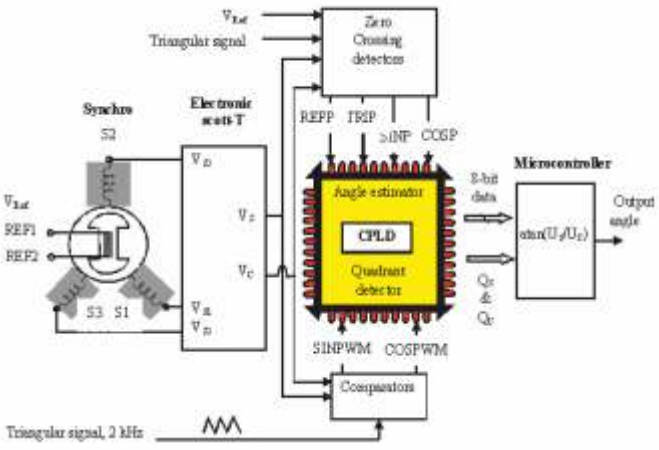

Figure 2.2.5 Block diagram of hardware implementation of SDC

circuit since the sine quadrant bit (Q_S) of quadrant detector itself provides speed information. Hence, it is cost-effective.

In addition, the diagnostic features such as Loss Of Signal (LOS) and stator terminal reversal connection detections between synchro and SDC coming as special features for modern converters are implemented. A practical SDC is developed and tested. From experimental results, the prototype SDC exhibits good linearity over 0^0-360^0 and this converter finds an application in motor driven mechanisms rotate at low speeds. The prognosis of synchro failure and wireless transmission of synchro shaft angle are other focus areas as future directions.

One of the students investigated into the fail safeness of safety critical instrumentation and control in a Sodium cooled fast reactor. This thesis proposes a novel method to detect "contact weld failure" of electromagnetic relay which helps in online diagnostics without disturbing the load connected to the relay contact. This method is online, continuous, automatic and facilitates simultaneous of redundant channels.Diagnostic method works on the principle of de-energizing followed by quick re-energization of relay coil before the contact starts moving apart. Further, the practical implementation and verification of relay contact weld detection circuit without any impact on functional circuit is verified with a relay output card as shown in Figure 2.2.6.

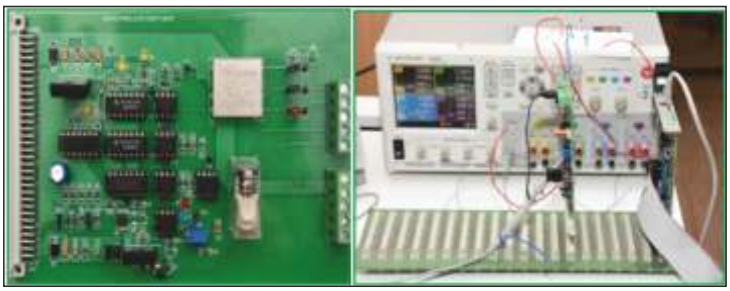

Figure 2.2.6 Experimental setup of weld detection circuit

Markov model is developed to demonstrate reduction in unsafe state probability of the system. The study has been shown that failure probability of each redundant channel is significantly reduced with this diagnostic technique.

Reliability demonstration testing as per MIL-HDBK-781A is carried out to confirm the failure data of EM contactor. Failure analysis of degraded contacts is performed with SEM and EDS. The impact of EM contactor failure on uncontrolled withdrawal of neutron absorber rods in Prototype Fast Breeder Reactor (PFBR) is analyzed. Inherent fail-safe circuits do not require diagnostics since any of the failures in the circuit will automatically lead to a safe state of the final control element. A novel inherently fail-safe AND gate is proposed. The basic idea is that energy is extracted from first input pulses through a pulse transformer and stored as DC in a capacitor. This, in turn, provides required current for the second input pulses to get transmitted further. An inherent fail-safe pulsating electronic logic based valve drive circuit with the AND gate is designed for a decay heat removal system.

2.3. Variable Energy Cyclotron Centre (VECC)

The requirements of low noise instrumentations for the detection of weak RF signal has found applications in several fields such as charged particle detection, beam diagnostics, atomic and nuclear spectrometry etc. Now a days, Penning ion trap has become one of the fundamental tools for carrying out high precision studies in the field of spectroscopy physics. At Variable Energy Cyclotron Centre (VECC), Kolkata, a Penning ion trap facility is developed to carry out precision measurement to address basic physics problem of fundamental significance. In this facility, initially cloud of electrons is trapped and their axial signal (~ 63 MHz) is detected using a high quality factor (Q) resonant LC circuit (tank circuit) and a low noise amplifier (LNA) with high input impedance as shown in Figure 2.3.1(a).

This thesis mainly focuses on the investigation of various engineering aspects related with the design and development of low noise detection circuit for VECC Penning ion trap. In this thesis, the detailed design and implementation of an inductively tuned common source amplifier is presented. An improved model of the amplifier is proposed which provides correct prediction of bandwidth enhancement due to a given load inductance and operating conditions of the amplifier. A 3-dB bandwidth of ~ 200 MHz is achieved with this amplifier. The input voltage noise density of the LNA is found to be ~ *2nV/√Hz*.

In this thesis, we have also proposed a novel scheme for in-situ trap capacitance measurement and excitation of trapped particles using an indigenously developed Colpitts oscillator. Using this oscillator, the capacitance of Penning ion trap electrodes as well as the overall system capacitance is measured. Based on the measured capacitance, a high Q resonant circuit is realized in the form of a quarter wave helical resonator. The effect of system capacitance on the performance of the resonator is simulated and experimentally verified. A loaded Q ~ 115 at a resonant frequency of ~ 61 MHz is achieved when the resonator is coupled with the ion trap and LNA. With the coupled detection circuit, cloud of trapped electrons is detected. The detailed results of the detected axial signal with variation of different trap parameters are presented in this thesis.

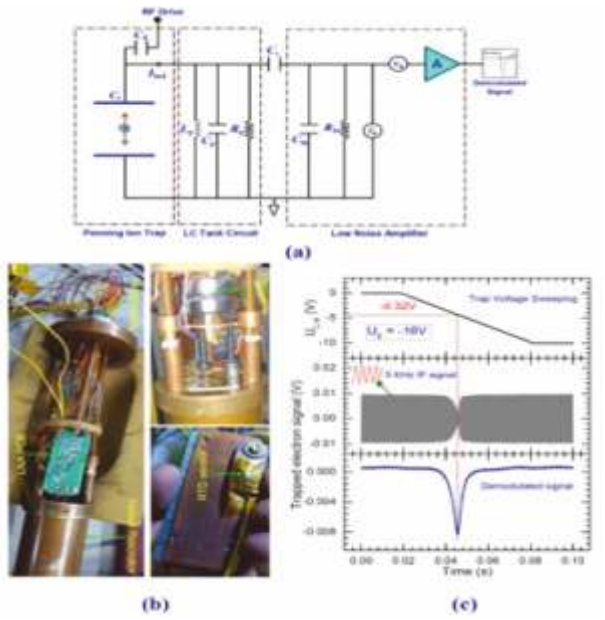

Figure 2.3.1 (a) Detection scheme in Penning ion trap

(b) Penning ion trap setup at VECC(c) Detected absorption signal of trapped electrons at VECC

Due to the dramatic increase of data volume in the modern High Energy Physics (HEP) experiments, a robust high speed data acquisition system (DAQ) is very much needed to gather the data generated during different nuclear interactions. As the DAQ works under harsh radiation environment, there is a fair chance of data corruption in different modules of DAQ system due to various energetic particles like alpha, beta or neutron. Hence, a major challenge in the development of DAQ in HEP experiment is to establish an error resilient communication between front-end sensors or detectors and back-end data processing computing nodes and to provide error mitigation techniques to different devices used in the DAQ chain.

Here we have developed a prototype of the DAQ system for MUCH detector system as shown in Figure

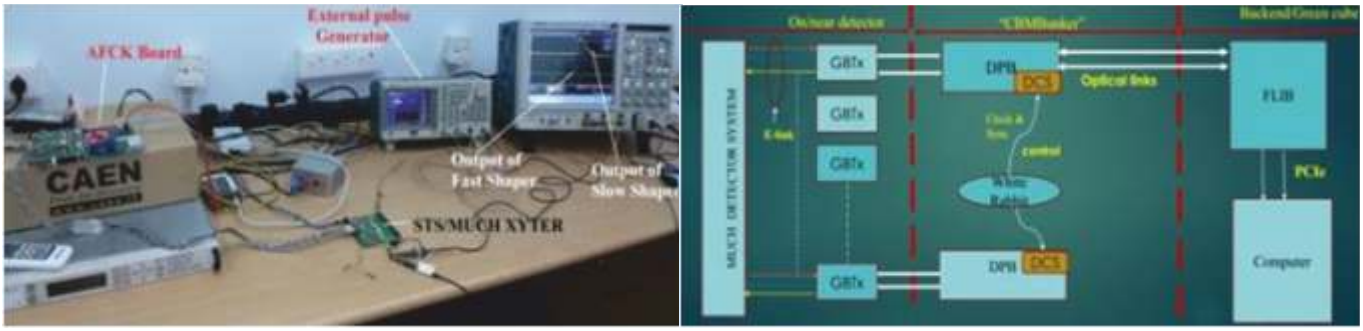

Figure 2.3.2 (a)Testing setup of MUCH-XYTER in VECC (b) Reaout chain of MUCH detector system

2.3.2 (b). DAQ system for MUCH detector consists of front end ASICs also known as MUCH-XYTER that will accept the data directly from the detector, Gigabit Transceiver (GBTx) Board, Data processing board (DPB) and First level interface board (FLIB). MUCH-XYTER and GBTx ASIC are placed near the detector and should be radiation hardened by both logical and physical design. Data from the highly radiated experimental cave will be sent to the DPB using optical fiber at the data rate of 4.8 gbps and DPB is connected with FLIB using 10 Gbps optical link. Finally data from FLIB will be sent to computer using PCIe where further data analysis will be taken place. DPB and other backend computing nodes are placed in the control room where radiation level is less compared to the experimental cave bt higher than the normal environment. Here we will use commercial FPGA to implement functionalities of DPB and FLIB and there is fair chance that their functionalities will be hampered by the soft error in the configuration memory of FPGA devices. We have used different error detection codes like modified matrix code, evenodd code along with dynamic partial reconfiguration and hardware scheduling algorithm to mitigate soft errors in the configuration memory of FPGA devices without hampering its normal operation. We have used highly densed solid state memory devices like multi-level (MLC) flash memory to store user data. With the increase of memory density probability of f ormation of adjacent MBUs or clustered error increases. Here we have proposed a novel product code using shortened block code as component code to mtigate the effect of clustered error in MLC flash memory and the proposed code has simple decoding structure and low error correction latency.

3. Health Sciences

During the period, HBNI has awarded Ph.D. degree to two students in Health Sciences on successful completion of academic programmes. Research topics are in the area of oncology. Highlights of the doctoral theses are outlined below.

3.1. Tata Memorial Centre

Gallbladder cancer is one of the most common cancers in the North and North-east India. The disease is highly lethal and 5 years survival rates were reported to be 5%. There are no large scale studies globally or within India to understand the aetiology of gallbladder cancer. The doctoral thesis in the area of health sciences titled “Risk factors for Gallbladder Cancer in India” is the first study to demonstrate the role of a few lifestyle related factors in development of gallbladder cancer. The major highlights of the work are as follows.

- It is observed that the place of birth is an important risk factor and that increased risk persisted even after migration from high risk to low risk regions, indicating the probable role of both gene and environment. Thus, large scale genetic studies required to understand the role of genetic factors and their interaction with environmental factors in development of gallbladder cancer.
- Higher waist-to-hip ratio was observed to increase risk of gallbladder cancer. Higher body size in early childhood and /or adulthood was associated with increased risk of gallbladder cancer.
- Higher consumption of fruits and vegetables was associated with reduced risk of gallbladder cancer. Use of mustard oil as cooking medium observed to increase the risk of gallbladder cancer.
- This is the first study globally to demonstrate the role of bidi smoking and tobacco chewing in development of gallbladder cancer. The attributable risk for developing gallbladder cancer has been estimated as 8% for bidi smoking and 11% for tobacco chewing.
- Study also confirms increase in risk with history of gallstone and higher number of pregnancies.

- No statistical significant association was observed between serum level of H. pylori antibodies and gallbladder cancer.
- The study provides strong evidence for prevention of gallbladder cancer by tobacco control, central obesity reduction, and moderate consumption of mustard oil and fresh fish.

Another thesis is titled as "A study of survival in oral cavity cancer patients". This study is one of the few Indian studies to comprehensively analyze and present a holistic picture of oral cancer survival in patients treated at a premier cancer hospital of India. This study shows that oral cancer mortality may be reduced if lesions are detected, diagnosed, and treated at an earlier stage. The survival rates of 5-year were better in patients with the early stages of OSCC (Oral Sqamous Cell Carninoma) than in those with the advanced stages. Therefore, it is concluded that the periodic screening of high risk populations for OSCC and early treatment may appreciably reduce oral cancer mortality in India. Thus, promotive and preventive public health approach holds the key to reduce the OSCC burden in India. Contrary to what is generally accepted socio-demographic factors such as education and marital status were not found to affect oral cancer survival in our study. Similarly, various time periods involved in evolution of cancer treatment in the hospital namely, time for diagnosis, treatment initiation, treatment completion and overall treatment time were not found to influence overall survival. Furthermore, cancer as a disease bears such an intense burden that role other chronic comorbities is often undermined, but our study shows that presence of co-morbidity has a significant influence on outcome of oral cancer patients. In addition, this is the only study in India to report prognostic role of heamatological parameters such as neutrophillymphocyte ratio (NLR) and monocyte counts in oral cancer patients. Given the low cost, easy accessibility, and reproducibility of a full blood count, both NLR and monocyte counts seem promising candidates for use in clinical practice. Finally, the study demonstrates that, in addition to TNM classification other clinical and pathological factors also have a significant role in predicting survival. Therefore, although the TNM classification harbors very important clinical information the role of other factors viz tumor differentiation, extracapsular spread and perineural invasion cannot be ignored and hence, there is a need to develop a more powerful and precise modular prognostic system that will not only be reliable and reproducible but also flexible and easy to use.

4. Life Sciences

During this period, HBNI has awarded Ph.D. degrees to 22 students in Life Sciences on successful completion of academic programmes. Research topics are from a variety of areas including multianalyte immunoassays, host directed therapeutics, radiation biology, biophysics, cancer cell biology, cancer epigenetics, cancer biology, protein biochemistry & structural biology, cancer genomics, stem cells & cancer, carcinogenesis & chemoprevention, cancer chemoresistance and drug delivery. Highlights of a few doctoral theses are outlined below.

4.1. Bhabha Atomic Research Centre (BARC)

The demand for rapid and reliable measurement of multiple analytes in clinical samples to increase the diagnostic specificity and sensitivity has encouraged the development of multianalyte immunoassays (MAIA). In this thesis, using thyroid diagnosis as a model, the student has studied the requirements for developing a MAIA for T4, TSH and Tg, with the required sensitivity and specificity. I-125- labelled antigens and antibodies, were used for detection, since they were readily available and easy to prepare in the RIA lab. Suitable polyclonal/monoclonal antibodies with the required specificity, affinity and titre were produced/procured and used. MAIAs were designed using the competitive assay format for T4 and non-

competitive assay formats for TSH and Tg. Selection of appropriate solid support and reproducible surface chemistry are important for antibody-chip fabrication, and microporous, polycarbonate track-etched membranes (TEM) was found to be an excellent and novel support for MAIA. Three different MAIA panels were developed (i)T4 and TSH (ii) TSH and Tg (iii) T4, TSH and Tg. MAIA panels were validated for all the QC parameters required for immunoassays. All analytes gave satisfactory dose-response curves with required

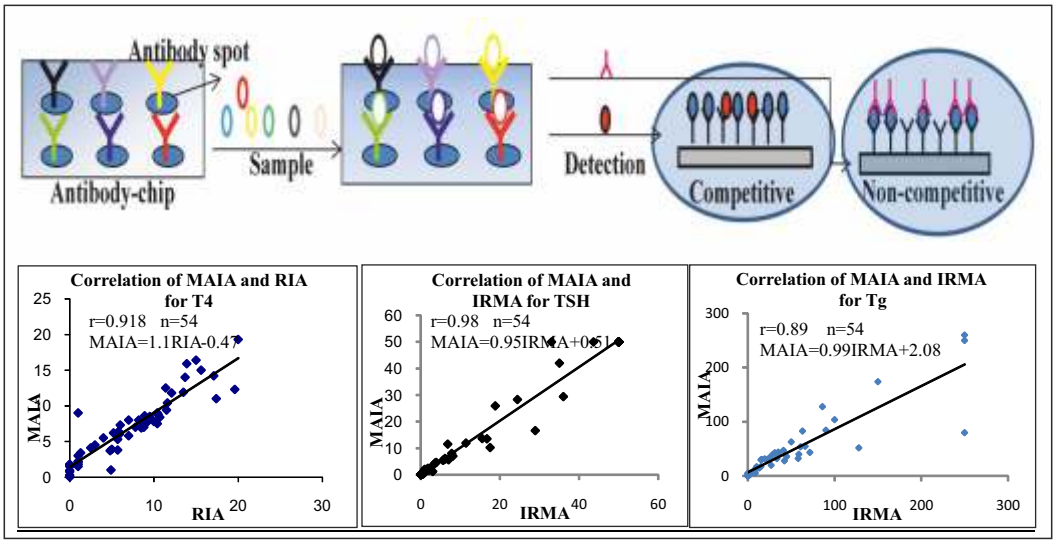

Figure 4.1.1 Schematic illustration of principle of MAIA and comparison of T4, TSH and Tg concentration in fifty-four human serum samples measured by MAIA & RIA/IRMA.

sensitivity and working range that is acceptable for clinical use. Cross interference between antibody spots was found to be insignificant for all MAIA panels. Comparison of estimates by MAIA and RIA/IRMA was done for a sufficiently large number of patients' samples and statistically analysed using correlation and regression tests. The results showed the MAIA method to be correlated very well ($p<0.01$) to individual RIA/IRMA tests. Further regression analysis showed the slope to be close to unity (as expected) with small intercepts. Since the antibody-chip and related experiments were done manually, the error factor is somewhat higher, but within acceptable limits. The thesis work has provided proof of concept for the hypothesis that MAIA is technically viable, and has shown that the MAIA for T4, TSH and Tg has performed comparably with the estimates obtained individually by RIA/IRMA, MAIA can save on assay time, assay costs and patients' sample required.

In another thesis entitled “Evaluation of in vitro and in vivo radioprotection and cytotoxic activities by novel selenium compounds”, dihydroxy selenolane (DHS), a water soluble organoselenium compound was evaluated for its radioprotective activity involving cellular and in vivo model systems. The study indicated that intraperitoneal administration of DHS improved 30 days survival of the mice and inhibited radiation induced inflammatory responses in radiosensitive organs. The anti-

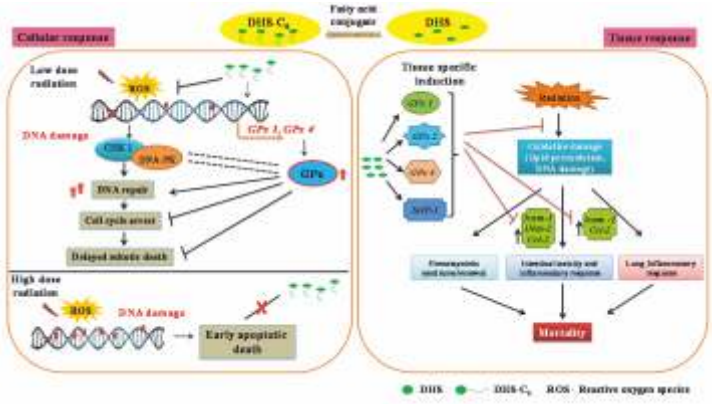

Figure 4.1.2 Proposed model for the radioprotective effect of DHS / DHS-C6

inflammatory effect of DHS was attributed to increase in the activity of glutathione peroxidise (GPx) and the reduction in levels of lipid peroxidation and pro-inflammatory genes. DHS-C6, a lipophilic derivative of DHS exhibited better antioxidant and radioprotective activity compared to DHS in CHO cells. DHS and DHS-C6 protected cells from radiation induced delayed mitotic death. This effect was associated with their abilities to augment DNA repair and prevent G2/M cell cycle arrest in a GPx dependent pathway. Taken together, our study proposes that selenium compounds mimicking GPx like activity may be a good candidate to reduce radiation induced inflammatory response.

Highly toxic strains of L. sphaericus (Ls) have proved to be highly efficient and eco-friendly mosquito larvicide. Their toxicity is mainly due to BinAB (binary) proteins that exist as a parasporal crystal in the bacterium. BinA (the toxic component) and BinB (the receptor binding component) recognize a specific receptor, Cqm1. Narrow target specificity and development of resistance among mosquitoes is limiting potential of binary toxin for extensive application. Also mechanism of action of the toxin is not established. The focus of studies world-over has been to develop more effective bacterial strains and to elucidate mechanism of larvicidal toxicity of BinAB. This thesis entitled “Molecular mechanism of action of Lysinibacillus sphaericus Binary toxin protein components” highlights some of these key aspects.

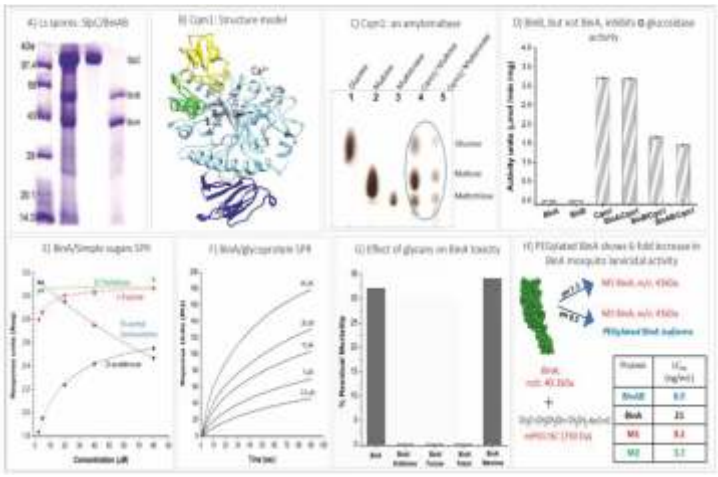

Figure 4.1.3 Understanding mode of action of BinAB toxin from Ls

It clearly establishes that larvicidal activity of Ls spores is attributed by binary toxin only. The other high molecular weight protein co-existing in the Ls spores is the surface layer coat protein, SlpC (*Panel A*), and not the oligomer of binary toxin. The SlpC displays poor toxicity against Culex larvae, as compared to BinAB. A detailed biophysical and biochemical characterization of the recombinant receptor protein (Cqm1) from Culex (*Panel B*) is also presented in the thesis.Recombinant Cqm1 protein exists as a stable dimer, which is consistent with its apical localization in lipid rafts.The thesis reports for the first time that Cqm1 is an amylomaltase with high glycosyltransferase activity (*Panel C*). This is suggestive of its role in carbohydrate metabolism in mosquitoes and can be explored as a potential target for mosquito control. The thesis also establishes that reduction in the catalytic activity of Cqm1 is not responsible for the larvicidal activity of binary toxin as the non-toxic BinB component, and not BinA, reduces the catalytic activity of Cqm1 to half (*Panel D*). The present thesis suggests that BinA-mediated intracellular cytotoxicity may involve BinA specificity against structurally diverse glycans (*Panels E, F, G*). The present thesis also discusses a novel approach of PEGylation resulting in successful enhancement of BinA larvicidal activity by six-folds (*Panel H*). The chemical modification improved thermal and enzymatic stability without affecting the native structure of BinA.

Keratin 8/18 (K8/18), a simple epithelia specific keratin pair, is aberrantly expressed in squamous cell carcinomas (SCCs) where it's expression is correlated with increased invasiveness and poor prognosis.Apart from its mechanical role,K8/18 is known to execute various regulatory functions. Majority of these functions are governed by its post translational modifications, most importantly; phosphorylation

at Serine[73] (Head domain) and Serine[431] (Tail domain) residues. Previous reports from our laboratory have shown a significant role of K8 and its site specific phosphorylation in neoplastic progression of oral SCC derived cells. Apart from our lab, few other groups have also shown deregulation of K8 and its phosphorylation to be associated with progression of different carcinomas, although its role in skin SCC and the underlying mechanism is still obscure.

In this thesis entitled "Role of keratin 8 phosphorylation in neoplastic progression of squamous cell carcinoma", it has been shown that loss of K8 leads to substantial reduction in tumorigenic potential of skin SCC derived A431 cells. The total quantitative proteomics data showed differential expression of many proteins including TMS1, MARCKSL1, RanBP1, 14-3-3 gamma, CDK6, RhoGDI2 after K8 knockdown. Further IPA analysis followed by functional validation showed two major pathways i. e. "cell death and survival" and "cellular movement" to be altered upon loss of K8. Furthermore, TMS1-NFκB-K17 degradation and MARCKSL1- Paxillin1-Rac axis were found to be the possible mechanisms associated with the above mentioned biological pathways, respectively. These findings substantiate the role of K8 in tumourigenic potential of skin SCC together with the probable mechanism involved. In addition to this re-expression of K8 wild type, phosphodead and phosphomimic mutants in K8 null background followed by TMT based quantitative phosphoproteomicsrevealed differential regulation of phosphoproteins associated with migratory, proliferative and invasive potential of these cells. These findings were also supported by subsequent phenotypic and biochemical validations emphasizing the probable role of site specific K8phosphorylationin neoplastic progression of A431 cells.Besides this,earlier reports have indicated a context dependent function of K8 phosphorylation in various carcinomas arising from different tissues. Therefore to elucidate the exact role of K8 phosphorylation in skin SCC, tissue specific transgenic mouse model expressing K8 wild type and phosphomutants were developed. These mice were then subjected to DMBA/TPA mediated skin carcinogenesis. The preliminary results of this experiment showed an early onset of tumors in K8 wild type expressing mice in comparison to K8S73A and K8 S431A expressing mice. In conclusion, the current study accentuates the role of K8 and its phosphorylation in neoplastic progression of skin SCC and also provides many new leads related to the possible mechanisms underlying this phenomenon.

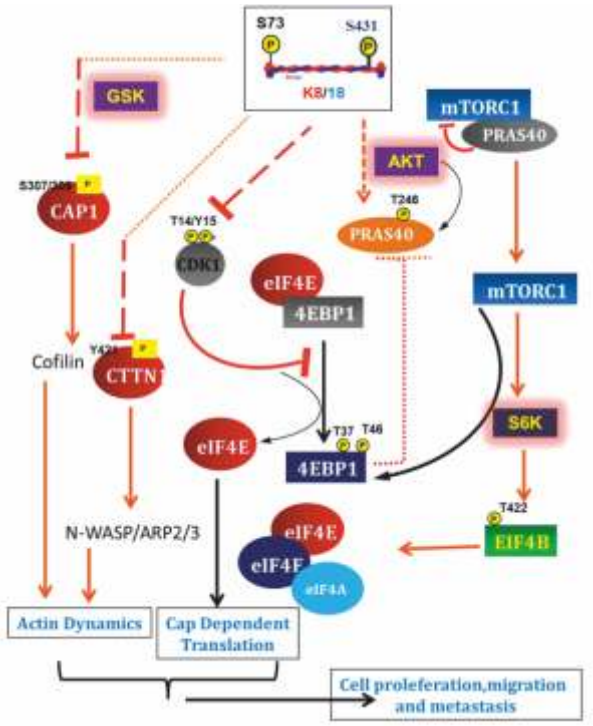

Figure 4.1.4 Keratin 8 phosphorylation regulates tumorigenic potential of skin SCC derived cells by altering an array of signaling pathways.

4.2. Tata Memorial Centre (TMC)

Histone isoforms and variants have been reported to be differentially expressed in various patho-physiological states including cancer. However, is there any correlation between them and do they work together for the attainment of such a state inside the cell have not been investigated yet. Moreover, previous reports have emphasized only on individual changes in the variant and or isoform profiles and

have not looked in depth into dysregulation of respective PTMs, chaperones and their interactors inside the nucleosome.

The work done in this thesis provides insights into these aspects of cancer epigenetics and also provides a novel strategy to circumvent the challenges faced during epi-drug based chemotherapeutic treatment in cancer patients.

Histone variants, H3.3 and H3.2 are dysregulated in HCC with H3.2 showing increased and H3.3 a decreased expression at both protein and transcript level. H2A isoforms and H3 variants are able to interact with each other, however, the nucleosomes formed from these combinations differ in stability with H2A.1/H3.2 being most and H3.2/H2A.2 least stable. Similar to the changes seen in H3 variant profile, there is a loss of histone activation PTM marks and a gain in repressive PTM marks not only in tissue samples but also in serum histones isolated by use of a developed novel technique. Further, tumor cells have pronounced heterochromatin and show a global gene repression. Histone H3.3 knock down led to compaction of chromatin, global transcriptional repression and elevated cell proliferation and clonogenic potential of cells similar to like a state of cancer cell. The balance of H3.3 and H3.2 acts as the master regulator governing the expression of various tumor suppressor genes either directly or indirectly, therefore, altering the expression status of these variants by H3.3 knockdown lead to attainment of cancer state by modulating the global epigenome profile of the cell.

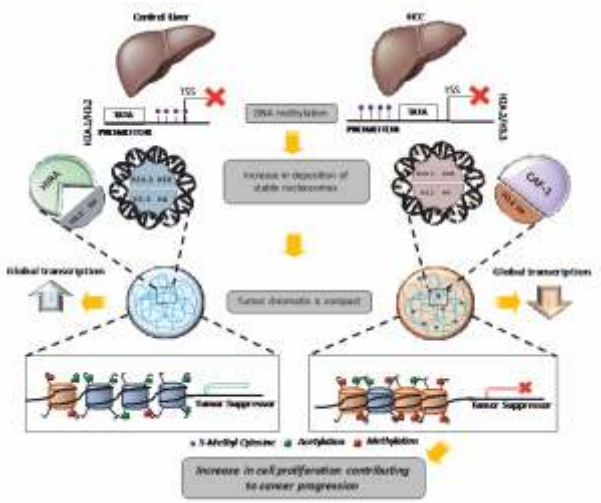

Figure 4.2.1 Depicts the changes in DNA methylation pattern governs expression status of histones and thus affecting chromatin compaction, transcription of tumor suppressor genes, influencing cell proliferation and influencing cancer progression.

Oligodendroglioma is one of the histologically defined subtypes of gliomas along with Astrocytoma and Oligoastrocytoma. Histopathological classification of glioma subgroups suffers from high intra-observer and inter-observer variability. Exome sequencingof oligodendrogliomas identified 10 to 46 somatic mutations in each tumour, that included recurrently mutated genes like IDH1, CIC, NOTCH1, FUBP1, MAML3, KRAS and ARID1A. Analysis of the exome sequencing data and copy number analysis of 251 adult grade II/III gliomas from the TCGA cohort identified three molecular subtypes indicating the need for molecular classification for accurate diagnosis. Homology modeling showed that the non-synonymous mutations in the CIC gene located in the exon 5 affected highly conserved amino acid residues that would be most proximal to DNA in the PDB derived co-crystal structures of the HMG domain bound to DNA. Transcriptome profiling of the CIC-mutant compared to that of CIC-wild type oligodendrogliomas showed significant upregulation of the ETV transcription factors viz. ETV1, ETV4, ETV5 as well as a number of negative regulators of the Receptor Tyrosine kinase / MAPK pathway indicating role of this signaling pathway in the pathogenesis of oligodendrogliomas. Analysis of chromosome 1p/19q codeleted 65 gliomas from the Cancer Genome Atlas Cohort (TCGA) further confirmed this finding. Thus, comparative transcriptome analysis suggests activated RTK/RAS/MAPK pathway to be a major driver of oligodendroglioma pathogenesis.

Fanconi Anemia pathway is activated specifically when DNA intercrosslink (ICL) damage occurs inside the cell. FA- pathway proteins comprises eighteen complementation groups of proteins which act in a common pathway to facilitate the DNA ICL repair. FANCI and FANCD2 together forms FANCI-FANCD2 complex known as I-D complex. These proteins also work independently and have multifunctional role in cellular milieu. However, not much have been explored at structural and functional level. In this dissertation, FANCI-FANCD proteins are structurally and functionally characterized, furthermore, protein-protein interactions analysis between FANCI, FANCD2 and BRCA2 were analyzed. It has been observed that FANCI ARM repeat protein is composed of α-helices and has stable and dynamic region. It also has DNA binding properties, and Helix-Turn-Helix (HTH) motif with conserved PHS signature. HTH motif is highly dynamic and binds to major groove of DNA with conserved amino acids. In FANCD2, the coupling of ubiquitin conjugation to endoplasmic reticulum domain (Cue domain) and its pathogenic Leu231Arg mutant were characterized, and observed that FANCD2 Cue domain wild-typehas more α-helicity and stability compare to Leu231Arg mutant. Since, it is ubiquitin binding domain, so protein-protein interactions studies using surface plasmon resonance (SPR) were performed. SPR data suggest that wild-typehas more specificity and affinity towards mono-ubiquitin unlike Leu231Arg mutant.Molecular dynamics data shows that wild type has less fluctuation and overall structural rearrangements than the mutant. Docking studies suggest that wild-typebind conserved hydrophobic patch of mono-ubiquitin unlike mutant.Furthermore, to get an idea of the commonness of FA-BRCA pathway, we performed protein-protein Interactions (PPIs)analysisbetween FANCI ARM repeat, FANCD2 Cue domain and BRCA2 C-terminal region using bacterial two hybrid assay. It has been observed that FANCD2 Cue domain interacts with BRCA2 CTR and FANCIARM repeat.These results presented in this thesis suggest that the functionaldomains present in FANCI, FANCD2, and BRCA2 play an important role in PPIs, and pathogenic mutation causes the binding impairment. In conclusion, protein – protein interaction network between different domains of

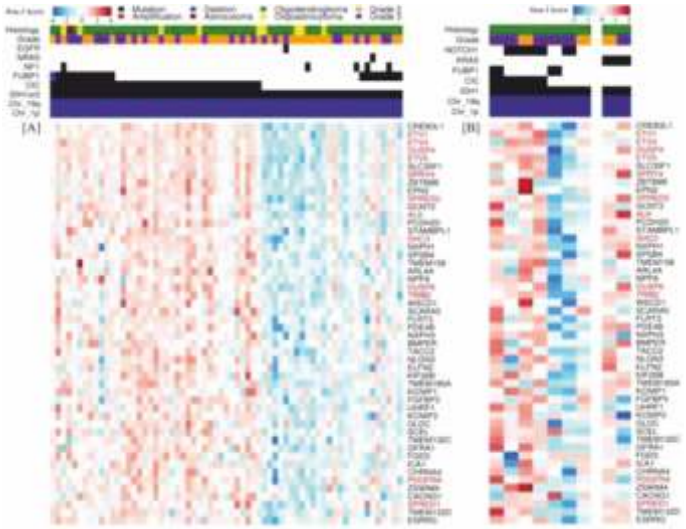

Figure 4.2.2 Heat map showing the top 50 genes most significantly differentially expressed in the CIC-mutant tumors in the TCGA cohort(A) and from the present study cohort (B).

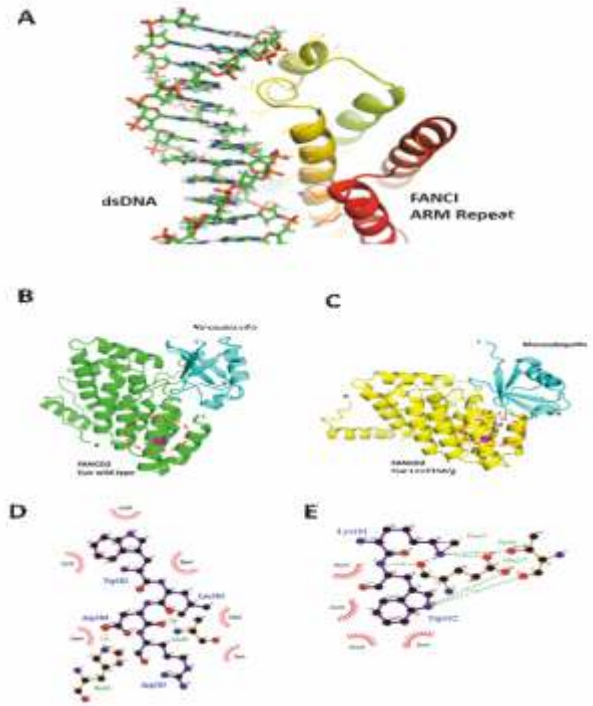

Figure 4.2.3 (A) FANCI ARM repeat interactions with major groove of dsDNA (B,D) FANCD2 Cue Domain interactions with monoubiquitin (C,E) FANCD2 Cue Domain Leu231Arg interactions with monoubiquitin

FANCI, FANCD2, and BRCA2, has important role in PPIs which in turn may regulate DNA ICL damage repair mechanism/FA pathway.

Genomic profiling of tumors offers great promise in cancer therapy. However, patients are unlikely to benefit in case of multiple co-occurring alterations. Hence, there is a need for convergence of information for co-occurring alterations to ensure the success of genomically matched therapies and clinical trials. Gallbladder cancer is an uncommon disease with relatively poor understanding of its pathogenesis and hence the current treatment regimens have not significantly improved the survival of patients. The high prevalence in the Indian subcontinent necessitates research using methodologies that are sensitive to identify genomic aberrations specific to the Indian cohort of patients. Moreover, there is an unmet need to identify molecular targets in gallbladder cancer.

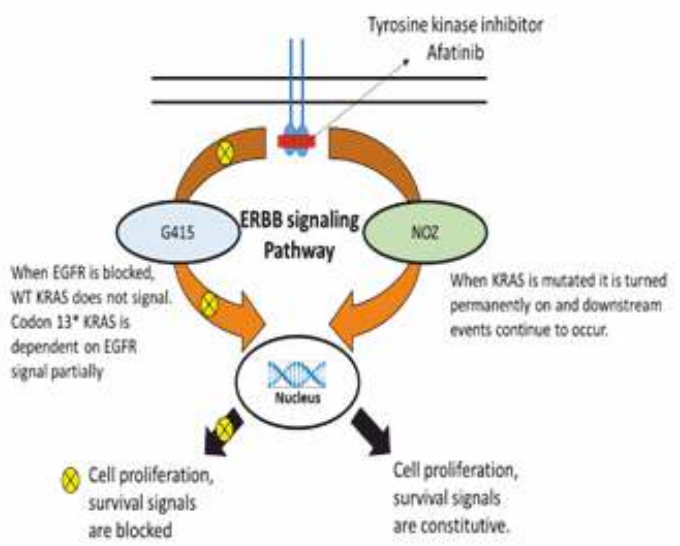

Figure 4.2.4 Response of gallbladder cell lines (G415 and NOZ) in response to afatinib- ERBB inhibitor with different KRAS status

As a first step, whole exome sequencing of gallbladder tumors and primary tumor-derived cell lines was performed. The student analyzed the data for the presence of Salmonella infections in these tumors using computational subtraction approaches. While existing epidemiological data suggests a strong association of typhoidal Salmonella infections, no reports suggest non-typhoidal Salmonella to be associated with gallbladder cancer. The findings for the first time reveal that non-typhoidal Salmonella infections are associated with gallbladder cancer as identified using next-generation sequencing data. Independently, in an attempt to identify somatic coding alterations in gallbladder cancer, our analysis revealed recurrent alterations in the *EGFR* gene family and identified activating alterations in the *ERBB2*. Furthermore, functional analysis in cell lines reveals the dependency of *EGFR* family pathway in gallbladder cancer and identifies *ERBB2* as a potential therapeutic target in gallbladder cancer. The findings also reveals that the *EGFR* family-based perturbation experiments have a pronounced effect in gallbladder tumor-derived cell lines with KRAS codon 13 mutation than in those with codon 12 mutations.

Furthermore, in-depth analysis of the whole-exome sequencing data presents a landscape of coding alterations and identifies ERBB2 as a novel therapeutic target in gallbladder cancer patients. We provide the first evidence that presence of KRAS (G12V) but not KRAS (G13D) mutation may preclude patients to respond to anti-EGFR treatment in gallbladder cancer, similar to the clinical algorithm commonly practiced to stratify patients for anti-EGFR treatment in colorectal cancer.

Stem cells regulation plays an important role in the development and maintenance of the tissue homeostasis. Stem cells are regulated by different intrinsic and extrinsic factors that include various signaling molecules and deregulation in these signaling molecular mechanism leads to a cancer. Recently various studies highlighted the importance of cancer stem cells in the maintenance and recurrence of cancer. The work done in this thesis entitled “Dissecting the molecular mechanism normal stem cell and cancer stem cell regulation” provides insights in the regulationof stem cells, cancer and cancer stem cells.

Secretory phospholipase A2-IIA (sPLA2-IIA) is involved in lipid catabolism and deregulated in various cancer.Overexpression of sPLA2-IIAshowed gradual depletion of hair follicle stem cell pool. This was accompanied with increased differentiation, loss of ortho-parakeratotic organization and enlargement of sebaceous gland, infundibulum and junctional zone.

Further, increased proliferation and differentiation of hair follicle stem cells is mediated through enhanced activation of mitogenic signaling and altered activation of c-Jun and FosB.Our results, first time uncovered that overexpression of sPLA2-IIA lead to depletion of hair follicle stem cells and differentiation.

Secreted frizzled-related protein 1 (Sfrp1) is a Wnt inhibitor and a tumor suppressor gene, which is upregulated in hair follicle stem cells and is downregulated in various cancers. Sfrp1 knockout mice showed the effect on proliferation and activation of hair follicle stem cells, with effect on slow cycling properties of the stem cells. The induced skin carcinogenesis study highlighted the role of Sfrp1 in tumor initiation, as loss of Sfrp1 enhances the sensitivity towards chemical carcinogenesis. Further, tumor characterization and functional study showed that loss of Sfrp1 enhanced tumorogenic potential of the cancer stem cells Thus, it is important to understand the target genes which are regulated by Sfrp1 in cancer stem cells regulation.

Lung cancer associated with cigarette smoking is a leading cause of death. The concept that dietary polyphenols can delay the process of carcinogenesis is receiving increasing attention because of its low toxicity and effects on diverse cellular targets. In this study, the student used polymeric black tea polyphenol (PBPs), one of the most abundant polyphenol, as a chemopreventive agent to study the effects on B(a)P and NNK induced experimental lung carcinogenesis model. Hence, she extracted PBPs from black tea powder using organic solvents. It was shown that the oral administration of these PBPs delayed the lung tumor multiplicity without affecting tumor incidence and latency period, macro and microscopically. PBPs exert its chemopreventive efficacy by modulating the process of inflammation, cell proliferation, apoptosis and activated form of signaling kinases like p38 & Akt.

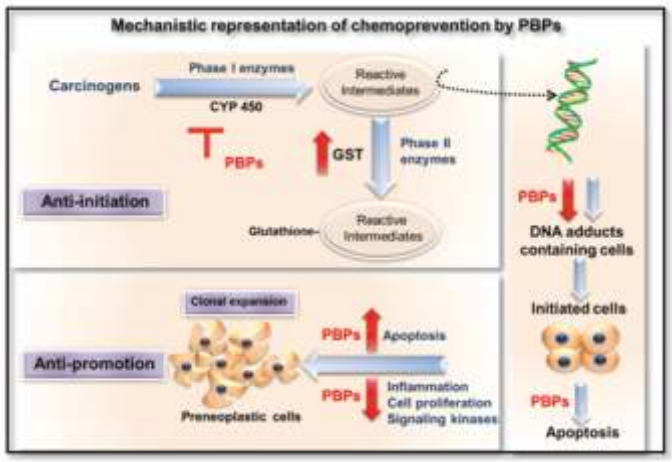

Figure 4.2.5 Mechanistic representation of chemo prevention by PBPs

Further they have also demonstrated that the dose response effect of PBPs on carcinogen metabolism using isoforms of phase I (CYP1A1 and CYP1A2) and phase II (GST mu, pi and alpha) xenobiotic metabolizing enzymes decreasing the B(a)P induced BPDE-DNA adducts. Additionally, the dose response effect of PBPs was further corroborated using B(a)P and NNK lung carcinogenicity A/J mice model showing dose dependent decreased lung tumor incidence and multiplicity, modulating various molecular markers. To dissect out the anti-initiation and anti-promotion effect of PBPs, effect of PBPs pre and post treatment was studied using B(a)P treatment. Out of various cell proliferation, inflammation molecular markers, apoptosis and DNA damage response markers were shown to be predominant modulators in driving the process of chemoprevention using PBPs.

In summary, the study contributes significantly in understanding the mechanism of chemopreventive efficacy of PBPs on experimental lung carcinogenesis and will further help inelucidating the cellular

Acquirement of chemoresistance is a major obstacle associated with the management of ovarian carcinoma, aggravating worldwide burden of mortality. Current chemotherapeutics hinder the homeostasis of cancer cells, however (resistant) cancer cells tent to evolve new (molecular or cellular) tactics to counteract such setbacks. How resistant cancer cells respond at molecular and cellular level towards therapeutics is one of the most confounding questions in cancer biology. Several molecular players are known to play a role in acquirement of cisplatin resistance controlling their cellular fate. Activation of PI3K/AKT survival axis is associated with the 50-70% of chemoresistant ovarian cancer, however it is not understood how does PI3K/AKT help in maintenance of chemoresistance Recent high throughput genetic analysis of high-grade serous ovarian cancer suggests ~16% of cases with elevated PIK3CA transcript level without any change in gene copy numbers. This distinguished expression of PIK3CA is probably due to its deregulated promoter activity. This study sought to dissect the mechanisms of differential activation of PIK3CA signaling in cisplatin-sensitive and resistant cells upon drug treatment. Here, it is shown that cisplatin-a chemotherapeutic drug exert differential cellular fate wherein it supresses PIK3CA expression in sensitive cells, while same drug up-regulates PIK3CA in resistant cells. In sensitive cells, cisplatin mediates HIPK2 and DYKR2 dependent phosphorylation of p53 at serine 46, which accelerates its interaction with PIK3CA promoter at p53-binding site 3 and 4. This interaction supresses PIK3CA expression and hence the activation of PI3K/AKT survival cue thereby imposing sensitive cells towards apoptotic fate. This p53-PIK3CA promoter interaction is decoupled in the cisplatin-resistant cells leading to abrogation of PIK3CA promoter attenuation and increased cell survival post cisplatin treatment. Intriguingly, in absence of p53 ordinance, NF-κB escalates PIK3CA expression, priming activation of PI3K/AKT cascade. Along with PIK3CA, NF-κB also escalates TNFα expression specifically in cancer stem cell (CSC) fraction of resistant ovarian cancer cells upon cisplatin treatment. This CSC-specific NF-κB-TNFα-PIK3CA bi-modal loop, on one hand,

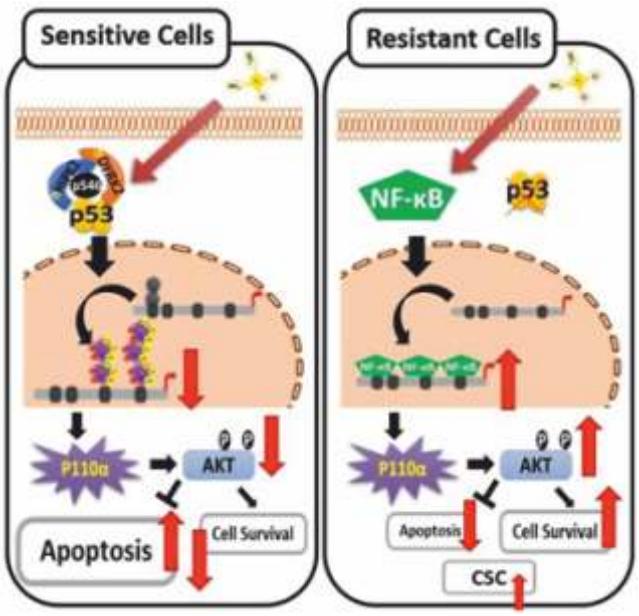

Figure 4.2.6 Cisplatin mediated differential regulation of PIK3CA/AKT endorse distinct cellular fates in sensitive and resistant cells.

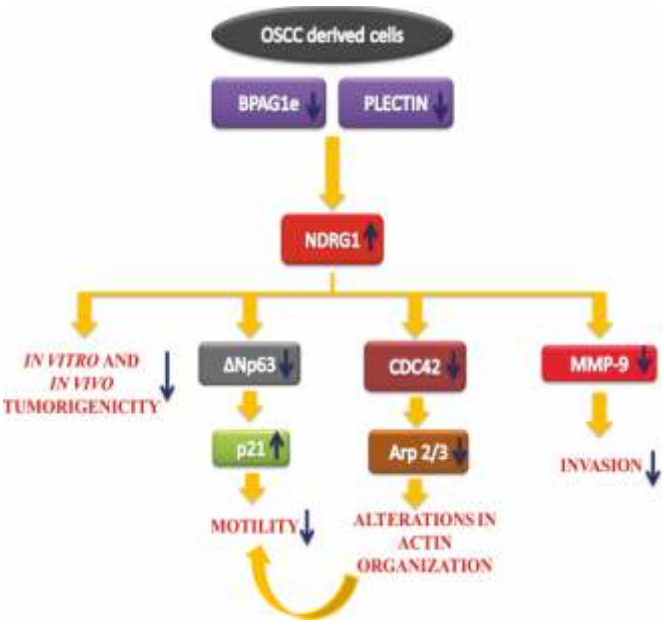

Figure 4.2.7 Schematic representation of the role of Hemidesmosomal linker proteins in OSCC derived cells

maintains persistent activation of NF-κB through TNFα- NF-κB autocrine loop, while NF-κB-PIK3CA loop nurture CSC population under cisplatin treatment.Overall, activation of PI3K/AKT and NF-κB signaling in resistant cells favours survival and enrichment of CSCs by acquiring anti-apoptotic, quiescent state. Thus, this study indicates that cisplatin could either induce cell death in chemo sensitive cells or cell survival and enhanced CSC population in chemo resistant cells by modulating PIK3CA/AKT signalling.

BPAG1e and Plectin are hemidesmosomal linker proteins which anchor keratins to the cell surface through β4 integrin. Recent reports indicate that these proteins play a role in various cellular processes apart from their known anchoring function. However, the existing literature related to these proteins is scanty and inconsistent. Also, the role of these proteins has not been explored in oral squamous cell carcinoma (OSCC). Previously, our laboratory has shown aberrant expression of keratin8/18 (K8/18) in human OSCC. Subsequent work from our laboratory revealed that K8/18 pair promotes cell motility and tumor progression by deregulating β4 integrin signaling in OSCC derived cells. As BPAG1e and plectin anchor keratin proteins to cell surface via β4 integrin, we hypothesized that these proteins may have a role in regulating cell motility and neoplastic progression of OSCC.

Downregulation of hemidesmosomal linker protein(s) in OSCC derived cells resulted in reduced cell migration, which could be attributed to decreased cdc42 activity, leading to reduced Arp2/3 expression which is known to regulate actin polymerization. Further, decreased invasive potential of linker protein(s) ablated cells can be attributed to reduced MMP9 activity. Moreover, loss of these proteins in OSCC derived cells resulted in reduced tumorigenic potential. The SWATH (sequential window acquisition of all theoretical fragment ion spectra) analysis demonstrated upregulation of NDRG1 in linker proteins knockdown cells as compared to vector control cells. Furthermore, the alterations in phenotype upon hemidesmosomal linker protein(s) loss were partially restored upon N-Myc downstream regulated gene 1 (NDRG1) knockdown in BPAG1e-Plectin downregulated cells. Altogether, this study demonstrated that hemidesmosomal linker proteins regulate cell motility, actin organization, cell invasion and tumorigenicity possibly through NDRG1 in OSCC derived cells (Figure 4.

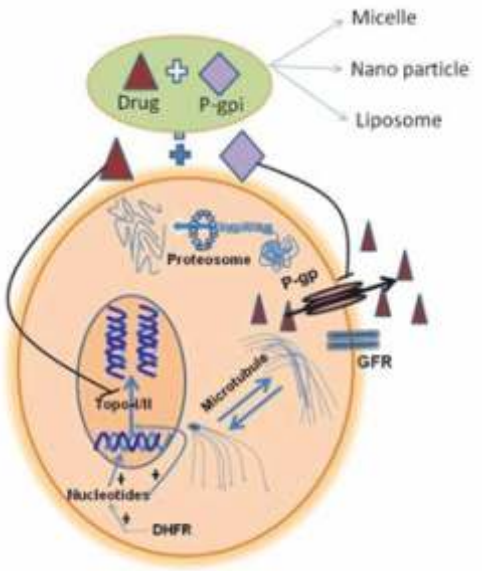

Figure 4.3.1 Combinational nano-formulation circumvents P-gp mediated drug resistance in cancer.

4.3. National Institute of Science Education and Research (NISER)

In recent years, different approaches for circumvention of drug resistance have been developed with some success. In this thesis work, an attempt was made to combine a p-glycoprotein (P-gp) inhibitor with a chemotherapeutic drug in a pharmaceutical nano-formulation for reversal of drug resistance. Here, theselection of P-gp inhibitor is important as P-gp expression varies in different resistant model systems. In addition, formulating a combinational nano-formulation is equally challenging owing to physicochemical difference between agents selected for the combination. For this study, doxorubicin (DOX) resistant counterparts of K562 (K562N) and COLO205 (ColoN) were developed as model system (K562R and ColoR respectively). Naturally occurring P-gp inhibitors (biochanin A, curcumin, daidzein, dihydrofisetin, genistein, resveratrol, silymarin) were screened for their P-gp inhibitory and reversal of DOX resistance

specifically in the developed cell lines. From the screening, curcumin was selected as a suitable agent for K562 while curcumin and biochanin A was selected for COLO205.

Both the selected agents are poorly aqueous soluble, therefore different strategies were adopted to improve their solubility. In case of curcumin, various nano-formulation of curcumin such as HP-β-CD encapsulated curcumin (CurN), liposomal curcumin (CurL), micellar curcumin (CurM) and DMSO assisted nano-dispersed curcumin (CurD) were developed and evaluated. In case of CurN, a freeze drying method was developed and optimized where the encapsulation efficiency of curcumin in HP-β-CD was increased from 1-5% to about 60%. From studies on P-gp inhibitory as well as reversal of resistance, CurN and CurL formulations were found to be optimal. However, CurN required a carrier for controlled release, therefore, CurL was considered for further studies. For formulations involving biochanin A, higher solubility was observed for biochanin A in basic medium. The combinational liposomes of curcumin of biochanin A with DOX were then prepared and evaluated. The prepared nano-formulations reversed acquired DOX resistance in K562R and ColoR cell lines via P-gp dependent and independent mechanisms respectively.

5. Mathematical Sciences

During this period, HBNI has awarded Ph.D. degree to 13 students in Mathematical Sciences on successful completion of academic programmes. Research topics are from a variety of areas including Differential Geometry, Number Theory, Lie Groups, Theoretical Computer Science, Parameterised Complexity and Operator Algebra. Highlights of a few doctoral theses are outlined below.

5.1. Harish-Chandra Research Institute (HRI)

In this thesis entitled “Maximal Surfaces and Their Applications”, a different formulation for describing maximal surfaces in Lorentz-Minkowski space L^3 = (R^3 , dx^2 +dy^2 − dz^2) using the identification of R^3 with C × R has been discussed. This description of maximal surfaces helps to give a different proof of the singular Björling problem for the case of closed real analytic null curve. As an application, it has been shown that the existence of maximal surfaces which contain a given closed real analytic space like curve and has a special singularity. It was observed that the maximal surface equation and Born-Infeld equation (which arises in physics in the context of nonlinear electrodynamics) are related by a Wick rotation. It was shown that a Born-Infeld soliton can be realised either as a space like minimal graph or time like minimal graph over a time like plane or a combination of both away from singular points. Connection of maximal surfaces to analytic number theory through certain Ramanujan's identities was also shown.

This thesis dealt with three problems in the theory of modular forms. The first problem is about the question 'when is an arbitrary product of Hecke eigenforms again an eigenform?' This problem in the context of nearly holomorphic modular forms and quasimodular forms was discussed. The second one is on finding the adjoint map of the Serre derivative map and as an application, a formula for the Ramanujan tau function in terms of special values of certain shifted Dirichlet series was found. The third problem is on finding an estimate for Fourier coefficients of Hermitian cusp forms of degree two over the imaginary quadratic field Q(i). This is the most technical part of the thesis and involves several estimates.

5.2. The Institute of Mathematical Sciences (IMSc)

A student investigated some graph modification problems from Parameterized Complexity point of view. A typical graph modification problem, for a fixed graph class Π, asks us to modify the input graph using small number of operations such that the resulting graph belongs to Π. Typical operations studied in the field are vertex and edge deletions. There are two choices of parameters for graph modification problems, one is

the size of the graph, we are looking for, and the other is the editing distance. The first part of the thesis deals with the former kind of parameterization and has results concerning many choices of the graph class Π. The first result establishes no polynomial kernelization under standard complexity theory assumptions for finding induced hereditary subgraphs for many choices of Π, including cographs, chordal, interval, split, perfect, and cluster graphs. In the other result, the class Π is the set of q-colorable graphs. We give efficient FPT algorithms for finding induced q-colorable subgraphs on graphs where either all maximal independent sets can be enumerated in polynomial time or where the maximum independent set can be found in polynomial time.

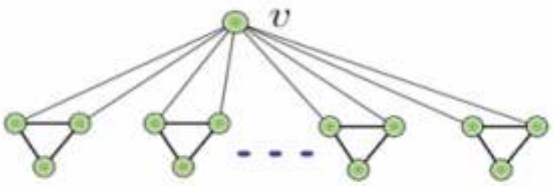

Figure 5.2. A hard example for the new parameterization proposed in the thesis. To make the graph into a bipartite graph, we need to delete (n-1)/3 edges, while after deleting one vertex, we just need to delete one edge from each connected component.

The second part of the thesis deals with the more conventional parameter choice, which is the edit distance, more commonly called the solution size. We first give efficient FPT algorithms for Split Vertex Deletion and Split Edge Deletion when parameterized by the solution size. We also give polynomial kernels for both the problems. Then we consider the problem of deleting both vertices and edges to get a forest, which is a generalization of classic Feedback Vertex Set problem, and show that it is FPT.

Then the student has proposed another parameterization for graph editing problems where after deletinga small number of vertices, they wanted every connected component of the resulting graph to be close to a well understood graph class Π, where the measure of closeness is the minimum number of edges to be deleted from that connected component to reach the graph class. It has been shown that how this parameterization is more powerful than the standard parameterizations for graph editing problems and this version to be FPT for two choices of Π, forests and bipartite graphs. While showing the latter, they also developed an algorithm for a generalization of the classic Min-Cut problem, called Mixed Cut, where it was allowed to delete both vertices and edges to disconnect the given terminals. They also showed that Mixed Cut is NP-complete.

Another student worked on Cohomology of locally symmetric spaces. This thesis consists of two parts. The first part addresses homotopy classification of maps between higher rank irreducible locally symmetric spaces. Assuming that the dimension of the domain is greater than or equal to that of the range, it is shown that the absolute value of the degree of any such map depends only on the two lattices involved. The question of when the degree can be negative has also been addressed.

The second part is about cohomology of a family of compact locally symmetric spaces. Let X be the quotient of the symmetric space SO*(2n)/U(n) by a uniform lattice G in SO*(2n). By a theorem of Matsushima, the cohomology of X can be written as a weighted sum of the relative Lie algebra cohomologies of (so*(2n),U(n)) with coefficients in irreducible components of the SO*(2n)-module L^2(G\SO*(2n)). Relative Lie algebra cohomology groups are non-zero for a finite set of coefficients which are denoted by A_q, where q runs over certain parabolic subalgebras of so(2n,C) (up to a certain equivalence). Relative Lie algebra cohomology groups with coefficients in A_q will be called A_q cohomology groups. They are zero in small dimensions, depending on q, unless q=so(2n,C). Thus the existence of a non-vanishing cohomology class of X, in a certain (small) dimension, can tell us if a particular

A_q cohomology appears with non-zero weight in the sum. If it does, then the corresponding A_q is a component in L^2(G\SO^*(2n)). We construct non-zero cohomology classes by considering Poincare duals of pairs of sub locally symmetric spaces and showing that the intersection number of each pair is non zero. We do this for a large family of commensurability classes of uniform lattices of SO*(2n). This method was initiated by Millson and Raghunathan who also proved that the classes constructed this way cannot be in the A_{so(2n,C)} cohomology groups summand. We observed that almost all the submanifolds we constructed are complex analytic, hence their Poincare duals will have Hodge type (p,p). This puts a restriction on the set of A_q components that these cohomology classes can have. We parameterize this restricted set by combinatorial objects named 'staircase diagrams', as shown in the figure. Then we identified the dimensions till which the A_q cohomologies from this restricted set vanish. Let k and l be the least and second least values of the dimensions. We noted that one of cohomology classes that we constructed is in a dimension which is between k and l. Thus this cohomology class has an A_q component, where the A_q cohomology is the unique one in the restricted set which vanishes till dimension k. The overall process described above has been carried out for groups other than SO*(2n), but according to our knowledge this is the first time that a specific A_q component has been detected. The key observation is to use the Hodge type of the constructed cohomology classes. Our result can be generalized to other compact Hermitian locally symmetric spaces.

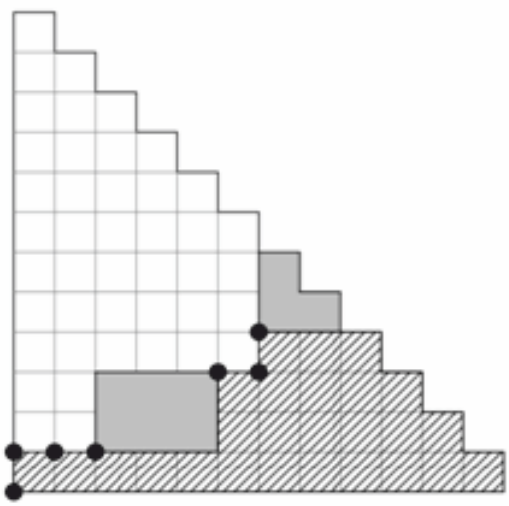

Figure 5.2.2 A staircase diagram

One of the students worked on the topology of nilpotent orbits in semisimple Lie algebras. In this thesis he contributed by studying two specific topological invariants, namely the second and the first de Rham cohomology groups, of nilpotent orbits in non-compact, non-complex simple Lie algebras.

The nilpotent orbits in the semisimple Lie algebras, under the adjoint action of the associated semisimple Lie groups, form a rich class of homogeneous spaces. Such orbits are studied at the interface of several

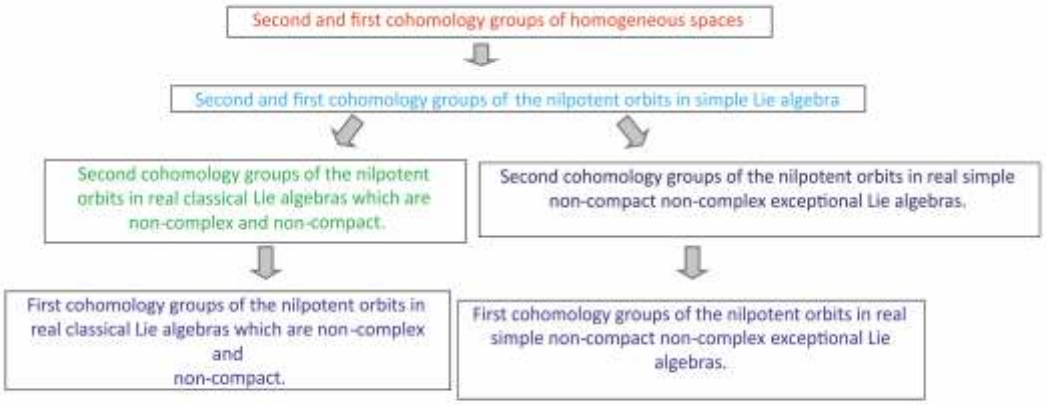

Figure 5.2.3 Interdependence of the topics in the thesis

disciplines in mathematics such as Lie theory, symplectic geometry, representation theory, algebraic geometry. Using involved computations we describe the second and the first cohomology groups of the

nilpotent orbits in real classical Lie algebras which are non-complex and non-compact. We also compute the second and first cohomology groups of the nilpotent orbits for most of the nilpotent orbits in real simple non-compact non-complex exceptional Lie algebras, and for the rest of cases of the nilpotent orbits, which are not covered in the above computations, upper bounds for the dimensions of the second cohomology groups are obtained.

A key component in the computation is a convenient description of the second cohomology groups of homogeneous space of a connected Lie group. On the other hand, in view of their applicability the above results may be of independent interest as they are general and hold under a very mild restriction. A stronger consequence of the above results was deduced in the special cases when the ambient Lie groups are complex semi-simple or real simple.

Another student worked on Parameterized Algorithms for Network Design. In this thesis we design algorithms for several network design problems in the framework of Parameterized Complexity and Exact algorithms. Along the way, we also give deterministic algorithms for some problems in matroid theory. Our results add to the small list of results on network design problems in the realm of parameterized and exact algorithms.

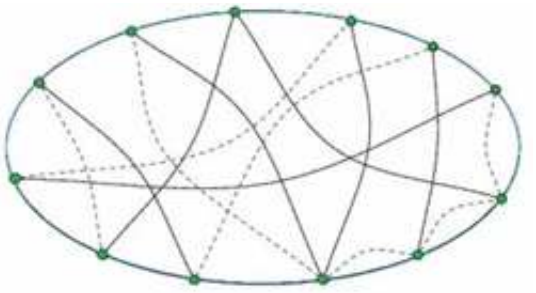

Figure 5.2.4 Augmenting a cycle to 3-connectivity

Network design problems are one of the most well studied class of problems studied in computer science and graph theory. We study the following network design problems in this thesis. (1)Eulerian Edge Deletion where we mustremove a minimum number of edges from an input graph to obtain an eulerian graph. We give a $2^{O(k)}n^{O(1)}$FPT algorithm for this problem, where k is the size of a solution.
(2)Exact algorithms for Survivable Network Design with uniform requirements, where the goal is to find a minimum cost subgraph of an input graph or digraph which is λ edge connected. A related problem is augmenting a given network with a minimum cost set of new links so the the network becomes λ connected. In this thesis, we design fast exact algorithms for both these problem that runs

in time $2^{O(|V(G)|)}$, which significantly improves upon the known algorithms of running time $2^{O(|E(G)|)}$. (3)Parameterized complexity of Augmentation by One, where we consider the parameterized complexity of network augmentation of a (λ – 1) connected graph to λ. First we parameterize it by the size of a minimum augmenting set and show that it admits a $2^{O(k)}n^{O(1)}$ FPT algorithm. Next we parameterize it by the size of the set of unused links, i.e. the complement of a minimum augmenting set. We show that the problems admits a $2^{O(k)}n^{O(1)}$ FPT algorithm and a polynomial kernel with this parameter. Our algorithms significantly improve upon the previous results. They are based on a novel connection between these problems and the Steiner Tree problem. (4)Minimum Equivalent Digraph where we are given a digraph D as input and the goal is to find a minimum spanning subgraph H which has the same reachability relations as D. We parameterize this problem by the number of arcs which may be safely deleted from the graph, and show that the problem admits a polynomial kernel, and hence it is FPT. Our results are based on a new structural property of strongly-connected digraphs, which can also be extended to higher connectivity.

Matroids and related algorithmic tools play an important role in many recent algorithmic results. In this thesis we obtain the following algorithms on matroids. (1)Deterministic truncation of linear matroids. We give a deterministic algorithm for computing the truncation of any linear matroid. Our algorithms are based on a connection of matroid truncation to the Wronskian matrix of polynomials which is well studied

in linear algebra, and it has found recent applications in coding theory and pseudo randomness. This derandomizes several algorithms in matroid theory and parameterized complexity including computation of representative sets in linear matroids, and exact algorithms for matroid parity. (2)Deterministic representation of gammoids in moderately exponential time. Gammoids are an important class of linear matroids which arise from graph connectivity, and one can find a representation of them in randomized polynomial time. In this thesis, a moderately exponential deterministic algorithm has been given for computing a representation of transversal matroid and gammoids.

One of the students worked on intermediate subfactors. This thesis primarily deals with the intermediate subfactors of a subfactor, say N Ì M, of type II_1. Interest in subfactors began when V. Jones introduced index, denoted by [M N], of the subfactor N Ì M of type II_1. He has shown that [M N] lies in the set {4cos ² π/n n≥3}∪[4,∞]. Pimsner and Popa have shown that for an inclusion N Ì M of II_1 factors, M is a finitely generated projective module over Nif and only if [M N] is finite by constructing a certain kind of family {m_j 1≤j≤n+1}of elements in M, with n=⌊[M N]⌋, which they called “orthonormal basis” for the pair N Ì M.

In the first chapter of this thesis, he has examined moregeneral bases for factors of type II_1 (as introduced in the book of Jones and Sunder) which are not necessarily orthonormal and showed that this can also be done for connected inclusion of finite dimensional von Neumann algebras (in the sense that the Bratteli diagram is connected). For both these cases we obtain a characterization of 'Jones basic construction' in terms of bases and prove the phenomenon of 'multistep basic construction'.

In the second chapter, we consider the subfactor planar algebra $P^{(N\grave{\imath}\ Q)}$ for an intermediate subfactor N Ì Q Ì M of an irreducible subfactor N Ì M of finite index. In an old unpublished paper Bina Bhattacharyya and Zeph Landau showed that this can be described in terms of the subfactor planar algebra $P^{(N\grave{\imath}\ M)}$. We give an alternative proof of this fact by showing that if T is any planar tangle, the associated operator $Z_T^{(N\grave{\imath}\ Q)}$ can be read off from $Z_T^{(N\grave{\imath}\ M)}$ by a procedure involving the so-called biprojection corresponding to the intermediate subfactor N Ì Q Ì M and a scalar $\alpha(T)$ carefully chosen so as to ensure that the formula defining $Z_T^{(N\grave{\imath}\ Q)}$ is multiplicative with respect to composition of tangles.

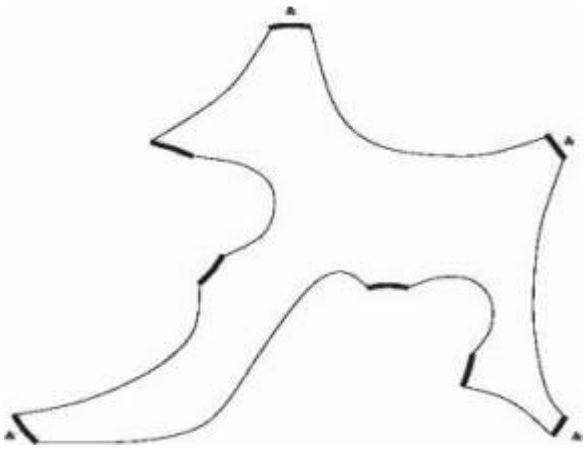

Figure 5.2.5 Black intervals and tangle

We denote by L(N Ì M) the set of all intermediate von Neumann sub-algebras for the subfactor N⊂M. The set L(N Ì M) forms a lattice under the two operations P∧Q=P∩Q and P∨Q=(P∪Q)''. If N⊂M is irreducible, that is N'∩M=C, then L(N Ì M) is exactly the lattice of intermediate subfactors. Watatani in has shown that in this case the lattice is a finite set. In the third chapter we improve existing upper bounds for the cardinality of this set. For this we have introduced a natural notion of 'angle' involving biprojections and investigated various properties of the same. In the final section of the third chapter we investigate the intermediate subfactors for general finite-index case. We show if the norm difference between two biprojections is less than half then the corresponding intermediate subfactors are actually isomorphic.

Another student worked on some decidable classes of the Distributed Synthesis Problem. In this thesis he has studied the distributed synthesis problem, which asks for an algorithm that synthesizes distributed systems from a given specification. We study this via the equivalent problem of determining the winning strategy of multi-player imperfect information games. More concretely, is there an algorithm, which given a multi-player imperfect information game as a game graph and a regular winning condition on the plays of the game, determines the existence of a winning strategy. The above problem is known to be undecidable, even for very simple winning conditions. The contribution of this thesis is in determining new decidable classes of games. In particular, we show that the winning strategy problem is decidable for the following

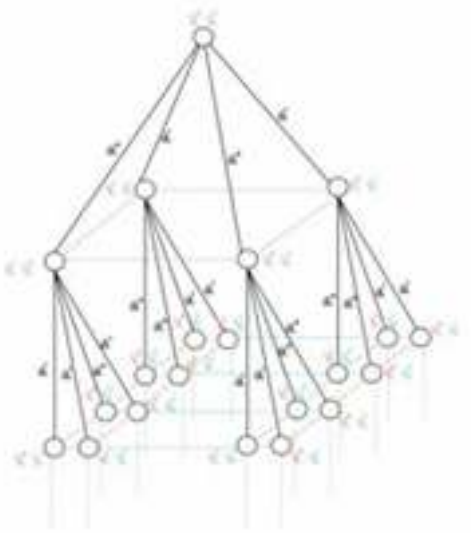

Figure 5.2.6 A game tree

1. Imperfect information games with Recurring Common Knowledge of State This condition relies on the fact that bounded common knowledge among the players of the game, leads to effective algorithms for the winning strategy problem. We show that under this condition, the existence of winning strategy can be decided in NEXPTIME and winning strategies can be synthesized in 2EXPTIME.

2. Imperfect information games with Retractable Witnesses We identify a generic approach to solving the winning strategy problem, which comprises of two steps first, we define a notion of a witness, the existence of which implies the existence of winning strategy; second, we define an operation called retraction that can transform witnesses into bounded-size witnesses. We then show that for classes of games whose witnesses admit a retraction to bounded-size witnesses, the existence of winning strategy can be determined. Using this approach, we solve the following classes of games

a. Imperfect information games with no Fork-Triples We define a property of games called fork-triple, the absence of which is a favorable criterion to decide the winning strategy problem. We show that in this case, the winning strategy problem is decidable with an algorithm whose complexity is non-elementary in the size of the inputs. We also show that the condition of absence of fork-triples on games is satisfied by many classes of games previously known to be decidable.

b. Imperfect information games obtained from Modular-Broadcast Architectures We show that games obtained from modular-broadcast architectures admit a decidable winning strategy problem, when restricted to local winning condition. Here again the complexity of the algorithm is non-elementary in the size of the inputs and includes all previously known decidable classes of games with local winning conditions.

Due to the rapid growth of data, algorithms that utilize the space efficiently are increasingly becoming important. A student worked on space efficient graph algorithms. This thesis focuses on an emerging area of designing algorithms for fundamental graph problems using little space without compromising on the speed as well.

He provided such algorithms for various graph search methods (depth-first search, breadth-first search, maximum cardinality search) and fundamental connectivity problems (bi-connectivity, 2-edge connectivity and strong connectivity) in the read-only memory model using linear bits of extra space. Most

of these results require techniques from succinct data structures along with suitable modifications of the existing graph algorithms.

We also provide sub-linear bits algorithms for various optimization problems on bounded treewidth graphs in the read-only memory model. In fact, we prove the following more general meta theorem which, roughly speaking, says, for bounded treewidth graphs, if any graph problem can be described in monadic second order (MSO) logic, we can obtain a smooth deterministic time-space trade-off from logarithmic words to linear space.

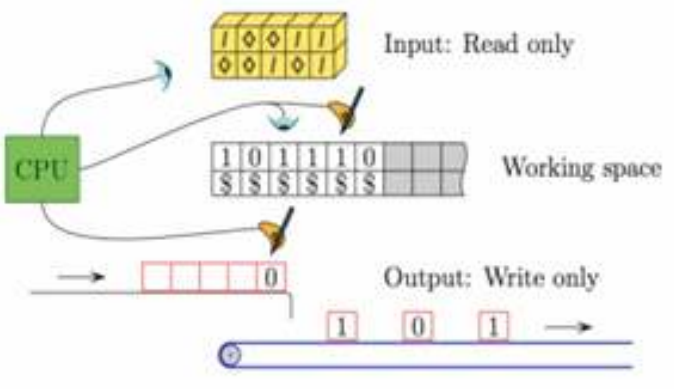

Figure 5.2.7 Read-Only Memory Model

Furthermore, we introduce two new frameworks for designing efficient in-place graph algorithms (where the input elements can be moved around in a restricted way) and obtain such algorithms for several basic algorithmic graph problems. In particular, we develop algorithms for depth-first search and breadth-first search in these models taking only logarithmic extra bit albeit taking super-linear time. In sharp contrast, we don't know of any algorithms for these problems taking sub-linear bits of space in the read-only memory model.

6. Physical Sciences

HBNI has awarded 104 Ph. D. degrees in Physical sciences category during the academic year 2017-18. The topics can broadly be categorized as (a) Condensed Matter Physics (b) Nuclear Physics (c) High energy physics, (d) Plasma physics, (e) Optics, (f) Quantum Mechanics, (g) Quantum Informatics and (h) Astrophysics. The reported works contain experiments, modeling, simulation and theoretical work in the above fields of research being pursued at various CII. Following are some of the highlights presented under the heading of the specific CII.

6.1 Bhabha Atomic Research Centre

A thesis presented work on the structure and magnetic properties of perovskite structures. Perovskite type compounds are the most widely studied compounds for their chemical and crystal structure diversity and thus prevalent in all technological applications. The thesis mainly deals with the crystal structure analysis and its physical property measurements of new complex double perovskite (DP) oxide systems. The cation (B&B') ordering in the double perovskite $A_2BB'O_6$ compounds has a profound effect on the magnetic ground state of the compounds. Three compounds in the $Sr_2Co_{2-x}Ru_xO_6$ (x=0.5, 1, 1.5) series were

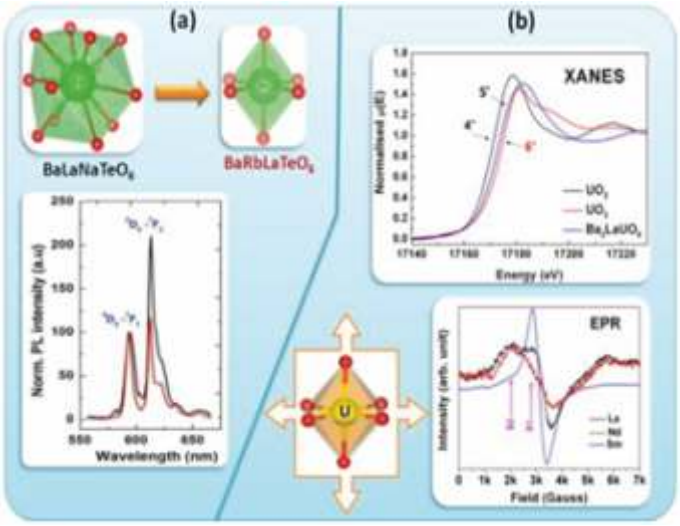

Figure 6.1.1(a) Change in PL emission due to the site swapping of La cation. (b) XANES spectra of Ba2LaUO6 showing U5+ and change in EPR signal with distortion of UO6

studied. In spite of variation in the composition, oxidation state and crystal structure; random distribution of the Co and Ru cations at the B-site cause these compounds to show spin glass behaviour. This shows that competing magnetic interactions plays a dominant role on the magnetic property of these compounds.

The size of the cations plays very important role in deciding the crystal structure and crystallographic site of the cations which in turn affects the physical properties like for photoluminescence (PL). Figure (a) shows the change in the emission spectra due to the change in the coordination of La in Eu^{3+} doped $BaLaNaTeO_6$ and $BaRbLaTeO_6$ compounds. Similar other compounds in the series BaLaBB'O6 and $Ba_2La_{2/3}M^{5+}O_{5.5}$ (B'= Nb, Sb, Te; B = metal or alkaline earth metals; M =Nb, Sb, Bi, and U were studied and effect of crystal structure and local coordination on PL and IR spectroscopy was investigated.

Pentavalent uranium double perovskite compounds Ba2REUO6 (RE=La, Nd, Sm) were synthesized and characterized. Figure (b) shows the XANES spectra confirming the pure U5+ oxidation state of uranium. Compounds show no long range magnetic ordering with weak moment of 0.4μB for U5+. The octahedral distortion around the U5+ was co-related to the split in the EPR signal at g>2.

Another thesis deals with plasma Processing of Carbon Nanostructures and Their Characterization Different carbon nanostructures have been deposited via low pressure plasma enhanced chemical vapour deposition (PECVD) process. Electron cyclotron resonance (ECR) plasma was used for deposition of carbon nanowalls (CNWs) and microwave plasma enhanced CVD (MPECVD) for the deposition of multi-walled carbon nanotubes (MWCNTs), graphene nanowalls (GNWs) and nano-crystalline diamond (NCD) and diamond films.

For the first time, it was shown that CNWs could be grown by ECR-CVD without application of any external bias. Apart from that, MWCNTs were deposited by MPECVD on Inconel 600 without use of any external

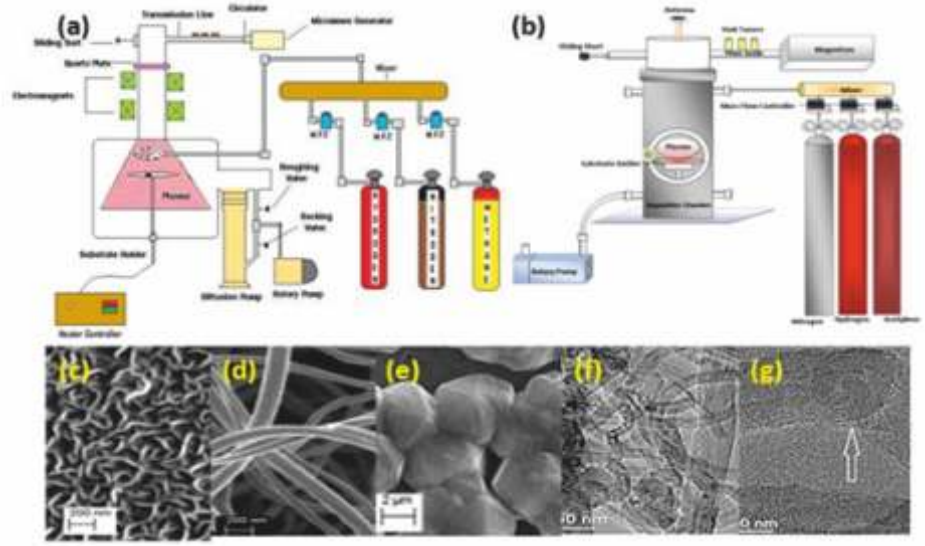

Figure 6.1.2 Schematic of (a) ECR-CVD system, (b) MPECVD system used in this work. FESEM images of deposited (c) GNWs, (d) MWCNTs, (e) diamond, HRTEM images of (f) MWCNT, (g) MWCNT with bamboo-like defects.

catalyst. It was seen that effect of heat-treatment and microwave attenuation on the substrate resulted in growth of long, dense CNTs with bamboo-like defects that contributed to enhanced field emission current density. A key output of the study was co-deposition of CNTs along with nano-crystalline diamond and

graphene nanowalls (GNWs).

Deposition and characterization of Refractory Oxide Thin Films and Multilayer Optical Coatings are important developing technologically important coatings. Refractory oxide materials such as HfO_2, ZrO_2, TiO_2, SiO_2 etc. are dielectric transparent materials, which are widely used for fabrication of different thin film Plasma Processing of Carbon Nanostructures and Their Characterization and multilayer optical coating devices such as antireflection coatings, high reflection mirrors, beam splitters, beam combiners, band pass filters etc. For high power laser applications, the thin films and multilayer coatings should withstand laser power without being damaged. For that purpose, an in-house experimental facility using Nd YAG pulsed laser as shown in Figure 1.1.3 (a) has been utilized to determine their laser induced damage threshold (LIDT) value. Apart from LIDT, the efficiency and performance of such devices depends strongly on the microstructure, residual stress and optical properties. These properties are investigated for HfO_2, SiO_2, ZrO_2-MgO and ZrO_2-SiO_2 dielectric thin films for optimized deposition oxygen partial pressure. Design of some challenging optical devices such as rugate notch filter, beam combiner etc. needs refractive index values which do not exist in conventional coating materials. In this direction, HfO_2-SiO_2 mixed oxide thin films with various compositions in the (x)HfO_2 (100-x)SiO_2 (x

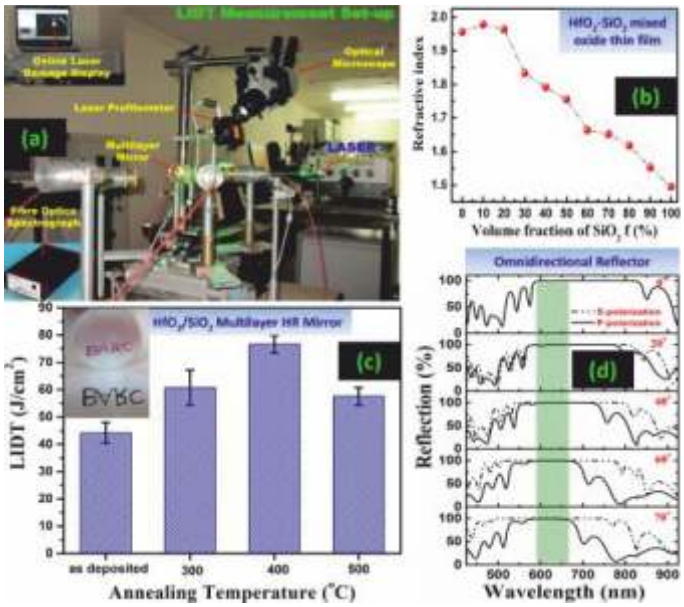

Figure 6.1.3(a) In-house developed LIDT measurement set-up, (b) Tuning of refractive index in mixed oxide thin film by varying silica fraction, (c) Enhancement of LIDT of HfO_2/SiO_2 multilayer high reflection mirror by annealing, and (d) Omnidirectional reflector using TiO_2/SiO_2 multilayer.

Figure 6.1.3(a) In-house developed LIDT measurement set-up, (b) Tuning of refractive index in mixed oxide thin film by varying silica fraction, (c) Enhancement of LIDT of HfO_2/SiO_2 multilayer high reflection mirror by annealing, and (d) Omnidirectional reflector using TiO_2/SiO_2 multilayer.= 0% to 100%) systems have been deposited using reactive electron beam co-evaporation of HfO_2 and SiO_2 to get wide range refractive index values as shown in Figure 1.1.3 (b). Multilayer high reflection (HR) mirrors have been prepared and post-deposition annealing is performed improve its LIDT from 44.1 J/cm² to 77.6 J/cm² as shown in Figure 1.1.3 (c). The multilayer structure can be used to fabricate omnidirectional reflector, which equally reflects a band of light irrespective of angle of incidence and polarization of light, which has potential applications in the field of optical fibre power transmission, filters in solar cells, wave guide communications, and laser cavities. We have successfully fabricated omnidirectional reflector by depositing TiO^2/SiO^2 multilayer using sputtering technique. The observed omnidirectional high reflection photonic band 592-668 nm ($\Delta\lambda$=76 nm) for reflectivity R>99% over the incident angle range of 0°-70° as shown in Figure 1 (d) is found close to the calculated values. The omnidirectional PBG is found much wider as compared to the values reported in literature so far in the visible region for TiO^2/SiO^2 periodic multilayer 1DPC.

Emission of non-equilibrium neutrons from low to intermediate energy heavy ion reactions is an important

area of study as it cannot be fully explained by either the statistical model or the direct reactions. A dissertation focuses on the estimation of neutrons beyond 20 MeV from heavy ion reactions using a pre-equilibrium (PEQ) model in the energy range upto a few tens of MeV per nucleon. In this work, a modified version of the previously developedPEQ model HION has been proposed. HION determines the energy angle distribution of PEQ neutrons from two body scattering kinematics.In the present work influence of nuclear mean field on the neutron emission has been investigated. Spatial density distribution of nucleons, determined from RMF theory and a semi-empirical formalism, is used to calculate nucleon-nucleon collision rates in the composite system. At incident energies above25 MeV per nucleon, simultaneous and sequential multi-particle PEQ emissions are considered. A time of flight (ToF)measurementfor^{16}O + thick ^{27}Al target has also been carried out at BARC-TIFR Pelletron-Linac facility. The model (HION4) is validated for old literature data on 10-30 MeV/A (^{20}Ne+^{165}Ho) and (^{12}C+^{165}Ho) reactions and forthe^{16}O +^{27}Al measurement. The results of HION4 and measured data corroborate well for neutron emission energies beyond 20 MeV (in Figure 1(a)). For beam energies above 25 MeV per nucleon sequential multiple PEQ emission becomes important. The integrated neutron dose estimated from the ToF yield data is higher compared to the doses measured using a neutron dose equivalent (NDE) meter for (O+Al)reaction. Equivalent doses obtained from the HION estimated yields when supplemented to NDE meter data agreed fairly well with the dose estimated from the ToF measurements. A theoretical estimate of neutron yield

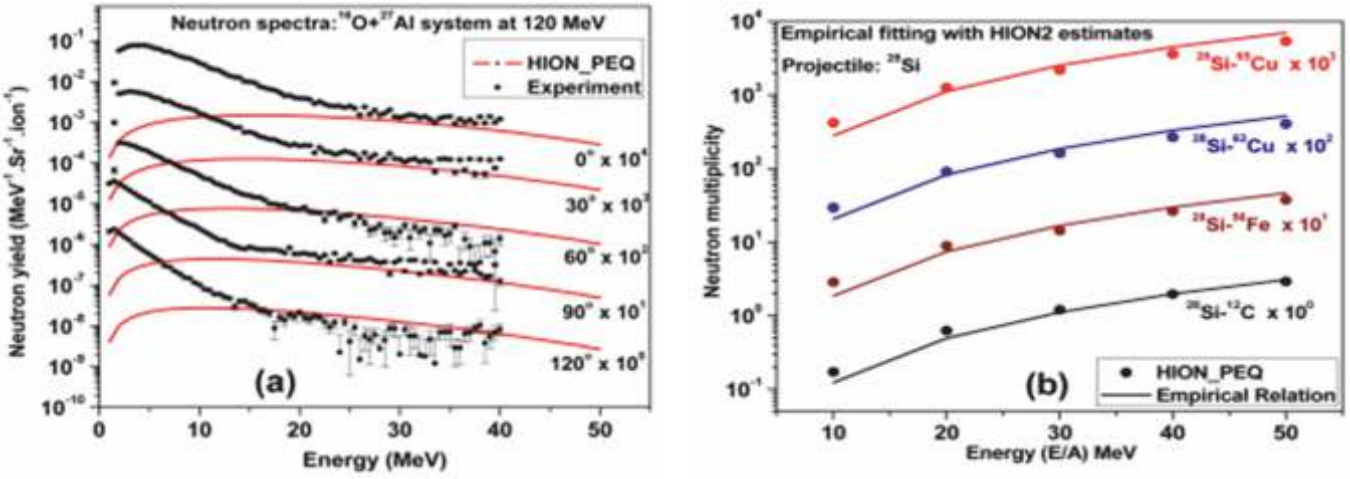

Figure 6.1.4 A comparison between (a) experiment and PEQ model and (b) empirical relation and the model estimates

and dose for different target-projectile systems is carried out using HION4 to estimate the neutron doses from the structural and dump materials in an accelerator. For different projectile beams with energies between 10 to 50 MeV per nucleon, PEQ contribution is found to be nearly 30% for low Z composite system and between 5-20% for high Z system. An empirical relation, (Figure 5.1.4(b)) is proposed to estimate the energy integrated yield of PEQ neutrons. This will help in calculating the PEQ neutron source term for shielding design calculations at various accelerator facilities.

This study helps to understand the reaction mechanisms at projectile energies up to few tens of MeV per nucleon and to ensure safe radiological practices during planning and operation for upcoming intermediate energy heavy ion accelerators. The PEQ model and the code will also help in minimizing the doses from shielding compositions based on the prior estimation of induced activity from the structural

and construction materials.

A thesis presented work on development of optimization techniques for fuel management in heavy water moderated reactors, which is of utmost importance for the department. Different optimization techniques for fuel management in initial core and during each refueling of a reactor were developed for AHWR which have ascertained enhanced utilization of fuel at any stage of reactor operation. A special refueling scheme has been developed where each refueling operation is followed by reshuffling operations. A computer code CARS has been developed, where the selection of fuel channels for refueling/reshuffling has been automated. By using this special refueling scheme, safe and economic operation of AHWR is demonstrated.

Computer codes based on two population based algorithms (Genetic algorithm (GA) and Estimation of distribution algorithm (EDA)) have been developed to address complex AHWR initial core loading pattern optimization (LPO) problem.

Various modifications in EDA for improving the performance and search for a better optimized LP have been tried which has lead to slight improvement in the performance.

Another thesis in astrophysics attempted Gamma-Hadron classification for the Ground Based Atmospheric Cherenkov Telescope MACE. The highlights of the thesis are

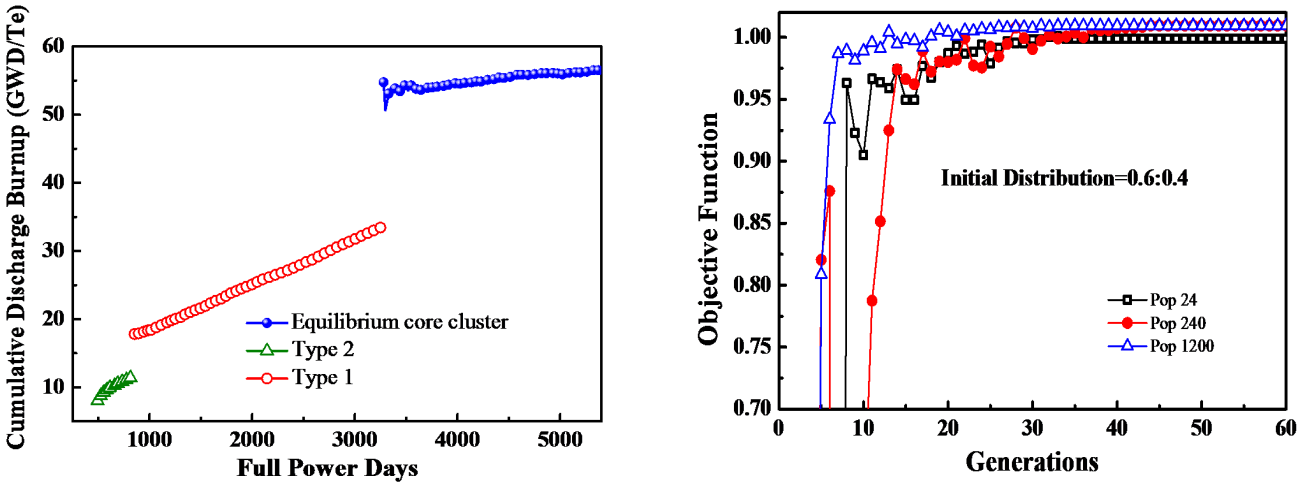

Figure 6.1.5 (a) On-power refueling in AHWR Cumulated burn-up of discharged cluster (using code CARS)
(b) Variation of Objective function with generations in Genetic Algorithm for initial core LPO of AHWR

1. By using the machine learning method Random Forest (RF), the gamma ray analysis energy threshold for the MACE telescope was estimated to be 38 GeV. The conventional gamma ray analysis method failed to achieve the energy threshold betterthan 140 GeV.
2. The integral sensitivity for point like sources with Crab Nebula-like spectrum above 38 GeV is estimated to ~2.7 of Crab Nebula flux at 5σ statistical significance level in 50 hrs of observation.
3. The estimated integral sensitivity of the MACE gamma ray telescope was demonstrate to be superior to the MAGIC-I telescope below 150 GeV (γ-ray energy).

4. Application of Random forest method for the analysis of active galactic nuclei Mrk421 using the TACTIC observation lead to an improvement of 26% in the signal detection strength and ~18% more gamma ray events compared to the conventional gamma ray analysis method.
5. Various machine learning methods like Random Forest (RF), Artificial Neural Network (ANN), Support Vector Machine (SVM), Linear Discrimination method (DISC), Naive Bayes Classifier (NB), Boosting Decision Tree (BDT), BDT with gradient boost (BDTG), BDT with decorrelation + Adaptive Boost (BDTD), TmlpANN (ROOT's ANN), Fisher Boost (Linear discriminant with Boosting) and Probability Density Estimator Range-Search (PDERS) were investigated by using the TACTIC simulation data and the superiority of RF method was demonstrated.

6.2 Indira Gandhi Centre for Atomic Research

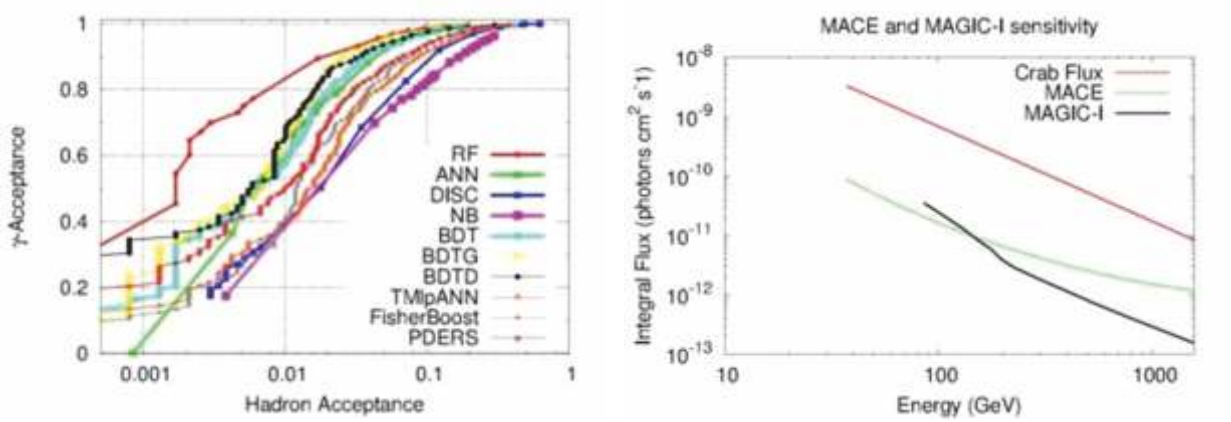

Figure 6.1.6 (a) ϒ acceptance bs hadron acceptance (b) Integrated flux vs Energy

A thesis presented work on inelastic light scattering studies on strong network Glasses Inorganic glasses with covalently bonded network structures formed by local atomic polyhedra are called as network glasses. Structure of network glasses is tunable using modifiers and intermediates. Two length-scales generally characterize the structure of a glass a short-range structure defining the nearest neighbour atomic polyhedra and an intermediate-range order defining regions of ordering beyond the second nearest neighbour. The evidence for the presence of intermediate-range order in glasses is the universal appearance of the first sharp diffraction peak (FSDP) observed in diffraction experiments and the Boson peak (BP) observed in inelastic light and neutron scattering experiments. Borate glasses exhibit a unique structure where some fraction of the initial three-coordinated units convert to four-coordinated borons with increasing modifier amount up to a certain concentration of doping. Borate and modified-borate glasses exhibit substantial intermediate-range order (~20 Å) arising from superstructural units. Network modifiers play an important role in defining the length-scale of the intermediate-range order. Here, the effect of glass modifiers on intermediate-range order in lead-borate glasses is captured from a detailed composition-dependent study of the BP, the FSDP and fragility. A comparison of the length-scales of intermediate-range order (L) obtained from the BP shows that it arises from the vibrations of the superstructural units, while the static correlations (D) from the FSDP arises from the correlation of voids between such structures. Here, experimental evidence of the dynamical properties such as BP and fragility in xPbO (1-x)B_2O_3 glasses have been shown to behave similar to short-range structural properties (average coordination number, glass transition temperature Tg and sound velocity) except an anomalous dip at x =

0.3. The anomalous behaviour at x = 0.3 is assigned to the formation of larger superstructural units (pentaborate units) which give rise to the ordering at intermediate-range length scale. This anomalous behaviour is found to be connected to the common origin of the dynamical properties in the intermediate-range ordered structures and reflects the critical role of Pb^{2+} in tuning the intermediate-range structure of the vitreous network.

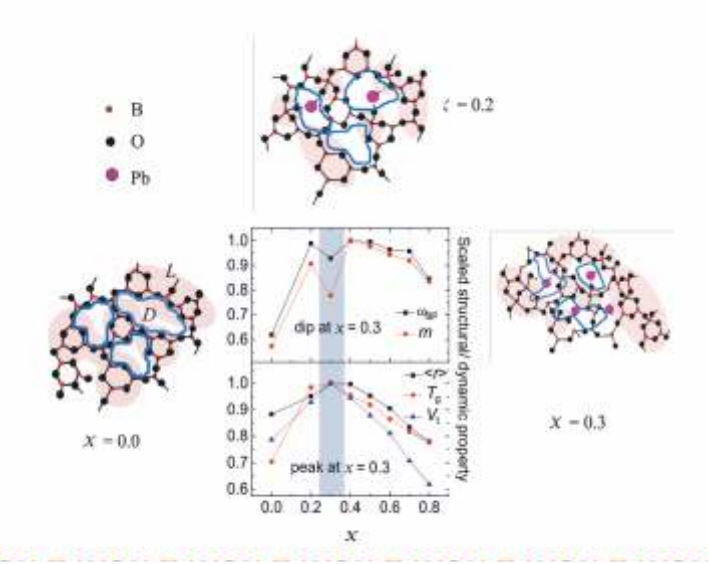

Figure 6.2.1 Short range structural properties exhibit a peak while anomalous dip at x = 0.3 is observed for the dynamic properties. Medium range ordering arises from vibrations of superstructures through dynamic correlation length L, while static correlations D arise from correlation of voids between such structures.

Diamond like Films (DLC) are of technological importance. Diamond Like Carbon (DLC) films, owing to their unique properties includes high hardness, ultra-low friction coefficient and extremely high wear resistance have become an obvious choice for electronic, optical and wear protection applications in nano to micro and macro-scale. A thesis presented work on correlation of tribological properties with chemical structure of modified DLC films Ultra smooth DLC films were grown on single crystal Si (100) substrates using plasma enhanced CVD technique as a function of substrate bias and nitrogen doping. The bonding, chemical structure and hydrogen content of these films were evaluated as function of the ion energy and nitrogen doping concentration. The variation in local elastic modulus of DLC films as a function of ion energy and nitrogen concentration was demonstrated by the acoustic force atomic microscopy. This provided the microscopic evidence for the graphitic phenomenon explained by the established sub-implantation growth model for DLC films. The measured elastic modulus of the films was well corroborated with the structural properties. Further the friction coefficient and wear rate of these films deposited as function of substrate bias and nitrogen concentration were obtained and correlated with bonding, film density and hydrogen content. Moreover, a detailed surface analysis using X-ray Photoelectron spectroscopy signified the role of adsorbed oxygen layer in controlling friction and wear properties. Additionally the sliding induced structural transformations also demonstrated using Raman spectra mapping of the wear tracks. This work provided an insight on various mechanisms governing the friction and wear depends on the test environment. The role of surface passivation and sliding induced graphitization in achieving super low friction and high wear resistance was substantiated. In this work we also achieved DLC surfaces with tunable wetting characteristics. Finally, the

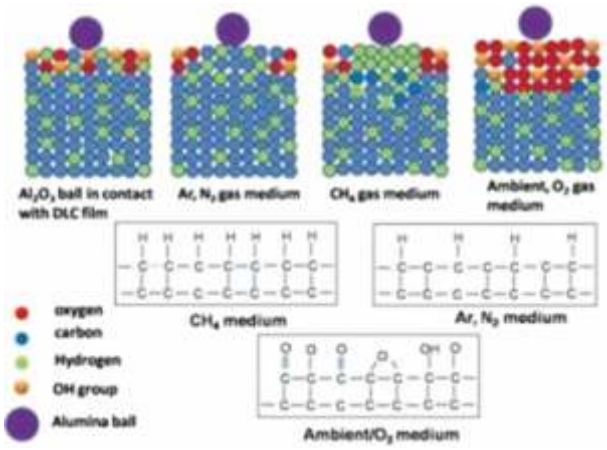

Figure 6.2.2 Schematic of tribo-chemical reactions at DLC surfaces tested in various gas medium

work summarized the influence of surface chemistry on tribological properties of DLC films.

Two-dimensional (2D) materials are a class of materials, consisting of a limited number of crystalline layers of atomic thickness. Among them graphene has been studied extensively due its unique physical properties. After the discovery of graphene, researchers have studied the structural and thermodynamic properties of different 2D materials in detail using harmonic, quasi-harmonic (QH) and anharmonic lattice dynamics (LD) methods. All the above methods fail to capture the true anharmonic nature of 2D materials. To compute the structural, thermal and vibrational properties of 2D materials with full anharmonicity of effective interaction between atoms, the student have developed a spectral energy density (SED) method and implemented in classical molecular dynamics (MD) simulation package LAMMPS. Using this method, he computed the temperature dependent structural stability, frequency shift, linewidth and coupling of normal modes of vibrations of graphene, 2D h-BN and monolayer (ML)-MoS2. The results obtained show significant differences from quasi-harmonic studies due to the inclusion of higher order phonon-phonon coupling processes, which were absent in quasi-harmonic approximation. The structural stability analysis envisages that the inclusion of higher order phonon-phonon coupling is a must to stabilize the graphene and 2D h-BN sheet at finite temperatures with the accompanying crumpling of sheets observed in experiments. Unlike graphene and 2D h-BN, in ML-MoS2, its finite thickness counteracts against the membrane effects and makes the sheet stable and prevents the crumpling transition. The student delineated the contributions of thermal expansion and anharmonic coupling of phonon modes to the frequency shift and linewidth, and found that the anharmonic coupling of phonon modes is the dominant source of observed frequency shift and broadening of peaks. The role of ripples on the thermal expansion properties of aforementioned 2D materials is analyzed. Ripples affect the thermal expansion properties of graphene and 2D h-BN significantly, while its effect is marginal in ML-MoS_2. The above discrepancy is attributed to the special S-Mo-S sandwich structure of ML-MoS_2, which reduces the rippling behavior considerably.

A thesis on quantum information worked on Discrete Wigner functions (DWFs). They are alternate formulation of quantum systems as a real valued functions in discrete phase space. These functions find

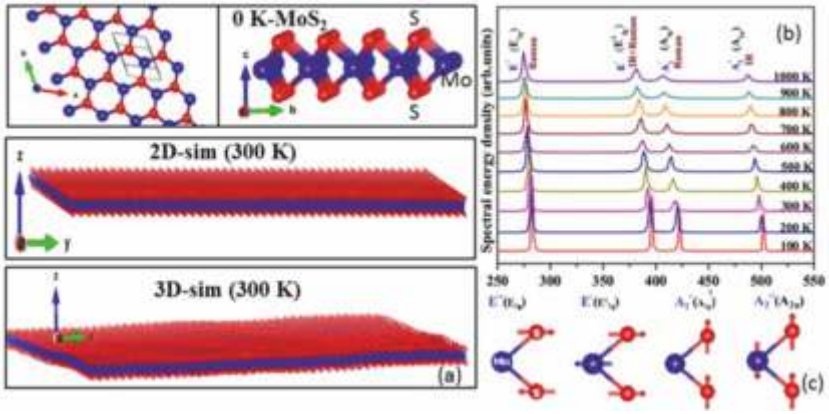

Figure 6.2.3 (a)(Top) Top view of the honeycomb lattice of ML-MoS2. The honeycomb lattice contains one Mo atom and two S atoms located at the corners of hexagons. (Middle & bottom) snapshots of sheets obtained from 2D and 3D simulations at 300 K. The thermally excited ripples are conspicuous in 3D simulations. (b)The Γ-point optic phonon modes as a function of temperature. The modes are labeled, the notations inside the bracket corresponds to bulk representation. IR and Raman active modes are indicated. (c) Eigenvectors of the corresponding modes

widespread application in the field quantum information and quantum computation.The present work provides tools to quantify and detect the entanglement present in multi-qubit DWFs. The DWF and its spin flip counterpart of a multi-qubit systems is shown to be related through a Hadamard matrix and it is independent of the quantum net. The direct relationship between DWF and Stokes vector of a multi-qubit systems is discussed. They are shown to be related through a Hadamard matrix (different from the previous one) and it depends on the choice of quantum net. A relationship between Stokes vector of the spin flippedsystem and DWF is given. A formula for computing n-concurrence for DWFs of a multi-qubit systems is derived. The reduction formula equivalent to the partial trace operation is derived to compute the DWF of any k-partite sub-systems from DWFs of multi-qubit systems. This result is valid for all possible quantum nets of composite and sub-systems. On the experimental side, bi-partite polarization entangled photons are generated through SPDC process. The DWF of these two qubit polarization entangled photons is reconstructed from series of projective measurements.

6.3 Raja Ramanna Centre for Advanced Technology

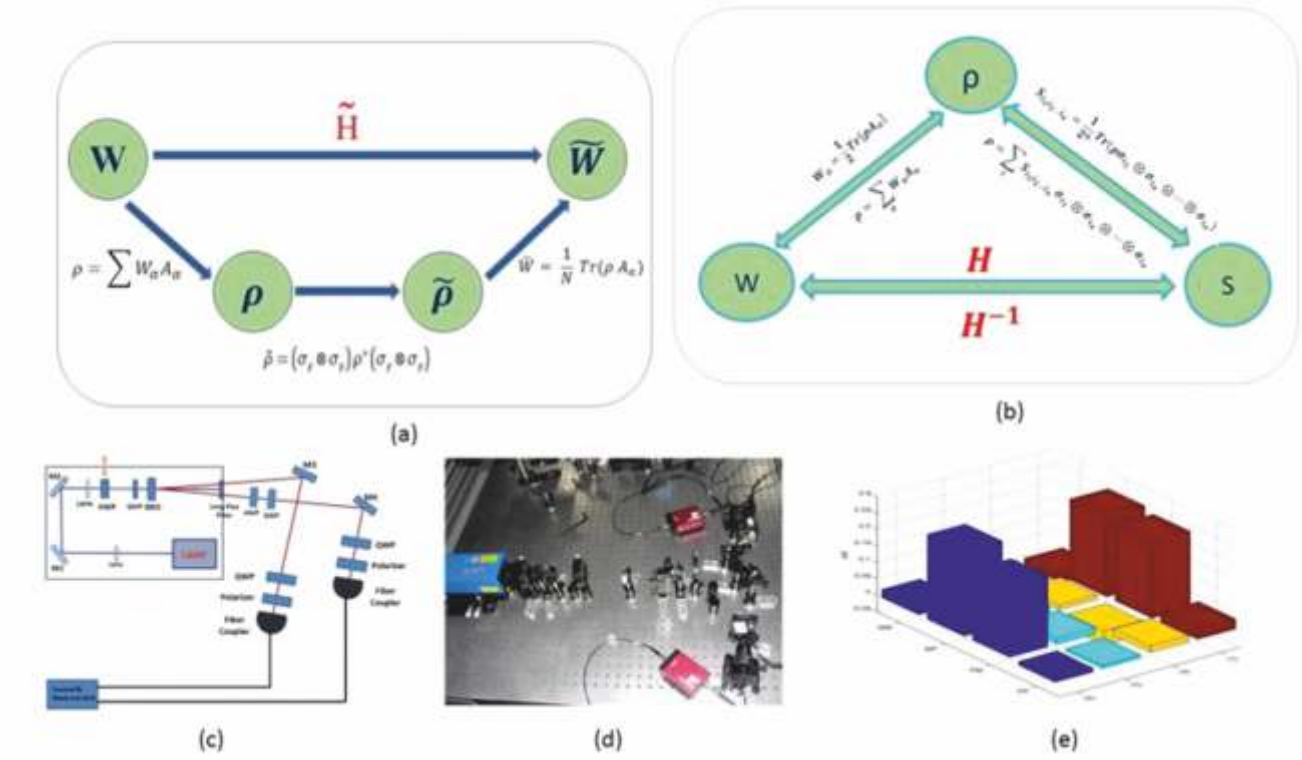

Figure 6.2.4 (a)Shows a relationship between DWF and its spin flip counterpart for multi-qubit systems. (b) Shows the direct relationship between DWFs and Stokes vectors of the multi-qubit systems. (c) Schematic of the experimental set upto generatepolarization entangled photons using SPDC process. (d) Experimental set up to generate entangled photon pairs and reconstruction of its DWF. (e) Reconstructed DWF of two photon polarization entangled states.

A thesis from RRCAT studied effect of substitution on electronic structure, magnetic and mechanical properties of ni, pt and mn-based heusler alloys. Heusler alloys have potential applications in diverse fields they can be probed as good thermoelectric, magnetocaloric, spin-injector, shape memory alloy (SMA) etc. Search for novel and promising Heusler alloys as well as in-depth understanding of their properties are

important. Here effect of substitution on electronic, magnetic and mechanical properties of Ni, Pt and Mn-based full Heusler alloys (FHAs) has been studied. Some FHAs are known to undergo a structural transition (from cubic to tetragonal symmetry) which is related to the shape memory property, if the alloy is cooled below a certain temperature (namely, martensite transition temperature, T_M). From the practical application point of view, it is desired that T_M and Curie temperature (T_C) be above room temperature (RT) and inherent crystalline brittleness (ICB) be low, as is shown in the literature. In the present thesis, a FHA Co_2PtGa has been predicted as a novel and promising Heusler alloy with high T_M and T_C (both above RT) and quite low ICB.

Present work (also studies in literature) show that one group of FHAs is likely to show a structural transition (related to SMA property) and is generally metallic in nature (set 1, example Co_2NbSn) whereas another group of FHAs possess high spin polarization at Fermi level (E_F) and is not typically prone to structural transition on cooling (set 2, example Co_2MnSn). An in depth study has been carried out on the similarities of and differences between electronic, mechanical and magnetic properties of these two classes of FHAs. Contrary to the second set, in case of the first set of materials, a softening of tetragonal shear constant and a high density of states (DOS) at or very close to EF have been observed (Figure 6.3.1). The closeness of DOS to EF causes a lowering of overall binding energy as a result of applied tetragonal distortion in the first set of materials.

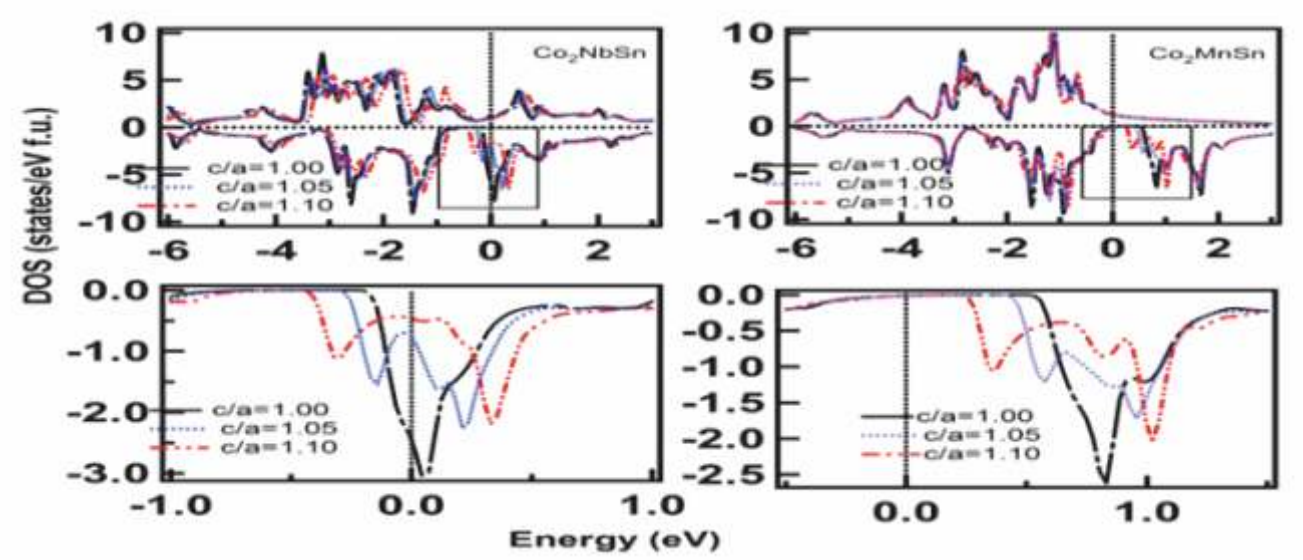

Figure 6.3.1 The density of states as a function of energy has been plotted for the cubic and tetragonal phases, from 1 to 1.10 in steps of 0.05 for materials Co2NbSn and Co2MnSn in left and right panels, respectively. Panels below show the down spin density near the Fermi level derived from eg states of the 3d electrons of the Co atom, for the respective materials.

6.4 Variable Energy Cyclotron Centre

A thesis entitled "Two particle correlations with identified trigger particles (pions and protons) in p-Pb and p-p collisions at the Large Hadron Collider (LHC) energies" has worked on CERN data. This work is based on collaboration between DAE and CERN in the field of particle physics. The thesis concentrates on a correlation observable which can be used to probe collectivity in small collision systems (p-p and p-Pb

collisions at LHC energies). Ridge, elliptic flow, mass ordering of the flow coefficient (v2) and baryon to meson enhancement at intermediate pT in small collision systems have remained a few of the most remarkable and surprising observations at LHC. However, no general consensus could be reached as ideas based on hydrodynamical evolution of the partonic medium or based on incoherent parton scattering along with quark coalescence or correlated emission from glasma flux tubes (CGC) could reproduce similar results. In this thesis, the presence of collectivity in small collision systems (pp and p-Pb collisions at LHC energies) has been investigated by using a measure of correlations with identified triggers at intermediate pT where the inclusive proton to pion enhancement has been observed. This enhancement is similar to the one already observed in the heavy-ion collisions at RHIC and LHC energies where it has been described in terms of radial flow and/or coalescence model of hadroniztion - indicating the presence of soft physics in the system. Now, applicability of the hydrodynamical scenario to p-p and p-Pb systems is in contradiction with the basic idea of hydrodynamics, i.e., the mean free path of partons must be smaller than the size of the system. The data taken by the ALICE collaboration for p-Pb collisions at √sNN = 5.02 TeV has been analyzed and proton triggered jet-like yield has been found to decrease gradually with multiplicity whereas the pion triggered jet-like yield remains almost constant as shown in Fig 1- commonly referred to as "trigger dilution". EPOS 3 (3+1D event-by-event hydro model) and AMPT with string melting (incorporates coalescence model of hadronization) can not reproduce the data quantitatively. But, EPOS 3 can qualitatively mimic the multiplicity evolution of the pion- and proton-triggered jet-like yields – indicating radial flow as a possible source of the observed trigger dilution in p-Pb collisions at 5.02 TeV. This thesis work also demonstrates that this correlation observable can disentangle the effect of hydrodynamical flow (in EPOS 3) from the effect of MPI based color reconnection (in PYTHIA 8) in case of p-p collisions at 7 TeV. In absence of significant jet-medium interplay, this trigger dilution may serve as a useful probe to investigate the presence of soft physics (coalescence model of hadronization, radial flow) in small collision systems where hydrodynamical collectivity is not so intuitive.

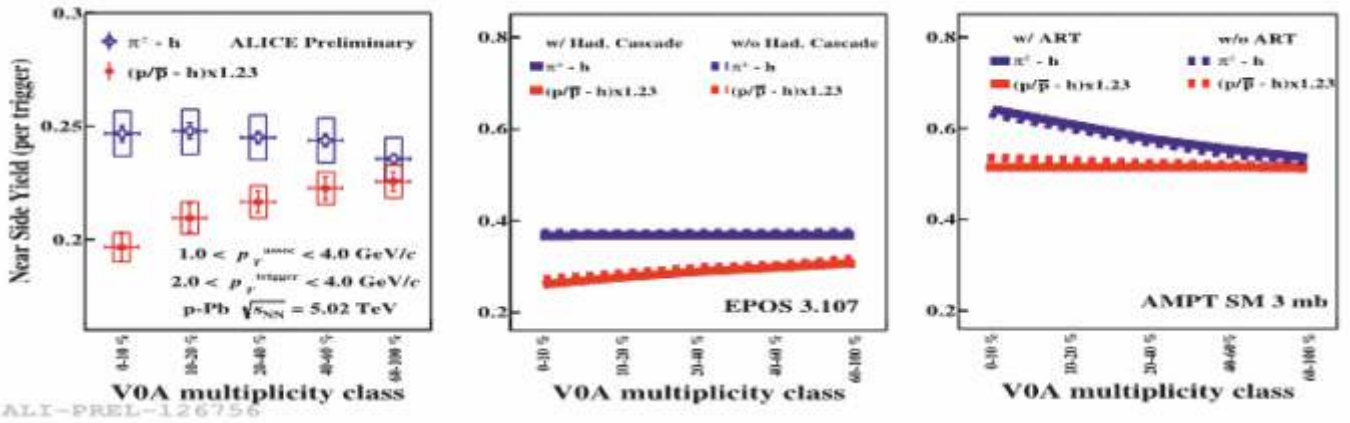

Figure 6.4.1. Near side yield from pion and proton triggered correlation in DATA (left), EPOS 3 (middle) and AMPT string melting (right).

The timescale of nuclear fission of highly excited fissile nuclei is a basic characteristic of the underlying fission dynamics. In this thesis the student have measured fission time for the first time from the intrinsic width of K x-ray lines of the ion containing the fissioning nucleus using only quantum mechanical energy-time uncertainty principle. The experimental challenge was to see the sharp Kα1 line of plutonium produced in the ^{4}He (60 MeV)+^{238}U fusion reaction as shown in Figure 1 (a). We obtained that most of the fission events are slow with a mean fission time > 1x10^{-18} sec. The long survival time obtained for this

system appears to be inconsistent with the short fission delays obtained from the nuclear experiments and calculations. Figure 6.4.2 a) Photon spectrum in coincidence with fission fragments with Pu Kα1 line (red curve) and fission fragment gamma lines (blue curves) simulated by GEANT3. b) Representative signal (blue curve) of electron cloud trapped in Penning Trap with ramp voltage (yellow curve) c) VECC Penning Trap setupSimilar inconsistencies have been found from the measurements of quasifission and fission time by nuclear and atomic techniques for Z=120 nuclei as well as many uraniumlike and transuranium nuclei that are far away from the island of predicted island of superheavy nuclei. So, the fission time measurement anomaly appears to be a general problem and could be beyond fission dynamics. We have discussed a probable solution of the fission time anomaly using a quantum decoherence model.

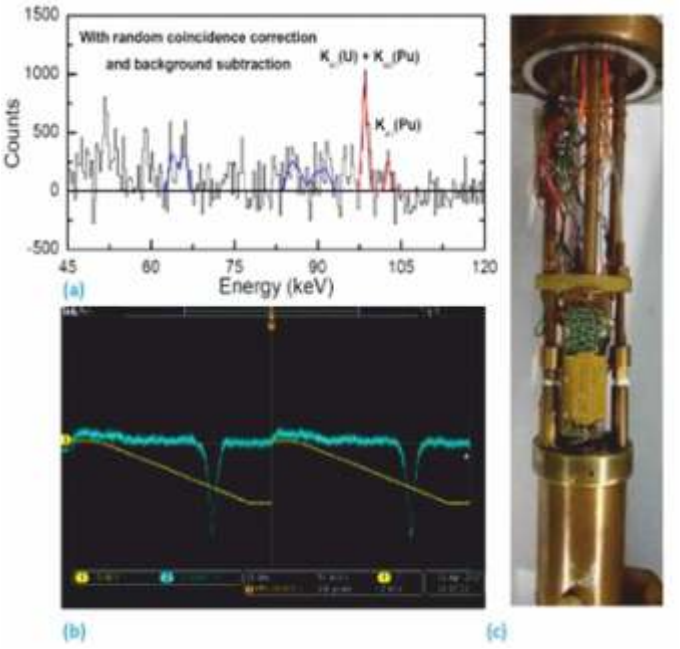

Figure 6.4.2 a) Photon spectrum in coincidence with fission fragments with Pu Kα1 line (red curve) and fission fragment gamma lines (blue curves) simulated by GEANT3. b) Representative signal (blue curve) of electron cloud trapped in Penning Trap with ramp voltage (yellow curve) c) VECC Penning Trap setup

The high precision mass measurement of very heavy nuclei would provide further information on this important topic and in this context a Penning trap facility would be very useful which has been developed as a part of this work. The commissioning of Penning Trap where a cloud of electrons had been trapped in a low magnetic field and at liquid nitrogen temperature was achieved and it has been reported in this work.

A thesis carried out study of Nuclear Viscosity and Isospin Mixing Utilizing Isovector Giant Dipole Resonance using K-130 cyclotron at VECC. . It contains the experimental investigations on two crucial properties of atomic nucleus; namely the ratio of shear viscosity (η) to entropy density (s) for finite nuclear matter at finite temperature and isospin mixing at high temperature in self- conjugate nucleus ^{32}S. Both studies were performed utilizing the isovector giant dipole resonance (IVGDR) as a probe. The IVGDR was populated in compound nucleus (CN) reaction using the ^{4}He beam of 28-50 MeV from the K-130 cyclotron at the Variable Energy Cyclotron Centre Kolkata. The γ-rays from the decay of the GDR Were detected using LAMBDA Spectrometer (B), while the CN angular momentum was determined by measuring the low energy multiplicity γ-rays by the multiplicity filter (B). Evaporated neutrons were detected using neutron time of flight detector (C) for proper determination of nuclear level density (NLD) parameter and nuclear temperature. The low energy γ-rays were also

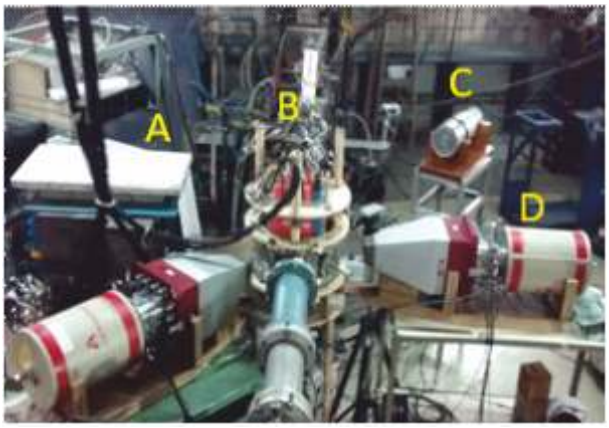

Figure 6.4.3 Experimental set-up used for present studies

detected using two clover detectors (D) for observing the isotopic impurity of the targets, if any. The theoretical analysis of the measured data was performed using statisticalmodel code CASCADE.

In the first part of the thesis, the shear viscosity for finite nuclear matter was determined from the measured GDR parameters (energy and width), while the entropy density was calculated from the measured NLD parameter and nuclear temperature. Thus, it has been observed experimentally, for the first time, that the nuclear fluid conform to the KSS conjecture and also establishes that strong fluidity is the universal characteristic of the strong interaction of the many-body nuclear systems. This result, along the results of low-temperature quantum fluids, suggests that large fluidity could also possibly be the intrinsic characteristic feature of strongly coupled systems.

6.5 Saha Institute for Nuclear Physics

Light-matter interaction at the nanometer scale has attracted significant interest in the area of photonics research in recent years due to its' huge applications in different fields such as cancer therapy, optical trapping, bio-sensing, drug delivery, solar cells, surface-enhanced Raman scattering (SERS)etc. All of these applications are based on the concept of localized surface plasmons (LSPs), i.e., collective charge density oscillations of the conduction electrons at the surface of metal nano particles (MNPs). For advancing different applications, it is very important to know the distribution of the electromagnetic field over MNPs with nanometer level spectral and spatial resolution. Recently cathode-luminescence (CL) has become a powerful tool for probing the LSP modes of MNPs with spatial resolution better than 10 nm. The main goal of this thesis is to understand plasmon assisted photon emission from anisotropic Au NPs using CL combined with finite-difference time-domain (FDTD) simulations with special emphasis on higher order modes and substrate effect.

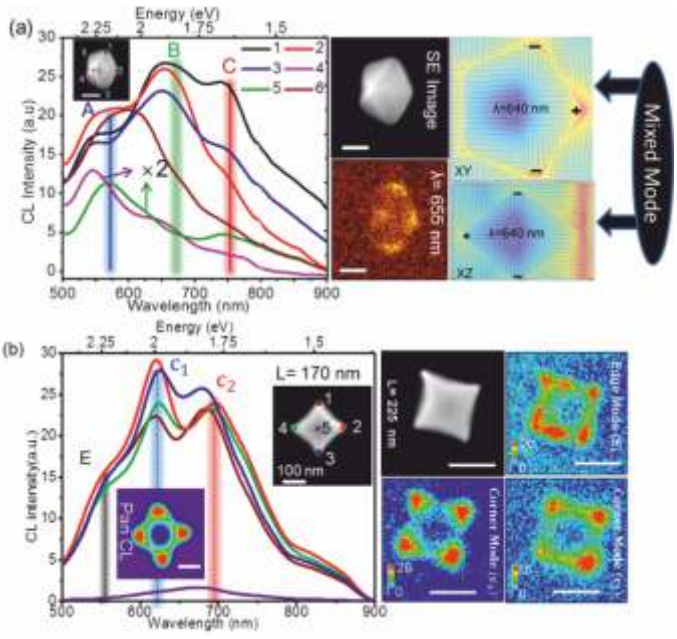

Figure 6.5.1: CL-FDTD combined studies of (a) Au decahedron and (b) Au concave nano cubeparticles.

In this thesis it is shown that mode mixing occur in the plasmonic properties of an isolated decahedron Au nanoparticle [Figure 6.5.1a] of side edge length 230 nm. Apart from a substrate induced LSPR mode in the near-infrared (750 nm) region, FDTD numerical analysis also identifies two prominent LSP modes in the visible region. While the shorter wavelength (560 nm) mode has a mixture of in-plane quadrupolar and out-of-plane quadrupolar charge distribution pattern, the longer wavelength (655 nm) mode has the dipolar charge pattern in both the direction.For Au concave nanocubes (CNCs), We observe that site-selective electron beam excitation gives rise to simultaneous excitation of edge and corner LSP modes [Figure 6.5.1b]. Extensive FDTD numerical analysis reveals effects of concavity, substrate and particle size on the amplitude and energy range of these plasmonic responses.Using FDTD simulations, we identify that mode E is related to the edge quadrupolar mode while the other two modes (mode C1 and mode C2) are hybridized octupolar mode and corner

quadrupolar mode respectively.

It is possible to obtain different shaped three dimensional nanostructures on substrate surface by this technique and subsequent thermal annealing. Since galvanic displacement reaction is a charge exchange reaction, controlling the particle size is a challenging part. Thermal evolution of nanoparticles on substrate surface plays an important role in substrate adhesion, phase separation, shape transformation. Now, to study the substrate supported nanoparticles and their interfaces transmission electron microscopy is an indispensable technique that has been utilized.

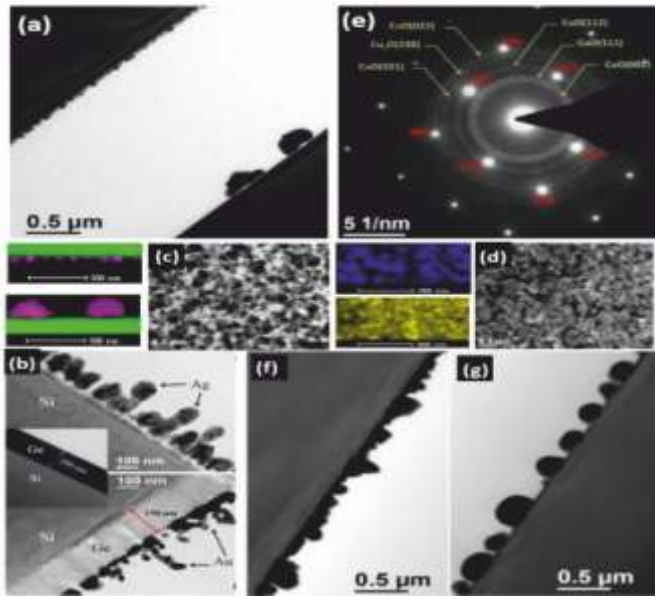

Figure 6.5.2 (a) Ag deposition on crystalline and amorphous Ge substrate, EDX maping of Ag (pink), and Ge (green); (b) substrate decomposition in Au and Ag deposition on Ge film; (c, d, blue and yellow color)wetting in oxidation of Cu nanoparticles and (e) the phase transformation by SAED; (f, g) dewetting in N2 environment annealing of Ag.

The main objective of this thesis work is to study the fundamental mechanisms occurring during three dimensional growths of nanostructures using GDR and their thermal evolution by investigating the influence of annealing environment on wetting and dewetting of nanoparticles on substrate surface. TEM and STEM-HAADF-EDX elemental mapping(Figure 6.5.2(a) a and green and pink color) shows the formation of Ag nanoparticles on crystalline and amorphous Ge surface and due to occurrence of electrochemical Ostwald ripening in GDR, bigger Ag particles are formed on crystalline Ge surface. Substrate decomposition in GRD of Ag is more than that of Au (Figure 6.5.2b).Thermal oxidation of Cu nanoparticles on Si surface (Figure 5.5.2c,d,e) and formation of cupric oxide shows unsual wetting rather than agglomeration (Figure 6.5.2.f-g).

Main finding of the thesis is the experimental detection of electrochemical Ostwald ripening in GDR. This observation provides the understanding of underlying mechanism inGDR and offers way to control particle size. The study of thermal evolution of Cu nanoparticle on Si surface shows that oxidation plays an important role in wetting at elevated temperature and it is possible to obtain CuO –an industrially important material in a quick and easy way by the combination of GDR and thermal annealing.

Studies on formation of coherent structures, their stability and their interactions in fluid dynamics as well as in plasmas have drawn a great attention to the physics community as they play a very important role in energy and particle transport in such medium. This thesis is concerned with the studies related to several novel phenomena associated with various kinds of nonlinear coherent structures related to both Alfvén wave in electron-ion plasma as well as transverse shear wave in strongly coupled plasma.

We have explored the linear and nonlinear behavior of linearly as well as circularly polarized Alfvén wavepropagation taking into account the electron inertial effect which is found to act as a source of dispersion. The governing equations describing the small amplitude nonlinear dynamics of the Alfvén wave,such as the modified Korteweg-de Vries equation (mKdV) in absence of collision and the mKdV-Bergers equation (mKdVB) in presence of collisional effects have been solved numerically and the solutions are compared with analytical predictions resulting in soliton and shock like coherent structures

respectively (shown in Figure 6.5.3 a). In the long wavelength limit, the weakly nonlinear Alfvénwave is shown to be governed by a damped nonlinear Schrödinger equation (NLSE). The numerical and analytical solution of this equation predicts weakly dissipative envelope solitons as shown in Figure 6.5.3 b.

We have also studied formation, interactions and stability of vortex structures analytically as well as numerically in strongly coupled dusty plasma in the frame-work of the GH model in presence of dust-neutral collisional drag.The interplay between the nonlinear elastic stress and the dust-neutral drag results in the generation of non-propagating monopole vortex. The generation of dipoles from the interaction between two counter-rotating vortices is shown in Figure 5.5.3 c. In addition, the stability analysis of the long scale equilibrium vortex to short scale shear wave perturbation has been presented The AdS/CFT duality is a very rich topic of research in String theory. In generally, it is limited in supersymmetric regime. But our present world and its physics are completely non-supersymmetric. The fundamental constituents

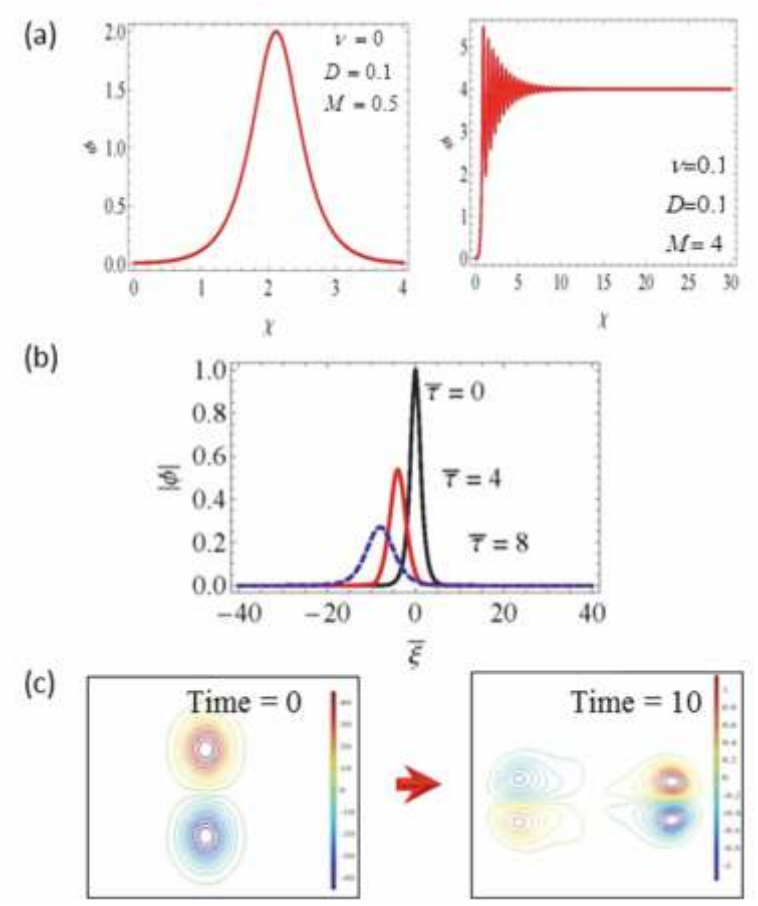

Figure 6.5.3 (a) Formation of solitonand shock in absence and presence of dissipation respectively(b) weakly dissipative envelope solitonand (C) vortex-vortex interaction.

follow the QCD theory which is mainly defined with the running coupling and Lambda-QCD. Another open challenge of String theory is to describe the various cosmologies from brane solutions.

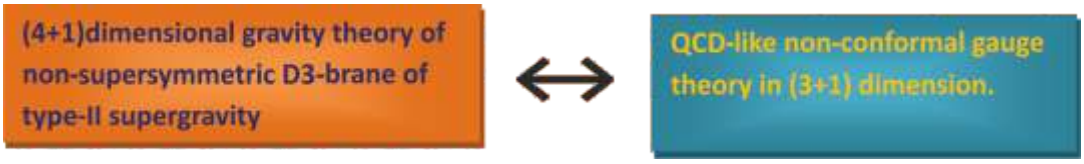

In this thesis, it has been shown that the non-supersymmetric brane solutions of type-II supergravity has

led to non-supersymmetric version of gauge/gravity correspondence. Here we have proposed the consistent decoupling limit to derive the decoupled geometry of non-susy D3 brane. The non-constant

dilaton field gives the running coupling of the QCD-like dual gauge theory. Some of the properties of QGP have been studied using this non-susy gauge/gravity duality.

In cosmology section, the space-like brane solutions have been used. The general isotropic SDp brane gives (p+1,1) dimensional cosmological model upon compactification of 8-p dimensional hyperboloid.

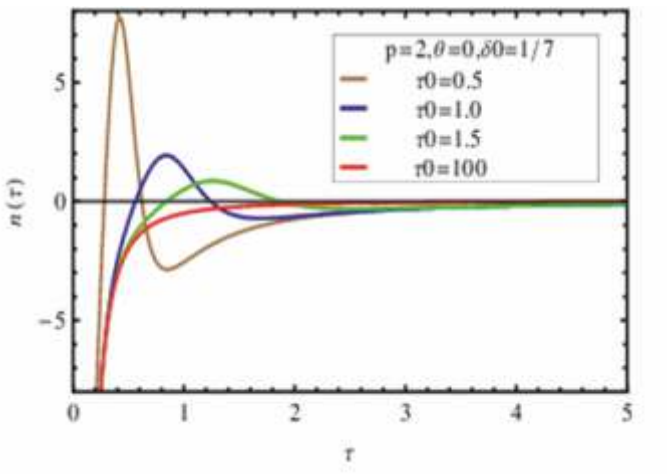

Fig.6.5.4 Index of acceleration vs. time for (3,1)dim FLRW cosmology

For p=2, it is (3,1) dim ever expanding FLRW cosmology. In addition, this expansion is accelerated for a certain window of time. However near τ=0 above FLRW metric reduces to de Sitter geometry. But this de Sitter universe expands with deceleration. Again the anisotropic SD2 brane has been considered. After compactification of transverse six dimensional hyperspace it gives an anisotropic, inhomogeneous (3,1) dim FLRW background. Near singularity it has been reduced to Kasner-like cosmology with two background scalar. Unlike known Kasner solution, this Kasner-like universe can expand in all of its spatial directions at same instance.

Neutron stars are one of the endpoints of stellar evolution. They are composed mostly of neutrons together with some small amount of protons, electrons and muons. The mass of a neutron star can be as high as twice the mass of the sun, whereas its radius is only of the order of 10 km. Consequently, the density of matter inside the neutron star is extremely high. Typically, the density at the center of a neutron star is a few times the normal nuclear density. Therefore, various important bulk properties of neutron stars are predominantly governed by the equation of state (EoS) of dense asymmetric nuclear matter. The crucial

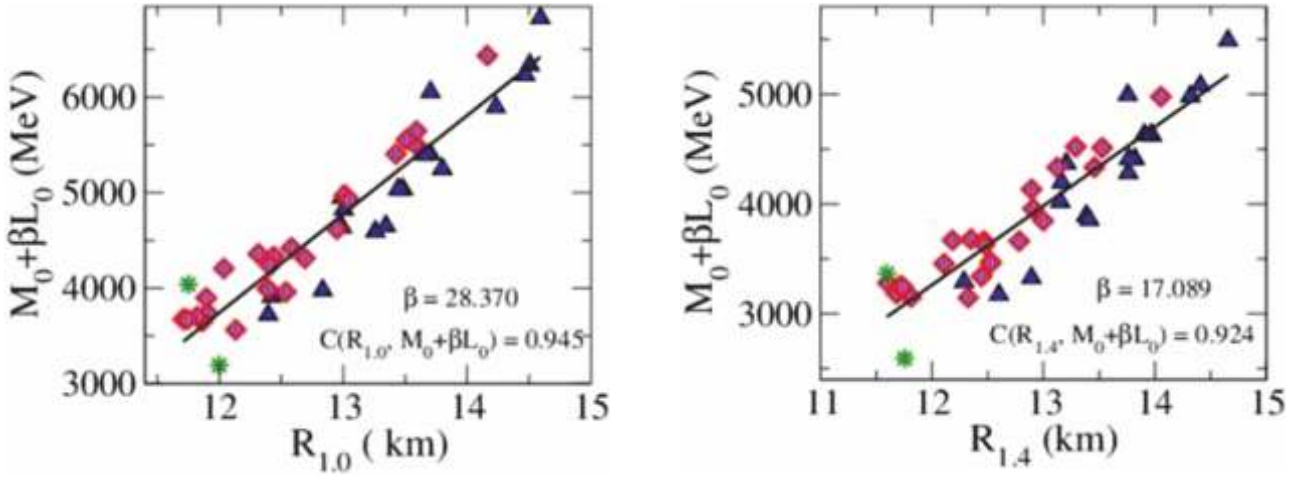

6.5.5 Neutron star radii R1.0 (top) and R1.4 (bottom) versus the linear combination M0+ βL0.

ingredients in determining theEoS of dense asymmetric nuclear matter are the nuclear incompressibility coefficient, symmetry energy coefficient and their density derivatives. But, we have limited knowledge about these key EoS parameters. One can extract the information about these EoS parameters through their correlations with finite nuclei observable or with various bulk properties of neutron stars. Figure The main objective of this thesis work is to study the correlations between the neutron star properties and various key parameters of nuclear matter EoS. The student has calculated different properties of neutron star, such as, core-crust transition properties, mass, radius, tidal deformability parameter etc., for a representative set of relativistic and non-relativistic nuclear models. Then, dependences of these neutron star properties on the key EoS parameters have been investigated. He found that the neutron star properties considered for our study are strongly depend on various EoS parameters. Most importantly, he observed strong and model independent correlations of neutron star radii with the linear combination of the slope of the nuclear matter incompressibility coefficient (M0) and slope of the nuclear symmetry energy coefficient (L0) at the saturation density for the first time (as displayed in Figure 5.5.4). Such correlations are found to be more or less independent of the neutron star mass over a wide range. This correlation is traced back to be linked to the empirical relation existing between the star radius and the pressure at a nucleonic density between one and two times saturation density.

Quantum integrable systems are closely associated with different areas of physics and mathematics such as quantum optics, condensed matter systems exhibiting generalized exclusion statistics, random matrix theory, quantum Hall effect etc. For one-dimensional systems, these models are exactly solvable and many statistical properties related to the spectra of these models can be studied from their exact solutions. Depending on the natures of interactions, they can be further classified into two categories, namely, short-range interactions(δ-function bose gas, Hubbard model, isotropic and anisotropic versions of Heisenberg spin-1/2chain) and long-range inertactions(one dimensional systems like Calogero model, Sutherland model, Haldane-Shastry (HS), Polychronakos spin chain).

In this thesis, the aim is to study some rational quantum integrable spin dynamical models and spin chains associated with polarised spin reversal operators (PSRO) and supersymmetric analogues of PSRO (SAPSRO). For the spin Calogero model of D_N type with polarized spin reversal operators, We computed the spectrum and the partition function of the former model in closed form, from which we derived an exact formula for the chain's partition function in terms of products of partition functions of Polychronakos-Frahm spin chains of type-A. Using a recursion relation for the latter partition functions that we derived in this case, we were able to numerically evaluate the partition function, and thus the spectrum, of the D_N type spin chain for relatively high values of the number of spins N. We analyzed several global properties of the chain's spectrum, such as the asymptotic level density, the distribution of consecutive spacings of the unfolded spectrum, and the average degeneracy. In particular, our results suggest that this chain is invariant under a

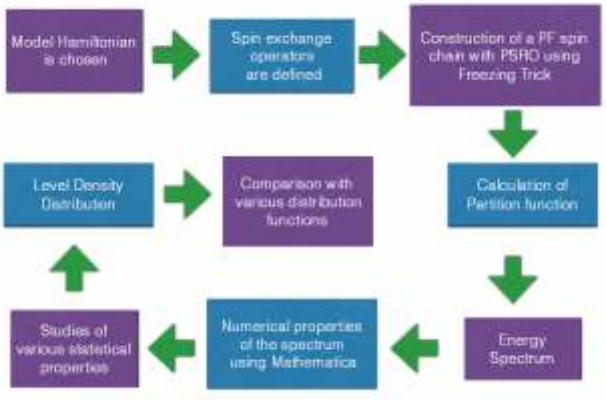

Figure 6.5.6 Schematic illustrating the workflow process as used to understand the Quantum Spin systems.

suitable Yangian group, and that its spectrum coincides with that of a Yangian-invariant vertex model with linear energy function and dispersion relation.

Similarly, the exact spectra as well as partition functions for a class of BCN type of spin Calogero models as well as its supersymmetric analogues, whose Hamiltonians were constructed by using supersymmetric analogues of polarized spin reversal operators (SAPSRO) were studied. It was observed that an extended boson-fermion duality relation is obeyed by the partition functions of the BC_N type of PF chains with SAPSRO.Some spectral properties of these spin chains, like level density distribution and nearest neighbour spacing distribution, were also studied.

6.6 Institute for Plasma Research

Synchronization among elements of an assembly of oscillators is a well-studied phenomenon and a useful paradigm for understanding collective behaviour observed in various natural and laboratory situations ranging from in-phase glowing of fireflies to understand phase transitions in material media. The thesis deals with synchronization Studies Between Two Coupled Glow Discharge Plasma Sources. A plasma is a highly complex system exhibiting various kinds of oscillations and instabilities that often give rise to turbulent or chaotic behaviour. The study of synchronization phenomena in such a system poses interesting experimental and theoretical challenges. In this thesis work, experimental and numerical investigation of synchronization phenomenon is presented for two coupled glow discharge plasma sources.

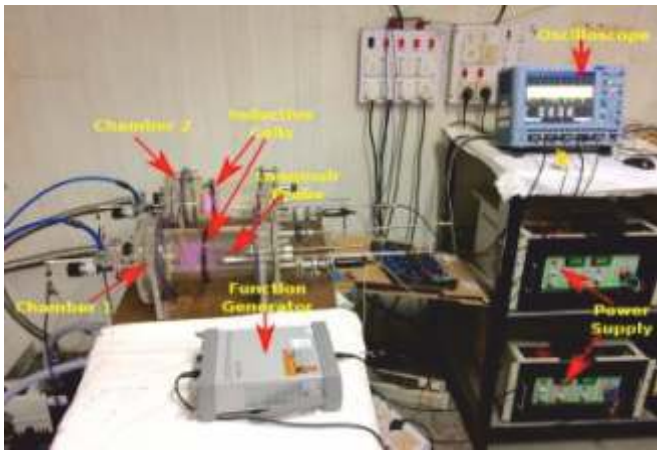

Figure 6.6.1 Experimental setup of two glow discharge plasma systems.

An experimental lab is setup for doing such studies (Figure 6.6.1). The experimental setup is consist of two glow discharge plasma systems with direct and indirect coupling mechanism. The major findings from this work are

(1) First time, it has been reported that oscillations of two plasma systems can be synchronized via indirect or inductive coupling mechanism. This result could have direct impact in future studies where instabilities or oscillations in plasma system can be remotely controlled.

(2) Phase-flip transition results are presented for two inductively coupled glow discharge plasma systems. In this result, it has been shown with change in the coupling strength between the oscillations of two plasma systems, oscillations of two systems abruptly jumps from in-phase to anti-phase synchronized state with simultaneous jump in their frequencies. Also, it has been shown that this transition have hysteric properties too (Figure 6.6.2).

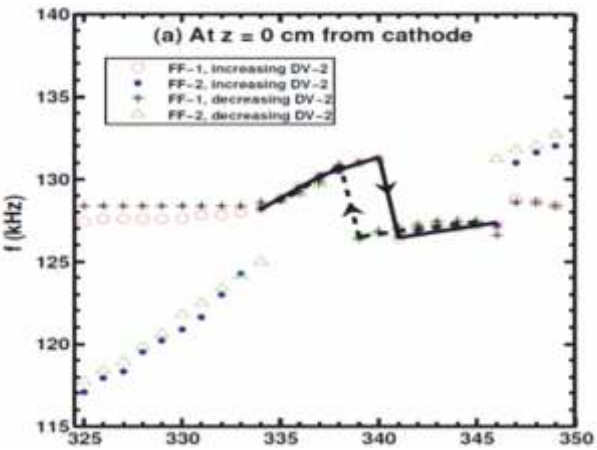

Figure 6.6.2 Phase flip bifurcations and hysteresis phenomenon between two inductively coupled plasma sources

(3) Mutual harmonic synchronization studies are done by forcing oscillations of one plasma system at different harmonic values from the oscillations of other plasma system. These results have unique properties because both the systems are mutually harmonic synchronized with each other which is first time done in any plasma systems.

The present work addresses a set of issues related to Scrape-off Layer (SOL) plasma transport in Adityatokamak using the steady-state Monte-Carlo transport simulation model EMC3-EIRENE.The 3D transport simulations treats plasma-fluid and kinetic neutral species for both, the original poloidally

continuous Ring Limiter (RL) and a toroidally distributed set of outboard Block Limiters (BL) installed on the Aditya-Upgrade configuration. In first part of the work, the 3D transport solutions and profiles simulated in this study are also applied to interpret the limited probe measurements available from the Aditya RL SOL. From complexity of connection length (LC) distribution, the poloidal structure of pressure profiles obtained from steady state transport equilibrium are quasi-periodic and are source of additional vorticity by generating secondary drifts. The resulting change in the ratio D_{EDGE}/D_{SOL} indicates a corresponding impact on the confinement properties of EDGE and SOL region. The second part of work shows the 3D poloidal variations are stronger function of diffusivity (D) in the low density cases indicating reduced stability on open field lines of SOL. The third part of work implements transport in Aditya-Upgrade relevant SOL setups and explores comparison between the SOL transport in original Aditya RL and upgrade-like outboard BL configurations. The central issue addressed is that of a finite diffusive flux of plasma to the main chamber wall as reported from observations on ALCATOR-C that might result in loss of neutral particle control. The recycling flux obtained from 3D simulations shows better stability and particlecontrol in Block Limiter (BL) configurations than Ring Limiter (RL) configuration.

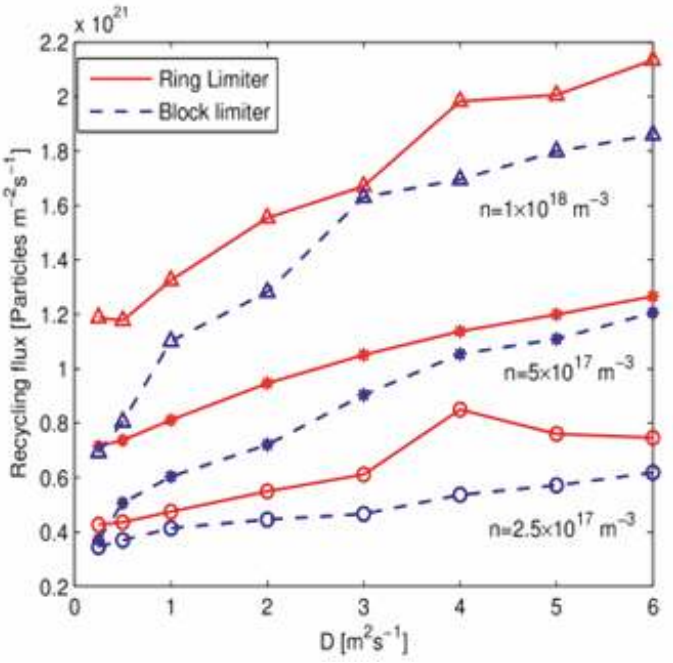

Figure 6.6.3 Recycling flux in Ring and Block Limiter obtained from EMC3 EIRENES imulation with Diffusivity at different Density values.

A thesis deals with experimental studies on collective phenomena in dusty plasma. The dusty plasma, which is an admixture of the electrons, ions, neutrals, and sub--micron to micron sized negatively charged solid particles has been a current topic of research due to its applications in space plasmas, plasma processing technologies, biological systems, condensed matters etc. In the background of plasma, the highly mobile electrons and slower ions impinge on the dust grain surface and make it negatively charged. In the low-temperature plasma, dust grains get negative charges up to 10^3 to 10^5 times of an electron charge (e). The collection of these highly negatively charged grains exhibits the collective dynamics similar to the conventional two component plasmas. The result of the collective response of the dusty plasma medium is encountered as dust-acoustic modes and vortex motion. The collective dynamics of the large volume dusty plasma is studied in a newly designed

Figure 6.6.4. Experimental device for Dusty Plasma studies at Institute for Plasma Research.

dusty plasma device, in which inductively coupled diffused plasma is used to create a potential well for confining the negatively charged dust grains.

The volume as well the characteristics of the dust grain medium changes with the change in discharge and plasma parameters. The confined 3D dusty plasma medium exhibits various self-excited motions depending on the discharge parameters. The confined dust grains exhibit dust acoustic waves (DAW) at lower dissipation and higher input rf power. Multiple co-rotating (anti-clockwise) dust vortices are observed in the dust cloud for a particular discharge condition. The transition from multiple to single dust vortex is observed when input rf power is lowered, as seen in Fig.5.6.5.

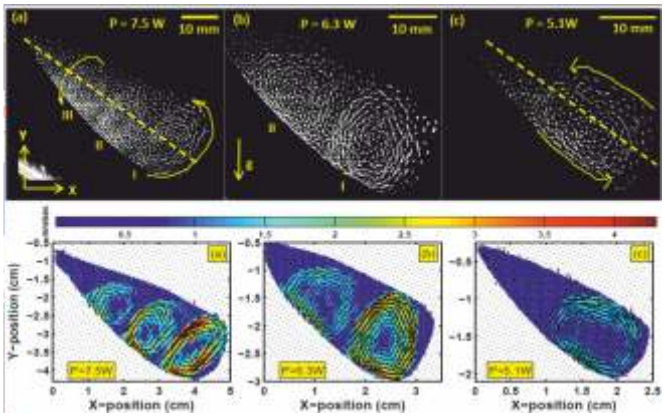

Figure 6.6.5 Results on the origin of co-rotating multiple vortices and velocity distribution of particles in the vortex structures in dusty plasma.

The velocity distribution of particles is estimated using the PIV software and found to be non-uniform throughout the vortex structure. The origin of vortex flow is due to the charge gradient of dust particles which is orthogonal to ion drag force. The charge gradient of dust grains is result of the plasma inhomogeneity in the background plasma parameters. There is a characteristic size of the vortex in the dusty plasma medium; therefore, multiple vortex structures are formed.

Present thesis describes a novel type of device with applications in basic plasma science and nanopatterning. Using a particular arrangement of magnets behind the anode plate, results in the confinement that restricts the contact of the plasma with the anode. The device shows formation of inverted droplet shaped fireball. Plasma, a quasi-neutral medium, is generally bounded by negatively charged boundaries due to highly mobile electrons. These boundaries usually have ion sheath, however in

Figure 6.6.6. Fireball formed at the magnetically constricted anode. Right side shows the schematic of the discharge and magnetic field near anode.

certain circumstances the electron sheath do form near an electrode. Such an electrode is then subject to a very large flux of electrons, consequently draws large electron saturation current and for this reason they

are kept smaller in dimension. It has been observed that these electron sheaths near small electrode can transform into a so called fireball. The fireball is formed by the ionization which neutralizes the negative space charge. The experimental studies of this fireball is difficult partly because small size of the structure, typically 1-2 cm which makes probing difficult. We have devised an experiment to create fireball on a relatively large anode of DC discharge. The magnetic field is used to constrict the effective area of the anode and the device is similar to conventional magnetron sputtering unit. We have found that a large fireball (4-7 cm) forms near the anode, mainly the magnetic field free region. The fireball is separated by a potential double layer of about the ionization potential from the bulk plasma. The plasma density inside the fireball is 1×10^{10} cm^{-3}, which is about an order of magnitude higher than average bulk plasma density. The inside of fireball has two temperature electron populations which is typical for such fireball. The device however, is stable only in low pressure regime. At pressure above 0.05 mbar it shows transition to another stable regime. The two modes are defined as C-Mode and P-Mode, respectively. The high pressure P-Mode shows low frequency oscillations in the range of few kHz. This device in C-Mode can be potentially used as miniature broad beam ion source for various material processing applications. To this end, an experiment was carried out to demonstrate formation of structured nanodots on the GaSb substrate with excellent hydrophobicity.

A thesis deals with Study of Localised Solution in Laser Plasma System. The coupled system of laser plasma permits a wide variety of exact nonlinear localized solutions. The detailed characterization and dynamical behavior of these solutions have been studied extensively in several earlier works. In the thesis, we have focused on three specific issues concerning these structures. (1) We have obtained analytical expressions for the cusp structures which occur when the ions undergo the wave breaking limit. Their numerical evolution shows that the structures are susceptible to Raman Forward scattering instability. (2) All previous studies were confined to a 1-D evolution of these structures. We study the evolution of these structure in 2-D and show that the erstwhile stable single peak solutions are unstable to filamentation instability. Even those structures which are unstable to 1-D forward Raman scattering instability have been shown to undergo the next phase of filamentation instability with 2-D character. (3) We have also investigated the evolution of localized solutions in which the precarious balance between ponderomotive force and the electrostatic force is disturbed significantly. We observe that the evolution exhibits interesting out of phase oscillations between field and kinetic energies. The density oscillations invariably suffer wave breaking ultimately leading to structures where radiation is trapped between density peaks. These studies have been performed both with fluid and PIC simulations.

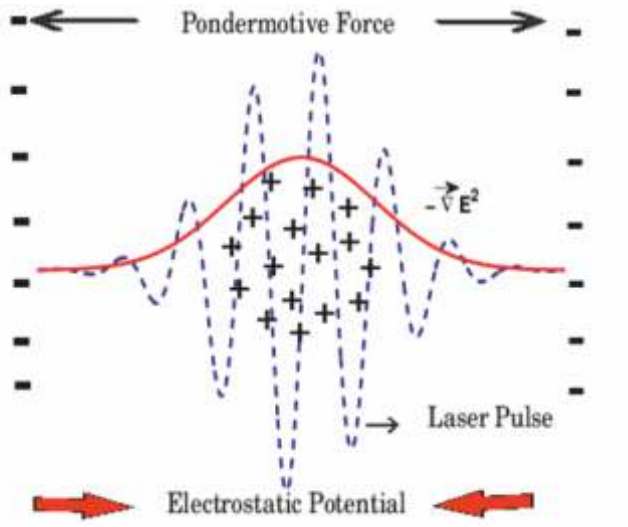

Figure 6.6.7 Schematic of soliton formation

This thesis was an attempt to investigate open physics problems in cylindrically confined non-neutral plasmas using the method of particle-in-cell (PIC)simulation.A suite of Electrostatic, OPEN-MP parallelized, PIC and PIC-with-Monte-Carlo-Collisions (MCC) codes have been developed to simulate collisionless and

collisional dynamics of plasmas of arbitrary neutrality in cross-sections of cylindrical magnetic traps. Simulations of the radial breathing modes on high density, i.e. high Brillouin ratio, electron clouds, revealed interesting nonlinear dynamics of the radial breathing modes such as spontaneous formation of density voids within the profiles of the electron clouds which in turn triggered transient azimuthal modes on these clouds[1]. Through numerical experiments performed with a 2D3v PIC code facilitated with 3D Monte-Carlo-Collisions it has been demonstrated in the thesis that contrary to existing theory, elastic collisions of electron with background neutrals have no destabilizing influence on the cloud dynamics[2]. A new theory has been put forward which explains that the non-ionizing collisions are incapable of drawing electrostatic energy from the negative energy Diocotron modes that is necessary for destabilizing these modes.1D PIC simulation have been used to demonstrate a novel scheme for axial heating of single component plasmas in cylindrical traps without driving the plasma far from thermal equilibrium [3]. 2D PIC simulations of the ion resonance instability reveal that the instability initially progresses in close adherence to the linear fluid model, but eventually becomes a fully kinetic, nonlinear phenomenon, exhibiting a whole palette of interesting nonlinear dynamics (for example Figure 1) and energetics that have been explained with the help of numerical diagnostics of the simulations[4]. For example the nonlinear phase revealed a characteristic potential energy pumping form the electrons to the ions.Simulations performed with the 2D3v PIC-with-MCC code reveal that the elastic and excitation collisions can dynamically alter the path of progression of the ongoing ion resonance instability by a feedback of the collisional relaxation of the electron cloud's profile on the instability[2]. The 2D3v PIC-with-MCC code has also been used to investigate the process of destabilization of a cylindrically confined electron plasma by impact-ionization of background neutrals. One of the major results obtained from this simulation is the curve of excited fundamental Diocotron mode's frequency as a function time[5].The fundamental mode's frequency is observed to fall rapidly in the linear phase of the instability, then decrease at a slow rate, pass through a minimum value, and then increase in the nonlinear growth phase of the instability. Finally in the saturation phase the fundamental mode's frequency oscillates about a mean value. This unique curve traced by the fundamental mode's frequency has been explained to be caused by opposing effects of increasing inertia of the 2-component plasma that tends to bring downthe value of the frequency and the nonlinear dynamics of the instability that tends to raise the value of the fundamental mode's frequency.

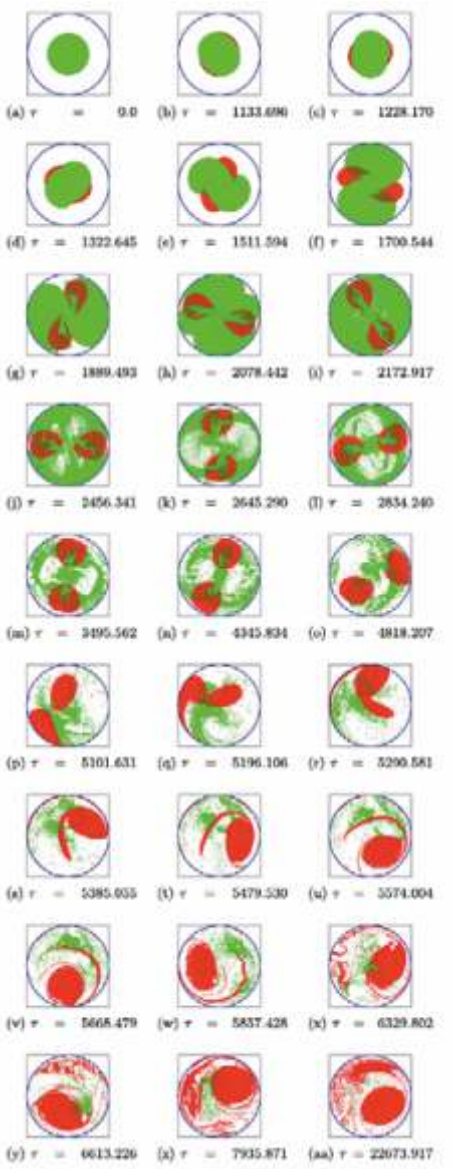

Figure 6.6.8 A simulation of the ion resonance instability. Electrons in red, and ions in green. M=2 mode excited here.

A study of the dynamics of delay coupled nonlinear oscillators and some model applications has been presented in this thesis. A network of coupled nonlinear oscillators can display a wide spectrum of

collective behavior ranging from synchronization to spatiotemporal chaos, and has therefore served as a useful paradigm to represent collective phenomena in a variety of applications in physical, chemical, biological, and social sciences. When the interactions between the interacting units are not instantaneous but are time-delayed, there can be significant changes in the onset thresholds or parametric domain of various collective states. Time delay is inevitable in real life systems due to finite interaction times between coupled units arising due to the propagation speed of signals, for instance, due to finite reaction times in chemical interactions or the conductance of neuronal connections. It is important therefore to include time-delayed interactions for realistic model applications. The work reported in this thesis presents the consequences of such time-delayed interactions in three model systems that can be of potential importance in realistic applications. In the first model problem, time delay effects on the collective dynamics of a geometrically frustrated network of phase oscillators are investigated. A well-known example of a frustrated system is that of three Ising spins that are anti-ferromagnetically coupled to each other and are placed on the corners of an equilateral triangle (Figure 6.6.9). In complex systems, frustration can arise from a combination of geometry and the nature of interaction among the subsystems, and it can give rise to a rich variety of collective behavior. Our results show that time delay significantly alters the amount of frustration in the system and thereby influences its collective dynamics. The second model problem aims to provide a dynamical understanding of the multisensory information processing involved in perception through a simple coupled-phase-oscillator based model consisting of the basic ingredients of any multisensory subsystem, two unisensory and one multisensory subunit, as shown in Figure 6.6.10. A particular focus is on explaining the principal experimental features associated with the so-called McGurk effect and its temporal constraints that show how the audio-visual integration in speech perception starts to break down when the lag between the onset of audio and visual inputs becomes too long. The results of our model show a remarkable qualitative agreement with the experimental observations of the McGurk effect. Since the populations of coupled oscillatory units in biological and physical systems must be robust against damages, the third and final model study investigates the effect of time delay on the robustness of the collective dynamics of a network of coupled oscillators against deterioration of some of its units, such as due to some elements turning non-self-oscillatory. Such a process can be interpreted as the aging of the system. Our results show that the presence of time-delayed interactions can lower the threshold of the aging transition of the system from a global oscillatory state to a non-oscillatory state and thereby degrades its functional robustness. The coupled oscillator model used for this investigation can serve as a simple paradigm for modeling the progress of neuro-degenerative diseases since such diseases are characterized by fall out of individual neurons.

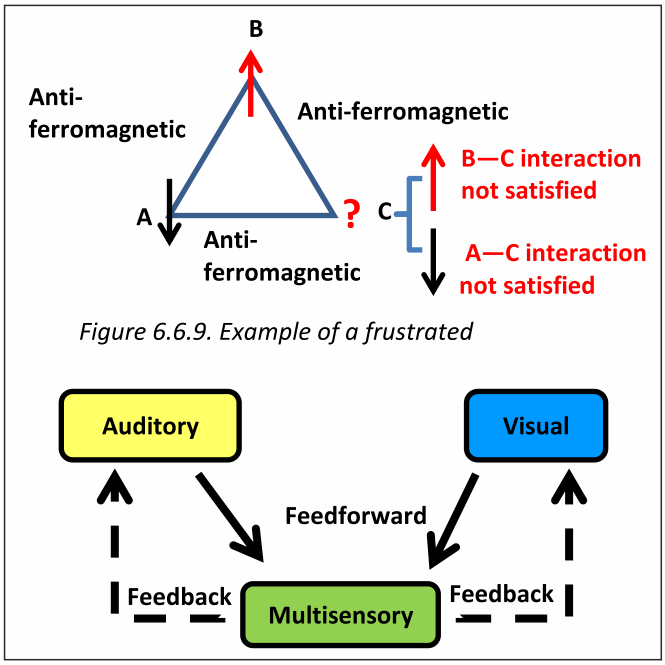

Figure 6.6.9. Example of a frustrated

Figure 6.6.10 . A dynamical model for multisensory perception

Our studies taken together highlight the important consequences of time-delayed coupling on the

collective dynamics of oscillator networks which can have potential practical implications in a variety of real life applications.

6.7 Institute of Physics

The thesis presents studies on Au-Ag Bimetallic nanostructures growth and characterization on ultra clean silicon substrates. Among the various bimetallic pairs, Au-Ag combination is specially studied because of complete miscibility with any desired Au Ag composition ratio and subsequent beneficial synergic effects in the field of catalysis (oxidation of CO), plasmonic (systematic tuning of SPR peak with variation Au Ag ratio) etc. Controlled fabrication of AuAg bimetallic nanowires (BMNWs) on ultra-clean Si(hkl) substrates comprised the combined advantages of one dimensional BMNW and usage for building block for metal-semiconductor junction in Si based technology. Our experimental outcomes explore that, reconstructed Si(5 5 12) template is superior than Hydrofluoric acid treated (with its 2-5% water solution) or native oxide covered template for growing metal (viz. Ag) nanostructures with its controlled morphology and good crystalline quality and motivates us to employ reconstructed Si(5 5 12) template for further growth of AuAg bimetallic nanostructures. We have explored that, followed by the modification of reconstructed Si(5 5 12) substrate with sub monolayer Ag, 1.5 ML Au growth on it at substrate temperature ~ 300 °C consequences formation of large aspect ratio AuAg BMNWs (as shown in Figure 1). Our detailed experimental studies with variation of growth parameters viz. Ag thickness, Au thickness, substrate temperature, substrate orientation enable us to find the optimum growth condition for achieving the unidirectional, large aspect

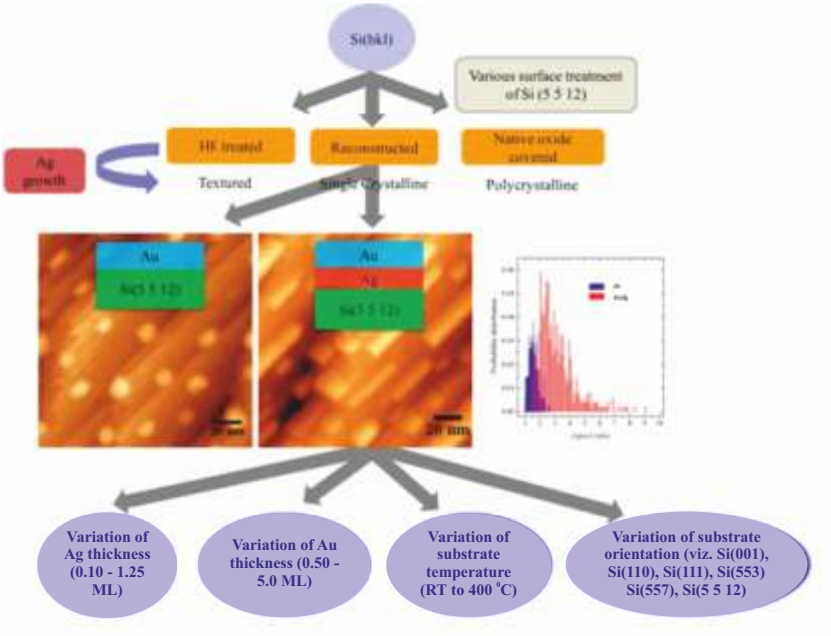

Figure 6.7.1 Effect of HF treated, reconstructed and native oxide covered Si(5 5 12) substrate on the crystalline quality of Ag nanostructures is investigated. Further reconstructed Si(5 5 12) template is used for bimetallic (AuAg) growth with variation of Ag thickness, Au thickness and substrate temperature. Experimental outcomes on Si(5 5 12) substrate are also compared with other substrate orientation viz. Si(001), Si(110), Si(111), Si(553) and Si(557).

ratio, uniformly intermixed AuAg BMNWs. Growth mechanism of formation of AuAg BMNWs has been investigated in the light of kinetic Monte Carlo simulation (with input from density functional theory) and

such phenomenon is attributed to co-occurrence of acting pre-grown Ag strip-like structure as nucleation centers for incoming Au ad-atoms and anisotropic surface mobility of Au and Ag adatoms. Remarkably, grown nanostructured substrate with AuAg BMNWs on ultra-clean Si(5 5 12) substrate is found extremely efficient for detecting Rhodamine 6G molecule with low concentration (10^{-7} M) in SERS method.

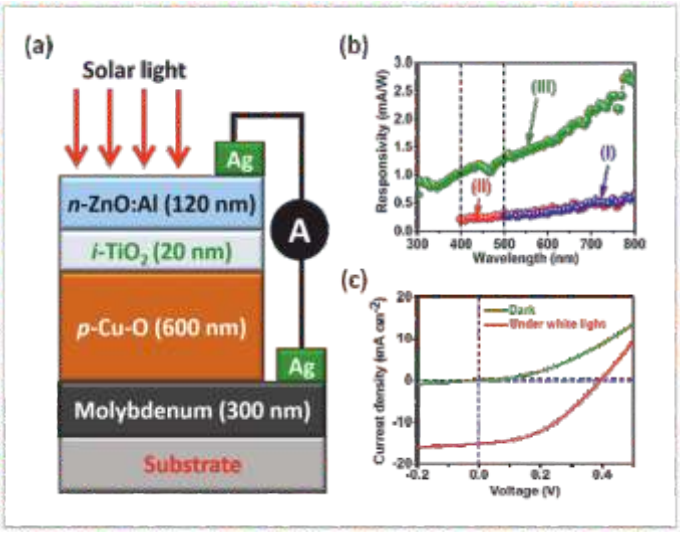

Figure 6.7.2 (a) Schematic diagram of Cu-O based solar cell. (b) Responsibility of AZO/Si junction and © current voltage characteristics of solar cell in dark and under while light.

A thesis deals with "Growth and characterization of Cu-O based solar cell". Solar cells are of prime importance due to their application in clean power generation. Present literature covers wide range of work done on growth and investigation of optical and electrical properties of the solar cells. The basic structure of the Cu-O based solar cell is ZnO Al/TiO_2/Cu-O/Mo/Si [Figure-1(a)] and theoretically, the efficiency of these type of solar cells should be around 20%; however, the best-known experimentally achieved efficiency is still less than 3%. Such a low efficiency is due to lack of clear understanding of the charge transport mechanisms in Cu-O and in its accompanying layers.My work focused on the optimization of the growth of the constituent layers at room temperature (RT) and studies of their electrical, optical, structural, and compositional properties, which has led to a superior cell efficiency of over 5%.

We demonstrated the growth of best optimized top transparent electrode in the form of ZnO Al (AZO) at RT and the effect of grain boundaries in these films on the charge transport. In addition, using local probe atomic force microscopy-based techniques (viz. cAFM, PFM, EFM, and KPFM) we have also shown direct evidence for local band bending at grain boundaries along with hitherto unexplored nanoscale pseudoferroelectricity in AZO films. The presence of polarization not only opens a new avenue to control the work function of the AZO film but also to control the charge transport in the same by applying external electric field. Further, we have shown how ultra-violet (UV) light absorption can influence the bulk as well as nanoscale conductivity of AZO thin films [Figure 6.7.2 (b)]. This contrasts with the common belief and is a novel finding of this thesis work. The main absorbing layer is Cu-O and we have not only optimized the growth angle but have also revealed the role of structural defects on nanoscale charge transport in the films using KPFM and cAFM. The study shows that in a highly defective sample, the resistance can be tuned from a low value to a high one by applying external electric field. The student have also deposited various thicknesses of TiO_2 thin films at different angles and studied their hole-blocking properties. Interestingly, hole-blocking nature is found to be independent of growth angles and of the nature of crystallinity in the films. Likewise, growth of back contact layer in form of Mo thin films has also been optimized to achieve a better performance of the Cu-O based solar cell. Finally, based on the experimental findings on individual layers, the student optimized his growth condition and layer thicknesses and constructed fully functioning Cu-O based solar cells and demonstrated efficiency of up to 5.2%, which constitutes by far the highest efficiency Cu-O solar cell[Figure-6.7.2(c)].

In the present thesis ,the student present studies on the electronic structure of some of the Bi based topological insulators (TIs) and Pd, Fe based new superconductors (Scs) using photoelectron spectroscopy in conjunction with first principles calculations. Content of the thesis is summarized in the Figure5.7.3. He observed Dirac like linearly dispersive surface state bands(SSBs) in the bulk energy gap region of Bi2Se3 and BiSbTe1.25Se1.75 while the SSBs in BiSe resemble Rashba split states. This difference in the observed SSBs highlights the correlation of structural geometry with the topological properties in Bi based compounds. The work finds that Dirac point (DP) in BSTS shifts by more than two times compared to that in Bi_2Se_3 to reach the saturation. From momentum density curves (MDCs) of the ARPES data we obtained an energy dispersion relation showing the warping strength of the Fermi surface (FS) in BSTS to be intermediate between those found in Bi_2Se_3 and Bi_2Te_3 and also to be tunable by controlling the ratio of chalcogen /pnictogen atoms. Further experiments also reveal that the nature of the BB effects are highly sensitive to the exposure of the fresh surface to various gas species. These findings have important implications in the tuning of DP in TIs for technological applications.

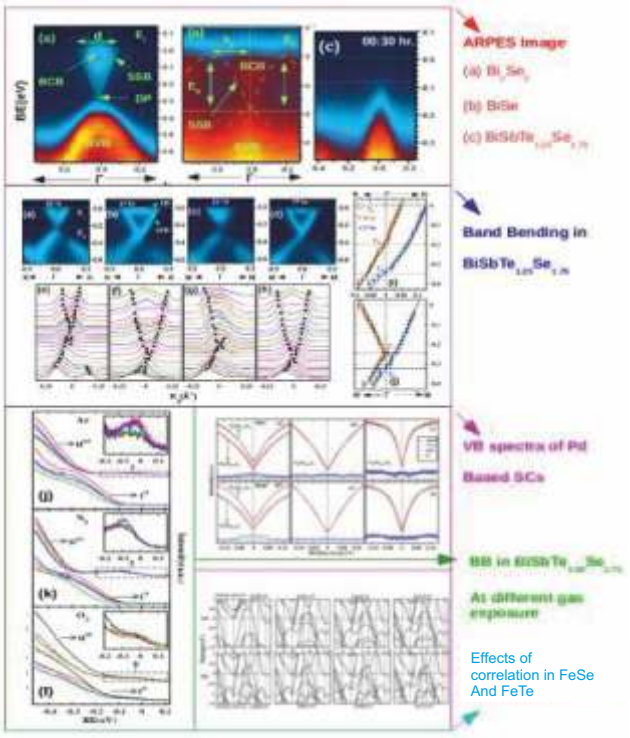

Figure 6.7.3 Electronic structure of TI s Bi2Se3, BiSe and BiSbTe1.25Se1.75; Pd based SC s and Fe chalcogenides obtained from ARPES studies and DFT calculations.

In the ARPES measurements on BiPd, which is considered to be a TI as well as non- centrosymmetric SC, he observed various electron and hole like bands crossing the FS. These results with DFT studies elucidate that BiPd could be a s-wave multiband superconductor. The r angle integrated photoemisson spectroscopy investigation reveals the nature of the valence band (VB) in Pd based Scs. In the continuation of present work on SCs, the student noticed that the correlation effects are orbital selective which dependent on the height of chalcogen atoms in FeSe and FeTe compounds in LDA + U study.

In the first part of this thesis, the student have studied the production of Λ(1520) resonance in pp collisions at √s = 7 TeV and in p-Pb collisions at $\sqrt{s_{NN}}$ = 5.02 TeV in the rapidity ranges |y|< 0.5 and -0.5 <y< 0, respectively, in the center of mass frame with the ALICE. The mean transverse momentum (<p_T>) and pT-integrated yield (dN/dy) of Λ(1520) has been calculated for minimum bias pp and p-Pb collisions, and also in different

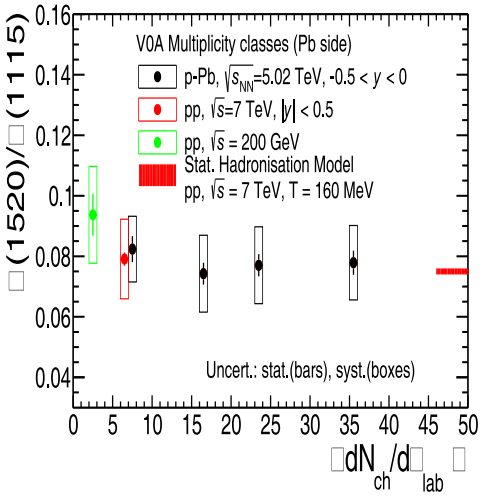

Figure 6.7.4 The yield ratio of Λ(1520) and Λ(1115) in pp and p-Pb collisions. Legends are defined on the plot.

multiplicity bins of p-Pb collisions. It has been found that yield ratios of Λ(1520) and its ground state particle Λ(1115) stay flat over all multiplicity bins of p-Pb collisions and matches with the same in pp collisions (see Fig.5.7.4). This suggests that the lifetime of the hadronic medium in p-Pb collisions is not so large to affect the yield of Λ(1520) significantly. The statistical hadronization models agree within uncertainty with the ALICE results.

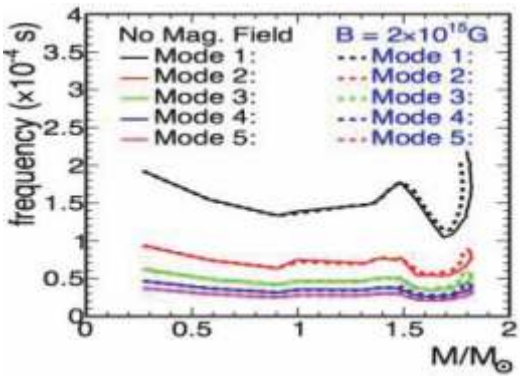

Figure 6.7.5 Nuclear modification factor for D-mesons in p-Pb collisions at √sNN= 5.02 TeV. Legends are defined on the plot.

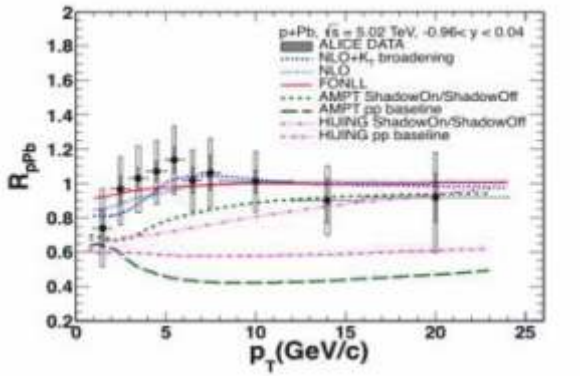

Figure 6.7.6 Period of oscillation against gravitational mass in solar mass unit with zero and non-zerovalues of magnetic field for fundamental mode (1) and higher harmonics (2-5) with density dependent bag pressure BGis 170 MeV/fm3.

In the second part, she studied the cold nuclear matter effect on D-mesons production in p-Pb collisions at $\sqrt{s_{NN}}$= 5.02 TeV using different simulation models (HIJING, AMPT, NLO (MNR) and FONLL) and compared with the ALICE results.HIJING and AMPT under-predict the p_T-differential production cross-section in p-Pb collisions at lower and intermediate $p_T$regions whereas NLO over-predicts the cross-section in higher p_T end. The average nuclear modification factor of D^0, D^+ and D^{*+} mesons has been calculated from all the models (see Fig.5.7.5) and found that all the systems predicts a cold nuclear matter effect for p-Pb collisions at $\sqrt{s_{NN}}$= 5.02 TeV.The NLO results with additional momentum broading effect (Cronin) predicts the shape of the ALICE data.

In the final part of the thesis, she studied the different modes of radial oscillations of compact stars by inclusion of hyperons in presence of a magnetic field. We have studied the effect of huge magnetic field on the matter inside the compact objects basically the equation of state (EOS). We have calculated the phase transition between hadronic and quark phases, maximum mass and eigenfrequencies of radial pulsation in the presence of a huge magnetic field. The mixed phase have been constructed by using Glendenning conjecture in between hadron and quark phases. It has been found that in the presence of magnetic field, the EOS in both matter becomes soft. As a result, the maximum mass has reduced and the period of radial oscillation has changed significantly and there is a sudden dip in the period of radial oscillations in the hybrid star, which signifies the transition from one to another matter (see Fig.6.7.6).

6.8 Harishchandra Research Institute

With the ever-increasing technological advancements towards processing of small-scale quantum systems and proposals of nano-scale heat engines, it is of paramount importance to investigate the thermodynamic perspectives of quantum features like coherence and quantum correlations. In the present thesis, the

student investigated the role of quantum coherence and quantum correlations in thermodynamics. This thesis is based on mainly three aspects of quantum thermodynamics where quantum information plays significant roles. Since a quantum state having coherence itallows transformations that are otherwise impossible and energy conservation restricts the thermodynamic processing of coherence, it can be viewed as an independent resource in thermodynamics. It can also improve the performance of quantum thermal machines. Considering the thermodynamic aspects of quantum coherence we explore the intimate connection between the resource theory of quantum coherence and thermodynamic limitations on the processing of quantum coherence. In particular, we study the creation of quantum coherence by unitary transformations with limited energy. The student goes on even further to present a comparative investigation of the creation of quantum coherence and total correlation (quantum mutual information) within the imposed thermodynamic constraints.

Studying co-operative quantum phenomena in many-body quantum systems using quantum correlations is an active field of research. He introduce a class of quantum correlation measures that are beyond the entanglement-separability paradigm, in terms of the Renyi and Tsallis entropies. He finds that these measures satisfy all the plausible axioms to be a good quantum correlation measure. He evaluated these measures for shared pure as well as paradigmatic classes of mixed states. It was shown that the measures can faithfully detect the quantum critical point in the transverse quantum Ising model. Furthermore, the measures provide better finite-size scaling exponents of the quantum critical point than the ones for other known order parameters, including entanglement and information-theoretic measures of quantum correlations, which can be useful to detect quantum phase transitions in this model in experiments.

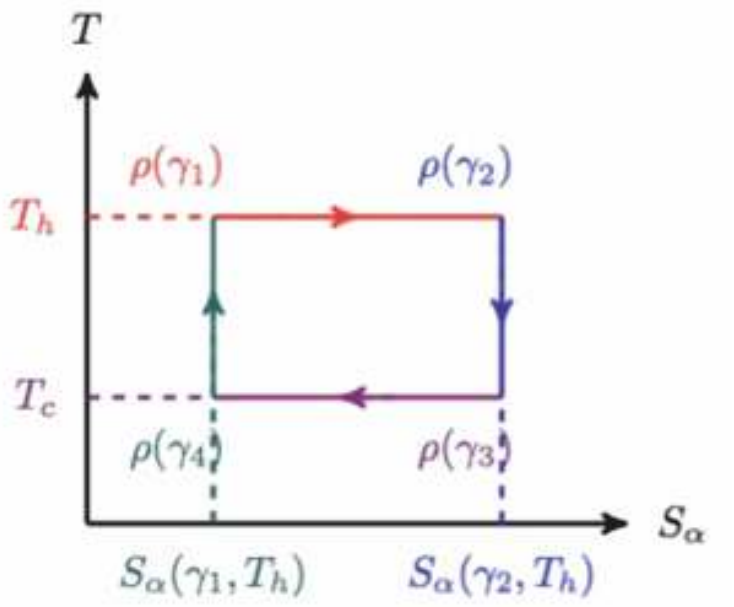

Figure 6.8.1 Schematic of Carnot Cycle 1→2 and 3→4 are the two isothermal steps at constant temperature Th and Tc respectively. 3→4 and 4→1 are the adiabatic isentropic steps. The different steps are performed by varying external parameter

In the domain of nano-thermodynamics, a major question is whether a quantum heat engine, more efficient than the Carnot engine, can be realized by harnessing the quantum nature of the systems. Exploiting the generalised entropy one can show that the principle of maximum entropy affirms that no engine can be more efficient than the Carnot engine even harnessing quantum resources. To establish the universality of the Carnot statement of the second law of thermodynamics, we formulate a complete theory of quantum thermodynamics in the Renyi entropic formalism exploiting the Renyi relative entropies, starting from the maximum entropy principle. In establishing the first and second laws of quantum thermodynamics, the student correctly identified accessible work and heat exchange both in equilibrium and non-equilibrium cases. The free energy (internal energy minus temperature times

entropy) remains unaltered when all the entities entering this relation are suitably defined. Exploiting Renyi relative entropies we have shown that this "form invariance" holds even beyond equilibrium and has profound operationalsignificance in quantifying accessible work in isothermal process. Moreover, it is shown that the universality of the Carnot statement of the second law is the consequence of the form invariance of the free energy, which is, in turn, the consequence of maximum entropy principle. Further, the Clausius inequality, which is the precursor to the Carnot statement, is also shown to hold based on the Renyi relative entropies.

Quantum correlations play an important role in various information-processing tasks, including quantum communication and quantum computation. Being a valuable resource, quantification of quantum correlations is useful in a variety of ways. A quantum physical system can be multipartite, and there can be correlations between its parties in several partitions and between several choices of subsets of parties. Although a number of quantum correlation measures for two-party systems have been studied extensively, investigation of quantum correlations in multiparty systems is hard, owing at least partially to the difficulty in defining and computing multipartite correlations. However, the notion of "monogamy" has proved to be a useful tool in exploring multipartite non-classical correlations. By monogamy of quantum correlations, one means a certain restriction on the distribution of quantum correlations of one fixed party with other parties of a multipartite quantum system. In particular, if party A in a tripartite system ABC is maximally quantum correlated with party B, then A or B cannot be correlated at all to the third party C. Monogamy appears to be the characteristic trait of multipartite quantum systems in the sense that "monogamy inequality" is satisfied by a large spectra of quantum correlations measures.An advantage of the monogamy inequality is that it is a multiparty property expressed in terms of bipartite quantum correlation measures, with the latter being relatively well-understood. Monogamy of non-classical correlations has important applications in several disciplines, ranging through quantum key distribution or quantum cryptography, classification of quantum states, black hole physics, etc. Quantification of monogamy property of quantum correlations in multiparty systems is however not straightforward. In this thesis, we have investigated various aspects of monogamy like (i) Figure 6.8.2. Schematic representation of the two-step protocol to distinguish quantum channels "conclusively" using monogamy of quantum correlations. Meanings of the symbols are explained in the thesis.which non-classical correlation measures and classes of quantum states, under what conditions, satisfy monogamy, (ii) do there exist bounds on distribution of quantum correlations in a multipartite quantum system, (iii) can monogamy be used to distinguish between quantum channels, etc.

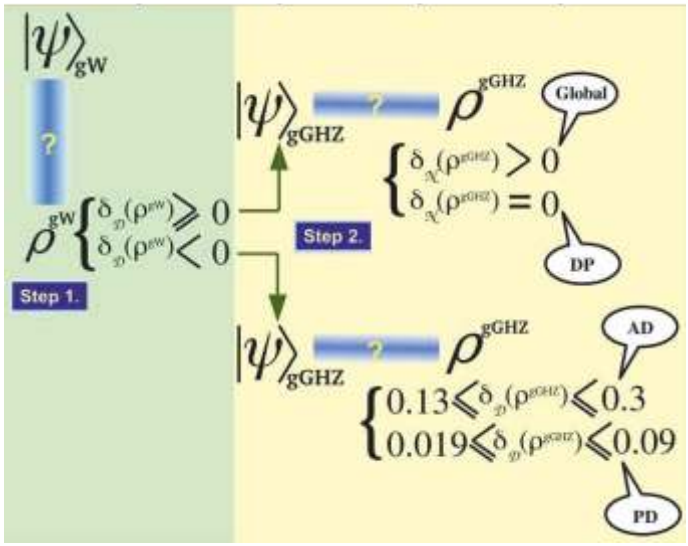

Figure 6.8.2. Schematic representation of the two-step protocol to distinguish quantum channels "conclusively" using monogamy of quantum correlations. Meanings of the symbols are explained in the thesis.

More specifically, a higher number of parties enforces monogamy of quantum correlations for “almost all” states, a monogamous quantum correlation measure remains so on raising its power, and monogamy of a convex quantum correlation measure for an arbitrary multipartite pure quantum state leads to its monogamy for mixed states in the same system. We obtained upper and lower bounds on the distribution of generic bipartite quantum correlations in multiparty systems. We also proposed a two-step protocol to distinguish quantum channels “conclusively” using monogamy ofquantum correlations (see Figure 6.8.2).

In the realm of quantum information and computation, it has been established fact that entanglement shared between two parties, situated in two distant locations is an essential ingredient for a vast majority of known quantum communication schemes. Specifically, it has been shown that in case of pure bipartite states, the capacity of classical information transmission by a shared quantum state (known as quantum dense coding (DC)) increases with the increase of shared quantum correlations.The practical usefulness of DC becomes prominent, when one consider a scenario involving multiple senders and multiple receivers. However, investigation of the communication protocol with more than a single receiver is quite limited due to mathematical complexity. This thesis mainly dealt with classical information transmission via quantum states between several senders and one or two receivers. On the other hand, it was also noticed that quantum correlations even for a multiparty pure state are not unique unlike the bipartite states. In this thesis, we have established a connection between multiparty DC capacity and multipartite quantum correlations measures in both noiseless and noisy scenarios.

Specifically, it has been proven that in the DC protocol with multiple senders and a single receiver, sharing gGHZstate is disadvantageous compared to an arbitrary multiqubit pure states, when both of them possess thesame amount of genuine multipartite entanglement. This is a striking result as it is commonly believed that the family of the gGHZ states among all multiparty states are the most useful states. However, we have also shown that the picture reverts, that is, the gGHZ state becomes advantageous, when there is sufficient amount of noise in the quantum channels, when the number of receivers become two.

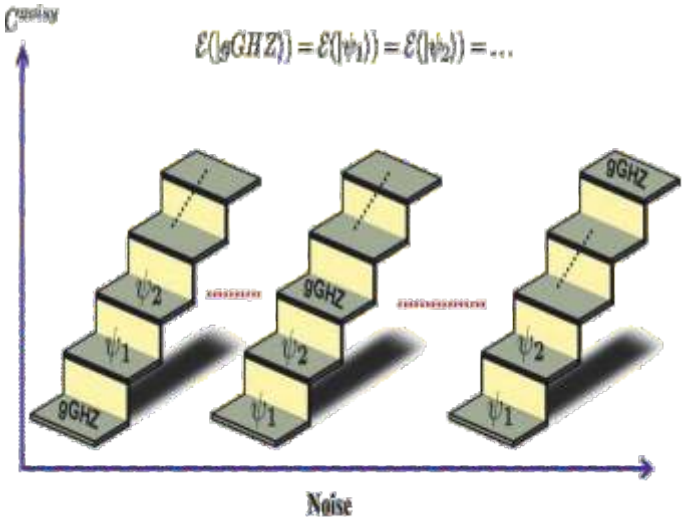

Figure 6.8.3 Schematic diagram of the change of status of the gGHZ state in comparison to other multipartite states with respect to multipartite DC capacity in the presence of noise.

One of the reasons behind the rapid development of quantum information processing science is due to the successful implementation of all the proposed quantum communicational schemes in the laboratories. However, there are some drawbacks in the possible realization of quantum communication networks in qubit systems in laboratories. Those disadvantageous can be overcome by considering continuous variable (CV) systems,including non-Gaussian states. The importance of non-Gaussian states in quantum information processing tasks have led to the discovery of several mechanism to creates such states in experiments. An important one is adding and subtracting photons, when the initial state is the squeezed vacuum state. In this thesis, we consider the four-mode squeezed vacuum (FMSV)

state as input and deGaussify it by adding and subtracting photons in different modes. We have investigated the entanglement patterns of photon-added and -subtracted four-mode squeezed vacuum states and observed that the photon-subtracted state can give us higher entanglement content and hence for quantum communication schemes than that of the the photon-added state which is in contrast of the two-mode case.The results obtained in this thesis is one step forward for establishing quantum communication networks.

6.9 Institute for Mathematical Sciences

Slender bodies capable of spontaneous motion in the absence of external actuation in an otherwise quiescent fluid are common in biological, physical and technological contexts. The interplay between the spontaneous fluid flow, Brownian motion and the elasticity of the body presents a challenging fluid–structure interaction problem. The student models the problem by approximating the slender body as an elastic filament that can impose non-equilibrium velocities or stresses at the fluid-structure interface. Then, an equation of motion for the active filament is derived by imposing momentum conservation in the fluid-structure interaction and assuming slow viscous flow. The fluid mediated interaction is obtained through a discretization which replaces the continuous filament by a series of connected beads. The activity of the beads is expressed by an "active slip" that generates spontaneous hydrodynamic flow. The spontaneous flow and resulting hydrodynamic torque and force can be computed, to any desired degree of accuracy, by solving Stokes equation using the boundary integral method. Further considering only the leading order contributions of hydrodynamic interactions, a simplified form of the equation of motion can be obtained. Using this simplified form, we study the dynamics of active filaments with different boundary conditions. We further investigate the dynamics of the active filament when it is subjected to an external field. Furthermore, attaching an active colloid to the terminus of a passive filament, we propose a new mechanism that can mimic actuation in the viscous environment. He concludes that the study by investigating collective dynamics of short filaments in an unbounded domain and near a wall. Throughout the thesis, He demonstrated that hydrodynamic interaction provides a novel route to out of equilibrium self-organization and collective motion. The investigations build the foundation to study collective phenomena in momentum-conserving, Brownian, active filament suspensions resolving the material at the scale of its constituents.

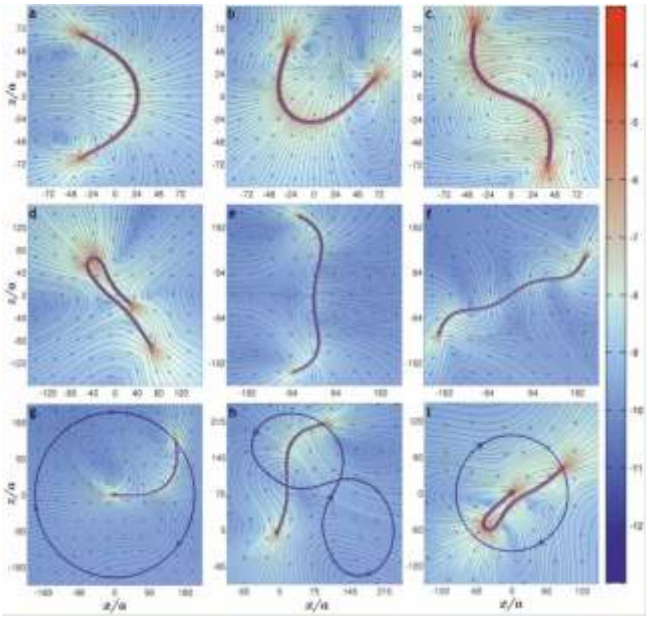

Figure 6.9.3 A. Outline of the thesis. B. Convective-rolls of active colloids in a harmonic trap. C. The exterior fluid flow and collective dynamics of active colloids are determined by the boundaries of the flow.

In this thesis, the student studied gauge theories with N = 2 supersymmetry in four dimensions. The low energy effective action of these theories on their Coulomb branch is described by a holomorphic function called the prepotential. In the first half, he studied linear conformal quiver theories with gauge group

SU(2). To compute the prepotential, he followed three approaches. These are (i) the classic Seiberg-Witten approach, in which we consider an M-theory construction of the Seiberg-Witten curve and the associated differential, (ii) equivariant localization as developed by Nekrasov, and (iii) the 2d/4d correspondence of the four dimensional gauge Figure 6.9.2 .Computing the prepotential and resumming the twisted superpotential of certain class S theoriestheory with the two dimensional Liouville conformal field theory. Matching the prepotential, he found out the precise map between the various parameters that appear in the three descriptions.

Figure 6.9.2 .Computing the prepotential and resumming the twisted superpotential of certain class S theories

In the latter half of the thesis, he studied surface operators in the context of N=2* theories with gauge group SU(N). These theories describe the dynamics of a vector multiplet, and a massive hypermultiplet in the adjoint representation of the gauge group. Surface operators are non-local operators that have support on a two dimensional sub-manifold of the four dimensional spacetime. They are defined by the singularities they induce in the four-dimensional gauge fields, or can be characterized by the two-dimensional theory they support on their world-volume. The infrared dynamics on the world-volume of the two-dimensional surface operator is described by a holomorphic function called the twisted superpotential. Using localization techniques which involves taking a suitable orbifold of the original action without the surface operator, he obtains the twisted superpotential. Imposing S-duality. He obtained a modular anomaly equation for the coefficients in the mass expansion of the twisted superpotential. Solving the anomaly equation, and comparing with the results obtained from localization, he resumed the twisted superpotential in a mass series, whose coefficient functions depend on (quasi-) modular forms and elliptic functions of the bare coupling constant and the continuous (complex) parameters that describe the surface operator.

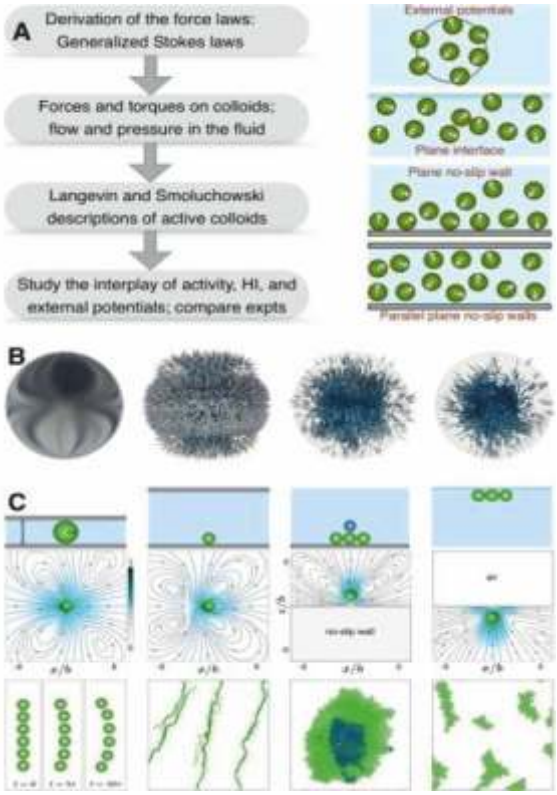

Figure 6.9.3 A. Outline of the thesis. B. Convective-rolls of active colloids in a harmonic trap. C. The exterior fluid flow and collective dynamics of active colloids are determined by the boundaries of the flow.

The outline of this thesis is given in Figure (6.9.3 A). The student usees the boundary integral representation of the Stokes flow to obtain the full expression of force per unit area on the surface of active colloids. The result is expressed as an infinite set of linear relations - generalized Stokes laws - between the tensorial spherical harmonic coefficients of the force per unit area and the boundary velocity. The expression of the force per unit is then used to derive forces, torques, and thus, to obtain the Langevin description of active colloids in terms of the familiar

mobility matrices and, the newly introduced, propulsion tensors. These Langevin equations have been implemented in a homegrown library to perform the numerical simulations reported in the thesis. The formalism is then applied to study the collective dynamics of active colloids in various experimentally realizable settings. His applications include the identification of the universal mechanisms of crystallization, observed in experiments of active colloids at a plane wall. In Figure 6.9.3, He showed the sustained convective-rolls of active colloids in a harmonic trap, maintained by the interplay of one-body active force and two-body hydrodynamic torque. In Fig 6.9.3 C he showed that the boundaries in the domain of the flow determine the collective behavior of active colloids. It was shown that the collective steady-states of momentum-conserving active matter systems are characterized using the flow-induced phase separation (FIPS) mechanisms. These are of dynamical origin and obtained from the balance of forces and torques. His predictions are in excellent agreements with recent experiments of active colloidal systems.

6.10 National Institute of Science Education and Research

To look for New Physics (NP) beyond the standard model, the rare B decays provide a unique opportunity to probe beyond the standard model (SM) through indirect searches where the observables of interest for a SM process are measured in the collider experiments. It would give a hint for new physics if significant deviation from the SM prediction is observed. The present thesis has addressed to test the consistency of the SM and NP beyond the SM through the study of B_s® $\mu^+\mu^-$ and B^+ ® $K^{*+}\mu^+\mu^-$ decay modes. The B_s® $\mu^+\mu^-$ decay is highly suppressed in the SM because the flavor changing neutral current transitions are forbidden at tree level and can only proceed through higher loop diagrams. By studying its decay rate, one can shed light on the consistency of SM. Similarly, the angular analysis of B^+ ® $K^{*+}\mu^+\mu^-$ is studied by looking at the observables e.g., Forward-backward asymmetry of the muons, AFB and the longitudinal polarization fraction of K*, FL and the measured values are compared to the SM predictions. The important observations of this thesis are outlined below

1. The branching fraction of B_s® $\mu^+\mu^-$ is consistent with the SM prediction (shown in Figure 1) which puts a stringent limit on the parameters in search of new physics.
2. The angular analysis of B^+® $K^{*+}\mu^+\mu^-$ is studied through A_{FB} and F_L. The measured values of A_{FB} and F_L are consistent with the SM predictions (shown in Figure 2).

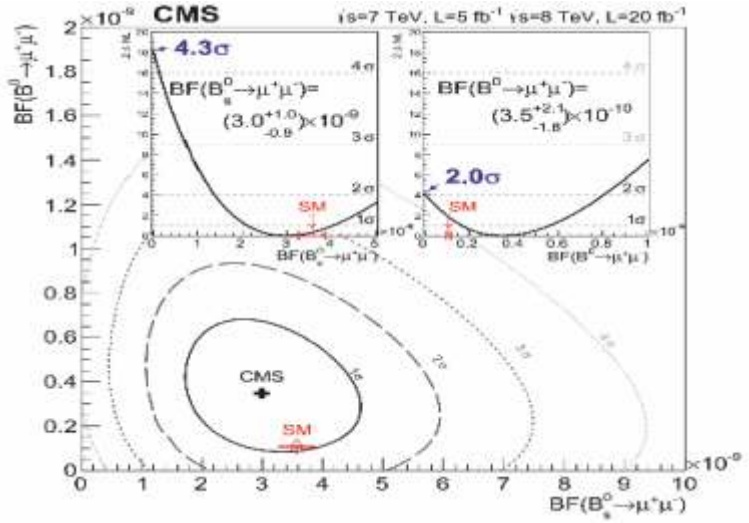

Figure 6.10.1 Result for the scan of joint likelihood ratio for Bsμ+μ-and B0μ+μ-. It is clear from the figure that the CMS measurement of Bsμ+μ-branching ratio agrees with the SM prediction within 1σ uncertainty and the corresponding observed significance is 4.3σ.

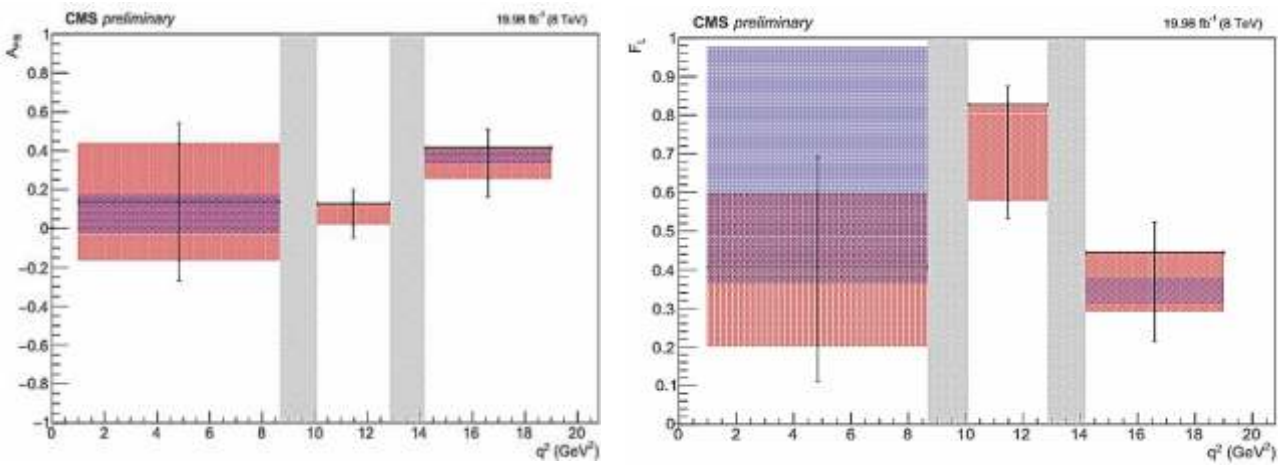

Figure 6.10.2 Results of the measurement of AFB (left plot) and FL (right plot) in data as a function of dimuon mass squared (q2). The red shaded region represents the statistical uncertainty whereas the systematic uncertaintiesare represented by black vertical error bars with edges. The standard model predictions are shown by the blueshaded region whereas the grey shaded regions represent the two resonance regions. The measurement agrees well with the standard model predictions within uncertainties.

Section-III

List of Students who have completed Ph.D. programs during 2017-18

Sr. No	Name of the student	CI/OCC	Discipline	Enrolment No.	Title
1	Abdul Nishad Padala	BARC	Chemistry	CHEM01201004021	Synthesis And Evaluation Of Specially Designed Polymeric Materials For The Removal Of Metals And Metalloids In Low Level Concentrations
2	Anil Boda	BARC	Chemistry	CHEM01201004005	Studies On Selected Metal Complexes: Computational And Experiments
3	Aruna Kumar M	BARC	Chemistry	CHEM01201204001	Understanding The Ultrafast Dynamics Of Molecular Rotor Based Probes In Amyloid Fibrils
4	Bholanath Mahanty	BARC	Chemistry	CHEM01201204010	Studies On The Diglycolamide-Functionalized Extractants Containing Polymer Inclusion Membrane For Actinide Separation And Sensor Development
5	Biswajit Manna	BARC	Chemistry	CHEM01201404003	Dynamics Of Excited States And Transient Species In Self Assembled Media
6	Biswajit Sadhu	BARC	Chemistry	CHEM01201304002	Binding And Transport Of Radionuclides In Natural And Synthetic Environment - A Computational Study
7	Jayanta Dana	BARC	Chemistry	CHEM01201304028	Ultrafast Charge Transfer Dynamics In Dye-Metal And Semiconductor Material
8	Joyeeta Mukhopadhyaya	BARC	Chemistry	CHEM01201104025	Synthesis And Characterization Of Nanomaterials For Uptake Of Radio Nuclides And Toxic Metal Ions
9	Lakshminarayanan N	BARC	Chemistry	CHEM01201104027	Synthesis And Evaluation Of [^{18}f] Labelled Amino Acids For Pet Imaging
10	M. K. Sureshkumar	BARC	Chemistry	CHEM01200804017	Application Of Biomaterials And Nanomaterials In Environmental Remediation

Sr. No	Name of the student	CI/OCC	Discipline	Enrolment No.	Title
11	Manoj Kumar	BARC	Chemistry	CHEM01201204019	Development Of Radioactive Sources For Insustrial And Meical Applications Through Different Chemical Methods
12	Milan Kumar Dey	BARC	Chemistry	CHEM01201104003	Preparation And Characterization Of Thin Film And Nano Phase Based Modified Electrodes For Electrochemical Sensor Application
13	Parvathi K.	BARC	Chemistry	CHEM01201204022	Hydration Of Acids: Towards Molecular Level Understanding
14	Pavitra V. Kumar	BARC	Chemistry	CHEM01201304031	Redox Reactions And Antioxidant Activities Of Organoselenium Compounds And Their Nanocomposites
15	Poonam P. Jagasia	BARC	Chemistry	CHEM01201104030	Studies On The Separation Of Cesium From High Level Liquid Waste
16	Rama Mohana Rao Dumpala	BARC	Chemistry	CHEM01201204019	Speciation Of Actinides Or Their Lighter Homologues In Aquatic Environment
17	Sabyasachi Rout	BARC	Chemistry	CHEM01201204012	Migration And Speciation Of Uranium In Terrestrial Environment
18	Sachin Gajanan Mhatre	BARC	Chemistry	CHEM01200804025	Development Of New Chemical Dosimeters For Radiation Processing Applications
19	Sandeep P.	BARC	Chemistry	CHEM01201104002	Physico-Chemical Characterization Of Airborne Particulate Matter And Source Apportionment Using Different Receptor Models
20	Santosh Kumar Suman	BARC	Chemistry	CHEM01201104028	Radiation Defects In Materials And Their Charazation Using Esr, Uv-Visble Spectrometry And Tl

Sr. No	Name of the student	CI/OCC	Discipline	Enrolment No.	Title
21	Satyapriya R. Sreejith	BARC	Chemistry	CHEM01201004020	Estimation Of Dietary Ingestion Intake Of Thorium For Inhabitants Of High Background Radiation Area Of Southern India
22	Sukanta Maity	BARC	Chemistry	CHEM01201204006	Studies On Transfer Factors Of Trace Metals In Marine Ecosystem
23	V. Kusum Vats	BARC	Chemistry	CHEM01201204011	DEVELOPMENT OF TARGET-SPECIFIC ^{99m}tc-RADIOTRACERS AS POTENTIAL RADIOPHARMACEUTICALS FOR DIAGNOSTIC APPLICATION
24	Vivekchandra Guruprasad Mishra	BARC	Chemistry	CHEM01201104010	Development Of Analytical Methodology For Trace Elements In Nuclear/Environmental Samples Using Chromatography Techniques
25	Yusufali C	BARC	Chemistry	CHEM01200904020	Interaction Of Aluminide Coated Ni-Cr-Fe Based Superalloy Substrates With Simulated Nuclear Waste And Borosilicate Glass
26	A. Rama Rao	BARC	Engineering	ENGG01200904013	A Comprehensive Study On The Detection Of Blade Vibration In Rotating Machineries
27	Abhijit Pandurang Deokule	BARC	Engineering	ENGG01201004005	Investigations Towards Enhancing Power Output Of A Pressure Tube Type BWR Using Annular Fuel Rod Cluster
28	Abhishek Tiwari (DGFS)	BARC	Engineering	ENGG01201304015	Characterization Of Fracture Behaviour Of Indian Reduced Activation Ferritic/Martensitic Steel In Ductile To Brittle Transition Region Using Master Curve Approach

Sr. No	Name of the student	CI/OCC	Discipline	Enrolment No.	Title
29	Ajith K J	BARC	Engineering	ENGG01200804016	Scalable Quantifier Elimination Techniques For Formal Verification
30	Ankur Kumar	BARC	Engineering	ENGG01201104019	Numerical Analysis Of Air Cooled Condenser And Selection Of Optimal Design Parameters
31	Anuj Kumar Kansal	BARC	Engineering	ENGG01201004014	Experimental And Computational Studies On Liquid Poison Injection In The Calandria Of Pressure Tube Type Reactor
32	Anupam Saraswat	BARC	Engineering	ENGG01201004010	Response Evaluation Of Freestanding System Subjected To Seismic Loading
33	Archana V.	BARC	Engineering	ENGG01201104010	Steady State And Transient Characteristics Of Supercritical Pressure Natural Circulation Loop
34	Arnab Dasgupta	BARC	Engineering	ENGG01200804005	Investigations On Mechanistic Models For Annular Flow Dryout And Post Dryout Heat Transfer Phenomena
35	Asit Baran Mukherjee	BARC	Engineering	ENGG01201004009	Design, Development And Qualification Of A Novel Bimetallic Joint Of Titanium-Stainless Steel
36	Gokhale Onkar suresh	BARC	Engineering	ENGG01201004016	Development And Experimental Validation Of Computation Model For Re-Flood Conditions In A Partially Degraed Reactor Core
37	Kundan Kumar	BARC	Engineering	ENGG01200804004	Evaluation Of Mechanical Properties Of Structural Materials Using Miniature Tensile And Small Punch Test Techniques
38	P. S. Somayajulu	BARC	Engineering	ENGG01200904023	Synthesis And Characterization Of Coated Agglomerate Pelletisation (Cap) Pellets Of Thoria Based Materials For Nuclear Fuels

Sr. No	Name of the student	CI/OCC	Discipline	Enrolment No.	Title
39	Paritosh Prabhakar Nanekar	BARC	Engineering	ENGG01200904028	An Integrated Approach To Sound Beam Focusing Using Phased Array And Saft For Flaw Characterization
40	Pradeep Kumar	BARC	Engineering	ENGG01201204023	Determination And Validation Of Fracture Properties Using Small Punch Test Specimens For Nuclear Reactor Materials
41	Priti Kotak Shah	BARC	Engineering	ENGG01200904026	Fracture And DHC Behavior Of As-Fabricated & Irradiated Indian PHWR Pressure Tubes
42	Rajasekhar Ananthoju	BARC	Engineering	ENGG01201104012	Computation Of Neutron Flux Distribution In Large Nuclear Reactors Via Reduced Order Modeling
43	Ratnesh Singh Sengar	BARC	Engineering	ENGG01201004024	Use Of Wavelets And Filter Banks In 2D Gel Electrophoresis Images In Spot Picker Robot For Precise Protein Identification
44	Reena Awasthi	BARC	Engineering	ENGG01200804009	Laser Cladding Of Nickel Based Hardfacing Alloy (Ni-Mo-Cr-Si) On Stainless Steel Substrate For Improvement Of Surface Properties
45	S. R. Gurumurthy	BARC	Engineering	ENGG01200904044	Investigations Into The Optimal Energy Extraction From Pm-Bldc Machine Based Flywheel Energy Storage System
46	Samiran Sengupta	BARC	Engineering	ENGG01200804003	Turbulent Mixingof Opposing Flows Inside Chimney Structureof Pool Type Research Reactor
47	Sanjay Kumar jha	BARC	Engineering	ENGG01201004022	Studies On Mechanisms Of Microstructure And Micro-Texture Development During Thermo-Mechanical Processes In Single/Multiphase Zirconium Based Alloys

Sr. No	Name of the student	CI/OCC	Discipline	Enrolment No.	Title
48	Suman Neogy	BARC	Engineering	ENGG01200904027	Studies On Phase Transformations In Zr-1 Wt. % Nb And U-9 Wt. % Mo Alloys And Their Metallurgical Interaction
49	V. Satish Kumar Reddy	BARC	Engineering	ENGG01201004003	Mobile Robot Navigation In An Outdoor Environment
50	Bharti Jain	BARC	Life Sciences	LIFE01200804002	Antibody-Chip For Multianalyte Immunoassay Of Thyroid Hormones
51	Mahima Sharma	BARC	Life Sciences	LIFE01201204008	Molecular Mechanism Of Action Of Lysinibacillus Sphaericus Binary Toxin Protein Components
52	Prachi Verma	BARC	Life Sciences	LIFE01201204009	Evaluation Of In Vitro And In Vivo Radioprotection And Cytotoxic Activities By Novel Selenium Compounds
53	Pramod Kumar Gupta	BARC	Life Sciences	LIFE01201204006	Tlr4 Mediated Immunomodulation In Tuberculosis
54	Amit Thakur	BARC	Physics	PHYS01201104008	Development Of Optimization Techniques For Fuel Management In Heavy Water Moderated Reactors
55	Ashish Kumar Agrawal	BARC	Physics	PHYS01201004002	Development Of X-Ray & Neutron Micro-Imaging Techniques And Their Applications In Material Science
56	Giri Dhari Patra	BARC	Physics	PHYS01201204017	Single Crystal Growth Of Lithium Tetra Borate And Its Characterization As A Multi-Functional Material For Personal Dosimetry
57	Himal Bhatt	BARC	Physics	PHYS01201004004	Infrared Spectroscopy Of Molecular Solids Under Extreme Conditions
58	Indresh Yadav	BARC	Physics	PHYS01201504017	Evolution Of Interaction And Structure Of Nanoparticle-Protein Complexes As Studied By Scattering Techniques

Sr. No	Name of the student	CI/OCC	Discipline	Enrolment No.	Title
59	Laishram Guneshwor Singh	BARC	Physics	PHYS01201004009	Groundwater Contaminant Source Identification Using Meshfree Radial Point Collocation Method And Particle Swarm Intelligence Based Simulation-Optimization Approach
60	Meghna K. K.	BARC	Physics	PHYS01200904012	Performance Of RPC Detectors And Study Of Muons With The Iron Calorimeter Detector At INO
61	Mradul Sharma	BARC	Physics	PHYS01201104002	Gamma-Hadron Classification For The Ground Based Atmospheric Cherenkov Telescope MACE
62	Partha Sarathi Ghosh	BARC	Physics	PHYS01201104018	THEORETICAL STUDIES ON PHASE TRANSFORMATIONS AND RELEVANT THERMAL PROPERTIES OF Zr- AND Tho_2-BASED NUCLEAR MATERIALS
63	Raj Bahadur Tokas	BARC	Physics	PHYS01201004013	Porous Optical Coatings By Oblique Angle Deposition
64	Rajesh Ganai	BARC	Physics	PHYS01201004015	Probing The Earth Matter Density Through INO-ICAL And Related Detector Development
65	Rajib kar	BARC	Physics	PHYS01201104016	Plasma Processing Of Carbon Nanostructures And Their Characterization
66	Raveendrababu Karnam ,(INO)	BARC	Physics	PHYS01201004019	Study Of Glass Resistive Plate Chambers For The INO-ICAL Detector
67	Rohan Phatak	BARC	Physics	PHYS01201104003	Study Of Crystal Structure And Magetc Properties Of Double Perovskite Oxides
68	Sabyasachi Paul	BARC	Physics	PHYS01201204009	Study Of Neutron Yield From Heavy-Ion Reactions Using Pre-Equilibrum Models
69	Sheo Mukund	BARC	Physics	PHYS01201104001	Laser Spectroscopy Of Some Transition-Metal-Contaning Diatomic Molecules: Nbn, Tan, Sch, Scn, Sco And Nic

Sr. No	Name of the student	CI/OCC	Discipline	Enrolment No.	Title
70	Shuvendu jena	BARC	Physics	PHYS01201304004	Deposition And Characterization Of Refractory Oxide Thin Films And Multilayer Optical Coatings
71	Suhail Ahmad Khan	BARC	Physics	PHYS01201004016	Development Of Transport Model For Whole Core Pin By Pin Calculation In 2d Geometry
72	A. S. Suneesh	IGCAR	Chemistry	CHEM02201104003	Development Of Extractants For The Mutual Separation Of Lanthanides And Actinides
73	Balija Sreenivasulu	IGCAR	Chemistry	CHEM02201104011	Studies Related To Spent Fuel Reprocessing Using Tri-Iso-Amyl Phosphate As An Alternate Extractant To Tri - N-Butyl Phosphate
74	Binoy Kumar Maji	IGCAR	Chemistry	CHEM02201004012	Synthesis And Thermo-Physical Properties Of Sr-Chloroapatite And Its Various Glass-Bonded Composites Loaded With Pyrochemical Chloride Waste
75	Meera A.V	IGCAR	Chemistry	CHEM02201004002	Thermochemical Investigations On Bi-Fe-O And Bi-Cr-O Systems
76	N. Desigan	IGCAR	Chemistry	CHEM02201004016	Chemical Aspects Of Dissolution Of Fast Reactor Nuclear Fuel
77	Prasant Kumar Nayak	IGCAR	Chemistry	CHEM02201104006	Development Of A Single-Cycle Approach For Minor Actinide Partitioning
78	R. Gopi	IGCAR	Chemistry	CHEM02201204008	Experimental Evidence For Blue And Red-Shifted Hydrogen Bond: A Matrix Isolation Infrared Spectroscopy And Ab Initio Studies
79	Rama R	IGCAR	Chemistry	CHEM02201204007	Solvent Extraction And Electrochemical Studies Of Lanthanides And Actinides In Room Temperture Ionic Liquid Medium Containng

Sr. No	Name of the student	CI/OCC	Discipline	Enrolment No.	Title
80	Sanjay Kumar D	IGCAR	Chemistry	CHEM02201104001	Studies On Some Novel Methods Of Synthesis And Sintering Of Nanocrystalline Ceramics
81	Satendra Kumar	IGCAR	Chemistry	CHEM02201004011	Luminescence Studies Of Eu^{3+} And Uo_2^{2+} Complexed With Aromatic Carboxylic Acid Ligands Inacetonitrile Medium
82	B. Babu	IGCAR	Engineering	ENGG02200904014	Development Of Real Time Leak Detection Systems For Steam Generators Of Sodium Cooled Fast Reactors
83	B. K. Sreedhar	IGCAR	Engineering	ENGG02200904004	Studies On Cavitation Erosion Resistance Of Reactor Materials
84	David Vijayanand V.	IGCAR	Engineering	ENGG02201104008	Aspects Of Integrity Assessment Of 316ln Austenitic Stainless Steel Weld Joint Under Creep
85	Deepak Ch	IGCAR	Engineering	ENGG02201104013	Study Of Synchro And Development Of Synchro-To-Digital Converter For Instrumentation & Control Applications
86	Ganesh Kumar J.	IGCAR	Engineering	ENGG02201104001	Assessment Of Tensile And Creep Behaviour Of 316ln Stainless Steel Using Automated Ball Indentation And Small Punch Creep Testing Techniques
87	Manas Ranjan Prusty	IGCAR	Engineering	ENGG02201104037	Studies On Supervised Classification Algorithms Based On Dataset Transformation For Monitoring Nuclear Power Plant Events
88	N.K. Sinha	IGCAR	Engineering	ENGG02200804005	Development Of Inflatable And Backup Seals For Sodium Cooled Fast Breeder Reactors: An Approach For Unification And Standardisation Of Elastomeric Sealing

Sr. No	Name of the student	CI/OCC	Discipline	Enrolment No.	Title
89	P. Selvaraj	IGCAR	Engineering	ENGG02200904003	Simulation Of Helium Jet Cooling For Spallation Targets
90	Ravi. L	IGCAR	Engineering	ENGG02201104031	Thermal Hydraulic Investigations On Total Instantaneous Blockage In A Fuel Subassembly Of Fast Reactor
91	Sambasiva Rao Kambala	IGCAR	Engineering	ENGG02201104038	Studies On Development Of A Pulsed Eddy Current System For Testing Thick Stainless Steel Components
92	Srikantam Sravanthi	IGCAR	Engineering	ENGG02201204006	An Investigation Into The Fail Safeness Of Safety Critical Instruement And Control In A Sodium Colled Fast Reactor
93	Anees P.	IGCAR	Physics	PHYS02201104011	Modeling And Simulation Of Structural Stability, Thermal Expansion And Anharmonicity Of 2d Materials
94	D. Karthickeyan	IGCAR	Physics	PHYS02201104009	Stimuli Responsive Microgel Particles And Microgel Crystals As Studied By Light Based Techniques
95	K. Srinivasan	IGCAR	Physics	PHYS02201204005	Investigations On Discrete Winger Functions Of Multi-Qubit Systems
96	Sivadasan A. K.	IGCAR	Physics	PHYS02201204003	OPTICAL PROPERTIES OF Aigan NANOSTRUCTURES
97	Soumee Chakraborty	IGCAR	Physics	PHYS02201004016	Inelastic Light Scattering Studies On Strong Network Glasses
98	Syamalarao Polaki	IGCAR	Physics	PHYS02201004018	Correlation Of Tribological Properties With Chemical Structure Of Modified DLC Films
99	Manoj Kumar Saxena	RRCAT	Engineering	ENGG03201004001	Study Of Non-Stationary Signal Models For Optical Fiber Based Sensors

Sr. No	Name of the student	CI/OCC	Discipline	Enrolment No.	Title
100	Ali Akbar Fakhri	RRCAT	Physics	PHYS03201004015	Study Of Beam Injection, Beam Optics And Insertion Devices For Synchrotron Radiation Source: A Case Study Of Indus-1 And Indus-2
101	Salahuddin Khan	RRCAT	Physics	PHYS03201004001	Effect Of Surface And Interface On The Carrier Dynamics Of Quantum Wells
102	Shailesh Kumar Khamari	RRCAT	Physics	PHYS03201104004	Transport Studies Of Spin Polarized Carriers In Semiconductors
103	Smritijit Sen	RRCAT	Physics	PHYS03201104010	Theoretical Studies On Superconducting And Normal State Properties Of Some Fe-Based Superconductors
104	Sujan Kar	RRCAT	Physics	PHYS03200904007	Growth And Characterization Of Doped And Undoped Lithium Niobate And Lithium Tetraborate Crystals In Bulk And Nano Form
105	Surendra Singh	RRCAT	Physics	PHYS03200804007	Development Of A Kr Magneto-Optical Trap For Efficient Loading And Collision Studies
106	Sushil Kumar Sharma	RRCAT	Physics	PHYS03200904009	Growth And Characterization Of Kdp, Lap And Zctc Crystals For Non-Linear Optical Applications
107	Tufan Roy	RRCAT	Physics	PHYS03201204009	Effect Of Substitution On Electronic Structure, Magnetic And Mechanical Properties Of Ni, Pt And Mn-Based Heusler Alloys
108	Yashvir Kalkal	RRCAT	Physics	PHYS03201104013	Theoretical Studies On Electron Beam Based Compact Terahertz Sources
109	Ashif Reza	VECC	Engineering	ENGG04201104004	Development Of Detection And Frequency Measurement Circuit For Penning Ion Trap

Sr. No	Name of the student	CI/OCC	Discipline	Enrolment No.	Title
110	Swagata Mandal	VECC	Engineering	ENGG04201304002	Development Of FPGA Based Error Resilient Self-Triggered Readout Chain For Muon Chamber (MUCH)Detector Of CBM Experiment
111	Arindam Kumar Sikdar	VECC	Physics	PHYS04201304002	Studies On Fission Time Anomaly In Fissile And Very Heavy Nuclei
112	Arnab Banerjee	VECC	Physics	PHYS04200904006	Development Of Micro-Pattern Gas Detector For Physics And Other Applications
113	Debasish Mondal	VECC	Physics	PHYS04201404004	Study Of Nuclear Viscosity And Isospin Mixing Utilizing Isovector Giant Dipole Resonance
114	Debojit Sarkar	VECC	Physics	PHYS04201104004	Two Particle Correlations With Identified Trigger Particles (Pions And Protons) In P-Pb And P-P Collisions At The Large Hadron Collider (LHC) Energies
115	Pratap Roy	VECC	Physics	PHYS04201304001	Study Of Nuclear Level Density Using Light Particle Evaporation As A Probe
116	Somnath Kar	VECC	Physics	PHYS04201104006	Measurement Of Angular Correlations Between D^0 Mesons And Charged Particles In *Ppb* Collisions At $\ddot{O}S_{NN}$ = 5.02 Tev With ALICE At The LHC
117	Sujoy Chatterjee	VECC	Physics	PHYS04201004010	Radiation Dosimetry Of Charged Particles And Neutrons By Passive And Active Dosimeters And Its Application To Radiation Personnel Monitoring
118	Sumit Basu	VECC	Physics	PHYS04201004002	Event-By-Event Temperature Fluctuations In High Energy Collisions At The LHC Energies In The ALICE Experiment

Sr. No	Name of the student	CI/OCC	Discipline	Enrolment No.	Title
119	Tanmoy Roy	VECC	Physics	PHYS04201104003	Study Of High Spin States In Nuclei Near Z=82
120	Abhijit Ghosh	SINP	Physics	PHYS05201104006	Study Of Drift Wave Instability In Rf Produced Magnetized Plasma
121	Achyut Maity	SINP	Physics	PHYS05201204003	Surface Plasmon Enhanced Optical Properties Of Complex Shaped Gold Nanoparticles
122	Aritra Bandyopadhyay	SINP	Physics	PHYS05201204004	Non-Perturbative Study Of Spectral Function And Its Application In Quark Gluon Plasma
123	Arpan Maiti	SINP	Physics	PHYS05201204008	Studying Surface Plasmons Of Individual Gold Nanoparticle On Silicon Substrate Using Cathodoluminiscence
124	Chiranjib Mondal	SINP	Physics	PHYS05201204016	Constraining The Density Dependence Of Symmetry Energy Using Mean Field Models
125	Chitralekha Datta	SINP	Physics	PHYS05201204014	Exact Solutions Of Some Quantum Integrable Systems Associated With Polarized Spin Reversal Operators
126	Goutam Das	SINP	Physics	PHYS05201304001	Precision Qcd Study For Spin-2 Production At The Large Hadron Collider
127	Kumar Das	SINP	Physics	PHYS05201204009	Aspects Of Inflationary Models In Supergravity
128	Kuntal Nayek	SINP	Physics	PHYS05201204011	Study On Some Aspects Of Non- Supersymmetric Brane Solutions In String Theory
129	Naosad Alam	SINP	Physics	PHYS05201204007	Correlations Of Neutron Star Properties With The Parameters Of Nuclear Matter Equation Of State
130	Pankaj Kumar Shaw	SINP	Physics	PHYS05201204006	Investigation Of Nonlinear Dynamics Of A Self - Excited Complex System Like Plasma

Sr. No	Name of the student	CI/OCC	Discipline	Enrolment No.	Title
131	Rajani Raman	SINP	Physics	PHYS05201004007	Computational Mechanism Of Filling-In In The Visual System
132	Rajeswari Roy Chowdhury	SINP	Physics	PHYS05201004006	Effect Of Substitution At The Transition Metal Site On The Magnetic Properties Of Rare Earth Ternary Silicides
133	Rome Samanta	SINP	Physics	PHYS05201304004	A Study On Impact Of Residual Symmetries In Some Neutrino Mass Models
134	Sabuj Ghosh	SINP	Physics	PHYS05201204019	On The Paths Of Transitions Among Different Kinds Of Nonlinear Oscillations In Glow Discharge Plasma
135	Sayanee Jana	SINP	Physics	PHYS05201204001	Nonlinear Coherent Structures In Plasmas
136	Sk Abdul Kader Md Faruque	SINP	Physics	PHYS05201104005	STUDY OF SPUTTER DEPOSITED Zro2 FILMS UNDER DIFFERENT OXIDATION AND ANNEALING CONDITIONS
137	Tapas Ghosh	SINP	Physics	PHYS05201204013	Study Of Galvanic Displacement Reaction Of Metal Nanostructures On Semiconductor Surfaces Using Transmission Electron Microscopy
138	Akanksha Gupta	IPR	Physics	PHYS06201104006	Shear Flows In 2d Strongly Coupled Fluids-A Theoretical And Computational Study
139	Bhumika Thakur	IPR	Physics	PHYS06201204002	A Study Of The Dynamics Of Delay Coupled Nonlinear Oscillators And Some Model Applications
140	Bibhu Prasad Sahoo	IPR	Physics	PHYS06201104002	3d Simulations And Analysis Of Plasma Transport In The Scrape-Off Layer Of Tokamak Aditya
141	Chandrasekhar Shukla	IPR	Physics	PHYS06201104004	Particle-In-Cell Simulations Of Fast Electron Time Scale Phenomena

Sr. No	Name of the student	CI/OCC	Discipline	Enrolment No.	Title
142	Debraj Mandal	IPR	Physics	PHYS06201204006	Collective Plasma Structures With Kinetic Nonlinearity: Their Coherence, Interaction And Stability
143	Deepa Verma	IPR	Physics	PHYS06201104010	The Study Of Localised Solution In Laser Plasma System
144	Harish Charan	IPR	Physics	PHYS06201104009	Yukawa Liquids Under External Forcing: A Molecular Dynamics Study
145	Laishram Modhuchandra Singh	IPR	Physics	PHYS06201204008	Studies On Driven Dust Vortex Flow Dynamics In Dusty Plasma
146	Mangilal Choudhary	IPR	Physics	PHYS06201104003	Experimental Studies On Collective Phenomena In Dusty Plasmas
147	Meghraj Sengupta	IPR	Physics	PHYS06201104012	Studies In Non-Neutral Plasmas Using Particle-In-Cell Simulations
148	Neeraj Chaubey	IPR	Physics	PHYS06201104013	Synchronization Studies Between Two Coupled Glow Discharge Plasma Sources
149	Samirsinh Ganpatsinh Chauhan	IPR	Physics	PHYS06201104008	Studies On Magnetically Constricted Anode Plasma Source
150	Vara Prasad Kella	IPR	Physics	PHYS06201104007	Ion-Flow Driven Instabilities In Sheath-Presheath Region Of Low Temperature Plasma
151	Anjan Bhukta	IOP	Physics	PHYS07201004001	Au-Ag Bimetallic Nanostructures Growth And Characterization On Ultra Clean Silicon Substrates
152	Bidisha Chakrabarty	IOP	Physics	PHYS07201204001	Studies On Non-Supersymmetric D1-D5-P Gravitational Bound States
153	Himanshu Lohani	IOP	Physics	PHYS07201004006	Electronic Structure Studies Of Some Topological Insulators And New Superconductors Using Photoelectron Spectroscopy And First Principles Calculations

Sr. No	Name of the student	CI/OCC	Discipline	Enrolment No.	Title
154	Indrani Mishra	IOP	Physics	PHYS07200904005	Modifications Of Siox , Tio_2 And PDMS Surfaces & Their Interactions With DNA And Cell
155	Mohit Kumar	IOP	Physics	PHYS07201004005	Growth And Characterization Of Cu-O Based Solar Cell
156	Rama Chandra Baral	IOP	Physics	PHYS07200904001	Study Of L (1520) Resonances & D Mesons At The LHC Energies And Phase Transition In Magnetized Compact Stars
157	Subrata Kumar Biswal	IOP	Physics	PHYS07201104002	Structural Properties Of Finite And Infinite Nuclear Systems And Related Phenomena
158	Arvind Kumar	HRI	Mathematics	MATH08201204002	On Some Problems Involving Nearly Holomorphic Modular Forms And An Estimate For Fourier Coefficients Of Hermitian Cusp Forms
159	Balesh Kumar	HRI	Mathematics	MATH08201104001	Some Topics In Number Theory
160	Rahul Kumar Singh	HRI	Mathematics	MATH08201104006	Maximal Surfaces And Their Applications
161	Ramesh Manna	HRI	Mathematics	MATH08201004003	Fourier Integral Operators, Wave Equation And Maximal Operators
162	Asutosh Kumar	HRI	Physics	PHYS08201104005	Monogamy Of Quantum Correlations
163	Avijit Misra	HRI	Physics	PHYS08200905008	Thermodynamic Aspects Of Quantum Coherence And Correlations
164	Debasis Mondal	HRI	Physics	PHYS08201104006	Quantum Uncertainnty, Coherence And Quantum Speed Limit
165	Mehedi Masud	HRI	Physics	PHYS08200905007	Study Of Cp Violation And Mass Hierarchy Sensitivities At Long Baseline Neutrino Experiments
166	Nabarun Chakrabarty	HRI	Physics	PHYS08201104007	Extended Higgs Sectors, Vacuum Stability And Related Issues

Sr. No	Name of the student	CI/OCC	Discipline	Enrolment No.	Title
167	Nyayabanta Swain	HRI	Physics	PHYS08200905003	The Mott Transition In Strongly Frustrated Lattices
168	Saurabh pradhan	HRI	Physics	PHYS08200805002	Studies In Strongly Correlated Systems
169	Shrobona Bagchi	HRI	Physics	PHYS08200905005	Explorations In Entanglement Of Purification And Multipartite Entanglement
170	Sudipto Sngha Roy	HRI	Physics	PHYS08201204007	Resonating Valence Bond States-A Quantum Information Perspective
171	Swapnamay Mondal	HRI	Physics	PHYS08200905006	Zero Angular Momentum Conjecture For Bps Black Holes In String Theory
172	Tamoghna Das	HRI	Physics	PHYS08201105007	Role Of Quantum Correlations In Quantum Communication Networks
173	Uttam Singh	HRI	Physics	PHYS08201104009	Resource Theories Of Quantum Coherence And Entanglement
174	Saurabh Chandrashekhar Bobdey	TMC	Health Sciences	HLTH09201304003	A Study Of Survival In Oral Cavity Cancer Patients
175	Sharayu Sitaram Mhatre	TMC	Health Sciences	HLTH09200904003	Risk Factors For Gallbladder Cancer In India
176	Bhushan Laxman Thakur	TMC	Life Sciences	LIFE09201204010	Identification Of Potential Regulators Of PIK3CA Promoter In Chemoresistant Ovarian Cancer Cells
177	Crismita Clement Dmello	TMC	Life Sciences	LIFE09201004021	Role Of Aberrant Vimentin Expression In Human Oral Pre-Cancer And Cancer
178	Gauri Ravindra Mirji	TMC	Life Sciences	LIFE09201004016	Genomic And Functional Studies In Leukemia Patients Exhibiting TCR Gd Gene Rearrangement
179	Hudlikar Rasika Rajendra	TMC	Life Sciences	LIFE09201104014	Molecular Analysis Of Tobacco Carcinogen Induced Experimental Lung Tumors And Chemoprevention Studies

Sr. No	Name of the student	CI/OCC	Discipline	Enrolment No.	Title
180	Madhura Gopal Kelkar	TMC	Life Sciences	LIFE09201004008	Imaging Human Sodium Iodide Symporter (Hnis) Gene Regulation In Breast Cancer Animal Model
181	Mohammad Quadir Siddiqui	TMC	Life Sciences	LIFE09201104013	Structural And Functional Basis Of Fanconi Anemia (FANCI-FANCD2) Pathway: Studies Of Protein-Protein Interactions Required For DNA Crosslink Repair
182	Pawan Kumar Upadhyay	TMC	Life Sciences	LIFE09201104001	Integrated Analysis Of Head And Neck Squamous Cell Carcinoma: A Genomics Approach
183	Prajish Sundaram Iyer	TMC	Life Sciences	LIFE09201204001	Genetic Approaches To Discover Novel Oncogenes In Human Cancer
184	Prasad Chandrakant Sulkshane	TMC	Life Sciences	LIFE09201004002	Regulation And Targeting Of MCL-1 In Human Oral Cancers
185	Pratik Rajeev Chaudhari	TMC	Life Sciences	LIFE09201204012	Role Of Hemidesmosomal Linker Proteins In Neoplastic Progression Of Squamous Cell Carcinomas
186	Rahul Maruti Sarate	TMC	Life Sciences	LIFE09201104006	Dissecting The Molecular Mechanism: Normal Stem Cell And Cancer Stem Cell Regulation
187	Richa Tiwari	TMC	Life Sciences	LIFE09201004011	Role Of Keratin 8 Phosphorylation In Neoplastic Progression Of Squamous Cell Carcinoma
188	Vijay Govindrao Padul	TMC	Life Sciences	LIFE09201104007	Identification Of Genes Instrumental In Pathogenesis Of Oligodendroglioma
189	Arghya Mandal	IMSc	Mathematics	MATH10201005002	Cohomology Of Locally Symmetric Spaces
190	Chandan Maity	IMSc	Mathematics	MATH10201004002	On The Topology Of Nilpotent Orbits In Semisimple Lie Algebras
191	Keshab Chandra Bakshi	IMSc	Mathematics	MATH10201304003	On Intermediate Subfactors

Sr. No	Name of the student	CI/OCC	Discipline	Enrolment No.	Title
192	Syed Mohammad Meesum	IMSc	Mathematics	MATH10201105003	Matrix Editing Via Multivariate Lens
193	Uday Bhaskar Sharma	IMSc	Mathematics	MATH10201104003	Counting Similarity Classes Of Tuples Of Commuting Matrices Over A Finite Field
194	Abhrajit Laskar	IMSc	Physics	PHYS10200905002	Microhydrodynamics Of Driven And Active Filaments
195	Aritra Biswas	IMSc	Physics	PHYS10201005005	Phenomenology Of The Charm Decays
196	Arya S.	IMSc	Physics	PHYS10201004003	On The Application Of The Two-Particle Self-Consistent Method To Some Problems In Many-Body Physics
197	Dhargyal	IMSc	Physics	PHYS10201104001	Phenomenological Studies Of The Observed Anomalies In Then T Sector
198	Rajesh Singh	IMSc	Physics	PHYS10201204001	Microhydrodynamics Of Active Colloids
199	Renjan Rajan John	IMSc	Physics	PHYS10201105001	Non-Perturbative Aspects Of Supersymmetric Gauge Theories With Surface Operators
200	Rusa mandal	IMSc	Physics	PHYS10201204003	Rare B Decays As A Probe To Beyond Standard Model Physics
201	Soumya Sadhukhan	IMSc	Physics	PHYS10201005007	The Phenomenology Of Beyond The Standard Model Scalars Due To Extended Symmetries With New Fermions
202	Subhadeep Roy	IMSc	Physics	PHYS10201005003	Interplay Of Stress Release Range And Disorder In Fracture
203	Taushif Ahmed	IMSc	Physics	PHYS10201005009	Qcd Radiative Corrections To Higgs Physics

Sr. No	Name of the student	CI/OCC	Discipline	Enrolment No.	Title
204	Tuhin Subhra Mukherjee	IMSc	Physics	PHYS10201004004	Effective Models Of Beyond The Standard Model Scalars Coupled To Vector -Like Fermions And Their Phenomenology
205	Ashutosh Rai (TCS)	IMSc	Theoretical Computer Science	MATH10201005006	Parameterized Algorithms For Graph Modification Problems
206	Pranabendu Misra	IMSc	Theoretical Computer Science	MATH10201204006	Parameterized Algorithms For Network Design
207	S. Raja	IMSc	Theoretical Computer Science	MATH10201004009	On Structure And Lower Bounds In Restricted Models Of Arithmetic Computations
208	Sudeshna Kolay	IMSc	Theoretical Computer Science	MATH10201105002	Parameterized Complexity Of Graph Partitioning And Geometric Covering
209	Adinarayana Bellamkonda	NISER	Chemistry	CHEM11201104009	Contracted And Expanded Porphyrinoids With Polycyclic Aromatic Units: Syntheses, Receptor Properties, Reactivity And Coordination Chemistry
210	Arindam Ghosh	NISER	Chemistry	CHEM11201204003	Novel Expanded Porphyrin Analogues: Syntheses, Conformation, Aromaticity And Structural Diversity
211	Basujit Chatterjee	NISER	Chemistry	CHEM11201104001	Catalytic Transformations Based On Pincer And Half-Sandwich Ruthenium Complexes
212	Chenikkayala Balachandra	NISER	Chemistry	CHEM11201104010	Syntheses Of Unnatural Amino Acids, Peptides And Novel Fluorescent Molecules From Tropolone
213	Manoj Kumar Janni	NISER	Chemistry	CHEM11201004002	Synthesis Of Deuterated And Novel Heterocyclic Compounds *Via* Metal Mediated Organic Transformations
214	Mriganka Sadhukhan	NISER	Chemistry	CHEM11201004007	Zero-Dimensional, Two-Dimensional Carbon Materials And Their Composites : Bottom Up Synthesis, Properties And

Sr. No	Name of the student	CI/OCC	Discipline	Enrolment No.	Title
215	Ramesh Mamidala	NISER	Chemistry	CHEM11201104012	Strategic Design, Syntheses Of Novel Pyrazole- Based Cyclometalated Palladcycles And Their Utilization As Pre-Catalysts In Organic Syntheses
216	Saikat Maiti	NISER	Chemistry	CHEM11201104007	Hypervalent Lodine(III) Mediated C-N Bond Formation Reactions
217	Somnath Koley	NISER	Chemistry	CHEM11201304002	Study Of Fast Photo-Physical Processes In Heterogeous Environments To Semiconductor Nanomaterials
218	Sourav Palchowdhury	NISER	Chemistry	CHEM11201204006	Molecular Dynamics Studies Of Ionic And Molecular Liquids In Aqueous And Non-Aqueous Multi-Component Systems
219	V. Mukundam	NISER	Chemistry	CHEM11201104014	Pyrazole And Imidazole Based Fluorescent Boron Compounds: Synthesis And Study Of Aggregation Induced Enhanced Emission Properties Of Tetraaryl Pyrazole Supported Polymers And Cyclophosphazenes
220	Biswaranjan Pradhan	NISER	Life Sciences	LIFE11201004014	Peptides And Probiotics As Alternative To Antibiotics: Report From *In-Vitro* And I*n-Vivo* Studies
221	Santosh Kumar Singh	NISER	Life Sciences	LIFE11201004005	Comparative Study Of Molecular Diversity In Environmental And Clinical Isolates Of *Klebsiella Pneumoniae:* Focus On Resistance Mechanism, Virulence Factors And Clonal Diversity
222	Tapan Kumar Dash	NISER	Life Sciences	LIFE11201004017	Combinational Nanoformulations For Circumvention Of Chemo-Resistance In Cancer

Sr. No	Name of the student	CI/OCC	Discipline	Enrolment No.	Title
223	Uday Singh	NISER	Life Sciences	LIFE11201004011	Transient Receptor Potential Vanilloid 3 (Trpv3) Ion Channel In The Rat Brain: Distribution And Functional Significance
224	Usha Pallabi Kar	NISER	Life Sciences	LIFE11201004007	Study Of Mechanism And Regulation Of A Nuclear Dynamin In Tetraymena Thermophila
225	Niladribihari Sahoo	NISER	Physics	PHYS11201004012	Study Of B_s ®m^+m^- And B^+®K^{*+} m^+m^- Using Cms Data At 7/8 Tev

Section-IV

List of Students who have completed M.Tech and M.Sc. (Engg.) programs during 2017-18

M.Tech.

Sr. No.	Name of the student	CI/OCC	Programme	Discipline	Enrolment No.	Title
1	Abhijit K.	BARC	M.Tech	Chemical	ENGG1A201401021	Development Of Numerical Model For Analysing Lekage In Liquefied Nitrogen Storage Tanek Of Pfbr
4	Amit Ranjan	BARC	M.Tech	Chemical	ENGG1A201401023	Rate Based Modelling And Simulation Studies On Mono-Thermal Ammonia-Hydrogen Exchange Process
2	Arijit Bhattacharya	BARC	M.Tech	Chemical	ENGG01201401064	Computational Study Of Heat Transfer And Pressure Drop Across Tube Bundle At High Reynolds Number
5	Divij Bhattacharjee	BARC	M.Tech	Chemical	ENGG1A201401024	Regeneration And Reuse Of Pickling Solution Through Precipitation Process And Optimization Of Process Parameters
3	Sankepally Phani Krishna	BARC	M.Tech	Chemical	ENGG01201401135	Mathematicval Modelling And Optimization Of A Geyser Pump For A Continuous Rotary Dissolver
6	Vivekanand Patel	BARC	M.Tech	Chemical	ENGG01201301103	Experimental Study On Heat Transfer In Gas-Solid Fluidized Bed And Determination Of Wall To Bed Heat Transfer Coefficient
7	Amul Kumar Jadhav	BARC	M.Tech	Civil	ENGG01201401086	Effect Of Strain Rate On The Failure Mode Of Reinfforced Concrete Structures Subjected To High Strain Impact Loading

Sr. No.	Name of the student	CI/OCC	Programme	Discipline	Enrolment No.	Title
8	Arnab Roy	BARC	M.Tech	Civil	ENGG01201401081	Finite Element Analysis Of Graded Composite Structural Members Under Mechanical Loads
9	Chandrani Chakraborty	BARC	M.Tech	Civil	ENGG01201401145	Structure Soil Structure Interaction Under Seismic Loading-A Case Study
10	Gurpreet Singh Bhatia	BARC	M.Tech	Civil	ENGG01201401084	Reliability Based Estimation Of Liquefaction Potential Of Alluvial Soil Site
11	Shuvodeep Chakraborty	BARC	M.Tech	Civil	ENGG01201401095	Finite Element Analysis Of Frp Wrapped Rc Beams And Beam-Column Joints Employing Cohesive Zone Model
12	Ayan Banerjee	BARC	M.Tech	Computer	ENGG01201501037	User Specific Automatic Organization Of Emails Using Machine Learning
13	Baldaniya Hardik Bhopabhai	BARC	M.Tech	Computer	ENGG01201501041	Analysis And Detection Of Abnormal Conditions In Nuclear Power Plant
14	Gaurav Rajguru	BARC	M.Tech	Computer	ENGG01201501040	Application Of Soft Computing Techniques For Improved Estimation Of Earthquake Source Parameters
15	Srishti Agrawal	BARC	M.Tech	Computer	ENGG01201501043	Study And Development Of Programming Primitives & Their Synthesis Techniques For Safety Test & Monitoring System
16	Vivek Latta	BARC	M.Tech	Computer	ENGG01201501045	Study Of Existing Methodologies Of Network Anomaly Detection And Design Of A Behaviour Based Network Anomaly Detection

Sr. No.	Name of the student	CI/OCC	Programme	Discipline	Enrolment No.	Title
17	Aditya Pandey	BARC	M.Tech	Electrical	ENGG01201501046	Analysis And Optimization Of Temperature Compensated Tunable Permanent Magnet Circuits
18	Ashish Kumar Pandey	BARC	M.Tech	Electrical	ENGG01201501048	Design,Analysis And Testing Of Three Level Inverter
19	Deshpande Ankit Vivek	BARC	M.Tech	Electrical	ENGG01201501049	Design & Development Of Control Algorithm For Robotic Arm
20	Gaurava Deep Srivastava	BARC	M.Tech	Electrical	ENGG01201301074	Design, Simulation And Implementation Of Digital Signal Processor-Controlled Shunt Active Filter For Incorporating In Electrical System At PARTH, Tarapur
21	Suman Kumar Mishra	BARC	M.Tech	Electrical	ENGG01201501057	Development Of Motor Condition Monitoring System For Detection Of Incioient Faults
22	Annu Sharma	BARC	M.Tech	Electronics	ENGG01201501059	Design And Development Of FPGA Based Digital Multichannel Analyzer For Nuclear Applications
23	Piyush Ahuja	BARC	M.Tech	Electronics	ENGG01201501062	Development Of Optical Sensor Based On Triangulation Method For Measuring FM Tilt With Respect To The End-Fittings Of The Coolant Channels
24	Pooja Chakraborty	BARC	M.Tech	Electronics	ENGG01201501063	Development Of Mathematical Model For Wavelength Control System Of High Repetition Rate Pulsed Laser And Its Experimental Validation
25	Saroj Kumar Jha	BARC	M.Tech	Electronics	ENGG01201501067	Development Of PLC Based Control System For Operation Of Induction Coil Gun

Sr. No.	Name of the student	CI/OCC	Programme	Discipline	Enrolment No.	Title
26	Shivam Agarwal	BARC	M.Tech	Electronics	ENGG01201501068	VHDL Based Approach For The Design Of Coincidence Analyzer For TDCR System Used For Radioactivity Measurement
27	Swati Hayaran Das	BARC	M.Tech	Electronics	ENGG01201301011	DESIGN AND DEVELOPMENT OF SCANNING SYSTEM FOR 500kev, 1A BEAM FOR Sox AND Nox REMOVAL
28	Puneet Jindal	BARC	M.Tech	Engineering	ENGG01201401108	Study And Development Of Techiques For Auto - Search Of Radioactive Source With UAV
29	Vismay Kumar Singh	BARC	M.Tech	Engineering	ENGG01201501113	Delopment Of HMI And Evaluation Of HMI Performance Using Eye Tracker
30	Ankit Kumar Gupta	BARC	M.Tech	Exploration Geosciences	ENGG1G201301021	Geophysical Investigation In Bhima Basin Over Hulkal Area Using IP And Electrical Resistivity Techniques To Delineate The Geological Structure For Uranium Exploration
31	Damodar K.	BARC	M.Tech	Exploration Geosciences	ENGG1G201501017	Integrated Interpretation Of Magnetic And Ip / Resistivity Studies For Delineating Structural Features And Sulphide Zone Favourable For Uranium Mineralization At Umra Area, Udaipur District, Rajasthan
32	Deepankar Sarma	BARC	M.Tech	Exploration Geosciences	ENGG1G201301014	Geology, Geochemistry, Petrography And Genesis Of Dhanota-Dhancholi-Dosi Granite, Mahendragarh District, Haryana And Its Bearing On The Uranium Mineralisation In The Delhi Super Group Of Sediments

Sr. No.	Name of the student	CI/OCC	Programme	Discipline	Enrolment No.	Title
33	Edadasi Lingamurty	BARC	M.Tech	Exploration Geosciences	ENGG1G201301012	Characterisation Of Acid Volcanics In And Around Selitiya-Chordongri Tract, Betul And Chhindwara District With Special Reference To Its Uranium Potential
34	Karri Rajesh	BARC	M.Tech	Exploration Geosciences	ENGG1G201501002	Modelling And Inversion Of Gravity And Magnetic Data For Delineation Of Lithological Contacts And Structural Features Controlling Uranium Mineralization In Thallitola-Maldongri-Sangli-Ambagarchowki Sector, Rajnandgaon District, Chhattisgarh
35	Md. Maruf Rahaman	BARC	M.Tech	Exploration Geosciences	ENGG1G201301015	Understanding The Genesis Of Uranium Mineralization Associated With Phosphorite And Black Shale At Krol-Talcontact Of Cambrian Metasedimentary Sequence, Along Durmala-Sila Tract, Mussoorie Syncline, Lesser Himalaya, Uttarakhand
36	Mukesh Kumar Singh	BARC	M.Tech	Exploration Geosciences	ENGG1G201301011	Structural And Geochemical Characterisation Of Host Rocks For Uranium Mineralisation In Gogi West-Ukinal Sector Along Gogi-Kurlagere Fault Zone, Yadgir District, Karnataka
37	Pankaj Das	BARC	M.Tech	Exploration Geosciences	ENGG1G201501003	Interpretation Of Heliborne Magnetic And Time Domain Electromagnetic Data For Uranium Mineralization In Parts Of Alwar Sub-Basin,

Sr. No.	Name of the student	CI/OCC	Programme	Discipline	Enrolment No.	Title
38	Parijat Mishra	BARC	M.Tech	Exploration Geosciences	ENGG1G201501013	Geological Study Of Uranium-Copper Association And Bearing Of Mafic Dykes On Uranium Mineralisation In Khetri, Along Kolihan-Chandmari Tract
39	POOJA TRIPATHI	BARC	M.Tech	Exploration Geosciences	ENGG1G201501013	Geochemical Characterisation And Uranium Potential Of Granitoids Around Amla, District Betul, Madhya Prasesh
40	Pradeep Kumar Upadhyay	BARC	M.Tech	Exploration Geosciences	ENGG1G201301009	Geology, Petrology And Structural Analysis Of Basment Rocks Between Sommalallapalle-Peddanagaripalle, South Of Tummalapalle Uranium Deposit, Kadapa District, Andhra Pradhesh
41	Prakash Mukherjee	BARC	M.Tech	Exploration Geosciences	ENGG1G201301020	Analysis Of EM Conductor Delineated From HTEM Surveys Using Ground IP/Resistivity Survey For Uranium Mineralisation In Parts Of Gegal-Ramner Area, Ajmer District, Rajasthan
42	Pritam Karmakar	BARC	M.Tech	Exploration Geosciences	ENGG1G201301013	Geological, Petromineralogical And Geochemical Characterization Of Nayagaon Uranium Occurrence, Rajsamand District, Rajasthan
43	Shashank Shekhar Mishra	BARC	M.Tech	Exploration Geosciences	ENGG1G201301019	Integration Of Induced Polarization (IP)/ Resistivity And Magnetic Techniques For Delineation Of Sulphide Rich Zones Associated With Brecciated/Sheared Quartzites

Sr. No.	Name of the student	CI/OCC	Programme	Discipline	Enrolment No.	Title
44	Sunil Prasad Singh	BARC	M.Tech	Exploration Geosciences	ENGG1G201301008	Characterization Of Migmatite And Their Bearing On Uranium Mineralization In Parts Of Naguar Dist., Rajasthan
45	Thadaka Mahesh	BARC	M.Tech	Exploration Geosciences	ENGG1G201301010	Geology And Geochemistry Of Khetabari Formation, Bomdila Group With A Special Reference To Its Uranium Mineralization In Nokonala-Kardo-Badak Area, West Siang District, Arunchal Pradhesh
46	Tirumareddi Manojkumar	BARC	M.Tech	Exploration Geosciences	ENGG1G201501004	Application Of Magnetic Method For REE Exploration In And Around The Amba Dongar Carbonatite Complex, India
47	Debjyoti Banerjee	BARC	M.Tech	Instrumentation	ENGG01201501107	Modelling And Application Of Advance Control Strategies To Brine Concentrator Unit
48	Elina Mishra	BARC	M.Tech	Instrumentation	ENGG01201301113	Study And Implementation Of Rf Tuning Methodology For Drift Tube Linac
49	Mrutyunjaya Pradhan	BARC	M.Tech	Instrumentation	ENGG01201401102	Development And Characterization Of CNT Based Mercury Vapor Analyzer Instrument
50	Rajakumar D	BARC	M.Tech	Instrumentation	ENGG01201501109	ECG Signal Processing For Telemdicine Application
51	Rohit Jain	BARC	M.Tech	Instrumentation	ENGG01201401103	Design And Simulation Of Corrugated Capsule As Sensing Element Of Differential Pressure Sensor For Nuclear Reactor Applications
52	S. Shri Shankari	BARC	M.Tech	Instrumentation	ENGG01201501112	Study, Design And Simulation Of Flow Through Type Conductivity Cell

Sr. No.	Name of the student	CI/OCC	Programme	Discipline	Enrolment No.	Title
53	Samrat Sahoo	BARC	M.Tech	Instrumentation	ENGG01201401148	On-Line Health Monitoring And Fault Identification In Pressure Sensors And Transmitters Used In Nuclear Facilities
54	Shalini	BARC	M.Tech	Instrumentation	ENGG01201501111	Study, Simulation And Experimentation Of Acoustic Velocity Independent, Fluid Velocity Measuring Instrument Using Ultrasonic Technique
55	Abhishek Sharma	BARC	M.Tech	Mechanical	ENGG01201401133	Modeling And Simulation Of Laser Shock Peening Process
56	Ajit Singh	BARC	M.Tech	Mechanical	ENGG01201401033	Design Optimization Of Dye Laser Flow Cell Using Computational Techniques And Validation
57	Amit Kumar Sharma	BARC	M.Tech	Mechanical	ENGG1A201301016	Thermal Modelling Of The Zirconium Sponge Production Unit To Optimize The Process Parameters
58	Ankit Jain	BARC	M.Tech	Mechanical	ENGG01201401036	Studies On Steady State Response Of Floating Pad Journal Bearing For High Speed Cryogenic Turboexpander
59	Ankit Tiwari	BARC	M.Tech	Mechanical	ENGG01201401037	DESIGN OPTIMIZATION OF STRONG-BACK SUPPORT SYSTEM FOR 650 Mhz SCRF CAVITY CRYOMODULE
60	Ashutosh Srivastava	BARC	M.Tech	Mechanical	ENGG01201501073	Establishing Ultrasonic Testing Threshold For Bond Strength Of Diffusion Bond Of Stainless Steel And Titanium
61	Asish Kumar	BARC	M.Tech	Mechanical	ENGG1A201401003	Investigation Of Mechanical And Fracture Behaviour Of Fuel-Clad Tubes Of Indian PHWR For Different Hydrogen Concentrations In Zircaloy4

Sr. No.	Name of the student	CI/OCC	Programme	Discipline	Enrolment No.	Title
62	Gowda Sunil Parashivaiah	BARC	M.Tech	Mechanical	ENGG01201501075	Simulation Studies Of Flow Over Existing Membrane Disc In Disc Tube Reverse Osmosis Plant And Validaton
63	Kolli Niharika	BARC	M.Tech	Mechanical	ENGG01201401031	Thermal Analysis For Design Of Dual Cooles Annular Fuel
64	Mukhar Sharma	BARC	M.Tech	Mechanical	ENGG1A201401007	Effect Of Loading Frequency On Fatigue Crack Growth Rate Of Type 304 L(N) Stainless Steel
65	Nadella Saikrishna	BARC	M.Tech	Mechanical	ENGG01201501082	Development Of Computer Code For Stability Analysis Of Molten Salt Natural Circulation Loop With And Without Internal Heat Genration
66	Ramkripankar Singh Parihar	BARC	M.Tech	Mechanical	ENGG01201501086	Study On Heat Transfer Enhancement In The Annulus Of Twisted Oval Tube Heat Exchanger In Laminar Region
67	Satish Yadav	BARC	M.Tech	Mechanical	ENGG01201401124	Fatigue Crack Growth Characterisation Of Alloy 617 At Elevated Temperature
68	Saurin Tikendra Bhatt	BARC	M.Tech	Mechanical	ENGG01201501094	Numerical Simulation Of Thermal And Deformation Behaviour Of Concentric Titanium Stainless Steel Cylinders Under Hot Pressing
69	Shilpa Kesarwani	BARC	M.Tech	Mechanical	ENGG01201401032	A Coupled Approach Based On Finite Element Analysis And Plate Impact Experiment To Establish The Strain Rate Properties Of ASTM A350 LF2 Material

Sr. No.	Name of the student	CI/OCC	Programme	Discipline	Enrolment No.	Title
70	Uppalancha Sushmanth	BARC	M.Tech	Mechanical	ENGG01201501097	Development Of New B And Hpl Equations To Evaluate Stress Intensity Factor And J-Integral For Pre-Cracked And Pre-Notched Small Punch Test
71	Harish	BARC	M.Tech	Metallurgical	ENGG01201401072	Effect Of Heat Treatments On Microstructure And Mechanical Properties Of 20mnmoni55 Pressure Vessel Steel
72	Sesetty Nagaraju	BARC	M.Tech	Metallurgical	ENGG01201401074	Effect Of Deformation On The Microstructure, Mechanical Properties And Precipitation Kinetics Of 350 Grade Maraging Steel
73	Shyam Maloo	BARC	M.Tech	Metallurgical	ENGG01201401075	Influence Of Process Temperature On Formability Of Hot-Rolled Beryllium Strips
74	Priyangshu Dhara	BARC	M.Tech	Rad. Safety Engg.	ENGG01201401122	Developpment Of Framework For Probabilistic Safety Analysis Of Radiation Safety Systems For Industrial Electron Accelerator
75	Rahul Sinha	BARC	M.Tech	Rad. Safety Engg.	ENGG01201301141	To Study, Analyze, Model & Carry Out Experimental Investigation
76	Samim Molla	BARC	M.Tech	Rad. Safety Engg.	ENGG01201501125	Systematic Study Radon Exhalation And Distribution In Tummalapalle Uranium Mie For Inhalation Does Assessment To Miners
77	Sarjan Singh	BARC	M.Tech	Rad. Safety Engg.	ENGG01201401152	Studies On Speciation Of Uranium In Mill Tailings And Its Role On Mobility Of Uranium At Jaduguda Mining Site
78	Saurav	BARC	M.Tech	Rad. Safety Engg.	ENGG01201501127	Establishment Of Radiological Parameters And Monte Carlo-Based Gamma Dose Estimation For Spent Fuel Bay Of A Research Reactor

Sr. No.	Name of the student	CI/OCC	Programme	Discipline	Enrolment No.	Title
79	Sreejith S.	BARC	M.Tech	Rad. Safety Engg.	ENGG01201501129	Study Of The Dosimetric Characteristics Of CR-39 Detector With Modified Badge Cassettee For Fast Neutron Pesonnel Monitoring
80	Amit Bhai Patel	IGCAR	M.Tech	Chemical	ENGG02201401018	Rheology Of A Low-Grade Uranium Ore Slurry
81	Anil Kumar	IGCAR	M.Tech	Chemical	ENGG02201401019	Study And Design Of Cryogenic Helium Gas External Purification System
82	Prateek Kumar Laxminarayan Mishra	IGCAR	M.Tech	Chemical	ENGG02201401022	Hydrodynamic And Chemical Studies Of Neodymium Extraction Using Pseudo-Emulsion Hollow Fiber Liquid Member
83	Ved Prakash Singh	IGCAR	M.Tech	Chemical	ENGG02201401023	Removal Of TBP From Diluent Washed Solution Of PUREX Process
84	Abhinav Kumar	IGCAR	M.Tech	Mechanical	ENGG02201301003	Extraction Of Support Impedance By Finite Element Model Updating Of Rotor Mounted On Squeeze Film Damper
85	Anu Krishnan	IGCAR	M.Tech	Mechanical	ENGG02201501001	Design And Analysis Of Offset Handling Machine For Future Fbrs
86	G. Vikram	IGCAR	M.Tech	Mechanical	ENGG02201401017	Development Of Thermal Hydraulic Models For Simulating Events With Coolant Boiling In Reactor Core
87	Kumar Jaideep	IGCAR	M.Tech	Mechanical	ENGG02201401005	Characterisation Of Tig Weld Between Dissimilar Alloys Ss321 And Sn42
88	Niraj Ganesh Jamdade	IGCAR	M.Tech	Mechanical	ENGG02201401007	Estimation Of Pressure Drop In Deformed Fast Breeder Reactor Fuel Subassembly
89	Priyanshu Jain	IGCAR	M.Tech	Mechanical	ENGG02201401008	Seismic Analysis Of Control And Safety Rod Drive Mechanism System Of A Fast Reactor

Sr. No.	Name of the student	CI/OCC	Programme	Discipline	Enrolment No.	Title
90	R. Nikhil	IGCAR	M.Tech	Mechanical	ENGG02201501006	FEM Based Evaluation Of Plastic H Factor For Heterogeneous Compact Tension Specimens
91	Ajmal Ansari	RRCAT	M.Tech	Engg. Physics	ENGG03201501003	Development Of Velocity Map Imaging Spectrograph
92	Avdhesh Kumar	RRCAT	M.Tech	Engg. Physics	ENGG03201501002	Study Of Self-Pulsing Phenomenon In Yb-Doped CW Fiber Lasers And Techniques For Its Suppression
93	Kulkarni Mandar Surendra	RRCAT	M.Tech	Engg. Physics	ENGG03201401004	MATLAB Based Simulation For Estimation And Minimization Of Harmonics Of Reprocessing Plant Power System For Operating Range Of Plant Equipment
94	Shardul Goel	RRCAT	M.Tech	Engg. Physics	ENGG03201401003	Design Improvements And Beam Development Through Multi-Cathode Cesium Sputter Source

M.Sc.(Engg.)

Sr. No.	Name of the student	CI/OCC	Programme	Enrolment No.	Title
1	Amit Kaushal	BARC	M.Sc (Engg.)	ENGG01201503008	Studies on hydrodynamic and kinetics of carbon nanotube synthesis by chemical vapor deposition process in a fluidized bed furnace
2	Amresh Kumar Jha	BARC	M.Sc (Engg.)	ENGG01201403007	Channel Equalization and Bandwidth Enhancement for Multi-Channel, High Speed Data Acquisition System and its Implementation using FPGA

Sr. No.	Name of the student	CI/OCC	Programme	Enrolment No.	Title
3	Nanda Kisor Prasad	BARC	M.Sc (Engg.)	ENGG01201403002	Some studies on laser welding of Oxygen Free High Conductivity (OFHC) copper
4	Tejinder Pal Sabharwal	BARC	M.Sc (Engg.)	ENGG01201403003	Development of New Correlation between Contact Angle and Texture Parameters for Generating Superhydrophobic Surfaces
5	A. Saikumaran	IGCAR	M.Sc (Engg.)	ENGG02201405017	Microstructural evolution in multiprincipal elemental CrFeNbNiV and CrFeNi2.6V alloys
6	Anuj Dubey	IGCAR	M.Sc (Engg.)	ENGG02201405005	Thermal hydraulic investigation of in-pin fuel motion during severe accidents
7	Chinapareddygari Teena Mouni	IGCAR	M.Sc (Engg.)	ENGG02201403013	Stretchability of Commercially Pure Titanium sheet metal
8	Gajji Aneesha	IGCAR	M.Sc (Engg.)	ENGG02201403014	Development of a plasticity correction procedure for online crack length measurement using DCPD during fracture testing
9	Kanhu Charan Sahoo	IGCAR	M.Sc (Engg.)	ENGG02201405008	Effect of thermal ageing on microstructure, tensile and impact properties of Indian RAFM steel
10	M. Sivakumar	IGCAR	M.Sc (Engg.)	ENGG02201405007	Characterization of sintered pellets of Fe-15Wt%.ZrO_2 and Fe-15Wt%Y_2O_3-5Wt%.Ti model ODS systems
11	P. Rohith	IGCAR	M.Sc (Engg.)	ENGG02201405016	Effect of aspect ratio on deformation behaviour of single crystal FCC Cu nanowires
12	Praveen C.	IGCAR	M.Sc (Engg.)	ENGG02201505003	Critical Assessment of Short-Term Stress Relaxation Studies for the Prediction of Creep Properties of P91 steel

Sr. No.	Name of the student	CI/OCC	Programme	Enrolment No.	Title
13	Ragavendran M.	IGCAR	M.Sc (Engg.)	ENGG02201405015	Optimization of Hybrid Laser - TIG Welding of 316LN Steel using Response Surface Methodology (RSM)
14	S. Kumar	IGCAR	M.Sc (Engg.)	ENGG02201505011	Evaluation of Weld Joints in DFRP Tanks by using Various NDE Methods - Experiments and Simulations
15	Sumana	IGCAR	M.Sc (Engg.)	ENGG02201505014	Focused- Time of Flight Diffraction(TOFD) Ultrasonic Imaging
16	Telagathoti Suresh Kumar	IGCAR	M.Sc (Engg.)	ENGG02201405018	Isothermal low cycle fatigue evaluation of 316 LN austenitic stainless steel weld joint in aged and unaged conditions
17	Vankadoth Shiva	IGCAR	M.Sc (Engg.)	ENGG02201403009	Influence of strain rate and temperature on the flow behavior of modified 9Cr-1Mo steel
18	Bidhan Chandra Mandal	VECC	M.Sc (Engg.)	ENGG04201403001	Design of High Power Beam dump for 50 MeV, e-LINAC at VECC
19	Niraj Chaddha	VECC	M.Sc (Engg.)	ENGG04201403002	Design, Analysi and Optimization of Measurement System for Magnet Characterization
20	Suman Kumar Guha	VECC	M.Sc (Engg.)	ENGG04201303002	Study of thermal instability of geographical region before earthquake using remote sensing network
21	Tamal Kumar Bhattacharyya	VECC	M.Sc (Engg.)	ENGG04201503002	Study, Modelling And Control Of The Liquid Helium Supply To Cryopanels Of Kolkata Superconducting Cyclotron
22	Yashwant Kumar	VECC	M.Sc (Engg.)	ENGG04201503001	Study, design and development of 55V/150A DC, regulated Switch Mode Power Supply (SMPS) for high power solid state Radio Frequency (RF) amplifier

Section –V

List of students who have completed D.M., M.Ch and M.D. during 2017-18

Sr. No.	Name of the student	CI/OCC	Programme	Enrolment No.
1	Dr (Ms.) Sangeetha .K.P	TMC	DM-Medical Oncology	HLTH09201410001
2	Dr. Turkar Siddharth Waman	TMC	DM-Medical Oncology	HLTH09201410002
3	Dr. Kothari Rushabh Kiran	TMC	DM-Medical Oncology	HLTH09201410003
4	Dr Tara Chand Gupta	TMC	DM-Medical Oncology	HLTH09201410004
5	Dr. Rohit Swami	TMC	DM-Medical Oncology	HLTH09201410005
6	Dr. Kushal Gupta	TMC	DM-Medical Oncology	HLTH09201410006
7	Dr. Nikhil Sanjeev Pande	TMC	DM-Medical Oncology	HLTH09201410007
8	Dr. Arun Chandrasekharan	TMC	DM-Medical Oncology	HLTH09201410008
9	Dr. Lingaraj Nayak	TMC	DM-Medical Oncology	HLTH09201410009
10	Dr. Doshi Vipul Arinjay	TMC	DM-Medical Oncology	HLTH09201410010
11	Dr (Ms.) Sushmita Rath	TMC	DM-Medical Oncology	HLTH09201410011
12	Dr. Raajit Chanana	TMC	DM-Medical Oncology	HLTH09201410013
13	Dr. Shrirangwar Sameer Sureshrao	TMC	DM-Medical Oncology	HLTH09201410014
14	Dr. Jayaprakash K. P	TMC	DM-Critcal Care Medicine	HLTH09201410015
15	Dr. Vikas Bhagat	TMC	DM-Critcal Care Medicine	HLTH09201410016
16	Dr. Anand .K.C	TMC	DM-Pediatric Onclgy	HLTH09201410017
17	Dr. Vasudeva Bhat K	TMC	DM-Pediatric Onclgy	HLTH09201410018
18	Dr. Srijan Mazumdar	TMC	DM-Gastroenterology	HLTH09201410019
19	Dr. Sridhar Sundaram	TMC	DM-Gastroenterology	HLTH09201410020

Sr. no.	Name of the student	CI/OCC	Programme	Enrolment no.
1	Dr. Abhay K. Kattepur	TMC	MCh.- Surgical Oncology	HLTH09201410021
2	Dr. Guru Prasad R.	TMC	MCh.- Surgical Oncology	HLTH09201410022
3	Dr. Khobragade Krunal Hareshchandra	TMC	MCh.- Surgical Oncology	HLTH09201410024
4	Dr. Balu Mahendra K.	TMC	MCh.- Surgical Oncology	HLTH09201410025
5	Dr. Thanky Harsh Bankimchandra	TMC	MCh.- Surgical Oncology	HLTH09201410026
6	Dr. Amitesh Anand	TMC	MCh.- Surgical Oncology	HLTH09201410029
7	Dr. Nawaz Usman	TMC	MCh.- Surgical Oncology	HLTH09201410030
8	Dr. Sajith P. Sasi	TMC	MCh.- Surgical Oncology	HLTH09201410033
9	Dr. Jitender Rohila	TMC	MCh.- Surgical Oncology	HLTH09201410035
10	Dr. Murali T.V.	TMC	MCh.- Surgical Oncology	HLTH09201410036
11	Dr (Ms.) Rao Amrita Balakrishna	TMC	MCh.-Plastic & Reconstructive Surgery	HLTH09201410037
12	Dr (Ms.) Belgaumwala Tasneem Jaffer	TMC	MCh.-Plastic & Reconstructive Surgery	HLTH09201410038

Sr. no.	Name of the student	CI/OCC	Programme	Enrolment no.
13	Dr (Ms.) Shweta Rai	TMC	MCh.- Gynecological Oncology	HLTH09201410040
14	Dr. Harsh Dhar	TMC	MCh-Head & Neck Oncology	HLTH09201410041
15	Dr. Devendra Kumar Gupta	TMC	MCh-Head & Neck Oncology	HLTH09201410042
16	Dr. Lakshmi Narasimman. P	TMC	MCh-Head & Neck Oncology	HLTH09201410043
17	Dr. Mair Manish Devendra	TMC	MCh-Head & Neck Oncology	HLTH09201410044
18	Dr. Sachin Khandelwal	TMC	MCh- Surgical.Oncology	HLTH09201410023
19	Dr. Rudresha	TMC	MCh- Surgical.Oncology	HLTH09201410027
20	Dr. Umasankar Tantravahi	TMC	MCh- Surgical.Oncology	HLTH09201410028
21	Dr. Bambarkar Supriya Shantaram	TMC	MCh- Surgical.Oncology	HLTH09201410031
22	Dr. Sanjeev Kumar	TMC	MCh- Surgical.Oncology	HLTH09201410032
23	Dr. Dharma Kumar K. G.	TMC	MCh- Surgical.Oncology	HLTH09201410034
24	Dr. Bansal Richa Ashok	TMC	MCh.- Gynecological Oncology	HLTH09201410039

Sr. no.	Name of the student	CI	Programme	Enrolment no.
1	Dr. Patil Roshankumar Anandrao	TMC	MD-Radiotheraphy	HLTH09201409001
2	Dr. (Ms.) Prachi Mittal	TMC	MD-Radiotheraphy	HLTH09201409002
3	Dr. Shaurav Maulik	TMC	MD-Radiotheraphy	HLTH09201409003
4	Dr. Shwetabh Sinha	TMC	MD-Radiotheraphy	HLTH09201409004
5	Dr. Gogy Jacob George	TMC	MD-Radiotheraphy	HLTH09201409005
6	Dr. Bhatia Jatin Vinod	TMC	MD-Radiotheraphy	HLTH09201409006
7	Dr. Kiran Kumar	TMC	MD-Radiotheraphy	HLTH09201409007
8	Dr. (Ms.) Naziba Karim Khondekar	TMC	MD-Radiotheraphy	HLTH09201409009
9	Dr. Gawande Ashutosh Suresh	TMC	MD-Radiotheraphy	HLTH09201409010
10	Dr. (Ms.) Revathy Krishnamurthy	TMC	MD-Radiotheraphy	HLTH09201409011
11	Dr. Gaikwad Utpal Shivram	TMC	MD-Radiotheraphy	HLTH09201409012
12	Dr. Pandey Saket Rajnarayan	TMC	MD-Radiotheraphy	HLTH09201409013
13	Dr. Tryambake Siddhesh Rajendra	TMC	MD-Radiotheraphy	HLTH09201409014
14	Dr. (Ms.) Pooja Babbar	TMC	MD-Radiotheraphy	HLTH09201409015
15	Dr. (Ms.) Riddhi Piyush Joshi	TMC	MD-Anesthesia	HLTH09201409017
16	Dr. Rohit Kumar Patnaik	TMC	MD-Anesthesia	HLTH09201409018
17	Dr. (Ms.) Ankita Lapalikar	TMC	MD-Anesthesia	HLTH09201409019
18	Dr. (Ms.) Kumar Pooja Prakash	TMC	MD-Anesthesia	HLTH09201409020

Sr. no.	Name of the student	CI	Programme	Enrolment no.
19	Dr. Praveen N.B.	TMC	MD-Anesthesia	HLTH09201409021
20	Dr. (Ms.) Nupur Karan	TMC	MD-Anesthesia	HLTH09201409023
21	Dr. Amit Raja Panigrahi	TMC	MD-Anesthesia	HLTH09201409024
22	Dr. Jain Vivek Arvindkumar	TMC	MD-Anesthesia	HLTH09201409026
23	Dr. (Ms.) Jibhkate Charushree Eknathrao	TMC	MD-Anesthesia	HLTH09201409027
24	Dr. Sushan Gupta	TMC	MD-Anesthesia	HLTH09201409028
25	Dr. Bhat Vishal Sadhu	TMC	MD-Anesthesia	HLTH09201409029
26	Dr. Amit Kumar	TMC	MD-Anesthesia	HLTH09201409030
27	Dr. (Ms.) Akshita Daga	TMC	MD-Anesthesia	HLTH09201409031
28	Dr. Kumbhare Pritish Pyarelal	TMC	MD-Anesthesia	HLTH09201409032
29	Dr. (Ms.) Kamalakar Maya Vilas	TMC	MD-Anesthesia	HLTH09201409033
30	Dr. (Ms.) Mohta Avani Sushil Kumar	TMC	MD-Anesthesia	HLTH09201409035
31	Dr. Katwale Bhushan Ashokrao	TMC	MD-Anesthesia	HLTH09201409036
32	Dr. Prakash Deb	TMC	MD-Anesthesia	HLTH09201509010
33	Dr. Anand Vijaya Narayanan	TMC	MD-Pathology	HLTH09201409037
34	Dr. (Ms.) Parul Tripathi	TMC	MD-Pathology	HLTH09201409038
35	Dr. (Ms.) Prerna Walecha	TMC	MD-Pathology	HLTH09201409039
36	Dr. Shyam B.	TMC	MD-Pathology	HLTH09201409040
37	Dr. (Ms.) Kulkarni Tanvee Shrikant	TMC	MD-Pathology	HLTH09201409041
38	Dr. (Ms.) Vidya R.	TMC	MD-Pathology	HLTH09201409042
39	Dr. Ingle Ketan Dadarao	TMC	MD-Pathology	HLTH09201409043
40	Dr. Sourav Sarkar	TMC	MD-Pathology	HLTH09201409044
41	Dr. (Ms.) Gauri Manoj Wagh	TMC	MD-Pathology	HLTH09201409045
42	Dr. (Ms.) Janjal Sneha Pandurang	TMC	MD-Pathology	HLTH09201409046
43	Dr. Patil Rahul Dhansing	TMC	MD-Pathology	HLTH09201409047
44	Dr. Barange Mukesh Shriramji	TMC	MD-Pathology	HLTH09201409048
45	Dr. Parayacade Joseph Sanal Bernard	TMC	MD-Immuno-Haematology & Blood Transfusion Medicine	HLTH09201409049
46	Dr. Gupta Abhaykumar Malind	TMC	MD-Immuno-Haematology & Blood Transfusion Medicine	HLTH09201409050
47	Dr. (Ms.) Navkudkar Anisha Appa	TMC	MD-Immuno-Haematology & Blood Transfusion Medicine	HLTH09201409051
48	Dr. (Ms.) Pande Shilpa Namdev	TMC	MD-Radio-Diagnosis	HLTH09201409052

Sr. no.	Name of the student	CI	Programme	Enrolment no.
49	Dr. Panbude Sushil Natthuji	TMC	MD-Radio-Diagnosis	HLTH09201409053
50	Sujeet Agrawal	TMC	MD-Radio-Diagnosis	HLTH09201409054
51	Dr. (Ms.) Anurima Patra	TMC	MD-Radio-Diagnosis	HLTH09201409055
52	Dr . Kabariya Amitkumar Himmatbhai	TMC	MD-Radio-Diagnosis	HLTH09201409056
53	Dr. (Ms.) Garima	TMC	MD-Radio-Diagnosis	HLTH09201409057
54	Dr. Ghaytidak Abhijeet Balbhim	TMC	MD-Radio-Diagnosis	HLTH09201409058
55	Dr. Peter Paul	TMC	MD-Radio-Diagnosis	HLTH09201409059
56	Dr. Mishra Arun RadheKrishna	TMC	MD-Radio-Diagnosis	HLTH09201409060
57	Dr. Kawthalkar Ameya Shirish	TMC	MD-Radio-Diagnosis	HLTH09201409061
58	Dr. (Ms.) Gauri Gauriya Chinchalker	TMC	MD-Palliative Medicine	HLTH09201409062
59	Dr. Pankaj Singhai	TMC	MD-Palliative Medicine	HLTH09201409063
60	Dr. Aravintho N.	TMC	MD-Nuclear Medicine	HLTH09201409064
61	Dr. Dhake Sanket Prakash	TMC	MD-Nuclear Medicine	HLTH09201409065
62	Dr. Niranjan Kumar Dash	TMC	MD-Radiotheraphy	HLTH09201409008
63	Dr. Thakur Ganesh Pandurangrao	TMC	MD-Radiotheraphy	HLTH09201409016
64	Dr. Milmile Ranjeet Meghraj	TMC	MD-Anesthesia	HLTH09201409022
65	Dr. Gotur Aparna Jagdish	TMC	MD-Anesthesia	HLTH09201409025

राष्ट्रीय मूल्यांकन एवं प्रत्यायन परिषद
विश्वविद्यालय अनुदान आयोग का स्वायत्त संस्थान
NATIONAL ASSESSMENT AND ACCREDITATION COUNCIL
An Autonomous Institution of the University Grants Commission

Certificate of Accreditation

The Executive Committee of the
National Assessment and Accreditation Council
on the recommendation of the duly appointed
Peer Team is pleased to declare the
Homi Bhabha National Institute
(Deemed to be University u/s 3 of the UGC Act 1956)
Anushaktinagar, Mumbai, Maharashtra as
Accredited
with CGPA of 3.53 on four point scale
at A grade
valid up to May 10, 2020

Date : May 11, 2015

Director

कुलपति

Vice Chancellor
प्रो. पी.डी. गुप्ता / प्रो. बिजन कु. दत्ता / प्रो. पी.आर. वासुदेव राव
Prof. P.D. Gupta / Prof. B.K. Dutta / Prof. P.R. Vasudeva Rao
Email : vasudeva@hbni.ac.in

डीन

Dean
प्रो. बिजन कु. दत्ता
Prof. B.K. Dutta
Email : bkdutta@barc.gov.in

सह डीन

Associate Dean
प्रो. डी.के माइति
Prof. D.K. Maity
Email : asso_dean@hbni.ac.in

सह डीन

Associate Dean
प्रो. सैबाल बासु
Prof. Saibal Basu
Email : sbasuhbni@hbni.ac.in

सह डीन

Associate Dean
प्रो. ए.के. दुरेजा
Prof. A.K. Dureja
Email : dureja@hbni.ac.in

कुलसचिव

Registrar
प्रो. बिजन कु. दत्ता / प्रो. डी.के माइति
Prof. B.K. Dutta / Prof. D.K. Maity
Email : asso_dean@hbni.ac.in

होमी भाभा राष्ट्रीय संस्थान
Homi Bhabha National Institute

प्रशिक्षण विधालय परिसर
Training School Complex

अणुशक्तिनगर, मुंबई, (भारत)
Anushaktinagar, Mumbai, (India)

www.hbni.ac.in